



Calhoun: The NPS Institutional Archive
DSpace Repository

Theses and Dissertations

1. Thesis and Dissertation Collection, all items

1948-09

A study of the magnetic amplifier

Betzer, William Eells; Werner, William Richard; Betzer,
William Eells; Werner, William Richard

Massachusetts Institute of Technology

<http://hdl.handle.net/10945/6571>

This publication is a work of the U.S. Government as defined in Title 17, United States Code, Section 101. Copyright protection is not available for this work in the United States.

Downloaded from NPS Archive: Calhoun



Calhoun is the Naval Postgraduate School's public access digital repository for research materials and institutional publications created by the NPS community. Calhoun is named for Professor of Mathematics Guy K. Calhoun, NPS's first appointed -- and published -- scholarly author.

Dudley Knox Library / Naval Postgraduate School
411 Dyer Road / 1 University Circle
Monterey, California USA 93943

<http://www.nps.edu/library>

A STUDY OF THE MAGNETIC AMPLIFIER

WILLIAM ELLS BETZER
WILLIAM RICHARD WERNER

Library
U. S. Naval Postgraduate School
Monterey, California.

Mont 154

8854

148
A STUDY OF THE MAGNETIC AMPLIFIER

by

William Ellis Betzer
Lieutenant Commander, United States Navy
B.S.
from the
United States Naval Academy
December 1941

and

William Richard Werner
Lieutenant Commander, United States Navy
B.S.
from the
United States Naval Academy
December 1941

Submitted in Partial Fulfillment of the Requirements
for the Degree of Master of Science
from the
Massachusetts Institute of Technology
Department of Electrical Engineering
September 1948

Thad
B48

A REPORT ON THE PROGRESS OF THE

BY

William John Baker
Lieutenant Commander, United States Navy
U.S.N.
From the
United States Naval Academy
December 1941

and

William Richard Turner
Lieutenant Commander, United States Navy
U.S.N.
From the
United States Naval Academy
December 1941

Submitted in partial fulfillment of the requirements

for the Degree of Master of Science

From the

Massachusetts Institute of Technology

Department of Electrical Engineering

September 1948

ACKNOWLEDGMENT

The authors wish to extend their grateful appreciation to Professor Samuel H. Caldwell, who made the facilities of the M.I.T. No. 1 Differential Analyzer available for this study; to Mr. John L. C. Lof and Mr. Herbert P. Grossimon, who assisted in the Analyzer studies; to Mr. Harold B. Rex and Mr. Arthur O. Black, of the Bureau of Ordnance, Navy Department, who provided the ferromagnetic cores for use in the experimental investigations; and especially to Professor William H. Radford, who supervised the research.

ACKNOWLEDGMENT

The author wishes to express their grateful appreciation to Professor Samuel H. Daniels, who made the facilities of the S.I.T. No. 1 Biological Analyzer available for this study; to Mr. John L. D. Lee and Mr. Herbert T. Groszmann, who assisted in the analyzer studies; to Mr. Harold A. Lee and Mr. Arthur G. Black, of the Bureau of Chemistry, Army Department, who provided the tetrahydrocannabinol used for use in the experimental investigations; and especially to Professor William H. Redford, who supervised the research.

TABLE OF CONTENTS

	Page
ACKNOWLEDGMENT	2
ABSTRACT	5
CHAPTER I	
INTRODUCTION	
The Magnetic Amplifier	8
Elementary Theory of Operation	12
Nature of the Thesis Study	17
CHAPTER II	
THE MAGNETIC CIRCUIT	
Introduction	20
Selection of the Cores	20
Measurement of Magnetic Properties	30
Winding the Toroids.	37
CHAPTER III	
EXPERIMENTAL STUDIES OF THE BASIC CIRCUIT	
Introduction	45
The Experimental Circuit	45
Static Performance of the Basic Circuit.	48
Amplifier Dynamics Studied by Transient Response	73
Amplifier Dynamics Studied by Frequency Response	82
Summary.	99
CHAPTER IV	
MATHEMATICAL ANALYSIS OF THE MAGNETIC AMPLIFIER	
Introduction to the Analytical Problem	100
Formulation of the Equations	102
Preparation of the Differential Analyzer Problem	108
Approximations, Limitations and Difficulties	115
Nature of the Analytical Solutions	120
The Concept of Buildup of Flux Bias.	131

TABLE OF CONTENTS

ACKNOWLEDGMENT	2
ABSTRACT	3
CHAPTER I	
INTRODUCTION	
The Magnetic Amplifier	4
Elementary Theory of Operation	12
Nature of the Device Used	17
CHAPTER II	
THE MAGNETIC CIRCUIT	
Introduction	20
Selection of the Core	20
Measurement of Magnetic Properties	22
Winding the Toroids	27
CHAPTER III	
EXPERIMENTAL STUDIES OF THE BASIC CIRCUIT	
Introduction	42
The Experimental Circuit	43
Static Performance of the Basic Circuit	48
Amplifier Dynamics Studied by Transient Response	73
Amplifier Dynamics Studied by Frequency Response	82
Summary	90
CHAPTER IV	
MATHEMATICAL ANALYSIS OF THE MAGNETIC AMPLIFIER	
Introduction to the Analytical Problem	100
Formulation of the Equations	102
Preparation of the Differential Analytical Problem	108
Approximations, Limitations and Difficulties	115
Nature of the Analytical Solutions	120
The Concept of Building of Flux Lines	121

	Page
The Analytical Steady-State Behavior	135
The Analytical Transient Behavior	148
Conclusions Regarding the Analytical Studies	166

CHAPTER V
REGENERATIVE FEEDBACK IN MAGNETIC AMPLIFIERS

The Use of Regenerative Feedback in Magnetic Amplifiers.	168
Theory of Regenerative Feedback in Magnetic Amplifiers.	169
Static Characteristics of Feedback Operation	174
Theory of Feedback Gain.	184
Dynamic Performance with Regenerative Feedback	188
Analytical Equations for Regenerative Feedback	191

CHAPTER VI
SUMMARY AND CONCLUSIONS

Summary of the Research	195
Results of the Research	196
Conclusions.	198
Suggestions for Further Work	201

APPENDIX
SAMPLE DESIGN PROCEDURE

Specifications	204
Flux Adjustment for Static Linear Operation.	204
Design for Dynamic Operation	205
Addition of Feedback Windings.	207
BIBLIOGRAPHY	208

120	The Analytical Steady-State Behavior
148	The Analytical Transient Behavior
160	Conclusions Regarding the Analytical Solution

CHAPTER V REGENERATIVE FEEDBACK IN MAGNETIC AMPLIFIERS

162	The Use of Regenerative Feedback in Magnetic Amplifiers
162	Theory of Regenerative Feedback in Magnetic Amplifiers
174	Static Characteristics of Feedback Operation
184	Theory of Feedback Gain
188	Dynamic Performance with Regenerative Feedback
191	Analytical Solutions for Regenerative Feedback

CHAPTER VI SUMMARY AND CONCLUSIONS

192	Summary of the Research
192	Results of the Research
198	Conclusions
201	Suggestions for Further Work

APPENDIX SAMPLE DESIGN PROCEDURE

204	Specifications
204	Flex Adjustment for Static Linear Operation
208	Design for Dynamic Operation
207	Addition of Feedback Windings
208	REMARKS

A STUDY OF THE MAGNETIC AMPLIFIER

ABSTRACT

In this thesis an attempt has been made to determine the fundamentals of magnetic-amplifier performance both from experimental and theoretical studies. Although the steady-state behavior of the magnetic amplifier has been discussed in some detail in the literature, relatively little concrete information is available in regard to the dynamic performance. Studies have been made in the thesis to put circuit performance on a quantitative basis. Steady-state behavior has been expressed in the form of modulation characteristics and power-gain and power-output curves. The dynamics of the system are expressed in terms of effective characteristic time as determined by means of both transient and frequency-response data.

The major portion of the effort was directed towards the investigation of the basic-amplifier circuit without feedback. The nonlinear loop-equilibrium differential equations which describe this system were set up and solved by means of the M.I.T. Differential Analyzer No. 1. Solutions thus obtained were then compared with experimental data. Satisfactory agreement between analytic and experimental steady-state performance was observed. Significant differences were noted, however, between experimental and analytic transients. Although the control

ABSTRACT

In this thesis an attempt was made to determine the fundamental characteristics of magnetic amplifier systems based upon experimental and theoretical studies. Although the steady-state behavior of the magnetic amplifier has been discussed in some detail in the literature, relatively little concrete information is available in regard to the dynamic performance. Studies have been made in the thesis to put directly performance on a quantitative basis. Steady-state behavior has been expressed in the form of modulation characteristics and power-gain and power-output curves. The dynamics of the system are expressed in terms of effective time constants. Time constants determined by means of both transient and frequency-response data.

The major portion of the effort was directed towards the investigation of the basic amplifier circuit without feedback. The amplifier loop-gain was varied and initial equations which describe this system were set up and solved by means of the M.I.T. Differential Analyzer. No. 1. Solutions thus obtained were then compared with experimental data. Satisfactory agreement between analytical and experimental steady-state performance was observed. Significant differences were noted, however, between experimental and analytical transients. Although the control

circuit appears to have been adequately described by the equations, the neglect of the functional dependence of core loss upon carrier-circuit constants and excitation introduced considerable error in the analytic transient. The value of the differential analyzer has not been confined to providing rapid solutions of difficult nonlinear equations, but is enhanced by giving a physical significance to the equations which is acquired from observation of the relative shaft motions which represent system variables.

Upon completion of the studies of the basic circuit, the remaining available time was allotted to experimental investigation of regenerative ampere-turn feedback. Careful balance of the feedback rectifier-bridge was found necessary to maintain symmetry in the carrier-current waveform. Further study of the feedback connection is indicated.

The magnetic-core material used in the saturable reactors was three-mil Allegheny Electrical Alloy #4750 which had been given a special magnetic anneal to produce high initial permeability and a sharp break at the knee of the magnetization curve. This was the best available material, although better cores now exist. The normal magnetization curve, which was measured by ballistic galvanometer techniques before winding the amplifier cores, was used in the machine solution as the nonlinear function

almost appears to have been adequately described by the equation, the neglect of the theoretical dependence of some loss upon certain physical constants and relations. Instead of considering a system in the analysis of the value of the differential coefficient, it has been found that in providing rapid solutions of differential equations, but as answered by giving a physical significance to the equation which is derived from observation of the relative effect of various physical constants.

Upon completion of the analysis of the basic principles, the remaining available data was applied to experimental investigation of representative known-unknown feedback. General balance of the feedback coefficient-physical was found necessary to maintain symmetry in the circuit-current wave-form. Further study of the feedback coefficient is indicated.

The negative-feedback material used in the experiments was three-lead alloy electrical alloy 60/40 which had been given a special negative anneal to produce high initial permeability and a sharp drop at the knee of the magnetization curve. This was the best available material, although better ones now exist. The normal magnetization curve, which was measured by ballistic galvanometer techniques before studying the regenerative circuit, was used in the machine solution as the nonlinear function

relating flux and magnetizing force.

The results of the amplifier studies indicate the way in which the various circuit parameters affect gain and bandwidth. It has been shown that a compromise between the two, consistent with the requirements of any specific application, must be sought. The principal limitation of this highly inductive device is its inherently narrow bandwidth. The use of positive feedback permits an improvement in the power gain by a factor of 100 or better, with an accompanying reduction of the pass-band. Further studies should indicate whether or not an overall gain-bandwidth improvement can be expected from the feedback connection.

relating time and magnifying factor.

The results of the amplifier studies indicate

the way in which the various circuit parameters affect gain and bandwidth. It has been shown that a compromise between the two, consistent with the requirements of any specific application, may be sought. The potential

limitation of this highly inductive device is its inherent narrow bandwidth. The use of resistive feedback permits an improvement in the power gain by a factor of 100 or better, with an accompanying reduction of the

pass-band. Further studies should indicate whether or not an overall gain-bandwidth improvement can be expected from the feedback operation.

It is noted that the feedback operation is a

very important factor in the design of

the amplifier circuit. It is noted that the

feedback operation is a very important factor in the design of the amplifier circuit.

A STUDY OF THE MAGNETIC AMPLIFIER

CHAPTER I

INTRODUCTION

The Magnetic Amplifier

Throughout the last thirty years, the use of the vacuum tube in all types of electrical circuitry has become widespread. The versatility and adaptability of this unique device has made it an indispensable part of the physical world, and its application has made possible scientific accomplishments which were undreamed of at the turn of the century. In 1925, however, the invention of the dry-disc rectifier by L. O. Grondahl marked the beginning of a period in which efforts were directed by many engineers toward the development of simple devices which would replace the vacuum tube in certain applications. This direction of interest into components which might compete with the vacuum tube, it should be remembered, occurred at a time when the use and application of the vacuum tube was in marked ascendancy, and it is obvious that a very small portion of the interest of the electrical engineering profession was directed into the more uninteresting competitive components when the triode and its variations seemed to supply most existing needs.

In the past decade, interest in vacuum-tube substitutes has achieved a new momentum marked by the practical use of germanium-diode and silicon-diode mixers and detectors in high-frequency-communications circuits, extensive utiliza-

The Scientific Revolution

Throughout the last thirty years, the use of the vacuum tube in all types of electrical circuitry has become widespread. The versatility and adaptability of this unique device has made it an indispensable part of the electrical world, and its application has made possible scientific developments which were impossible of attainment at the beginning of the century. In 1907, however, the invention of the triode vacuum tube by L. V. De Forest marked the beginning of a period in which efforts were directed to many experiments toward the development of single vacuum tubes which would replace the vacuum tubes in certain applications. This direction of interest led to experiments which might compete with the vacuum tube, it should be remembered, occurred at a time when the use and application of the vacuum tube was in marked ascendancy, and it is obvious that a very small portion of the interest in the electrical engineering profession was directed into the more substantial cooperative experiments with the tube and its variations seemed to occupy most existing funds.

In the past decade, interest in vacuum-tube applications has exhibited a new momentum added by the practical use of pentode-diode and triode-diode mixers and detectors in high-frequency communication circuits, extensive utilization

tion of dry-disc rectifiers of the selenium type in power-supply circuits, the use of mechanical rectifiers in power circuits, the development and application of the magnetic amplifier, and very recently, the introduction of the Bell Laboratories' "transistor" amplifier. The inevitable replacement of the vacuum tube in many useful applications is a foregone conclusion, and undoubtedly the magnetic amplifier, when its dynamic and steady-state behavior is fully understood, will provide a useful addition to the tools of the electrical engineer.

Amplification is obtained in the magnetic amplifier through utilization of the saturation effects in an iron core under excitation by either an alternating current and a direct current, or by two alternating currents of different frequencies. The magnetic amplifier is a direct-current amplifying circuit of the carrier-frequency type in which the carrier is modulated by an input signal in a magnetically biased saturable-reactor unit. The amplified input signal is subsequently recovered in a demodulator system. The inductance of the magnetic circuit of this type is high, and an inherently slow time-response is associated with highly inductive devices of this type. Investigations of magnetic amplifier circuitry require attention to the improvement of either the gain or the time-response of the amplifier without undue sacrifice of the other factor.

The magnetic amplifier was originally developed in

The negative amplifier was originally developed in 1940 for the purpose of amplifying signals from the output of the negative feedback amplifier. The amplifier is a simple circuit which consists of a single stage of a vacuum tube or transistor. The input signal is applied to the grid of the tube or the base of the transistor. The output is taken from the plate or collector. The amplifier is designed to have a gain of approximately 10. The amplifier is used in a variety of applications, including as a pre-amplifier for the negative feedback amplifier.

successful form in 1912 by E. F. W. Alexanderson, of the General Electric Company, who used the device as an amplifier-modulator for voice-frequency amplitude-modulation of the output of a radio-frequency alternator. The magnetic amplifier enjoyed an early prominence in the field of wireless communications, but was soon superseded by the vacuum-tube amplifier as the triode was perfected and applied.

During the period between the great World Wars, various improvements of the magnetic amplifier appeared. The perfection of the dry-disc rectifier in 1925 provided the necessary component for the construction of a tubeless amplifier, the use of cascaded magnetic amplifiers, and the use of regenerative-feedback for the improvement of magnetic amplifier gain. In general, however, magnetic amplifier development was retarded because of the intense interest in vacuum-tube circuitry.

The nonlinear character of the inductance of the saturable core has made analytical study of the magnetic amplifier very difficult. Various methods of approach involving linear approximation of the magnetizing characteristic have been developed from the original method proposed by A. Boyajian in 1931. In general, however, most magnetic amplifiers have been designed from empirical considerations.

In the years preceding the outbreak of the recent war, German engineers recognized the fact that improvements in magnetic materials and in rectifier units gave the mag-

netic amplifier a new potential value. Extensive studies were conducted in Germany during the War, and the successes of these researches have been viewed with great interest in this country and in England.

The time-response problem has been studied rather extensively at the Servomechanisms Laboratory at the Massachusetts Institute of Technology. Degenerative-feedback techniques were applied to this problem, but results were not wholly encouraging, primarily because of the low quality magnetic materials from which the cores were constructed. The device has, however, proved to be a satisfactory servo-amplifier for limited applications when the period of cyclic variations of the system is long.

The magnetic amplifier is admirably suited to many military and industrial applications in which ruggedness and freedom from the need for frequent attention are of paramount importance. In contrast with the vacuum-tube amplifier, the magnetic device is totally shock and impact resistant, is not subject to deterioration with age or with use, and, with proper design, may display efficiencies of the order of 90%. The vacuum tube amplifier represents a variable ohmic resistance, and is, therefore, an inherently lossy device. The magnetic amplifier can be designed to be nearly purely reactive, and is, therefore, capable of theoretically lossless performance. Magnetic amplifiers are free from the need for complicated power supplies since all power is furnished by an a-c source. The magnetic

better results than the present value. The results obtained
 were obtained in many cases during the war, and the success
 of these operations have been noted with great interest in
 this country and in England.
 The time-temperature problem has been solved by the
 application of the thermodynamic law of the mass-
 action law of chemistry. The results have been
 obtained and applied to this problem, but there is also
 not only a theoretical, but also a practical, basis of the law which
 magnetic materials have which has been well established.
 The device has, however, proved to be a satisfactory power-
 amplifier for heated conditions when the need of a
 variation of the system is large.
 The magnetic amplifier is a device which is used to
 amplify and deliver electrical energy in which the
 and transfer from the heat the present situation is at
 present important. In contrast with the vacuum-tube
 amplifier, the magnetic device is easily made and is not
 resistant, is not subject to deterioration with age or with
 use, and, with proper design, may display efficiency of
 the order of 90%. The vacuum tube amplifier requires
 various other conditions, and is, therefore, an inherently
 lossy device. The magnetic amplifier can be designed to
 be nearly totally lossless, and is, therefore, capable of
 theoretically infinite performance. Magnetic amplifiers
 are used from the need for amplified power output also
 all power is provided by an a-c source. The magnetic

amplifier can provide high gains while maintaining compact construction.

The response of the vacuum-tube amplifier is essentially, within the designed band-width, independent of frequency. The magnetic amplifier, being a reactive device, is frequency dependent in response over a relatively narrow band. The inductive inertia of the magnetic amplifier has been a constant restraint against the use of the device. The nature of this inductive effect is discussed in this report.

The availability of new superior magnetic materials and efficient rectifier units has given the magnetic amplifier renewed prominence, and there is promise that the magnetic amplifier will soon find far wider acceptance and use.

Elementary Theory of Operation

The magnetic amplifier is a particular adaptation of the saturable-core reactor. Power magnification is obtained through utilization of the variation of the permeability of the core material of the reactor in the region of the knee of the normal magnetization curve. The incremental permeability of ferromagnetic cores may be defined as the ratio of the incremental flux density in the material to the incremental value of the applied magnetizing force. Furthermore, the incremental inductance of a wire-wound core of this type is a function of the incremental permea-

regulator and provide high water with automatic control.

The response of the human body is also affected, with the nervous system, independent of the body. The nervous system, being a sensitive device, is strongly dependent in response with a relatively narrow band. The nervous system of the human body is not a simple system, but a complex system which is not of the same type. The nature of this nervous system is discussed in this report.

The regulation of the nervous system is not a simple matter, but a complex one. It is not only the nervous system, but also the body, which is affected. The nervous system, being a sensitive device, is strongly dependent in response with a relatively narrow band. The nervous system of the human body is not a simple system, but a complex system which is not of the same type. The nature of this nervous system is discussed in this report.

Regulation of the Nervous System

The nervous system is a complex system, and its regulation is not a simple matter. It is not only the nervous system, but also the body, which is affected. The nervous system, being a sensitive device, is strongly dependent in response with a relatively narrow band. The nervous system of the human body is not a simple system, but a complex system which is not of the same type. The nature of this nervous system is discussed in this report.

bility. Figure 1-1 illustrates the variation of flux density and permeability with magnetizing force. It is clear, from the figure, that in the region of the knee of the normal magnetization curve there is a rapid change in permeability, and consequently of inductance, with relatively small changes in magnetizing force.

As shown in Figure 1-2, a typical magnetic amplifier consists of a pair of properly-wound toroidal cores. The alternating-current series circuit is composed of a high power a-c source, a load, and the a-c windings on the cores. The a-c source supplies essentially sinusoidal flux variations to the cores. The direct-current coils are connected in series opposition such that the induced fundamental alternating voltages in these coils are balanced out across the input windings. A source of low-level d-c or slowly fluctuating a-c power is supplied to the input terminals.

A slight change in the d-c control current will cause a large variation in the inductance of the a-c windings. This variation will effectively modify the total impedance presented to the a-c source in a manner related nonlinearly to the instantaneous magnitude of the control current. Such action will amplitude-modulate the voltage supplied by the a-c source with the signal applied to the control windings. The signal is then recovered from the carrier circuit in a system of dry-disc demodulators. Since the source voltage was applied at a much higher power-level

1. The first step in the design of the control system is the selection of the control variable. This is the variable which is to be controlled. It is usually the output of the system, but it may be any other variable which is of interest.

2. The next step is the selection of the control signal. This is the signal which is to be used to control the system. It is usually a voltage or a current, but it may be any other physical quantity.

3. The third step is the selection of the control element. This is the element which is to be used to convert the control signal into a control action. It is usually an amplifier or a motor, but it may be any other device.

4. The fourth step is the selection of the control law. This is the law which is to be used to determine the control signal from the control variable. It is usually a proportional, integral, or derivative law, but it may be any other law.

5. The fifth step is the selection of the control system. This is the system which is to be used to implement the control law. It is usually a computer or a control unit, but it may be any other device.

6. The sixth step is the selection of the control parameters. These are the parameters which are used to adjust the control system. They are usually the gain, the time constant, and the reset time.

7. The seventh step is the selection of the control hardware. This is the hardware which is used to implement the control system. It is usually a computer or a control unit, but it may be any other device.

8. The eighth step is the selection of the control software. This is the software which is used to implement the control system. It is usually a computer program or a control algorithm, but it may be any other software.

9. The ninth step is the selection of the control test equipment. This is the equipment which is used to test the control system. It is usually a computer or a control unit, but it may be any other device.

10. The tenth step is the selection of the control operator. This is the operator who is responsible for operating the control system. It is usually a person, but it may be any other device.

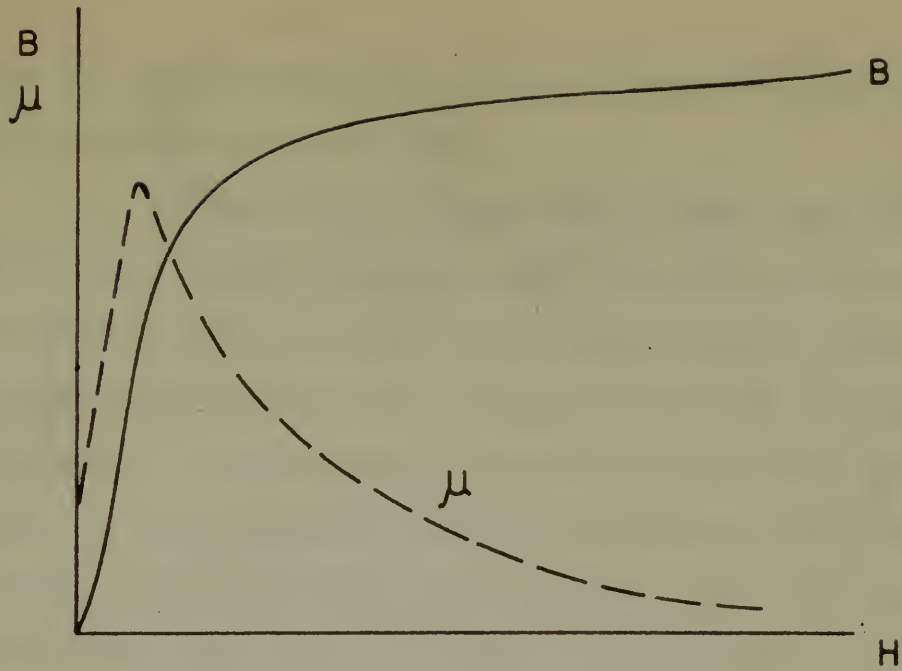


FIG. 1-1 NORMAL MAGNETIZATION CURVE.

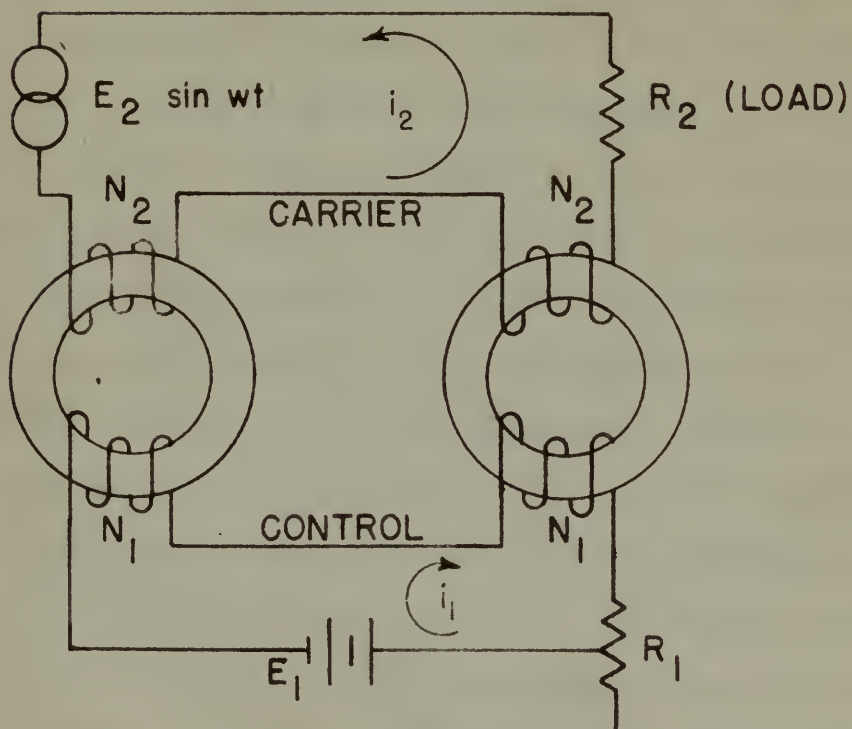


FIG. 1-2 BASIC MAGNETIC AMPLIFIER

than the control current, overall amplification of the control signal is obtained.

Figure 1-3(a) depicts the normal magnetization curve of a typical magnetic amplifier under excitation of a sinusoidal flux as is shown in Figure 1-3(b), when a small control magnetizing force, NI_{dc} , is applied to the control windings. A simple graphical construction will give waveforms of the resultant a-c circuit magnetizing forces expressed in ampere-turns as shown in Figure 1-3(c). The use of harmonic analysis will permit the separation of the even and odd harmonic terms of the magnetizing currents. Such an analysis will indicate that the odd-harmonic terms are of the same magnitude and sign, while the even-harmonic terms are of equivalent magnitudes, but of opposite sign. These magnetizing forces are plotted in Figure 1-4. If the a-c coils of the amplifier are connected in series, and if the impedance of the d-c source is low, the phases of the harmonics will then be such that the even-harmonic currents will flow in the control circuit, while the odd-harmonic currents will flow as an output current in the a-c circuit. Actually, then, it is the odd-harmonic currents in the a-c circuit which are modulated by the applied control signals. Magnetization of the cores under these conditions is designated as "natural" magnetization. If, on the other hand, the cores are connected in series and the impedance of the d-c circuit is high to second-harmonic frequencies of the applied carrier, the second-harmonic currents are unable

from the control circuit, overall amplification of the
output signal is obtained.

Figure 1-2(a) depicts the control system.

curve of a typical magnetic amplifier with saturation of a
magnetic core is shown in Figure 1-2(b), where a small
control magnetizing force, H_{dc} , is applied to the control
windings. A single symmetrical saturation will give zero
force at the residual H_{dc} and a linear magnetizing region at
positive and negative forces as shown in Figure 1-2(a). The rise
of magnetic flux is all linear the saturation of the core
and the magnetic force of the magnetizing windings. Such
an analysis will indicate that the odd-symmetry curve is
at the zero magnetic and also, with the even-symmetry
force at of equivalent magnetizing, but of opposite sign.
These magnetizing forces are plotted in Figure 1-2. If the
odd coils of the amplifier are connected in series, and if
the inductance of the 2-2 branch is low, the phase of the
magnetization will then be such that the even-symmetry magnetic
will flow in the control circuit, while the odd-symmetry
magnetization will flow as an output current in the 2-2 circuit.
Actually, then, it is the odd-symmetry magnetization in the 2-2
circuit which is regulated by the applied control signal.
Regulation of the even-symmetry branch conditions is design-
ated as "magnetic" magnetization. If, on the other hand,
the even-symmetry is series and the inductance of the
2-2 circuit is high so that the even-symmetry magnetization of the
applied current, the even-symmetry magnetization is the

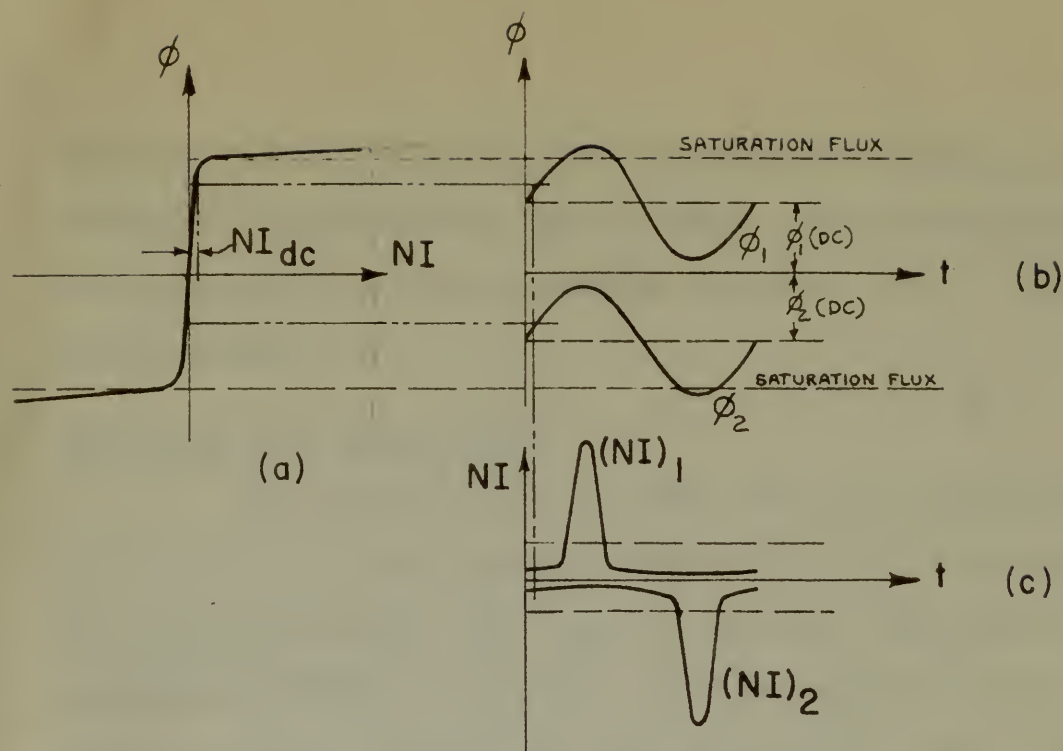


FIG. 1-3 (a) THE MAGNETIZATION CURVE.
(b) FLUX AS A FUNCTION OF TIME.
(c) MAGNETIZING FORCE AS A FUNCTION OF TIME.

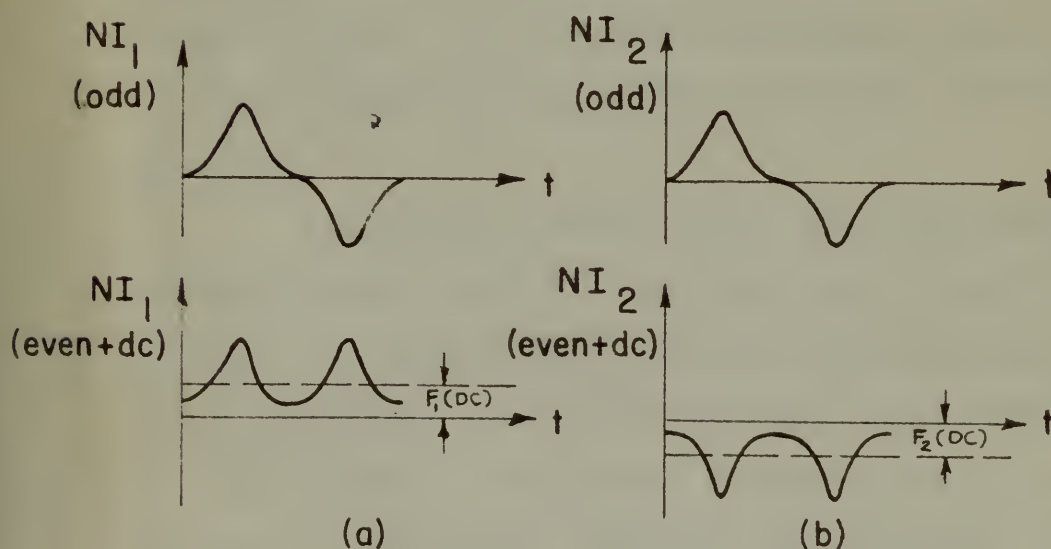


FIG. 1-4 (a) HARMONIC COMPONENTS OF MAGNETIZING FORCE IN CORE NO. 1.
(b) HARMONIC COMPONENTS OF MAGNETIZING FORCE IN CORE NO. 2.

to flow, and the condition of magnetization known as "constrained" magnetization will prevail. This report will deal primarily with the magnetic amplifier under "natural" magnetization.

Nature of the Thesis Study

The first phases of this study are devoted to investigations of the magnetic characteristics of magnetic-core materials which will present optimum performance in magnetic-amplifier circuitry. The performance of the amplifier is associated with the normal induction curve of the core-material and the performance is justified with mathematical relationships whenever linear approximations are possible. Comparison of available magnetic materials is made and the choice of the material from which the cores were constructed is justified by empirical and theoretical considerations. In connection with this phase of the work, magnetic characteristics of the available materials were measured.

The second phase of this investigation involves an experimental study of the basic magnetic-amplifier circuit. An experimental magnetic amplifier was designed, and an extensive series of laboratory tests were conducted on this circuit. The effects of the magnitudes of the load and input resistances, frequency and magnitude of the a-c source supply voltage, number of turns on the input and output circuits, and magnitude of the control current on

to flow, and the condition of magnetization known as "open-circuit" magnetization will be reached. This report will deal primarily with the magnetic amplifier under "closed-circuit" magnetization.

History of the Magnetic Amplifier

The first phase of this study was devoted to the investigation of the magnetic characteristics of magnetic amplifiers which will present certain advantages in magnetic-amplifier circuits. The performance of the amplifier is associated with the internal induction curve of the core material and the permeability is justified with mathematical relationships whenever linear approximations are possible. Comparison of available magnetic materials is made and the choice of the material from which the core was constructed is justified by empirical and theoretical considerations. In connection with this phase of the work, magnetic characteristics of the available materials were presented.

The second phase of this investigation involves

an experimental study of the basic magnetic-amplifier circuit. An experimental magnetic amplifier was designed and an extensive series of laboratory tests were conducted on this device. The effects of the magnitude of the load and input resistance, frequency and magnitude of the a-c source supply voltage, number of turns on the input and output circuits, and magnitude of the control current on

gain of the amplifier, power-output of the device, and dynamic response of the system were observed. Dynamic response of the amplifier was observed for both step-functions applied to the input circuit and for sinusoidal variations of the control voltage. Effects of the various parameters on gain and power output are based on steady-state operational considerations. The observed variations are correlated with theoretical considerations and explained, whenever possible, by the use of accepted formulae.

The third phase of this investigation is comprised of an analytic study of the magnetic amplifier based upon solution of the nonlinear equations of circuit operation on the #1 Differential Analyzer. A set of simultaneous differential equations describing the behavior of the amplifier circuit was prepared, and a series of analytical solutions to these equations was obtained mathematically on the analyzer. Circuit parameters for these theoretical solutions were made to closely approximate the actual experimental parameters under which laboratory observations were made. The analytical solution was found to be an invaluable aid to the understanding of circuit performance. The results of the analytical solutions are correlated with observed phenomena.

The use of positive, or regenerative, feedback was investigated in the fourth phase of this study. Again the effects of variations in the circuit parameters were

observed experimentally. Steady-state and dynamic characteristics of the feedback circuit are discussed and explained on the basis of information obtained on experimental and analytical studies of the basic circuit.

In the final phase of this study, certain design criteria are established. These criteria are based on analytical and empirical considerations of the performance of the magnetic-amplifier circuit. The nature of the gain, power output, and dynamic performance of the amplifier are correlated, and definite criteria for methods of design for a particular performance are formulated. In connection with these considerations, a typical magnetic-amplifier design is carried out. Finally, a series of suggestions for future work in this field is presented.

observed experimentally. Velocity-state and dynamic character-
istics of the system must be determined and explained
on the basis of information obtained on experimental and
analytical studies of the system itself.

In the final phase of this study, certain design
features are established. These features are based on
analysis and synthesis of the characteristics of the system
of the specific system. The nature of the gain,
phase output, and dynamic behavior of the system are
correlated, and relative output for a range of design for
a particular performance are indicated. In connection
with these considerations, a typical transfer function de-
sign is carried out. Finally, a series of experiments for
testing and in this study is indicated.

CHAPTER II

THE MAGNETIC CIRCUIT

Introduction

Since the action of the magnetic amplifier depends in a large measure upon the ferromagnetic properties of its saturable-reactor unit, the design of the magnetic circuit is of utmost importance. Considerations involved in the selection of the core material, the measurement of its properties, and the winding of the reactors will, therefore, be discussed in detail.

Selection of the Cores

The factors which must be investigated in choosing the magnetic circuit for magnetic-amplifier design are:

1. Normal magnetization curve,
2. Permeability,
3. Saturation flux density,
4. Core losses,
5. Core shape.

These will be discussed in order and their significance in relation to the amplifier design will be pointed out.

The normal magnetization curve of a ferromagnetic core is a qualitative sensitivity-index for a magnetic amplifier utilizing such cores. To achieve the highest amplifier sensitivity, the magnetization curve should have the idealized form shown in Figure 2-1, which exhibits a finite discontinuity at the origin. This idealized function is

CHAPTER II

THE MAGNETIC CIRCUIT

Introduction

Since the action of the magnetic circuit depends in a large measure upon the characteristics of its various parts, the design of the magnetic circuit is of great importance. Considerations involved in the selection of the core material, the determination of its properties, and the winding of the circuit will, therefore, be discussed in detail.

Definition of the Core

The factors which must be investigated in choosing the magnetic circuit for magnetic-circuit design are:

1. Normal magnetization curve,
2. Permeability,
3. Saturation flux density,
4. Core losses,
5. Core shape.

These will be discussed in detail and their significance in relation to the magnetic design will be related out.

The normal magnetization curve of a ferromagnetic core is a qualitative sensitivity-index for a magnetic circuit. It is a qualitative index of the magnetic properties of the material. The magnetic circuit design must have the same sensitivity, the magnetization curve must have the same shape as shown in Figure 2-1, which exhibits a typical magnetization curve. This is the typical function of the design.

often used in the literature as an approximation in the analysis of magnetic-amplifier performance.^{1,2} Such a function implies, of course, infinite initial permeability and no hysteretic effects. The manner in which the magnetization curve indicates amplifier sensitivity can be seen by plotting the static permeability as a function of direct magnetizing force from the defining relation

$$\mu = \frac{B}{H} . \quad (2-1)$$

For the idealized case this function is shown in Figure 2-2. The transfer characteristics of the amplifier depend upon the variation of inductance with direct magnetization, and hence upon the permeability, since the inductance is directly proportional to the permeability. The steeper the slope of the permeability function, the more sensitive will be the amplifier. Comparison of the ideal static-permeability function with the measured functions of two different magnetic materials, which are shown in Figures 2-9 and 2-10, reveals that the sensitivity of the practical amplifier is less than that of the ideal amplifier. This criterion is only of qualitative interest because the reactor inductance depends not upon the static permeability but upon the incremental permeability, there being no direct mathematical relation between the two. Although it is smaller than the static permeability, the incremental permeability exhibits, however, the same

-
1. Lamm, U., "The Transducer, a D.C. Pre-Saturated Reactor," (Stockholm, Esselte Aktiebolag, 1943).
 2. Rex, H.B., "The Transducer," Instruments, 20, (1947), 1102-1109.

often used in the literature as an approximation in the analysis of negative-amplitude performance.^{1,2} Such a function implies, of course, infinite initial power and no transient effects. The manner in which the negative-amplitude response is actually achieved can be seen by plotting an actual waveform as a function of direct magnitude taken from the negative relation

$$(2-1) \quad \frac{d}{dt} = \frac{1}{2} \frac{d}{dt}$$

For the idealized case this function is shown in Figure 2-5. The transient characteristics of the amplifier depend upon the variation of impedance with direct magnitude, and hence upon the relationship, since the impedance is directly proportional to the power density. The closer the value of the power density function, the more sensitive will be the amplifier. Comparison of the ideal and the power density function with the function shown in Figure 2-5 and 2-10, reveals that the sensitivity of the power density function is less than that of the ideal amplifier. This relation is only of qualitative interest because the power density function depends upon the actual sensitivity but upon the impedance relationship. There being no direct relationship between the two, it is evident that the power density function, the impedance sensitivity analysis, however, the same.

1. James, H. "The Transducer, a D.C. Two-Port Network," *Electronic Engineering*, 1957.
2. For H. S. "The Transducer," *Electronic Engineering*, 1957.

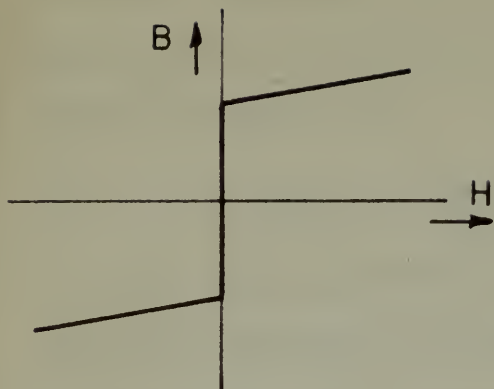


FIG. 2-1

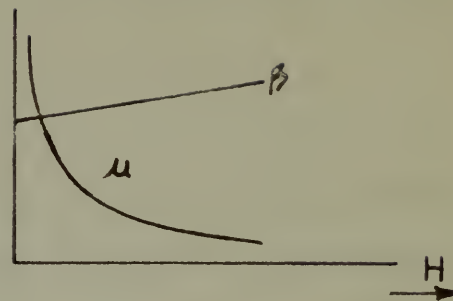


FIG. 2-2

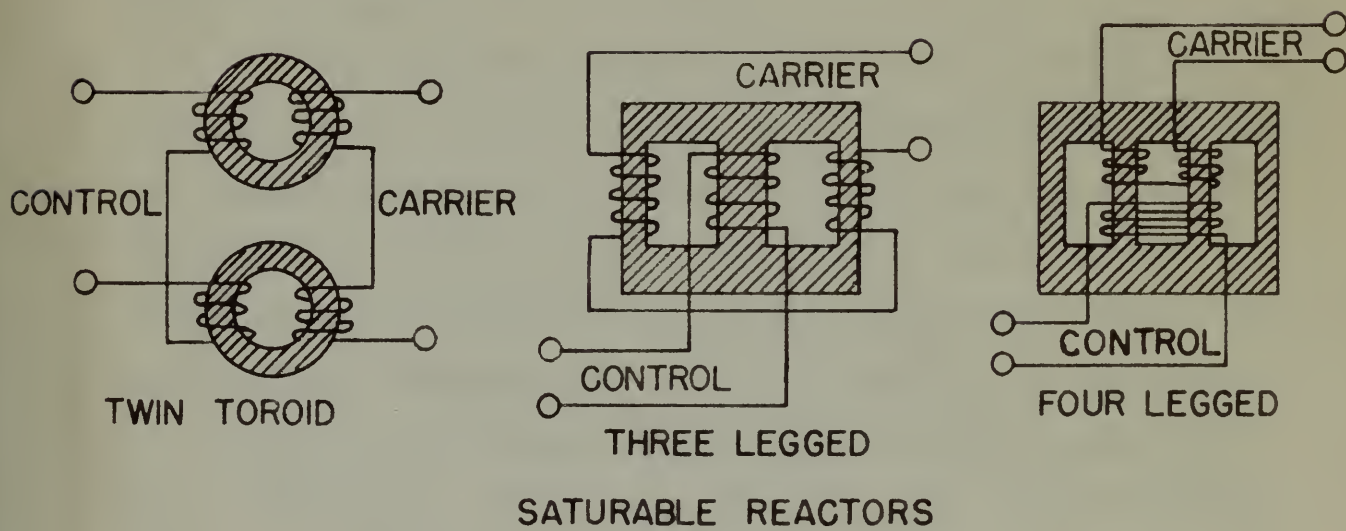


FIG. 2-3

general trend for a given alternating flux-density amplitude, and renders the above-cited criterion of practical interest. This criterion is particularly valuable as a guide to the metallurgist seeking to improve the properties of core materials for magnetic-amplifier design. Several ways of defining incremental permeability appear in engineering literature.^{1,2} It may be defined as

$$\mu_{ac} = \frac{B_{rms}}{H_{rms}} \quad (2-2)$$

in which the root-mean-square values of alternating induction and magnetization are taken. If one of these quantities is assumed sinusoidal, the other will not have a sinusoidal waveform because of the nonlinearity of the magnetization curve. Incremental permeability, therefore, is merely a definition which has meaning only in the sense in which defined, in this case being the ratio of the root-mean-square values of the alternating components of B and H.

The saturation flux-density is of importance in determining the relation between the cross-sectional core area, the carrier voltage, the carrier frequency, and the number of turns in the carrier winding. The carrier circuit power supply is a sinusoidal-voltage source which gives rise to an alternating sinusoidal flux in the cores provided the impedance of the input circuit of the induced even-harmonic voltages is kept low. Under this condition, the magnetization is natural. If the impedance of the input circuit to these

-
1. Lamson, H.W., "Alternating-Current Measurements of Magnetic Properties," I.R.E. Proc., 36, (1948), 266-277.
 2. M.I.T. Staff, "Magnetic Circuits and Transformers," (New York, John Wiley & Sons, 1943), 198.

General trend for a given alternating flux-density amplitude, and therefore the above-cited criterion of practical interest. This criterion is particularly valuable as a guide to the coefficient needed to improve the properties of core material for magnetic-coupled design. Several ways of obtaining instrumental permeability appear in engineering literature.^{1,2} It may be defined as

$$\mu_{ac} = \frac{W_{mag}}{W_{in}} \quad (2-5)$$

in which the post-mean-square values of alternating induction and magnetization are taken. If one of these quantities is assumed sinusoidal, the other will not have a sinusoidal waveform because of the nonlinearity of the magnetization curve. Instrumental permeability, therefore, is merely a definition which has meaning only in the sense in which defined, in this case being the ratio of the post-mean-square values of the alternating components of B and H .

The saturation flux-density is of importance in determining the relation between the cross-sectional core area, the carrier voltage, the carrier frequency, and the number of turns in the carrier winding. The carrier circuit power supply is a sinusoidal-voltage source which gives rise to an alternating sinusoidal flux in the cores provided the impedance of the input circuit of the induced cross-sectional voltage is kept low. Under this condition, the excitation is natural. If the impedance of the input circuit is chosen

1. Lamson, H.W., "Alternating-Current Measurements of Magnetic Properties," I.R.E. Trans., 56, (1948), 268-277.
2. K.I. Smith, "Magnetic Circuits and Transformers," (New York, John Wiley & Sons, 1947), 198.

even-harmonic voltages is high, the magnetization is constrained and the core flux is not sinusoidal.¹ The present studies involve only natural magnetization, a high-pass filter being shunted across the input windings such that it offers a high impedance to the signal-frequency currents and yet insures a low-impedance path for the even-harmonics of the carrier frequency. Under these conditions the flux in the core may be derived from the law of induction,

$$e = -N_2 \frac{d\phi}{dt} \quad (2-3)$$

$$\phi = \beta A = -\frac{1}{N_2} \int e \, dt \quad (2-4)$$

$$\beta = -\frac{1}{N_2 A} \int E \sin \omega_2 t \, dt \quad (2-5)$$

$$\beta = \frac{E}{\omega_2 N_2 A} \cos \omega_2 t \quad (2-6)$$

where

e is the voltage across the carrier winding of one reactor,

ϕ is the flux in webers,

β is the flux density in webers/sq. meter,

A is the cross-sectional core area in sq. meters,

ω_2 is the angular carrier frequency,

N_2 is the number of carrier turns on one core.

With zero direct magnetization and with the carrier windings connected in series, the alternating voltage across one reactor will very nearly equal one-half of the carrier voltage, the difference being a result of the voltage drop in the load caused by the exciting current. For best amplifier

1. Rex, H.B., "The Transductor," Instruments, 20, (1947), 1102-1109

performance, the flux density in the cores should be so adjusted that for no direct magnetization the flux-density amplitude just reaches the knee of the magnetization curve. If the flux-density amplitude is chosen too large, the exciting current will be excessive. If too small an amplitude is chosen, the linear portion of the modulation characteristic will be severely restricted. These effects may be seen by referring to the modulation characteristics shown in Chapters III and V. The circuit parameters which may be adjusted to achieve this condition, consistent with other considerations such as power output, space and weight, bandwidth, and linearity, are A , H_2 , E_2 , and ω_2 .

Because it is a variable reactance, the magnetic amplifier is ideally a lossless circuit in contrast with the electronic amplifier, which is a variable resistance, and inherently dissipative. For efficient operation, the core and copper losses in the magnetic amplifier should be minimized. Or, stated in another fashion, it is desirable to minimize the exciting current of the saturable reactors and to obtain a coil with as high a Q as possible. Exciting current which flows in the load when no signal is applied represents a useless component of load power. It has the further disadvantage of causing cumulative saturation when magnetic-amplifier stages are cascaded. If the demodulated exciting-current output of the first stage were fed to a second stage of amplification, a signal would flow in the second stage tending to saturate this stage even though no

performance, the first tendency is the more marked as the ad-
justment is made to the more marked the first tendency.
regulation just reaches the end of the regulation curve.
If the first tendency is marked as shown in figure, the ad-
justing element will be excessive. It too will be an element
is chosen, the linear portion of the regulation character-
istic will be severely restricted. These effects may be
seen by referring to the regulation characteristics shown
in Figures III and V. The amount of regulation which may be
adjusted is reduced this element, constant with the other
characteristics such as power output, speed and weight, load-
ing, and efficiency, etc., etc., etc.

Figure II is a typical characteristic, the regulation
characteristic is usually a constant element in adjustment. The
the characteristic amplifier, which is a variable resistance,
and inherently dissipative. For efficient operation, the
loss and output power in the amplifier should be
minimized. Or, stated in another fashion, it is desirable
to minimize the resulting output of the amplifier network
and to obtain a gain with as high a β as possible. Limiting
current which flows in the load when no signal is applied
represents a constant amount of load power. If the gain
factor decreases of amplification network, the
regulation-amplifier, the more the increased. If the regulation-
amplifier-current output of the first stage is fed to a
second stage of amplification, a signal which flows in the
second stage feeding to regulate this stage, the result, on

signal had been applied to the first stage. This cumulative-saturation effect in cascaded amplifiers must usually be compensated for by one method or another.¹

The core-loss is made up of two components, hysteresis and eddy-current loss. Hysteresis loss may usually be expressed by the relation

$$P_h = \eta V f \beta_m^n \quad (2-7)$$

where:

P_h is the hysteresis power loss,

n is the Steinmetz coefficient,

η is a constant of the material,

V is the core volume,

f is the alternating-current frequency,

β_m is the maximum flux density.

This formula is strictly applicable only to a core which is in the symmetrically cyclically magnetized condition.²

Since the magnetic amplifier is asymmetrically magnetized by virtue of the superposed direct magnetization, the validity of this formula applied to a magnetic-amplifier circuit is open to question. It serves to point out, however, that the hysteresis loss is a function of both the frequency and the quality of the core material. Since the carrier frequency will be limited by the available alternating-current source or by bandwidth requirements, hysteresis can be minimized by proper selection of core material. Another manner in which

-
1. Fitzgerald, A.S., "Magnetic Amplifier Circuits-Neutral Type," J.F.I., 244, (1947), 249-265.
 2. M.I.T. Staff, "Magnetic Circuits and Transformers," (New York, John Wiley & Sons, 1943), 129-130.

...has been applied to the first stage. This qualitative-
 induction effect is described and illustrated usually by
 accompanied for by the method as mentioned.

The core-loss is made up of two components,
 hysteretic and eddy-current loss. Hysteretic loss may
 usually be expressed by the relation

$$P_h = k_h f^n B_m^n \quad (2-7)$$

where:

- P_h is the hysteretic power loss,
- k_h is the Steinmetz coefficient,
- f is a constant of the material,
- B_m is the core volume,
- n is the eddy-current frequency,
- B_m is the maximum flux density.

This formula is strictly applicable only to a core which is
 in the magnetically saturated condition.

Since the magnetic coefficient is experimentally determined
 by virtue of the supposed direct magnetization, the validity
 of this formula applied to a magnetic-coefficient circuit is
 open to question. It serves to point out, however, that the
 hysteretic loss is a function of both the frequency and the
 quality of the core material. Since the carrier frequency
 will be limited by the existing alternating-current source
 or by mechanical requirements, hysteretic loss can be minimized by
 proper selection of core material. Another manner in which

1. Steinmetz, A. A. "Magnetic Coefficient Circuit-Theory"
 Trans. A.I.E.E., Vol. 1 (1907), 249-252.
 2. K. I. T. Smith, "Magnetic Coefficient and Transformation," (New
 York, John Wiley & Sons, 1931), 122-130.

hysteresis might be reduced is by making use of the Elmen effect.¹ If an electromagnetic device is excited by current of a given frequency, it is possible to reduce the hysteresis loop for the low frequency by the superposition of a second alternating-current of considerably higher frequency, the effect being that the high-frequency current supplies most of the hysteresis loss. This method of approach to the hysteresis-reduction problem, however, would require an additional alternating-current source of higher frequency than the carrier. If such additional windings were used, the available window space would be reduced. Effects of intermodulation also would have to be considered.

The other component of core loss is that of eddy-current dissipation. This may be written to a first approximation² as

$$P_e = k_e f^2 r^2 \beta_m^2 V$$

where

P_e is the eddy-current power loss,

k_e is a constant of the material,

f is the alternating-current frequency,

r is the lamination thickness,

β_m is the maximum flux density,

V is the core volume.

To minimize eddy-current loss it is apparent that the core should be kept small, the material should possess as high a

-
1. Elmen, G.W., "High-Frequency Detector," U.S. Patent 1,289,418, (1918).
 2. M.I.T. Staff, "Magnetic Circuits and Transformers," (New York, John Wiley & Sons, 1943), 132-138.

resistivity as possible consistent with the magnetic properties, the material should be as thinly laminated as practicable, and the interlaminar insulation should be efficient. Spirally-wound tapes of one-mil thickness are now commercially available, and the processing of even thinner tapes is in the developmental stage.

A further effect of the eddy currents is to distort the flux by reducing the field at the center of the laminations. This effect increases with frequency as the skin depth of the eddy currents decreases. This effect, known as eddy-current shielding, reduces the effective cross-sectional area of the core.

The shape of the magnetic circuit is, likewise, an important consideration. Currently used configurations include the twin-toroidal, the three-legged, and the four-legged saturable reactor units, illustrated in Figure 2-3. As previously discussed, the permeability must be maximized for optimum performance, and hence the presence of even a minute air gap must be avoided. This requirement indicates that dust cores or interleaved punchings should be avoided. Stacked annular laminations or spirally-wound tapes are preferred. Since it is desirable to keep the coupling between the windings as high as possible, the leakage flux must be minimized. The toroidal-core reactor, in which each winding is distributed over the entire periphery, offers the best solution to this problem. The advantage of the three and

possibly as possible consistent with the highest proper-
 time, the student should be fully instructed in proper-
 time, and the instruction should be as follows:
 actively-learned cases of well-known characters who have consistently
 available, and any discussion of such cases should be in the
 development stage.
 A further effort at the early stage is to discuss
 the time by relating the time to the action of the lesson-
 time. This effort involves with frequency as the early stage
 of the early stage involves. This effort, however, is only-
 current thinking, because the student is not-learned and
 of the case.
 The case of the student should be, however, as
 important considerations. Especially when considerations in-
 clude the two-learned, the three-learned, and the four-learned
 students teacher will, however, in Figure 2-3. As pro-
 viously discussed, the responsibility must be extended for
 optimum development, and hence the process of such a minute
 bit may not be avoided. This responsibility includes that
 group cases or individual cases should be avoided.
 Groups should involve of actively-learned cases and
 preferred. Since it is impossible to have the student learn
 the student as well as possible, the student should be
 minimal. The student's effort is to be made when
 is discussed over the entire period, where the best
 position is that should be. The student of the time and

four-legged reactors over the twin-toroidal type is that no fundamental or odd harmonic voltage is induced in the control windings, whereas in the latter type these voltages are actually induced, although bucked out by the connection of the two windings in series opposition. Since these induced voltages may be high enough under certain conditions to cause breakdown, the three or four-legged reactor may be preferred in some designs.

Magnetic materials which are now being used in magnetic-amplifier design include permnorm 5000-Z, Allegheny Electrical Alloy Steel #4750, mumetal, permalloy, hipernik, and silicon steel. The requisite magnetic properties are not ensured by alloy composition alone. Such metallurgical processes as grain orientation and magnetic annealing are most essential in determining the performance of the specimen. The most outstanding among these magnetic materials is permnorm 5000-Z, which is a very recent development of the Naval Ordnance Laboratory and attributed to G.W. Elmen and E.A. Gaugler.¹ Characterized by a maximum permeability of about 300,000 and a saturation flux density of about 15 kilogauss, the most distinctive feature is its almost rectangular hysteresis loop. From a performance viewpoint, silicon steel is the poorest choice for magnetic-amplifier reactors, although the cost is much less than the nickel alloys. The recent work of Minihara, however, indicates that much better performance may be obtained from silicon-iron, if properly

1. Rockett, Frank, "Improved Material for Magnetic Amplifiers," Electronics, (August 1948), 128-130.

treated.¹

Measurement of Magnetic Properties.

Four matched toroidal cores of Allegheny Electrical Alloy #4750 and four matched toroidal cores of Allegheny Mumetal were available for this study. The former type cores, shown in Figure 2-4, are spirally-wound metallic tapes of three mil thickness whose convolutions are separated by a magnesium-oxide insulating layer. The latter type cores, shown in Figure 2-5, are assembled from three-mil annular stampings. In order to evaluate magnetic circuit performance and to check the consistency of magnetic properties among the samples, the normal magnetization curve and typical hysteresis loops were measured with a Leeds and Northrup type P-2239-D ballistic galvanometer using standard techniques.² The results are shown in Figure 2-6 for the Allegheny Electrical Alloy #4750, and in Figure 2-7 for the Allegheny Mumetal. The approximately rectangular hysteresis loop of the Allegheny #4750 is contrasted with the more conventional curvature of the mumetal loop. This rectangular effect is achieved by reducing impurities to a minimum in the original melt, by annealing the spiral tapes in a hydrogen atmosphere, and by cooling slowly in a magnetic field applied in the direction of rolling. Ferromagnetic materials are well-known to be magnetically anisotropic, that is, they have a direction of easiest magnetization. For a single crystal of

1. Target Report K-34N (unclassified), U. S. Naval Technical Mission to Japan, "Magnetic Development in Japan during World War II, (1946).
2. Ricker and Tucker, "Electrical Engineering Laboratory Experiments," (New York, McGraw-Hill, 1940), 91-100.

THE UNIVERSITY OF CHICAGO

of the system and the system is not a simple system.

...and the ...

Copyright © 2000 by John Wiley & Sons, Inc.

RECEIVED AT THE OFFICE OF THE SECRETARY OF THE ARMY
WASHINGTON, D. C. 20315

by a commercial-grade label like 1407. The latter two dates,

gafompo lio-ando' woti basompo woti, 2-2 woti' ni mudi

—Laminated. In order to retain its strength during burning.

ADDRESS: 1000 N. 1st St., Suite 100, Phoenix, AZ 85004

Journal has been written through the year 2011 and 2012.

Copyright © 2000 by John Wiley & Sons, Inc.

Downloaded from ascelibrary.org by University of California - San Diego on 06/09/15

© 2007 Pearson Education, Inc. All rights reserved.

[illegible]

models. The second half presents the results from the

Importances were not significantly different in any of the comparisons.

Source: *Journal of the American Medical Association*, 1964, 191: 1000-1001.

will have to be a major consideration in the future.

... by answering the initial question in a hypothetical

ALL INFORMATION CONTAINED HEREIN IS UNCLASSIFIED EXCEPT WHERE SHOWN OTHERWISE

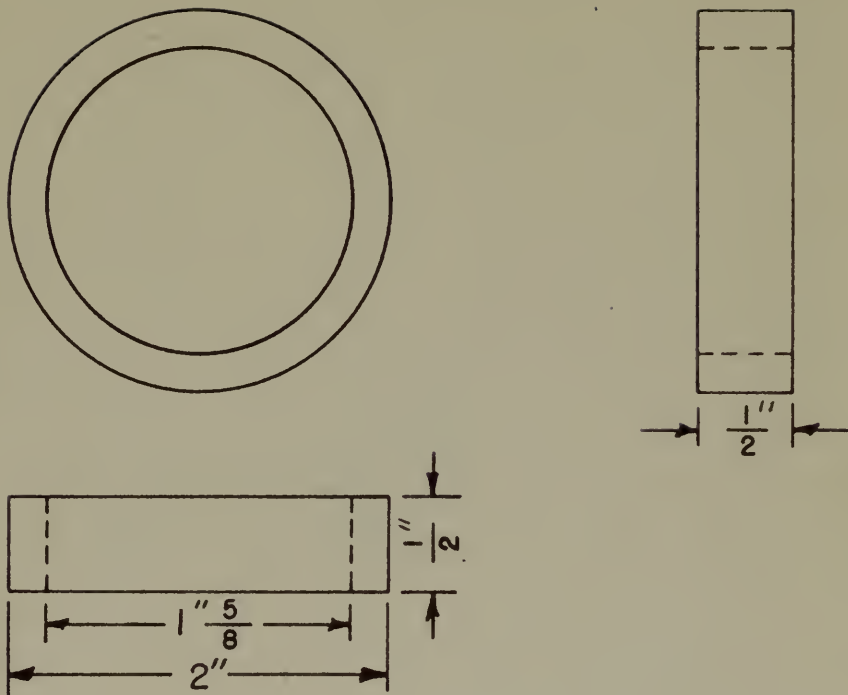
Elaboration of the following hypotheses is provided:

From the Department of Psychology, University of Illinois at Chicago, Chicago, Illinois 60607

14-00000

[illegible]

1001-10 (C-1), 1118-1120, 1121-1122, 1123-1124



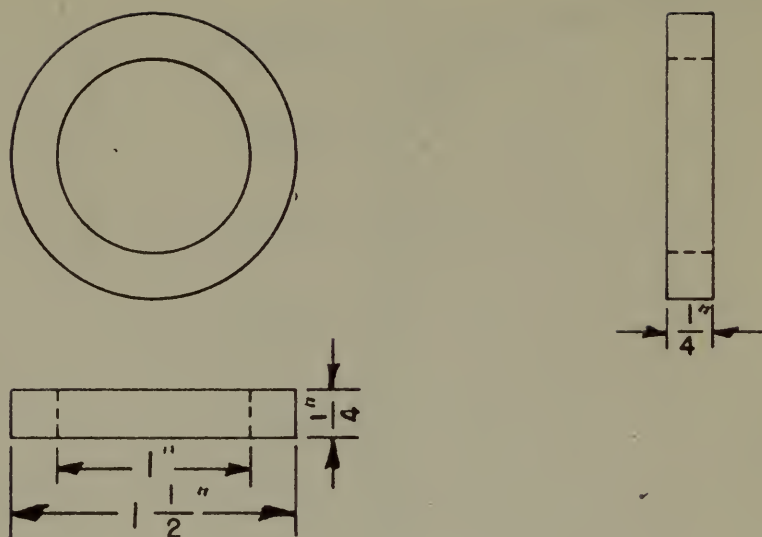
CORE CONSTRUCTION

48 SPIRALLY WOUND TURNS OF ALLEGHENY LUDLUM NO. 4750 ALLOY OF 0.003 INCHES THICKNESS. MAGNESIUM OXIDE INSULATION APPLIED DURING WINDING. CORES HEAT-ANNEALED IN HYDROGEN ATMOSPHERE BY NAVAL ORDNANCE LABORATORY OF WHITE OAK, MARYLAND.

WINDING DATA

7200 TURNS OF NO.30 FORMVAR ENAMELED COPPER WIRE, TAPPED EACH 200 TURNS.

FIG.2-4 SPECIFICATIONS FOR NO.4750 CORES



CORE CONSTRUCTION

70 LAMINATIONS OF ALLEGHENY LUDLUM MUMETAL
OF 0.003 INCHES THICKNESS, STACKED AS SHOWN.
HEAT TREATED BY ALLEGHENY LUDLUM.

WINDING DATA

2000 TURNS OF NO. 36 MAGNETIC WIRE,
TAPPED EACH 200 TURNS.

FIG.2-5 SPECIFICATIONS FOR MUMETAL CORES

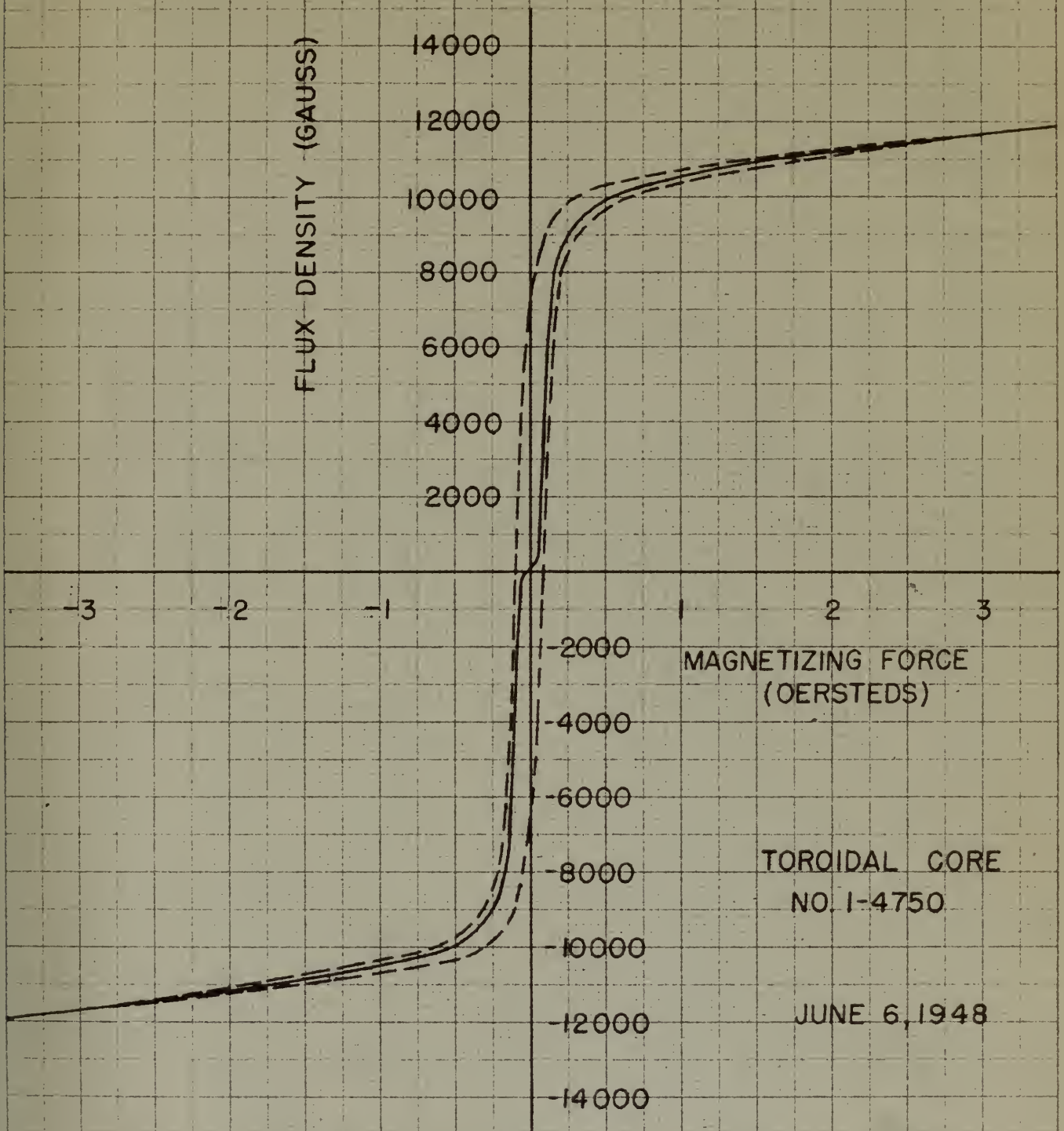
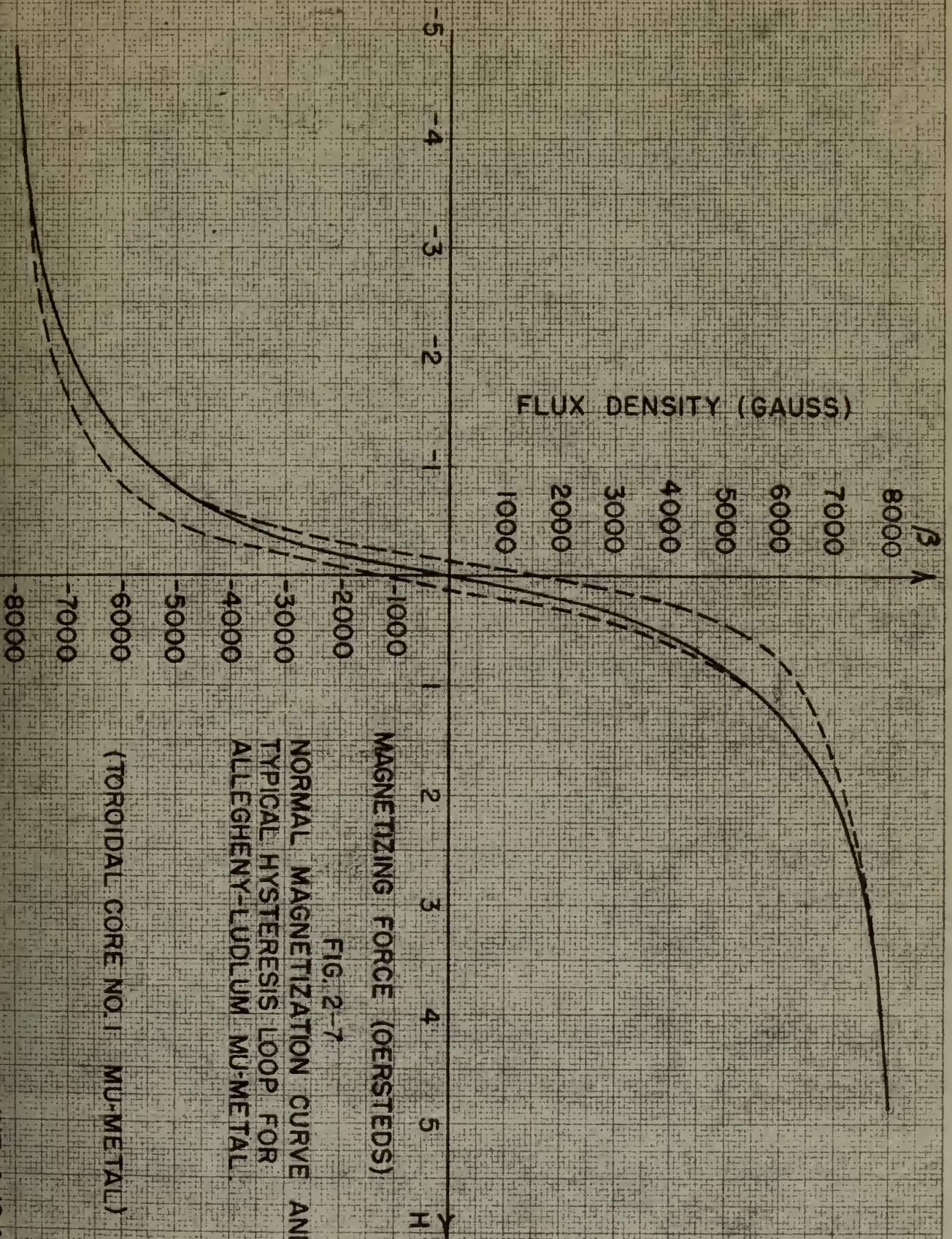


FIG.2-6 NORMAL MAGNETIZATION CURVE AND TYPICAL
HYSTERESIS LOOP FOR ALLEGHENY LUDLUM NO.4750
MAGNETIC ALLOY



MAGNETIZING FORCE (OERSTEDS)

FIG. 2-7

NORMAL MAGNETIZATION CURVE AND
 TYPICAL HYSTERESIS LOOP FOR
 ALLEGHENY-LUDLUM MU-METAL.

(TOROIDAL CORE NO. 1 MU-METAL)

fifty percent nickel-iron this is the crystal edge or the 1,0,0 axis. In this direction the electron spins can be aligned with minimum energy. In grain-oriented material, achieved by rolling in the 1,0,0 plane, the crystal lattice of the grains is aligned such that the entire mass exhibits magnetic behavior similar to a single crystal. The magnetic anneal, on the other hand, orients the domains by means of internal magnetostrictive forces without changing the crystal alignment. The effects of domain growth and rotation in the direction of an applied alternating magnetic field are thereby eliminated, leaving only the sudden 180-degree reversals of the electron spins as the direction of the field is changed. This results in a rectangular hysteresis loop. As seen from Figure 2-6, this effect is achieved to considerable degree in the Allegheny #4750 cores which were given a magnetic anneal by the Naval Ordnance Laboratory at White Oak, Maryland.

The consistency of the magnetic properties between the various samples of Allegheny #4750 was found to be quite good, as shown in Figure 2-8. The control of the complex metallurgical processes to produce uniformity in magnetic properties between different lots of material, or even between different samples of the same melt, is one of the most difficult problems in the manufacture of core materials. Lack of uniformity of the core properties in a magnetic amplifier will produce an unbalanced current-waveform.

fifty percent nickel-iron this is the expected value of the
 1,0,0 ratio. In this situation the electron spin can be
 aligned with nickel atoms. In this situation the
 observed by rotation is 1,0,0 ratio, the observed ratio
 of the spin is aligned with the nickel atom without
 magnetic behavior similar to a single crystal. The magnetic
 field, on the other hand, rotates the domain by means of
 induced magnetization forces without changing the crystal
 alignment. The effect of domain growth and rotation is
 the direction of an applied alternating magnetic field and
 thereby eliminated, leaving only the uniaxial 100-degree re-
 version of the electron spin as the direction of the field
 is changed. This results in a uniaxial structure.
 As seen from figure 1-4, this effect is observed in condis-
 tion center in the Alnico alloy some years ago given
 a reaction caused by the heat treatment laboratory at which
 the material was used.

The relationship of the magnetic properties between
 the various samples of Alnico alloy was found to be quite
 good, as shown in figure 1-5. The control of the complex
 metallurgical processes in various ways is required
 properties between different lots of material, or even
 between different samples of the same lot, is one of the
 most difficult problems in the manufacture of such materials.
 Lack of uniformity of the same composition is a serious ob-
 stacle will produce an unbalanced system.

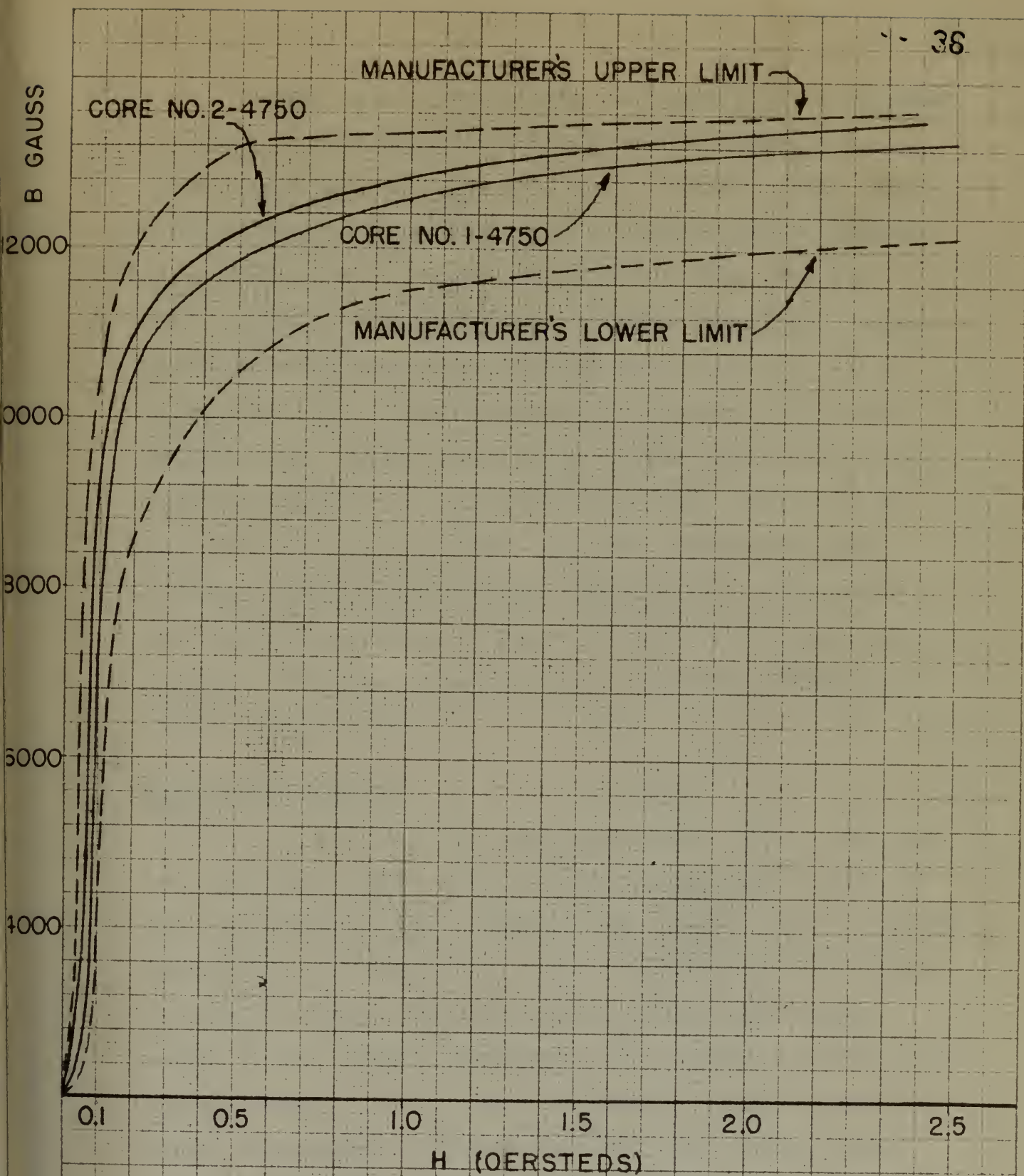


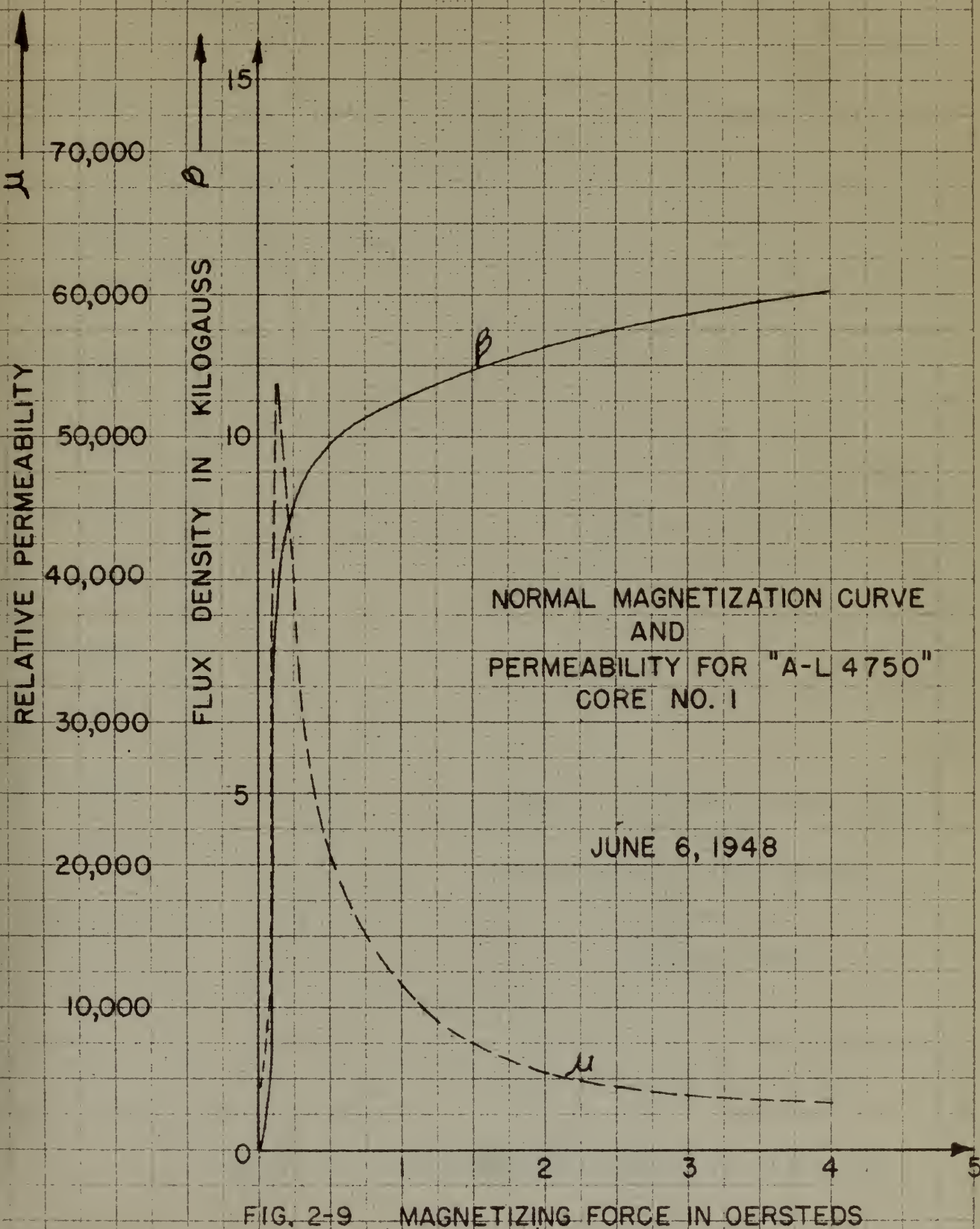
FIG. 2-8 COMPARISON OF MEASURED NORMAL MAGNETIZATION CURVES FOR CORES NO. 1-4750 AND 2-4750

The static permeability was computed as a function of direct magnetizing force and plotted in Figure 2-9 for a #4750 sample and in Figure 2-10 for a mumetal sample. The maximum static permeability of the Allegheny #4750 is seen to be much higher than for the mumetal. This indicates that a #4750 reactor would have a higher magnetizing inductance and a lower exciting current than one using mumetal. Furthermore, the rate of change of inductance with direct magnetization, being proportional to the slope of the permeability function, is observed to be much greater in the case of the Allegheny #4750. Magnetic amplifiers using Allegheny #4750 reactors would, therefore, be expected to give higher sensitivity. Since time limitations precluded a study of both type cores, those of Allegheny #4750 were chosen for this study.

Winding the Toroids.

A pair of #4750 cores were wound using a toroidal-core winding machine. When winding ferromagnetic cores of high permeability, it is necessary to enclose them in protective insulating containers, such as linen-covered bakelite, in order to relieve the cores of any mechanical strains caused by the winding procedure.¹ The containers should fit loosely enough to insure that no external magnetostrictive forces are applied, while at the same time fitting snugly enough to hold the cores securely in place. The application of a magnetic field to a ferromagnetic body disturbs the

1. Burton, E.T., "Transformer," U.S. Patent #1,880,412 (1930).



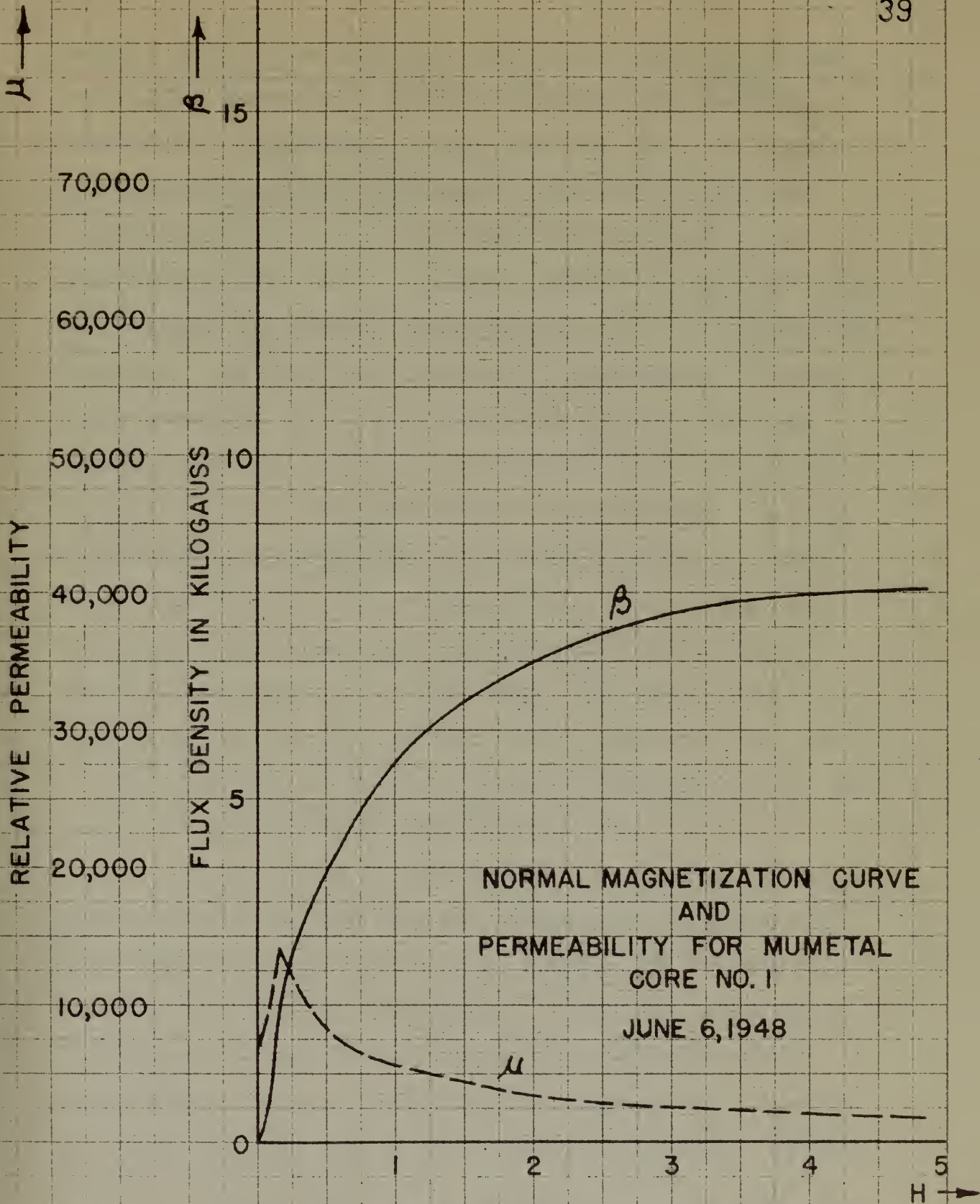


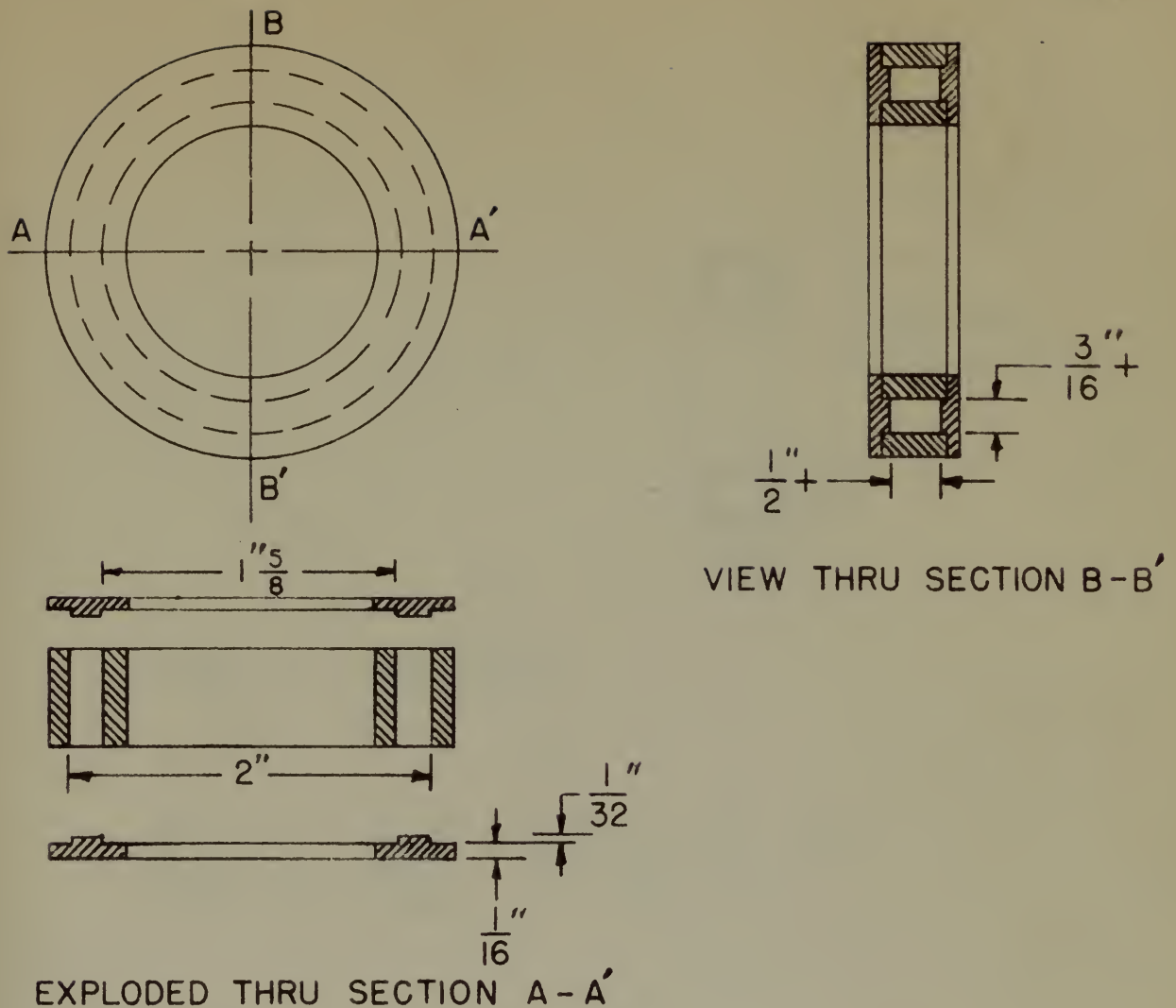
FIG. 2-10 MAGNETIZING FORCE IN OERSTEDS

balance between the internal electric and magnetic forces, and hence, changes the physical dimensions of the body. Conversely, a mechanical strain resulting from the application of an external mechanical stress will alter the magnetic properties. These effects are referred to as magnetostriction. It is apparent, therefore, that in order to preserve the magnetic properties of a given ferromagnetic specimen, provision must be made for the natural expansion and contraction of the core under the influence of magnetizing forces. Another consideration in the design of the containers is that they should be constructed as small as possible consistent with mechanical rigidity in order to prevent undue loss of window space. Accordingly, the Allegheny #4750 cores were provided with linen-covered bakelite boxes, shown in Figure 2-11. The mumetal cores were also provided with similar boxes, shown in Figure 2-12, in the event that it became feasible to include them in the study of magnetic-amplifier circuits.

The pair of Allegheny #4750 cores which had been selected for the study were each wound with 7200 turns of #30 Formvar enameled copper wire. During the winding process, caution must be exercised to prevent scraping the insulation and thereby short-circuiting adjacent turns. Shorted turns result in lowering the Q of the coil because of the copper loss caused by the high short-circuit currents induced. A low Q reduces the efficiency of the amplifier and increases the exciting current.

relation between the internal stimulus and response factors,
 and hence, through the physical characteristics of the body.
 Conversely, a mechanical stimulus resulting from the appli-
 cation of an external mechanical stimulus will alter the
 response properties. These effects are referred to as
 adaptation. It is important, therefore, that in order
 to preserve the response properties of a given transduction
 system, provision must be made for the removal of sensory
 and stimulation of the body under the influence of the
 external forces. Another consideration in the design of
 the equipment is that they should be constructed so as to
 be possible associated with mechanical stimuli in order
 to prevent undue loss of system space. Accordingly, the
 equipment should be provided with the following
 facilities: being shown in Figure 2-11. The control system
 were also provided with similar facilities shown in Figure 2-12.
 In the event that it becomes necessary to include more in the
 study of response-related phenomena.

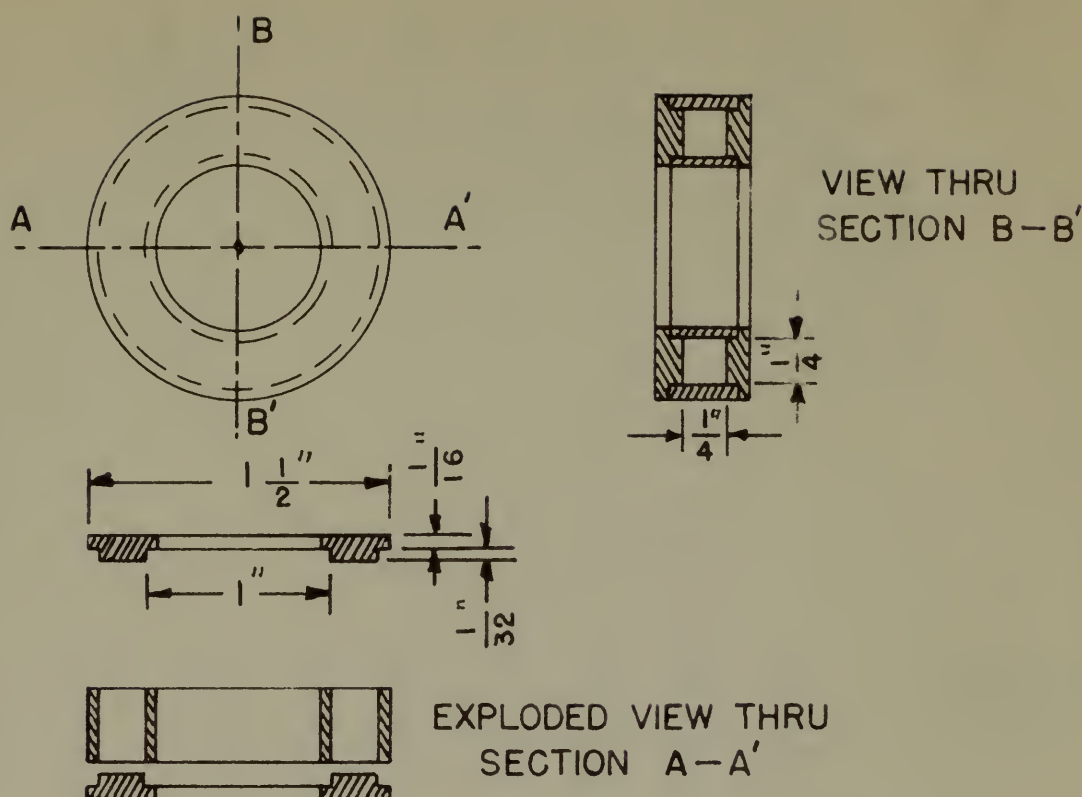
The part of the equipment which controls the response
 selected for the study were each shown with 7000 units of
 400 response channels output after being the stimulus
 process, control must be provided so that the response
 facilities and thereby short-circuiting the response system.
 Shorter time periods in response to the stimulus will be
 of the response time caused by the high short-circuit response
 interval. A low response time interval is the result
 and therefore the resulting response.



MATERIAL — LINEN COVERED BAKELITE

NOTE — INSIDE DIMENSIONS OF THE BOX ARE VERY SLIGHTLY GREATER THAN THE OUTSIDE DIMENSIONS OF THE CORE IN ORDER TO AVOID PLACING ANY MECHANICAL STRAIN ON THE CORES WHEN WINDINGS ARE APPLIED.

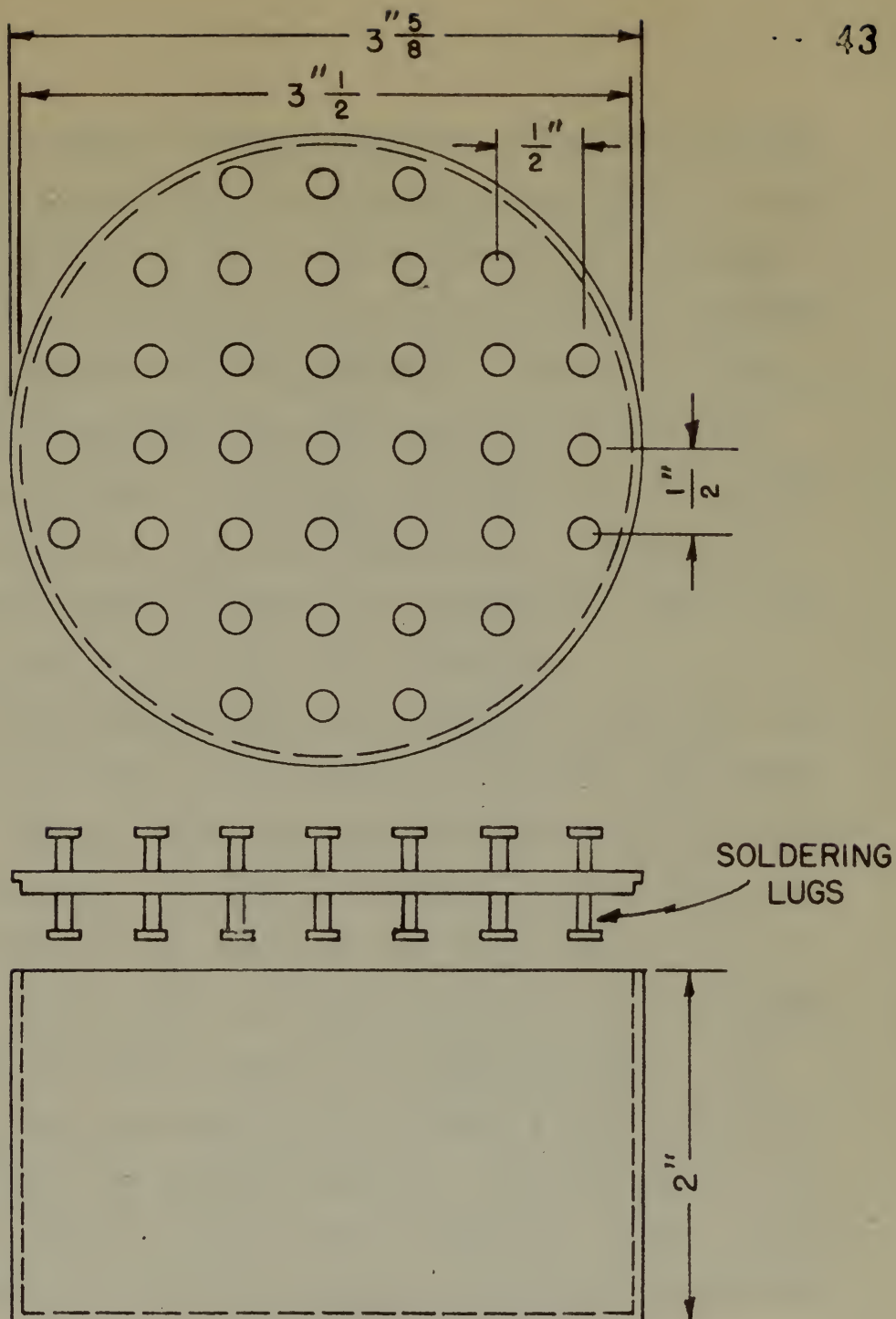
FIG. 2-II SPECIFICATIONS FOR SPECIAL INSULATING BOXES FOR NO. 4750 CORES



MATERIAL— LINEN COVERED BAKELITE

NOTE — INSIDE DIMENSIONS OF THE BOX ARE VERY SLIGHTLY GREATER THAN THE OUTSIDE DIMENSIONS OF THE CORE IN ORDER TO AVOID PLACING ANY MECHANICAL STRAIN ON THE CORES WHEN WINDINGS ARE APPLIED.

FIG.2-12 SPECIFICATIONS FOR SPECIAL INSULATING BOXES FOR MUMETAL CORES.



MATERIALS - LINEN COVERED BAKELITE AND STANDARD SOLDERING LUGS.

NOTE - THE 37 SOLDERING LUGS ARE CONNECTED TO TAPS ON THE CORE WINDINGS EVERY 200 TURNS, PROVIDING A CONVENIENT METHOD FOR CHANGING THE ARRANGEMENT OF THE VARIOUS WINDINGS.

FIG. 2-13 SPECIFICATIONS FOR TEST COIL BOXES.

To achieve maximum coupling between the various windings it is necessary to minimize leakage flux. It is desirable, therefore, that each of the several windings required by the amplifier design be distributed around the entire circumference of the toroid. In order to reduce capacitance parasitics, the cores should be wound such that large potential differences between turns are avoided whenever possible. The separation of the windings from the metallic cores by means of the protective boxes is an additional aid in reducing stray capacity.

All reactor windings were tapped every 200 turns in order to provide a ready means for changing the number of turns. Each finished coil was then enclosed in a cylindrical container. As shown in Figure 2-13, the covers of these containers were provided with 35 soldering lugs to which the various coil taps were attached in a systematic manner and labeled to permit easy identification. The coils were then impregnated with Ceresine Wax to improve the insulation and exclude moisture. The convenience with which the number of turns could be adjusted in the various windings was of great value while conducting experimental studies.

To achieve maximum coupling between the various
windings it is necessary to minimize leakage flux. It is
desirable, therefore, that most of the several windings
imposed by the various coils be distributed around the
entire circumference of the stator. In order to reduce
space harmonics produced, the stator should be wound with
three large potential differences between phases and should
whenever possible. The arrangement of the windings from
the metallic core of each of the stator coils is an
additional aid in reducing space harmonics.

All reaction windings are wound with 120 turns
in order to provide a fairly small for designing the number
of turns. Each finished coil was then wound in a split
stator consisting. As shown in Figure 2-11, the stator of
these coils was wound with 120 turns in a split
which the stator coil was wound in a split
manner and intended to provide a split stator. The
stator was then impregnated with lacquer and the
the insulation and winding material. The dimensions with
which the number of turns would be adjusted in the stator
windings was of great value with designing experimental
stator.

CHAPTER III

EXPERIMENTAL STUDIES OF THE BASIC CIRCUIT

Introduction

Although the basic magnetic-amplifier circuit, whose properties will be discussed in this chapter, is not the case of most practical interest, conclusions drawn from its study will provide certain fundamental concepts as to the static and dynamic performance of the magnetic amplifier. Because the problem of designing magnetically-biased saturable reactors involves nonlinear differential equations, the usual approach has been to approximate mathematically the empirically determined nonlinear functions, or to carry out experimental investigations on a prototype.^{1,2} A third method of attack, which to the knowledge of the authors has not yet been applied to the problem, is the solution of the system equations by machine methods. This latter method has been carried out using the M.I.T. Differential Analyzer Number One. The analytic results obtained therefrom are compared in Chapter IV with the experimental results set forth in the present chapter.

The Experimental Circuit

The basic magnetic-amplifier circuit studied in this chapter is the series-connected saturable reactor with a direct-current input and an alternating-current power

-
1. M.I.T. Staff, "Magnetic Circuits and Transformers," (New York, John Wiley & Sons, 1943), 199.
 2. Lamm, U., "The Transductor, A D.C. Pre-Saturated Reactor," (Stockholm, Esselte Aktiebolag, 1943).

CHAPTER III EXPERIMENTAL STUDY OF THE BASIC CIRCUIT

Introduction

Although the basic magnetic-coupled circuit, whose properties will be discussed in this chapter, is not the case of most electrical circuits, distinguished from them in its ability to provide certain fundamental concepts as to the static and dynamic behavior of the magnetic amplifier. Because the process of designing magnetically biased magnetic circuits involves nonlinear differential equations, the usual approach has been to approximate mathematically the magnetically nonlinear circuit functions, or to carry out experimental investigations in a prototype.^{1,2} A third method of attack, which is the knowledge of the circuit has not been applied to the problem, is the solution of the static equations by means of methods. This latter method has been carried out using the E.I. differential analyzer circuit. The analysis of the results obtained therefore the computer is carried out with the experimental results are given in the present chapter.

The Experimental Circuit

The basic magnetic-coupled circuit shown in this chapter is the series-connected magnetic transformer with a direct-current input and an alternating-current output.

1. W. I. Bell, "Magnetic Circuits and Transformers," (New York, John Wiley & Sons, 1947), 190.
2. L. L. L. The Transformer, A. C. The Transformer, (Brooklyn, Nassau Publishing, 1947).

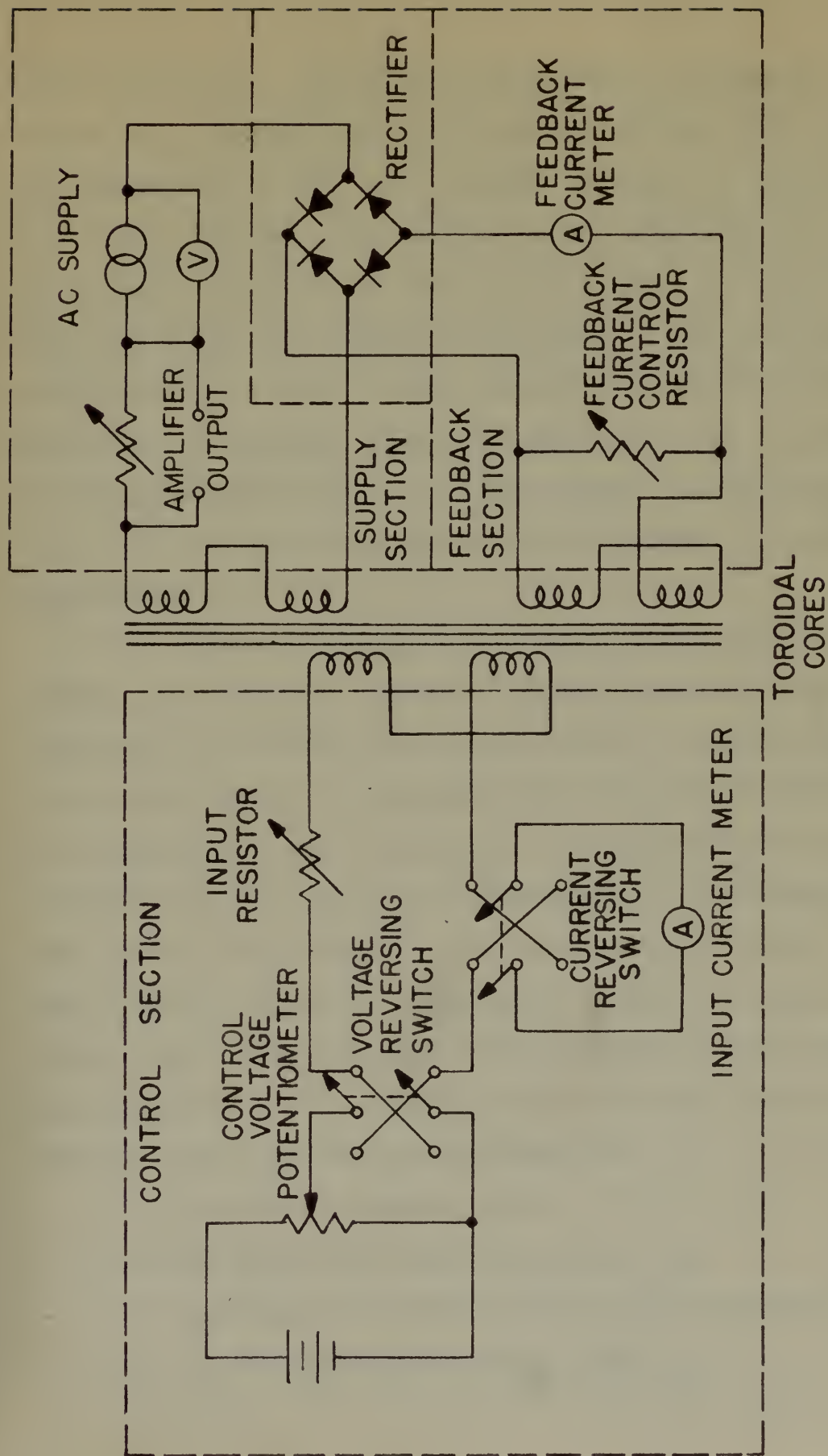


FIG.3-1 BREADBOARD CIRCUIT FOR EXPERIMENTAL MAGNETIC AMPLIFIER STUDIES.

supply and load. The circuit arrangement is shown in Figure 3-1, disregarding the feedback section, which is not applicable to the basic circuit and will be discussed in a later chapter. The purpose of the experimental study is to show the effect of the various circuit elements on both the static and dynamic performance of the magnetic amplifier with a view towards establishing certain design criteria. A thorough study of these effects in a prototype amplifier permits the use of model theory in scaling the size and winding data of the reactors to meet a specific application.

Because the magnetic amplifier is a nonlinear circuit, its behavior cannot be characterized by a system function, or transform, as in the case of a linear device. The system itself, more specifically the circuit inductance, is a function of the excitation. The nonlinearity is attributable to the saturation phenomenon of the ferromagnetic core which is prescribed by the magnetization curve. Since the amplifier cannot be analyzed as a linear system, this chapter will discuss the empirical approach, based upon experimental data, for optimizing the following excitation variables and lumped-circuit parameters:

1. the control current, i_1 ,
2. the control-circuit resistance, R_1 ,
3. the number of turns in the control winding, N_1 ,
4. the carrier-excitation voltage, E_2 .

mainly and used. The circuit arrangement is shown in Figure 3-1, illustrating the feedback action, which is not applicable to the basic circuit and will be discussed in a later chapter. The purpose of the experimental study is to show the effect of the various circuit elements on both the static and dynamic performance of the negative amplifier with a view towards establishing certain design criteria. A thorough study of these effects is a prerequisite amplifier permits the use of actual theory in testing the static and dynamic data of the response to meet a specific application.

Because the negative amplifier is a nonlinear circuit, its behavior cannot be described by a system function, or transfer, as in the case of a linear device. The system itself, more specifically the circuit impedance, is a function of the excitation. The nonlinearity is attributable to the nonlinear phenomenon of the ferroelectric core which is described by the magnetization curve. Since the amplifier cannot be analyzed as a linear system, this chapter will discuss the analytical approach, based upon mathematical form, for obtaining the following excitation variables and input-output parameters:

1. The control current, i_c
2. The control-output resistance, R_o
3. The number of turns in the control winding, N_c
4. The output-resistance voltage, V_o

5. the carrier-excitation frequency, f_2 ,
6. the load resistance, R_2 , and
7. the number of turns in the carrier winding, N_2 .

The response variable will be considered to be the carrier current, i_2 , from which the ampere-turn sensitivity, the power output, and power gain can be readily computed.

Static Performance of the Basic Circuit.

The modulation characteristic, or functional relationship between the control current and the average-carrier current, is the most useful transfer curve for describing the static behavior of the magnetic amplifier. This characteristic is more significant when average output ampere-turns are plotted as a function of input ampere-turns, giving the relationship between control and carrier magnetizing forces. For the ideal case of infinite initial permeability, this relationship would be a straight line through the origin having a forty-five degree slope; that is, the average carrier ampere-turns would equal the control ampere-turns within the amplifying range of control excitation. In the practical case, this relationship is closely approximated and has been discussed in detail by Buchhold.¹ Because of the exciting current which is required to furnish the no-load core losses in the practical amplifier, the average carrier ampere-turns exceed the control ampere-turns in the lower control range, whereas in

1. Rex, H.B., "The Transductor," Instruments, 20, (1947), 1102-1109.

the higher control range they fall off and become less than the control ampere-turns. A modulation characteristic is plotted in Figure 3-2 for constant voltage across the reactors, a case of no practical interest because it implies the absence of load resistance. The manner in which this characteristic arises is explained by reference to Figure 3-3, which shows the relation between the flux and the ampere-turns in the cores. Only the action of one core need be given. As long as the peak excursions of the flux lie below the saturation line, the ampere turns are small and essentially constant in amplitude, as shown by Figure 3-3, (1) and (2). As the peak flux-excursions begin to exceed the saturation line, linear amplifying action takes place. The end of the linear range, point (4) of Figure 3-2, occurs when the direct flux biases the alternating flux to the saturation line shown in Figure 3-3 (5). As the input increases beyond this point, the characteristic begins to flatten out, becoming horizontal when the direct flux is so large that the entire excursion of the alternating flux lies above the saturation line shown in Figure 3-3 (5). Regardless of further increases of the control current, the carrier current will remain constant by virtue of the fact that the core is now completely saturated at all times with respect to the alternating components.

In the practical magnetic amplifier the voltage across the reactor is not constant, but falls off as the voltage-drop across the load resistor rises with increasing

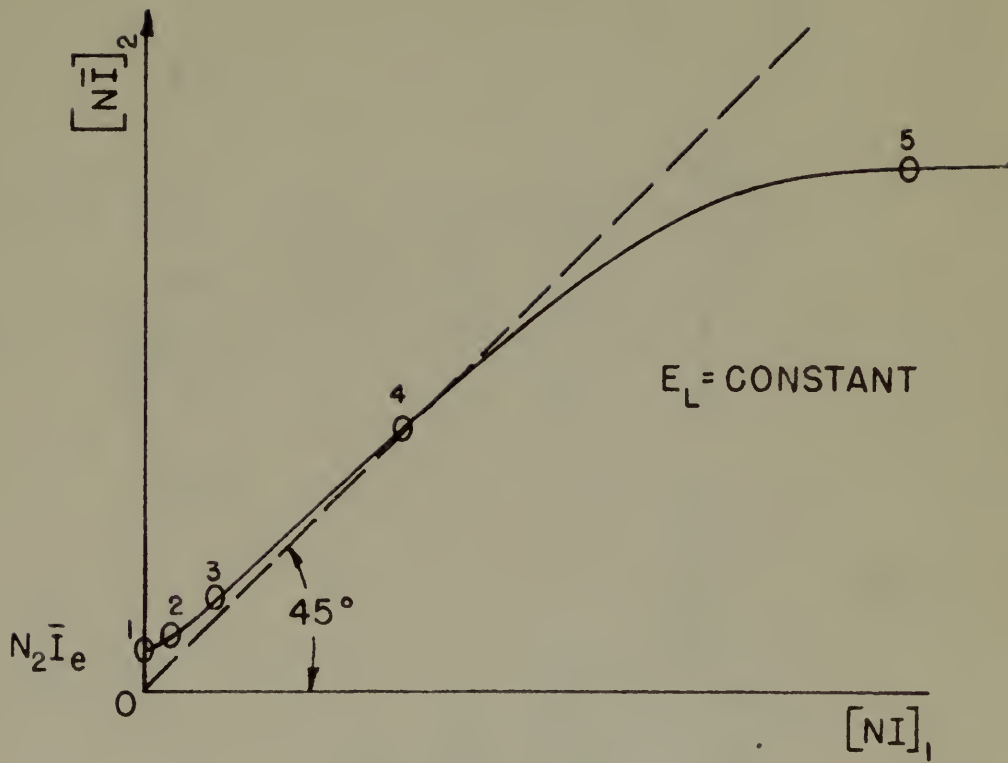


FIG. 3-2 MODULATION CHARACTERISTIC.

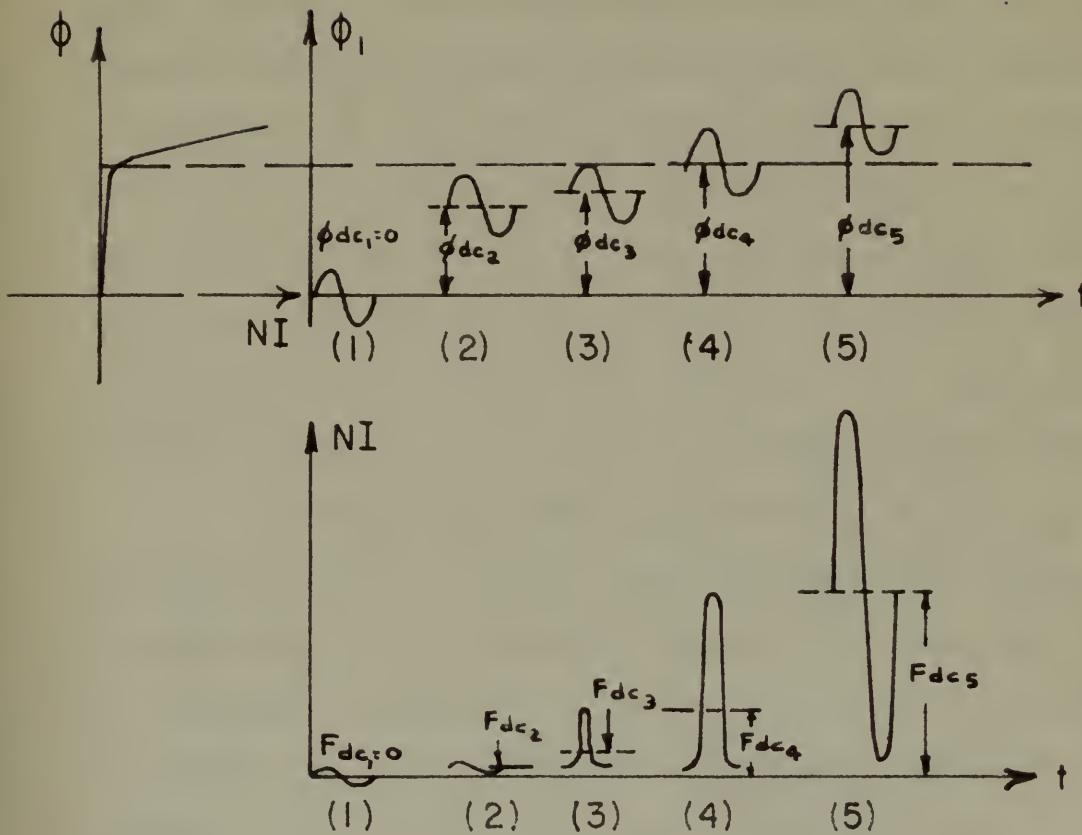


FIG.3-3 FLUX AND MAGNETIZING FORCE FOR VARIOUS VALUES OF DIRECT EXCITATION.

carrier current, and hence the actual modulation characteristic flattens out somewhat sooner. The observed effect of the circuit variables upon the modulation characteristic will be taken up and explained individually in order. A Western-Electric type 142A amplifier fed by a Hewlett-Packard model 205A4 audio-frequency generator was used as the carrier-power supply. The load voltage was read from a Hewlett-Packard model 400A vacuum-tube voltmeter whose deflection is proportional to the average value of the voltage although calibrated to read the root-mean-square value of a sine wave. The average value of the carrier current was then computed from Ohm's law, knowing the value of the load resistance and the average value of the load voltage. The value of input current was read directly from a direct-current milliammeter.

The control circuit parameters, N_1 and R_1 , were observed to have no effect upon the modulation characteristic. R_1 was taken from a minimum value of 165 ohms, the resistance of the input winding, to a maximum value of about 10,000 ohms. No effect would be anticipated unless the impedance of the control circuit to the induced even-harmonic carrier currents is high. If, for example, a choke coil were placed in series with the control windings, the flow of the even harmonics would be restricted and the magnetization of the cores would be constrained. The flux, as explained by Buchhold,¹ would no longer be sinusoidal and the waveform of the carrier current would be altered. To ensure natural magnetization, and

1. Rex, H.B., "The Transducer," Instruments, 20, (1947), 1102-1109.

driving current, and hence the actual conduction character-
 istics of the circuit are not affected. The circuit is
 of the circuit variables when the conduction characteristics
 will be taken up and explained later in detail. A
 vacuum-tube type 12A6 amplifier fed by a heater-
 model 30A6 multi-frequency generator was used as the carrier-
 power supply. The load voltage was read from a Hewlett-
 Packard model 800A vacuum-tube voltmeter whose deflection is
 proportional to the average value of the voltage waveform
 delivered to load the root-mean-square value of a sine wave.
 The average value of the carrier current was then computed
 from Ohm's law, knowing the value of the load resistance and
 the average value of the load voltage. The value of input
 current was read directly from a current-voltage milliammeter.
 The control circuit parameters, R_1 and R_2 , were
 observed to have an effect upon the conduction characteristics.
 R_1 was taken from a minimum value of 100 ohms, the resistance
 of the input winding, to a maximum value of about 10,000 ohms.
 No effect could be anticipated unless the impedance of the
 control circuit is the loaded even-harmonic carrier circuit
 is high. If, for example, a choke coil were placed in series
 with the control winding, the flow of the even harmonics would
 be restricted and the magnification of the carrier would be
 diminished. The flow, as explained by equation (1), would no
 longer be sinusoidal and the waveform of the carrier current
 would be altered. To ensure network magnification, and

sinusoidal flux, a capacitor should be shunted across the control-current windings of a magnetic amplifier. This filter should present a low impedance to the even-harmonic frequencies of the carrier, and a high impedance to the signal frequencies.

While the control circuit has little effect upon the modulation characteristic, the carrier-circuit variables were all observed to have quite a pronounced effect. The effect of the load resistor, R_2 , will first be considered.

The effect of R_2 is to reduce the alternating voltage which appears across the carrier windings of the saturable reactors as a result of the voltage drop in the load, thereby reducing the magnitude of the alternating-flux amplitude in the cores. If, for the moment, the carrier current is assumed sinusoidal, an assumption which is quantitatively invalid because of the high odd-harmonic content of this current, linear-impedance concepts, based on sinusoidal excitation and response, may be used to give a qualitative picture of the effect of load resistance on the modulation characteristic. Figure 3-4 may be taken as the equivalent carrier circuit where L_2 is an inverse function of the control current. The core losses are lumped into R_2 for convenience. The ratio of the voltage, E_L , across the reactors to the carrier-supply voltage, E_2 , is obtained as follows:

arranged that a separate should be printed as soon as the
 general-purpose printing of a separate edition. This
 latter would serve as the basis for the two-volume
 production of the series, and a high impression for the
 single production.

While the general should be the effect upon
 the production characteristics, the production characteristics
 were all intended to have a high impression effect. The
 effect of the low volume, for which first to consider.
 The effect of p_1 is to reduce the amount of
 volume which appears across the entire volume of the
 entire volume as a result of the volume being in the
 low, thereby reducing the amount of the entire volume.
 The volume in the case, p_1 , is the amount, the
 entire volume is reduced, in the entire volume which
 is the entire volume of the entire volume, and
 the entire volume, linearly, is the entire volume, and
 on the entire volume and volume, may be used to give
 a relative picture of the effect of the entire volume on
 the entire volume. Figure 1-1 may be taken as
 the entire volume, which is an entire volume.
 The entire volume, the entire volume, the entire volume are
 into p_1 for the entire volume. The entire volume, p_1 ,
 across the entire volume, the entire volume, p_1 , is
 the entire volume.

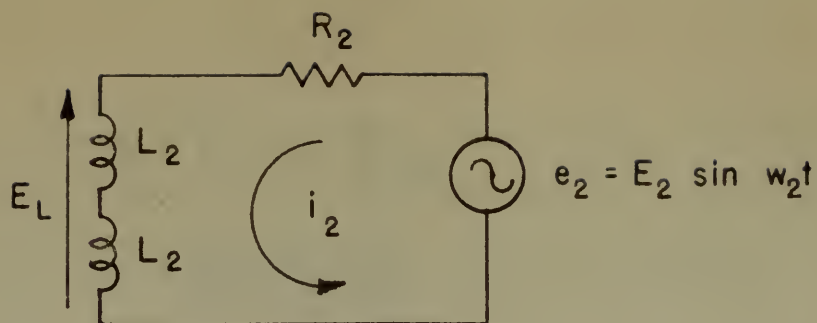
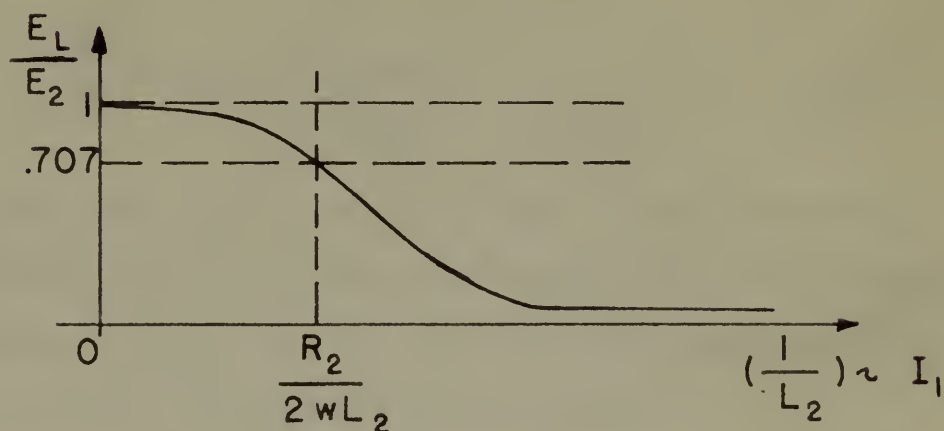
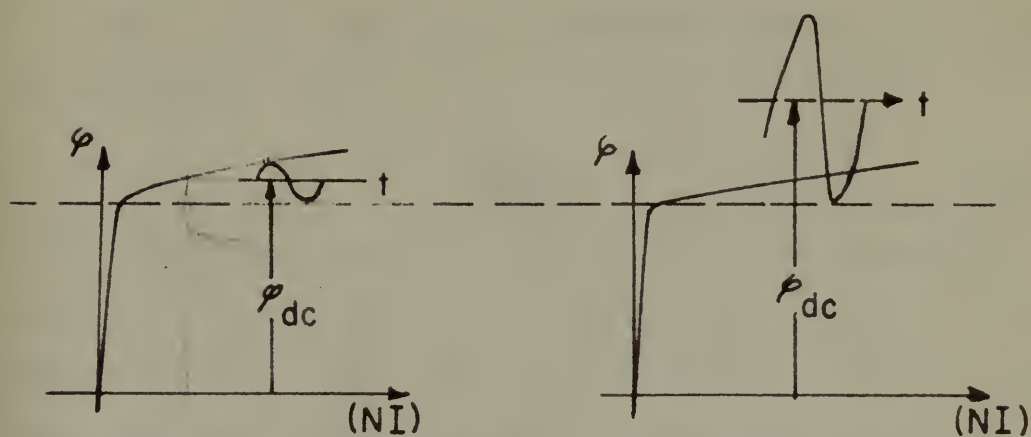


FIG. 3-4 EQUIVALENT CARRIER CIRCUIT

FIG. 3-5 $\frac{E_L}{E_2}$ AS A FUNCTION OF I_1 

(a) SMALL FLUX AMPLITUDE. (b) LARGE FLUX AMPLITUDE.

FIG. 3-6

$$E_L = I_2 X_2 = \frac{E_2}{Z_2} X_2 \quad (3-1)$$

$$= \frac{E_2 (2j\omega_1 L_2)}{R_2 + 2j\omega_1 L_2} \quad (3-2)$$

$$\frac{E_L}{E_2} = \frac{1}{1 - j\left(\frac{R_2}{2\omega_1 L_2}\right)} \quad (3-3)$$

$$\left| \frac{E_L}{E_2} \right| = \frac{1}{\sqrt{1 + \left[\frac{R_2}{2\omega_1 L_2} \right]^2}} \quad (3-4)$$

Since, for zero I_1 , L_2 is very large, ideally infinite, the ratio is initially unity, or nearly so. As I_1 increases and L_2 decreases, the ratio falls off and approaches zero for small L_2 . The ratio is down 3 db when

$$\frac{R_2}{2\omega_1 L_2} = 1 \quad (3-5)$$

The E_L/E_2 function is plotted in Figure 3-5. For higher load resistances, therefore, the ratio drops from unity at a higher rate. Since the alternating flux-density amplitude is given by

$$\beta = \frac{\frac{1}{2} E_L}{\omega_2 N_2 A} \quad (3-6)$$

the alternating component of core-flux experiences the same rate of change of amplitude with I_1 as does the voltage E_L . The modulation characteristic, therefore, tends to flatten out for lower values of input ampere-turns as the R_2 is made larger. This effect may be pictured physically by reference to Figure 3-6, from which it is seen that a smaller value of direct flux is needed to bias the entire alternating flux

(3-1)

$$L_1 = L_2 \times \frac{L_2}{L_1}$$

(3-2)

$$= \frac{L_2 (L_2 + L_1)}{L_1 + L_2}$$

(3-3)

$$\frac{L_1}{L_2} = \frac{1}{1 - \frac{L_2}{L_1}}$$

(3-4)

$$\left| \frac{L_1}{L_2} \right| = \frac{1}{\sqrt{1 + \left(\frac{L_2}{L_1} \right)^2}}$$

Since, for zero L_1 , L_2 is very large, ideally infinite, the ratio is initially unity, as nearly so. As L_1 increases and L_2 decreases, the ratio falls off and approaches zero for small L_2 . The ratio is then 1/2 when

(3-5)

$$\frac{L_2}{L_1} = 1$$

The L_1/L_2 function is plotted in Figure 3-5. For higher load impedances, therefore, the ratio drops from unity at a higher rate. Since the alternating flux-density amplitude is given by

(3-6)

$$\frac{1}{2} \frac{L_1}{L_2} = \frac{1}{2} \frac{L_1}{L_2}$$

the alternating component of core-flux experiences the same rate of change of amplitude with L_1 as does the voltage E_1 . The modulation characteristic, therefore, tends to flatten out for lower values of input square-wave as the L_1 is made larger. This effect may be pictured physically by reference to Figure 3-6, from which it is seen that a smaller value of direct flux is needed to bias the entire alternating flux

above the saturation line with a small flux amplitude as compared with a large flux amplitude. This effect was observed experimentally, as shown by Figures 3-7, 3-13 and 3-18.

The manner in which E_2 affects the modulation characteristic can best be explained by again referring to the ratio E_L/E_2 which is expressed by Equation 3-4 and shown in Figure 3-5. E_2 does not affect the rate at which E_L falls off with I_1 , but does control its magnitude. Thus, for higher E_2 there exists a larger core-flux amplitude from the Equation 3-6, and the modulation characteristic tends to flatten out for higher values of control ampere-turns. This effect was observed as shown in Figures 3-8, 3-14 and 3-17. Another effect which should be pointed out is that if, with no control current applied, the value of the alternating-flux amplitude is such that it exceeds the saturation line, an excessive exciting current is drawn. As stated in Chapter II, the flux should be so adjusted that it just fails to exceed the saturation line when no control current is applied. A good illustration of excessive exciting current as a result of incorrect alternating-flux adjustment is the $E_2 = 80$ volts (rms.) curve at a carrier frequency of 100 cycles per second, shown in Figure 3-14.

Unlike the effects of E_2 and R_2 , the carrier frequency, f_2 , affects both the core flux and the carrier-circuit impedance. The flux-density amplitude is seen from Equation

above the saturation line with a small flux amplitude as compared with a large flux amplitude. This effect was observed experimentally, as shown by figures 3-7, 3-13 and 3-18.

The reason in which E_2 affects the modulation characteristic can best be explained by again referring to the ratio E_2/E_1 which is expressed by equation 3-4 and shown in figure 3-5. E_2 does not affect the rate at which E_1 falls off with I_1 , but does control its magnitude. Thus, for higher E_2 there exists a larger core-flux amplitude from the equation 3-5, and the modulation characteristic tends to flatten out for higher values of control voltage. This effect was observed as shown in figures 3-6, 3-16 and 3-17. Another effect which should be pointed out is that E_2 , when in control current applied, the value of the saturating-flux amplitude is such that it exceeds the saturation line, an excessive exciting current is drawn. As stated in Chapter II, the flux should be so adjusted that it just fails to exceed the saturation line when no control current is applied. A good illustration of excessive exciting current as a result of increased saturating-flux adjustment is the $E_2 = 50$ volts (var.) curve at a carrier frequency of 100 cycles per second, shown in figure 3-18.

Unlike the effects of E_1 and E_2 , the carrier frequency, f_c , affects both the core flux and the carrier-current amplitude. The flux-density amplitude is seen from equation

3-6 to be inversely proportional to the frequency. If the frequency is raised, the flux-density amplitude is lowered and the modulation characteristic would be expected to flatten out for lower I_1 by reason of the effect pointed out in Figure 3-6. The E_L/E_2 ratio, however, would fall off at a slower rate for the higher frequency tending to counteract the former effect. Experimental results plotted in Figure 3-9 show that the lowering of the flux-density amplitude is the more significant effect, since the modulation characteristics flatten out sooner at higher frequencies.

The final system parameter to be considered is N_2 . Similar to the effect of f_2 , N_2 affects both the core flux and the carrier-circuit impedance. A larger number of turns would decrease the core flux, as shown by Equation 3-6, and the modulation characteristic would tend to flatten out at a smaller value of I_1 from this consideration. The way in which N_2 affects the carrier-circuit inductance is indicated by the relation

$$L_2 = k N_2^2 \mu_{ao} \quad (3-8)$$

In the case of the frequency effect, the reactance went up directly with the frequency, whereas with N_2 , the reactance goes up as the square of the number of turns. The E_L/E_2 ratio has considerably more effect here than in the case of the frequency variation. For larger N_2 the effect of this ratio is to cause the modulation characteristic to flatten out at higher values of I_1 . These two effects, as in the case of the frequency variation, tend to oppose one another,

It is to be inversely proportional to the frequency. If the frequency is raised, the flux-density amplitude is lowered and the modulation characteristics would be expected to flatten out for lower f by reason of the effect pointed out in Figure 3-6. The f ratio, however, would still be at a lower rate for the higher frequency range as compared to the lower effect. Experimental results plotted in Figure 3-7 show that the flattening of the flux-density amplitude is not very significant effect, since the modulation characteristics flatten out more at higher frequencies. The flux density parameter to be considered is f . Similar to the effect of f , f affects both the flux and the carrier-amplitude dependence. A larger increase of f would increase the flux, as shown by equation 3-6, and the modulation characteristics would tend to flatten out at a smaller value of f for the same reason. The way in which f affects the carrier-amplitude dependence is indicated by the relation

$$f = \frac{1}{2\pi} \frac{d\phi}{dt} \quad (3-8)$$

In the case of the frequency effect, the response was directly with the frequency, whereas with f , the response goes up as the square of the number of turns. The f ratio has essentially no effect here in the case of the frequency variation. For larger f , the effect of this ratio is to cause the modulation characteristics to flatten out at higher values of f . These two effects, as in the case of the frequency variation, tend to oppose the carrier,

but because of the squared relation there is an optimum value of N_2 to be sought such that the modulation characteristic follows along a forty-five degree slope as long as possible before tending to flatten out. The fact that an optimum N_2 exists can be seen by examination of Figures 3-10, 3-11, 3-12, 3-15 and 3-18.

From this qualitative discussion it is seen that two factors must be kept in mind when predicting a modulation characteristic, namely: the initial value of the flux-density amplitude and the rate at which this amplitude falls off with respect to increasing control current. As stated at the beginning of this discussion, these concepts are only of a qualitative nature because the impedance concept itself is based upon the assumption that the carrier current is sinusoidal, an assumption which is highly approximate, as can be seen by reference to the actual waveforms encountered, as illustrated in Chapter IV.

From a knowledge of the modulation characteristics of a given circuit, the values of power output and power gain may be obtained directly by computation. Since the exciting current which flows in the load when no signal is applied does not represent useful power, it is usually compensated for in the practical case by one method or another.¹ If I_e represents the root-mean-square value of the exciting current, the power output is then obtained from the expression

1. Fitzgerald, A.S., "Magnetic Amplifier Characteristics - Neutral Type," J.F.I., 244, (1947), 415-439.

but because of the various relations there is an extreme value
 at 20 to be sought and the condition characteristic
 follows along a path of values along the line as possible
 before reaching the limit. The limit is an optimum
 value can be seen by examination of figures 1-10, 1-11,
 1-12, 1-13 and 1-14.

From this qualitative discussion it is seen that
 the factors must be kept in mind when considering a system
 from characteristic, namely: the initial value of the line
 density, amplitude and the rate at which the density falls
 off with respect to increasing angular distance. As shown
 at the beginning of this discussion, the rate of the
 rate of a qualitative nature shows the important concept
 itself is based upon the assumption that the system is
 is assumed, or assumption which is highly complex, as
 can be seen by reference to the actual system considered,
 as illustrated in Chapter IV.

From a knowledge of the qualitative characteristics
 of a given system, the value of peak density and power
 gain may be obtained directly by computation. Since the
 action current which flows in the line when an signal is
 applied does not represent actual power, it is usually con-
 sidered for in the practical case by the ratio of amplitude.
 It represents the root-mean-square value of the voltage
 current, the value which is then obtained from the equation

$$I = \frac{P}{V} \quad \text{or} \quad V = \frac{P}{I} \quad \text{or} \quad I = \frac{P}{V}$$

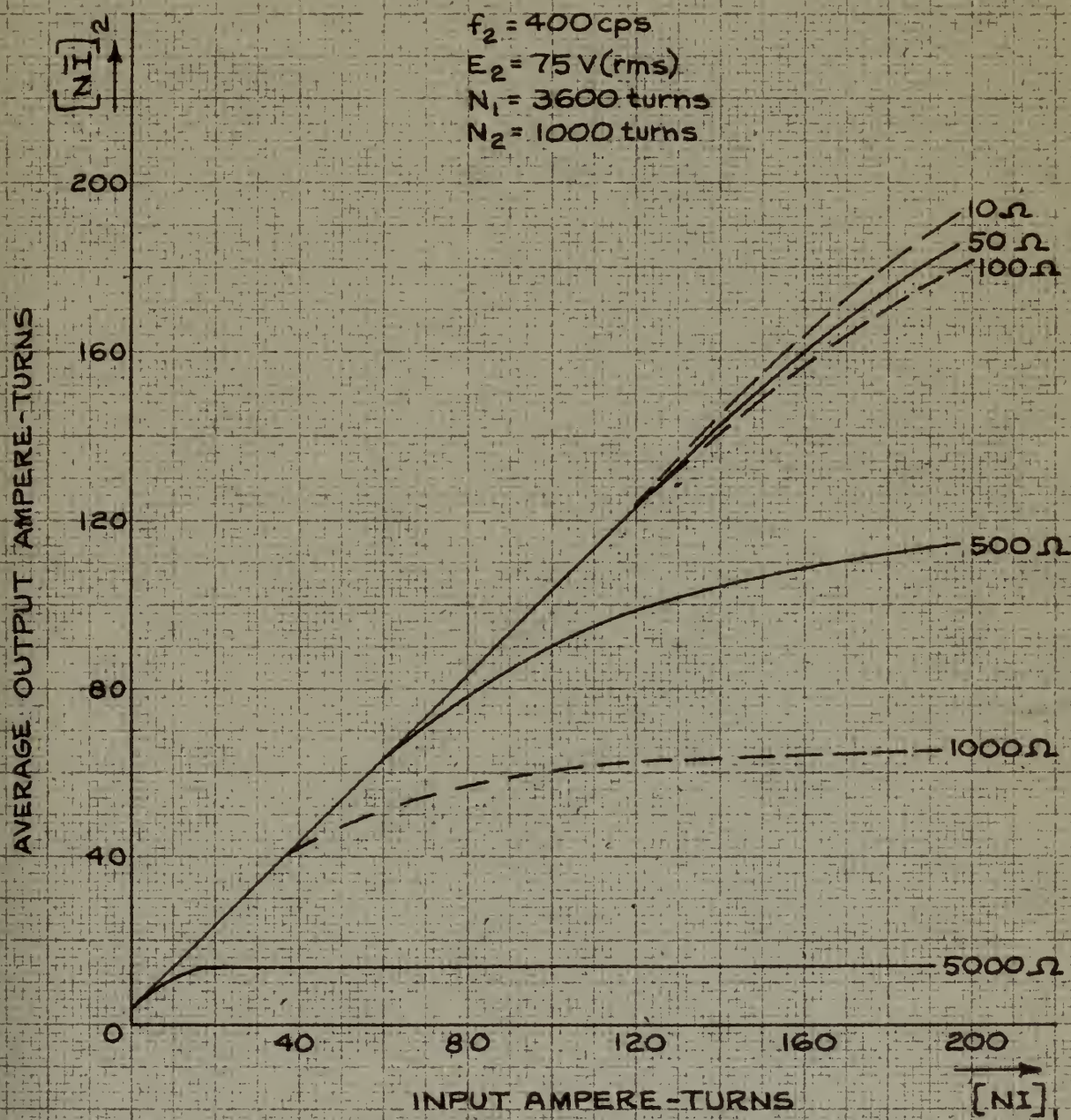


FIG. 3-7 MODULATION CHARACTERISTIC OF THE BASIC MAGNETIC AMPLIFIER SHOWING EFFECT OF LOAD RESISTANCE.

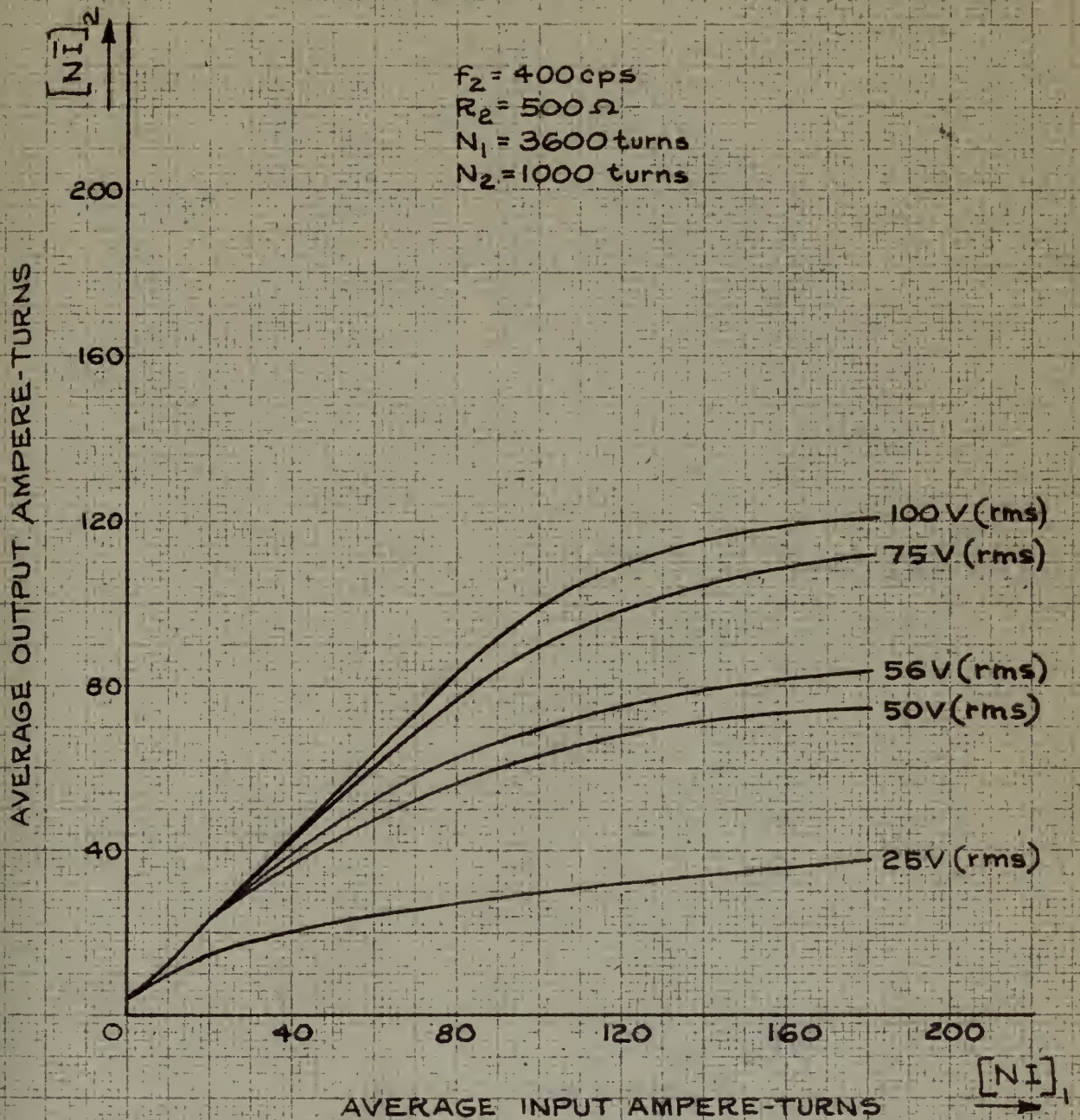


FIG. 3-8 MODULATION CHARACTERISTIC OF BASIC MAGNETIC AMPLIFIER SHOWING EFFECT OF ALTERNATING-CURRENT VOLTAGE.

$E_2 = 75 \text{ V (rms)}$
 $N_1 = 3600 \text{ turns}$
 $N_2 = 1000 \text{ turns}$
 $R_2 = 500 \Omega$

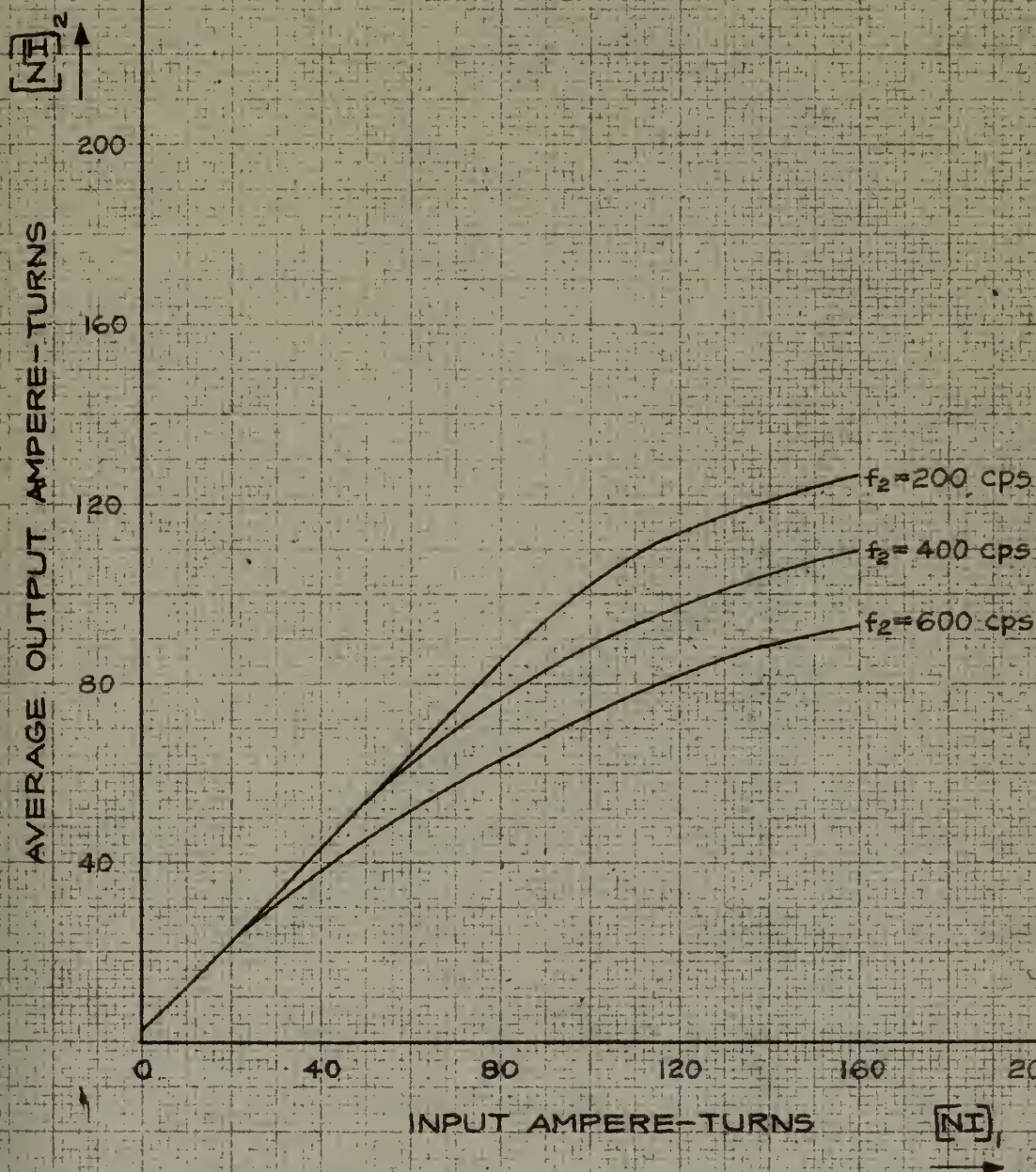


FIG. 3-9 MODULATION CHARACTERISTIC OF THE BASIC MAGNETIC AMPLIFIER SHOWING THE EFFECT OF CARRIER FREQUENCY

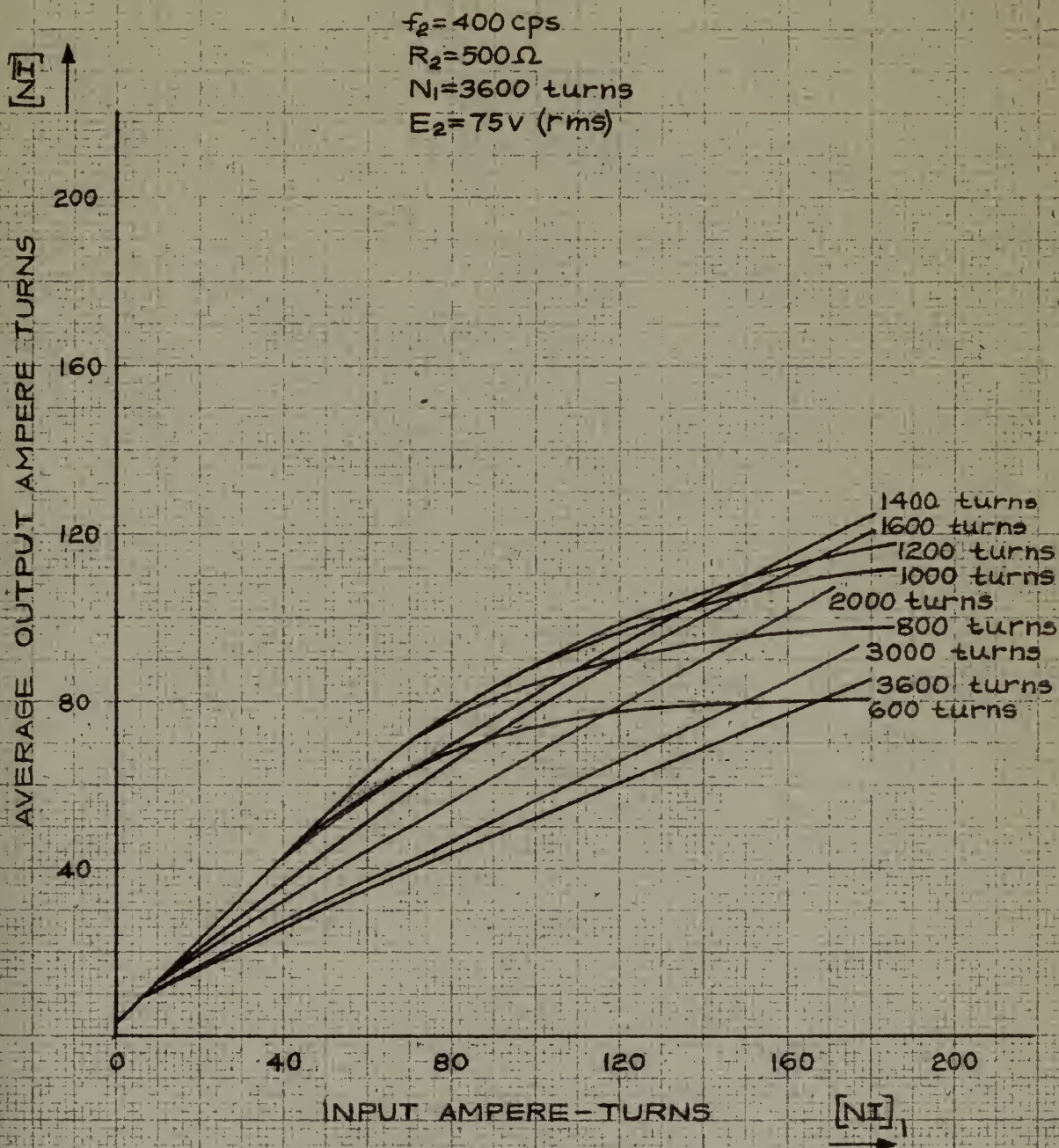


FIG. 3-10 MODULATION CHARACTERISTIC OF THE BASIC MAGNETIC AMPLIFIER SHOWING THE EFFECT OF OUTPUT TURNS

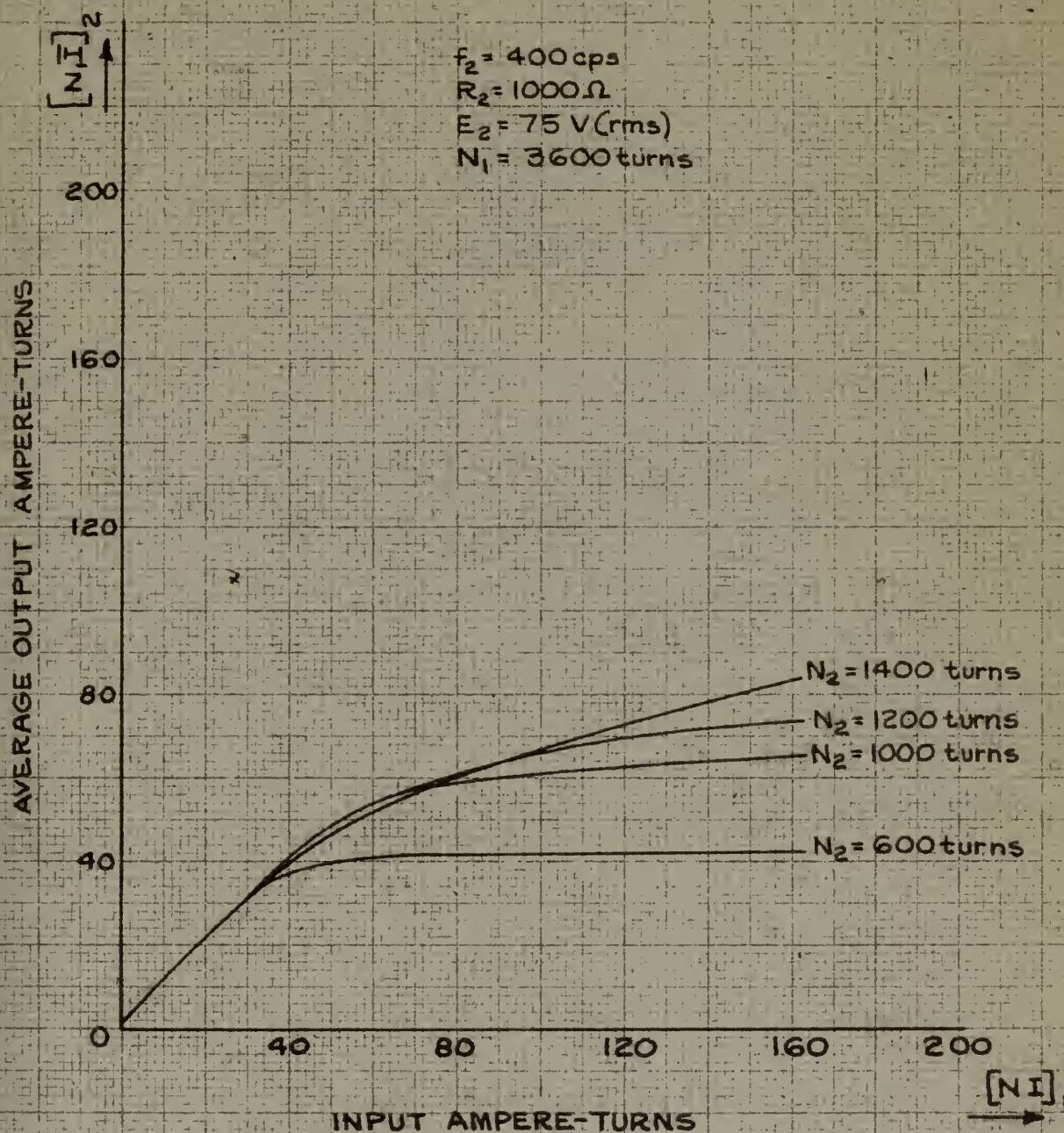


FIG. 3-II MODULATION CHARACTERISTIC OF THE BASIC MAGNETIC AMPLIFIER SHOWING THE EFFECT OF OUTPUT TURNS.

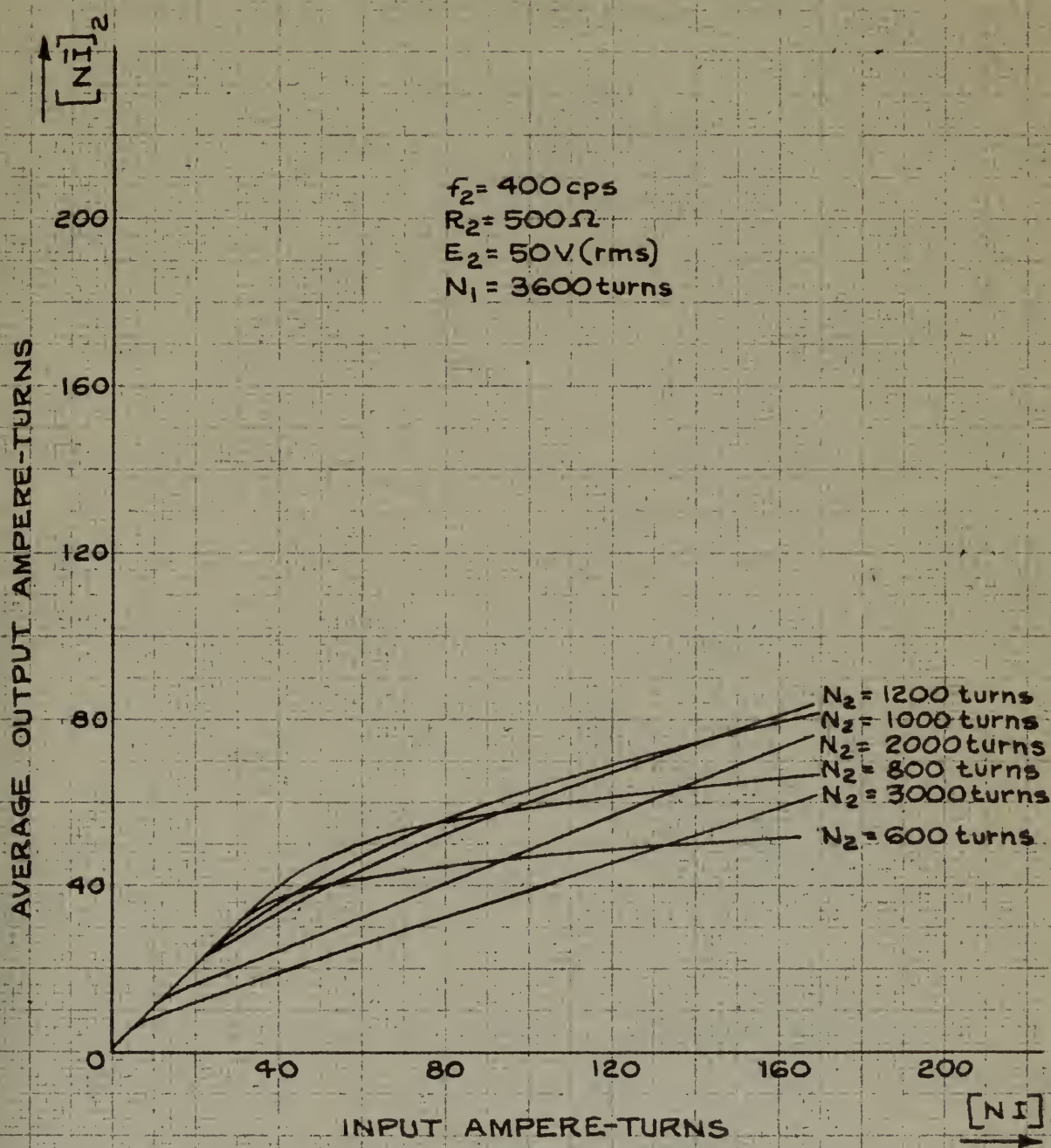


FIG. 3-12 MODULATION CHARACTERISTIC OF THE BASIC MAGNETIC AMPLIFIER. SHOWING THE EFFECT OF OUTPUT TURNS.

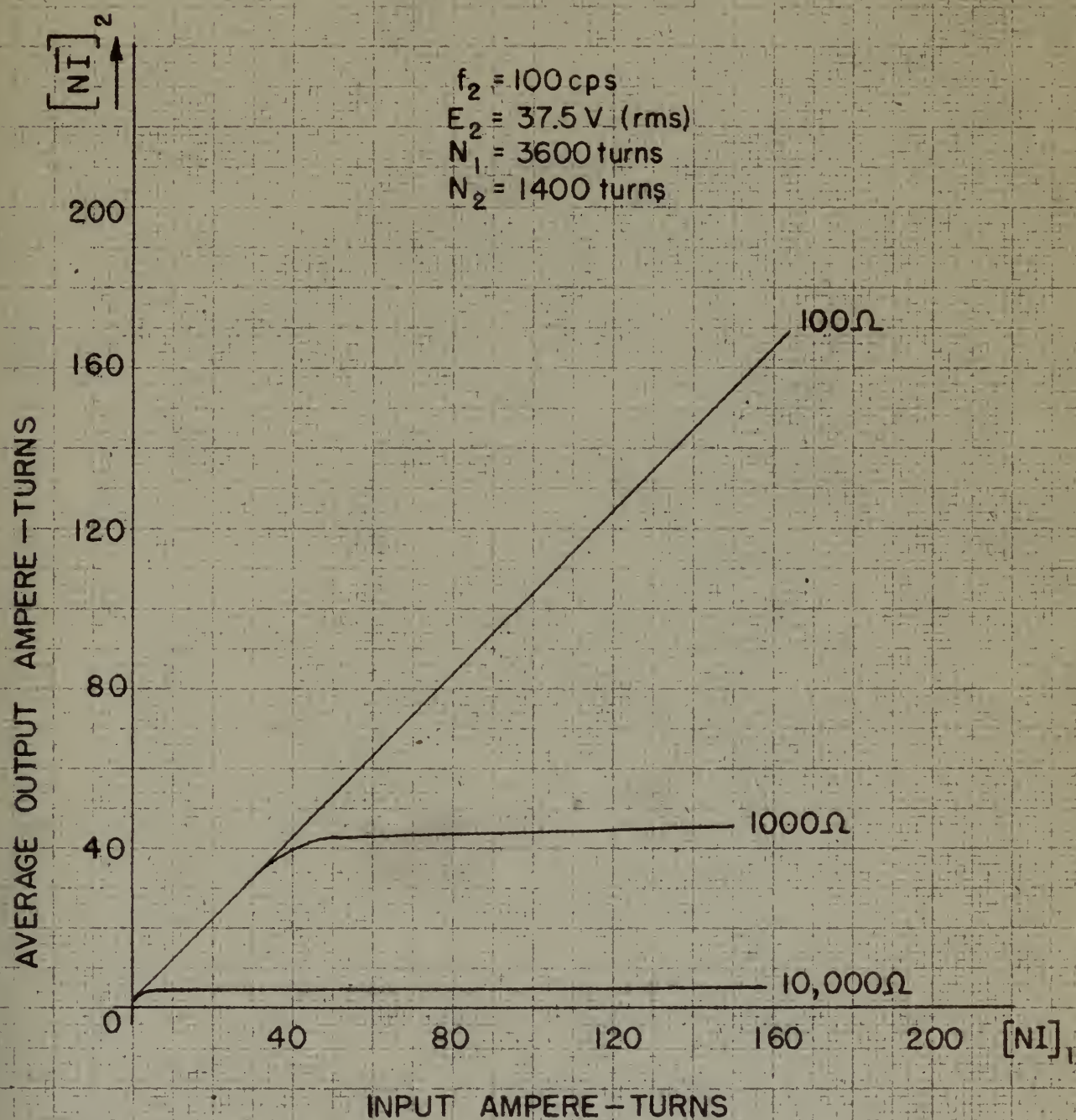


FIG. 3-13 MODULATION CHARACTERISTIC OF BASIC MAGNETIC AMPLIFIER SHOWING EFFECT OF LOAD RESISTANCE.

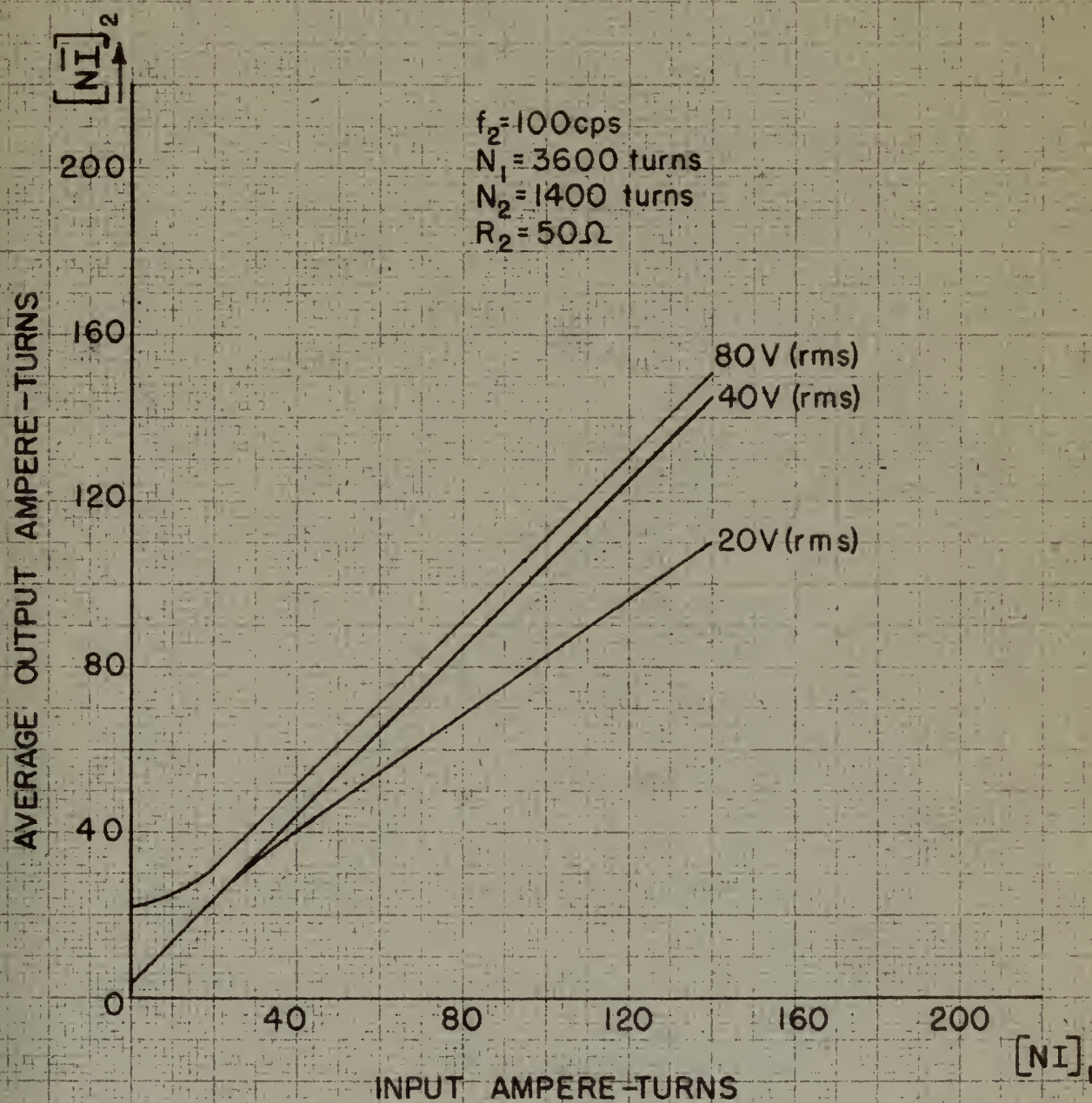


FIG. 3-14 MODULATION CHARACTERISTIC OF BASIC MAGNETIC AMPLIFIER SHOWING EFFECT OF ALTERNATING CURRENT VOLTAGE.

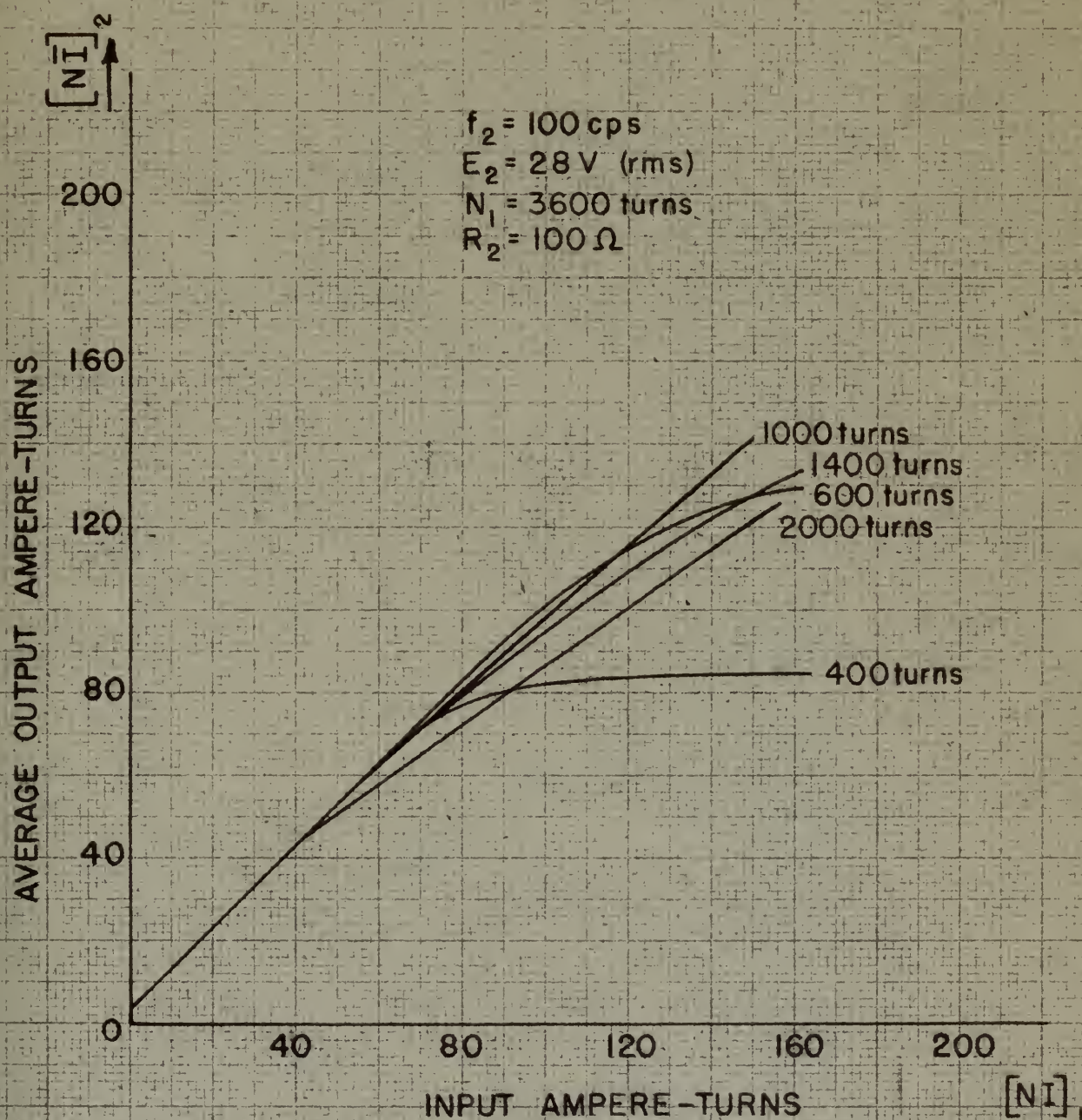


FIG. 3-15 MODULATION CHARACTERISTIC OF BASIC MAGNETIC AMPLIFIER SHOWING EFFECT OF OUTPUT TURNS.

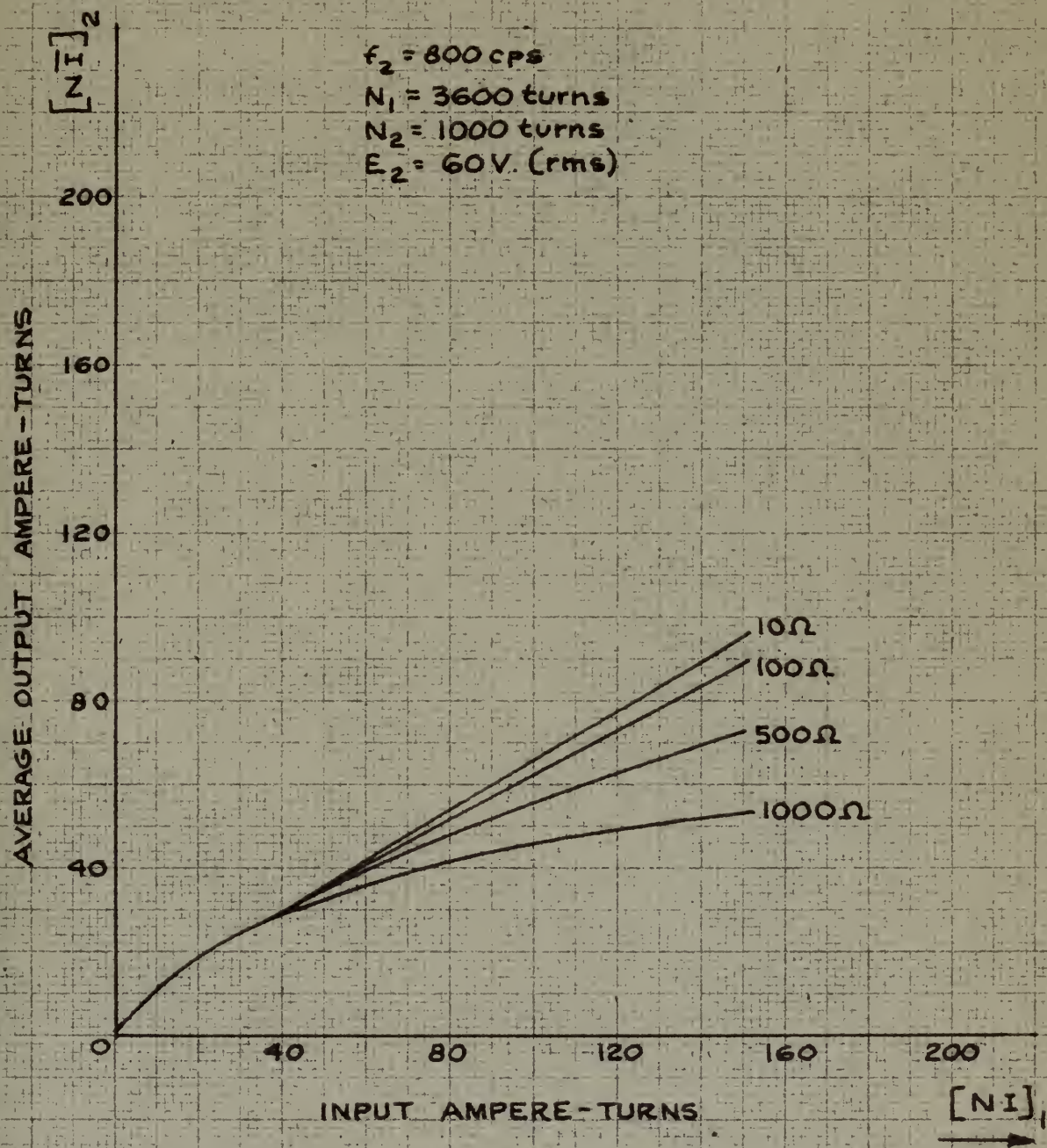


FIG. 3-16 MODULATION CHARACTERISTIC OF THE BASIC MAGNETIC AMPLIFIER SHOWING EFFECT OF LOAD RESISTANCE.

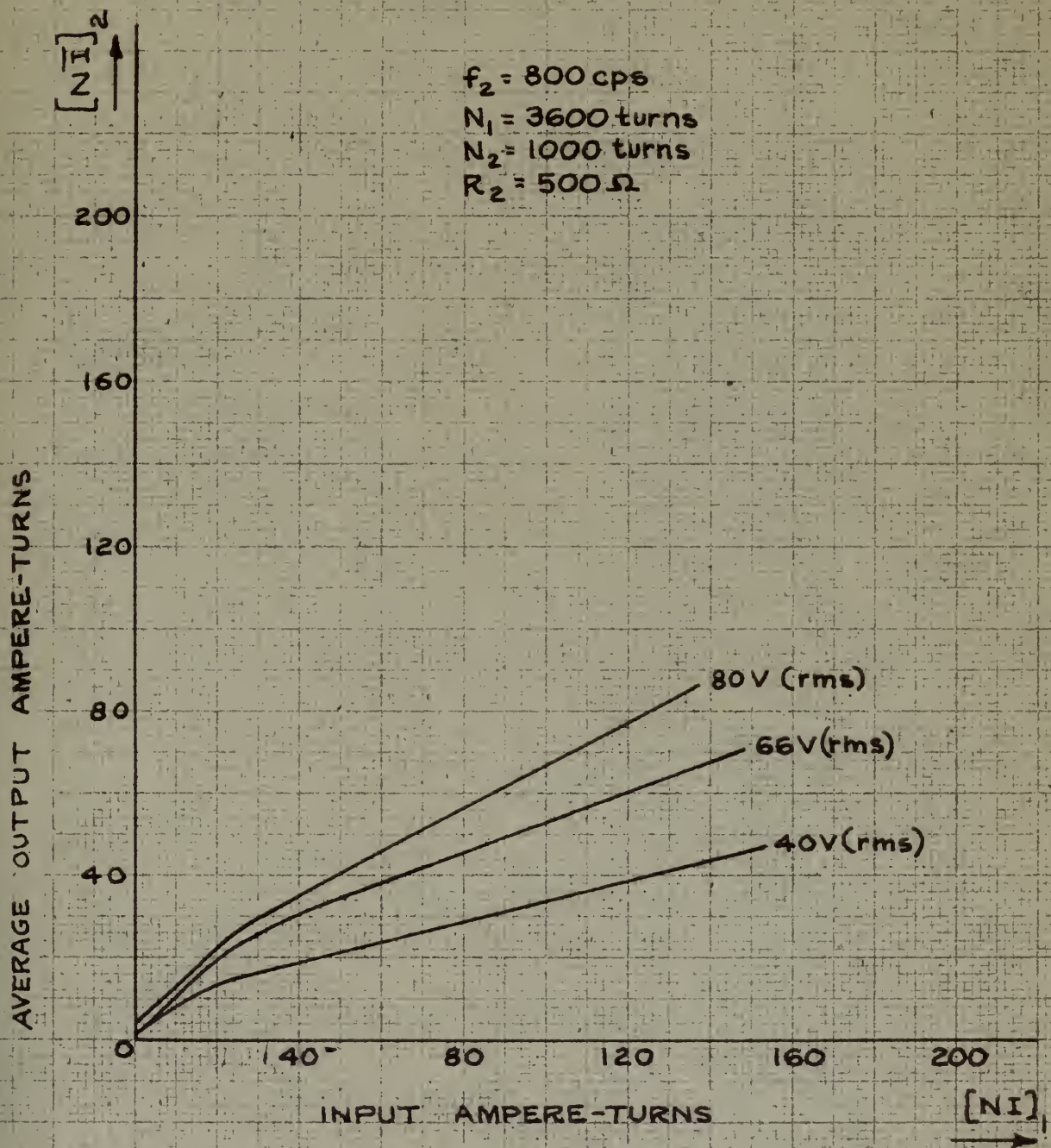


FIG. 3-17 MODULATION CHARACTERISTIC OF THE BASIC MAGNETIC AMPLIFIER SHOWING EFFECT OF ALTERNATING CURRENT VOLTAGE.

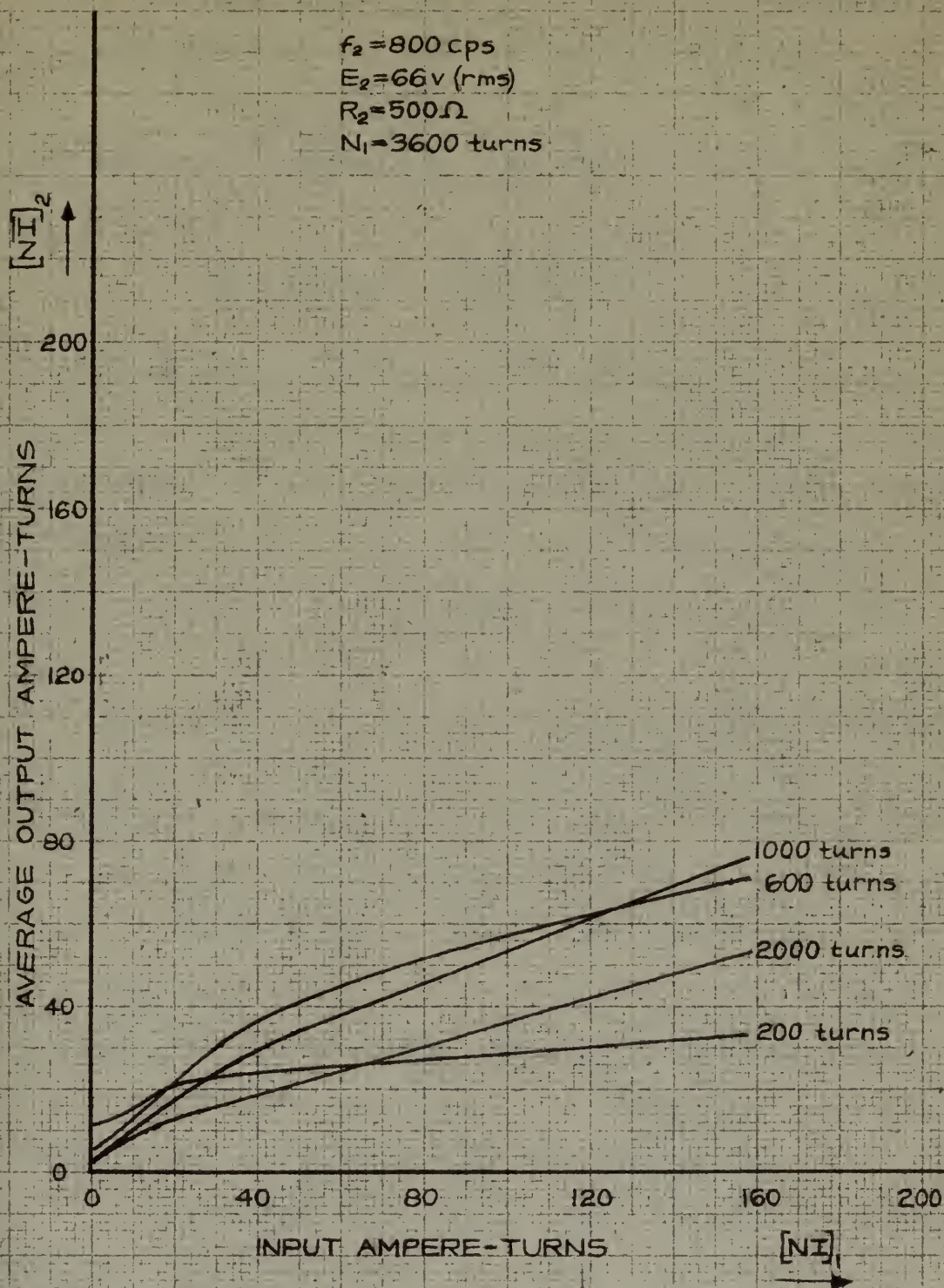


FIG. 3-18 MODULATION CHARACTERISTIC OF THE BASIC MAGNETIC AMPLIFIER SHOWING THE EFFECT OF OUTPUT TURNS.

$$P_2 = (I_2 - I_e)^2 R_2 \quad (3-9)$$

The power input may be obtained from the relation

$$P_1 = I_1^2 R_1 \quad (3-10)$$

From these two expressions, the power gain may be defined as

$$K_p = P_2/P_1 = \frac{(I_2 - I_e)^2 R_2}{I_1^2 R_1} \quad (3-11)$$

From these relations power output and power gain may be plotted as a function of power input, or more conveniently, as functions of I_1^2 , in order that the choice of R_1 , based on dynamic considerations, may be made independently.

Figure 3-19 shows P_2 and $(R_1 K_p)$ plotted as functions of I_1^2 . The parameter is chosen as R_2 , since the choice of f_2 has been assumed fixed by bandwidth or power-supply requirements, and the value of N_2 has been assumed optimized from studies of the modulation characteristic. These families of curves reveal that the value of R_2 chosen is a compromise between power gain, power output, and linear range. As will be shown in the discussion of circuit dynamics, a higher R_1 decreases the response time, but also lowers the gain. The actual design must, therefore, be a compromise between power output, power gain, linearity, and response time.

An approximate formula for estimating the power gain of a magnetic amplifier without feedback may be developed using the relation

$$N_1 I_1 \approx N_2 I_2 \quad (3-12)$$

$$(2-9) \quad X_2 = (X_1 - I_1) \frac{1}{A_2}$$

The power input may be obtained from the relation

$$(2-10) \quad P_1 = I_1^2 R_1$$

From these two expressions, the power gain may be defined as

$$(2-11) \quad G_p = \frac{P_2}{P_1} = \frac{(I_2 - I_1) \frac{1}{A_2}}{I_1^2 R_1}$$

From these relations power output and power gain may be plotted as a function of power input, or more conveniently, as functions of I_1^2 . In order that the choice of I_1 be made on dynamic considerations, may be made independently. Figure 2-13 shows P_2 and $(I_2 - I_1) \frac{1}{A_2}$ plotted as functions of I_1^2 . The parameter is chosen as R_1 , since the values of I_1 has been assumed fixed by constraints of power-output, frequency, and the value of R_1 has been assumed specified from studies of the amplifier characteristics. These results at various values show that the value of R_1 chosen is a compromise between power gain, power output, and linear range. As will be shown in the discussion of circuit elements, a higher R_1 decreases the response time, but also lowers the gain. The actual design must, therefore, be a compromise between power output, power gain, linearity, and response time.

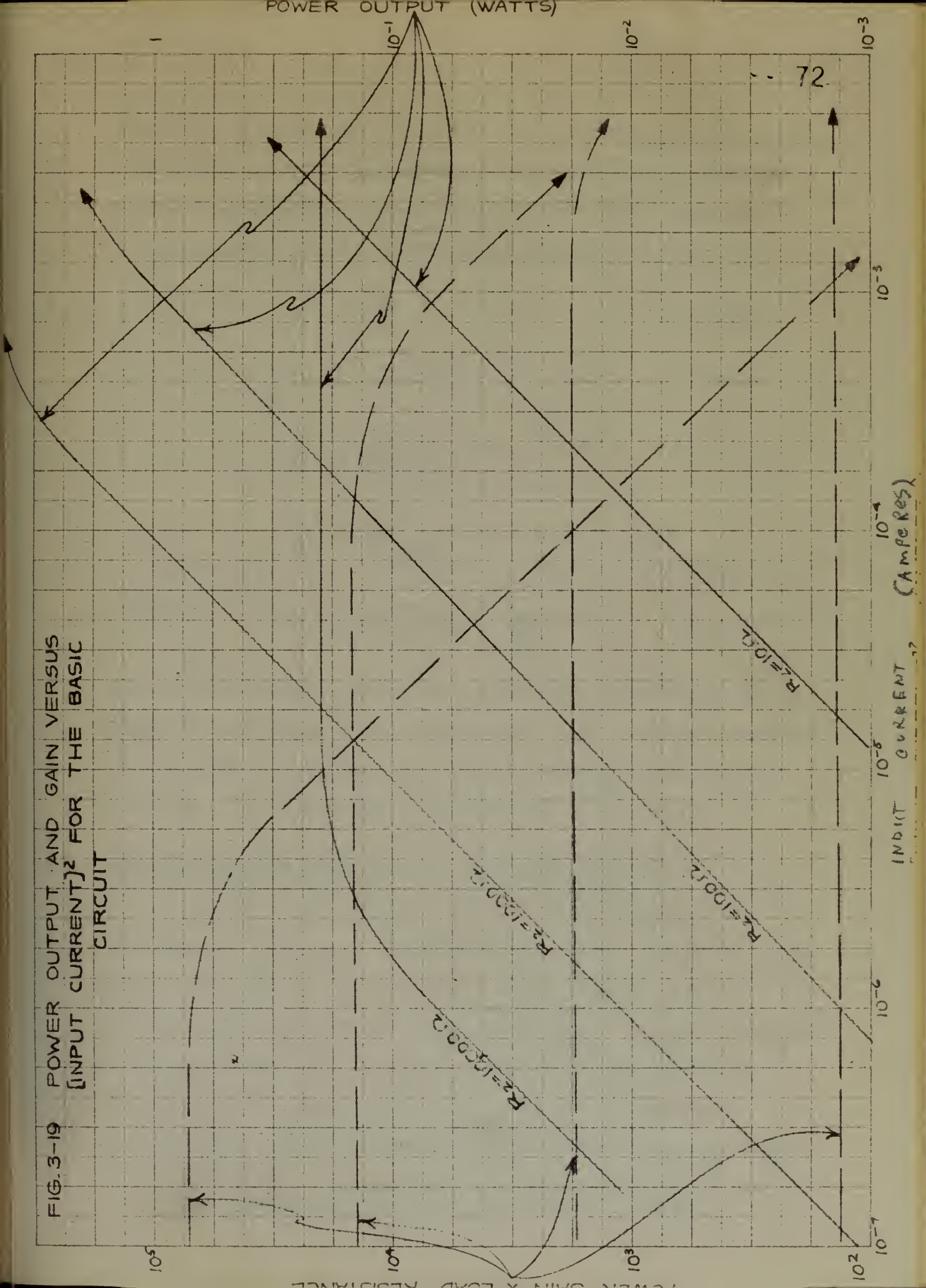
The approximate formula for estimating the power

gain of a magnetic amplifier coupled feedback may be de-

veloped using the relation

$$(2-12) \quad G_p \approx \frac{1}{R_1 A_2^2}$$

FIG. 3-19 POWER OUTPUT AND GAIN VERSUS
[INPUT CURRENT]² FOR THE BASIC
CIRCUIT



which is a fairly good approximation over the region where excitation current, I_e , is small and where the modulation characteristic has a slope of approximately 45 degrees.

The power gain may be developed as follows:

$$\frac{\bar{I}_2}{\bar{I}_1} \approx \frac{N_1}{N_2} \quad (3-13)$$

$$I_2 \approx 1.11 \bar{I}_2 \quad (3-14)$$

$$\frac{I_2}{I_1} \approx \frac{N_1}{1.11 N_2} \quad (3-15)$$

$$K_p \approx \frac{I_2^2 R_2}{I_1^2 R_1} \quad (3-16)$$

$$K_p \approx \left(\frac{N_1}{1.11 N_2} \right)^2 \frac{R_2}{R_1} \quad (3-17)$$

This relation shows which factors are most important for consideration in obtaining high gains with the basic amplifier circuit, assuming that the alternating flux has been properly adjusted by correct choice of E_2 and f_2 .

Amplifier Dynamics Studied by Transient Response

Although a great deal of material has appeared in engineering literature concerning the static characteristics of the magnetic amplifier, very little detailed analysis of the transient behavior has been published. In 1943, Buchhold established that the speed of response was proportional to the ratio of input-circuit inductance to input-circuit resistance.¹ Lamm, in the same year, published a transient

1. Buchhold, T., "On the Theory of the Magnetic Amplifier," Archiv fur Elektrotechnik, 37, (1943), 197-211.

which is a fairly good approximation over the region where
excitation current, I_m , is small and where the modulation
characteristic has a slope of approximately 50 degrees.
The power gain may be developed as follows:

$$\begin{aligned} (7-17) \quad \frac{P_o}{P_i} &= \frac{I_m}{I_0} \\ (7-18) \quad \frac{P_o}{P_i} &= \frac{I_m}{I_0} \\ (7-19) \quad \frac{P_o}{P_i} &= \frac{I_m}{I_0} \\ (7-20) \quad \frac{P_o}{P_i} &= \frac{I_m}{I_0} \\ (7-21) \quad \frac{P_o}{P_i} &= \frac{I_m}{I_0} \end{aligned}$$

This relation shows which factors are most important for
consideration in obtaining high gain with the basic ampli-
fier circuit, assuming that the modulating line has been
properly adjusted by correct choice of I_m and I_0 .

Amplifier Dynamics Studied by Frequency Response

Although a great deal of material has appeared in
engineering literature concerning the audio characteristics
of the magnetic amplifier, very little detailed analysis of
the transient behavior has been published. In 1947, McDonald
established that the speed of response was proportional to
the ratio of input-circuit inductance to input-circuit
resistance.¹ Later, in the same year, published a transient
I. McDonald, "On the Theory of the Magnetic Amplifier,"
Study for Electronics, IV, (1947), 197-211.

analysis of a three-phase saturable-reactor in which he states that the response time is proportional to the carrier frequency.¹ In 1946, Grafinger pointed out that the magnetic amplifier could be characterized by a first-order time constant.² Therkelsen confirmed this observation from frequency-response studies, showing the time constant to be essentially the ratio of inductance to resistance in the input circuit.³ The purpose of the present study is to extend these investigations in order to establish the effect of all circuit parameters upon the dynamics of the amplifier.

Because the magnetic amplifier is a nonlinear system, it is inherently incorrect to characterize its dynamic performance by means of a time constant unless additional defining restrictions are imposed. Since the input inductance is a function of the degree of saturation of the core, which is, in turn, a function of the excitation current, any time constant defined in terms of the ratio of input inductance to input resistance is, in reality, a variable. If, however, a sinusoidal signal is superimposed upon a biasing-current level, the amplifier response has the characteristics of a first-order system as first shown by Therkelsen and extended later in this chapter.

The speed of response will be studied in this section in terms of the time required for the amplifier to respond to an applied step voltage. Because the system is

-
1. Lamm, U., "The Transducer, A D.C. Pre-Saturated Reactor," (Stockholm, Esselte Aktiebolag, 1943).
 2. Grafinger, L.N., "A Study of Magnetic Amplifiers for Servomechanisms," E.E. Thesis (M.I.T., 1946).
 3. Therkelsen, E.B., "A Low-Power Magnetic Amplifier for Servomechanisms," E.E. Thesis (M.I.T., 1946).

analysis of a three-phase astable-multivibrator in which the
 states that the response time is proportional to the output
 frequency. In 1946, Swamy² pointed out that the mag-
 nitude of the output voltage is determined by a time-order
 time constant. Theoretical analysis of this operation from
 frequency-response studies, showing the time constant to be
 essentially the ratio of inductance to resistance in the
 input circuit. The purpose of the present study is to ex-
 tend these investigations in order to establish the effect
 of all circuit parameters upon the dynamics of the amplifier.
 Because the amplifier is a nonlinear
 system, it is inherently intractable to characterize the
 dynamic performance by means of a time constant unless ad-
 ditional defining restrictions are imposed. Since the input
 inductance is a function of the degree of saturation of the
 core, which is, in turn, a function of the excitation cur-
 rent, any time constant defined in terms of the ratio of
 input inductance to input resistance is, in reality, a
 variable. If, however, a sinusoidal signal is superimposed
 upon a biasing-current level, the amplifier response has
 the characteristics of a time-order system as long as the
 by induction and extended later in this chapter.
 The speed of response will be treated in this sec-
 tion in terms of the time required for the amplifier to re-
 spond to an applied step voltage. Because the system is

1. Jones, U. S. "The Transistor," R. D. MacDonald, Ed.,
 McGraw-Hill, New York, 1957.
 2. Swamy, S. V. "A Study of Magnetic Amplifiers for
 Servomechanisms," R. D. MacDonald (Ed.), 1957.
 3. Swamy, S. V. "A Study of Magnetic Amplifiers for
 Servomechanisms," R. D. MacDonald (Ed.), 1957.

nonlinear, the term, time constant, will not be used. A more appropriate expression is effective characteristic time, (CT), which will be defined as that time required for the output to rise or fall through 63% of the total change in response to a step-function input.¹ This concept is based on an analogy with the simple exponential curve which characterizes a first-order linear system, in which the time constant is defined as the time for the step-function response to rise or fall through $(1-1/e)$, or 63%, of the total change. Thus, the characteristic time of the nonlinear system is analogous to the time constant of the linear system. The characteristic time will, therefore, be the index used in specifying the speed of response of the magnetic amplifier.

The laboratory technique used to measure (CT) involved the application of a step voltage to the input terminals and observation of the carrier-current transient on a calibrated oscilloscope. A DuMont type 215 low-frequency linear time-base generator was used to furnish the sweep voltage to a DuMont type 208 cathode-ray oscilloscope which was modified by the substitution of a high-persistence cathode-ray tube. The time for the carrier envelope to rise or fall from its initial value through 63% of the total change could be read directly from the oscilloscope once the horizontal sweep had been calibrated in milliseconds. The step voltage

1. Draper, C.S. and McKay, W., "Instrument Analysis," M.I.T., 1946.

was applied by means of a switch in the input circuit whose closure also triggered the sweep.

Circuit conditions were chosen as nearly identical as possible with those used on the differential analyzer in order that a comparison of analytic and experimental transient data could be made. A standard condition was selected and the circuit parameters were varied one at a time in order to observe their effect upon the transient.

The effects of changes in the control-circuit parameters, R_1 , I_1 , and N_1 , were investigated first. The results indicate that (CT) varies inversely with R_1 . This conclusion is drawn from the fact that when (CT) is plotted as a function of R_1 on logarithmic coordinates, the function has a negative slope of unity. The experimental data is shown in Figure 3-20. This result confirms the observations of previous experimenters. The effect of the input current upon the transient response showed that (CT) varies inversely as the square-root of I_1 , as can be seen from the negative slope of one-half which the function exhibits on the logarithmic plot in Figure 3-20. When the effect of input turns was examined, (CT) was observed to vary directly as N_1 , the logarithmic plot of Figure 3-20 having a positive slope of unity. Pease has shown that the reactor inductance is inversely proportional to the control current to a first approximation.¹ On this basis, the following relation holds,

1. Pease, W.M., "Design of a 400 Cycle Servomechanism," E.E. Thesis, (M.I.T., 1943).

There is a small amount of material in the file which is not included in the report.

(continued from page 6)

one at a time in order to observe their effect upon the
diffusion rate selected and the electric resistance were varied
systematically through out the range of 0.1 to 1.0 ohm-cm.
analysis in order that a comparison of results and con-
clusions as regards the effect of the different

The effects of changes in the constant-diffusion parameters, D_1 , D_2 , and D_3 , were investigated first. The results indicate that (DT) varies inversely with D_1 . This conclusion is shown from the fact that when (DT) is plotted as a function of D_1 on logarithmic coordinates, the data plot has a negative slope of unity. The experimental data is shown in Figure 3-20. This result defines the dependence of various experiments. The effect of the length of the constant-diffusion region on the (DT) varies inversely as the square root of D_1 , as can be seen from the negative slope of one-half which the function exhibits on the logarithmic plot in Figure 3-20. When the effect of input terms was examined, (DT) was observed to vary directly as D_1 . The logarithmic plot in Figure 3-20 having a positive slope of unity. There has been no effect on the (DT) when the input is varied by a factor of 10. In this case, the following relation holds:

1. Nelson, R.H., *Treatment of a Low Cycle Seismicity*,
R.H. Nelson, (Ed.), 1997.

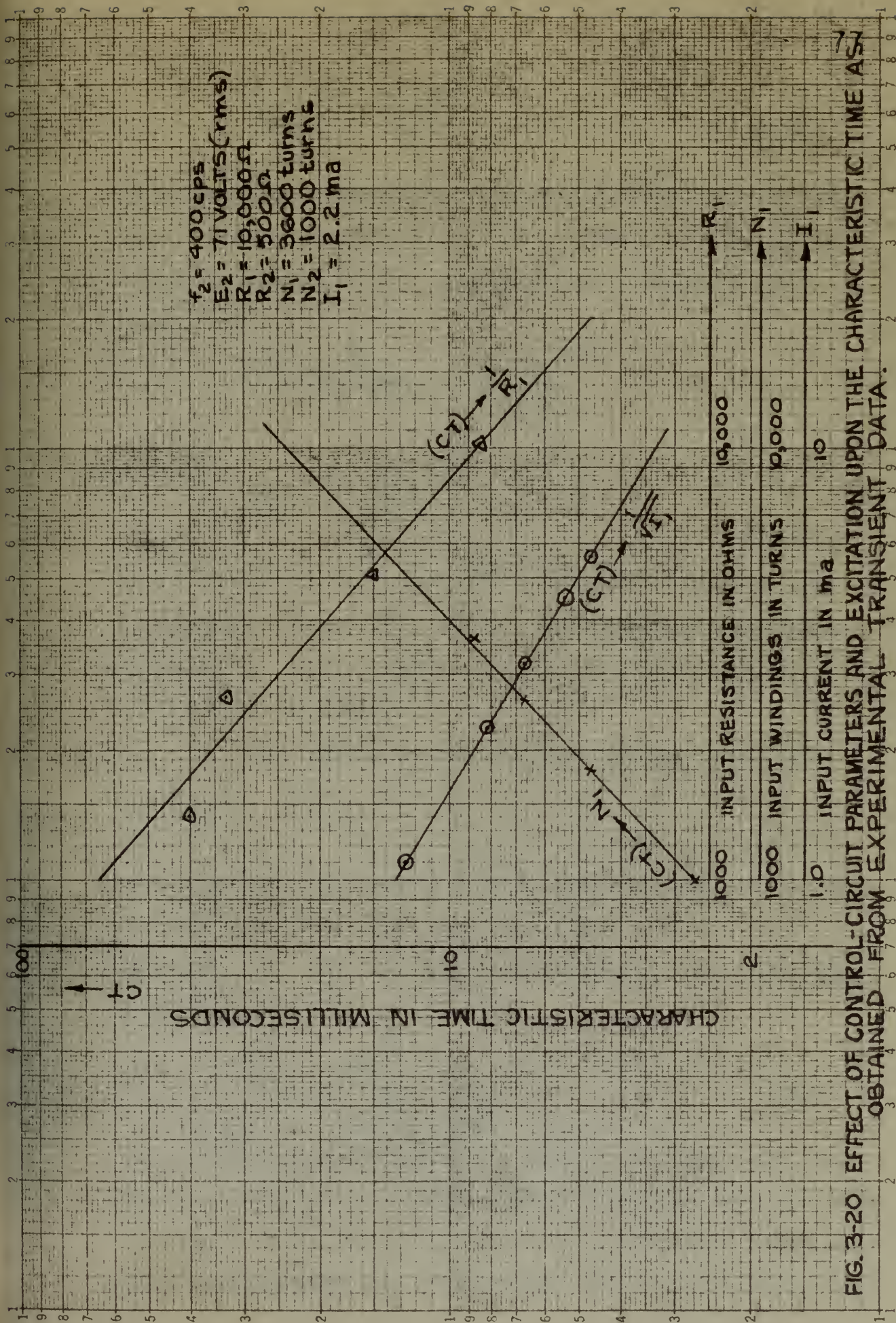


FIG. 3-20 EFFECT OF CONTROL-CIRCUIT PARAMETERS AND EXCITATION UPON THE CHARACTERISTIC TIME CONSTANT OBTAINED FROM EXPERIMENTAL DATA.

$$L_1(I_1) \cong \frac{k' N_1^2}{I_1} \quad (3-18)$$

in which k' is a constant of proportionality, and L_1 , because it is a function of I_1 , is identified by the additional subscript, (I_1) . The following relations can be seen:

$$(CT) \rightarrow \frac{N_1}{R_1 \sqrt{I_1}} \rightarrow \frac{1}{R_1} \left[\frac{N_1^2}{I_1} \right]^{1/2} \quad (3-19)$$

or

$$(CT) \rightarrow \frac{\sqrt{L_1(I_1)}}{R_1} \quad (3-20)$$

It is concluded, therefore, that the characteristic time is directly proportional to the square-root of the final value of the input inductance, and inversely proportional to the input resistance.

The effects of the carrier-circuit parameters, R_2 , N_2 , E_2 , and f_2 , were next observed. As shown in Figure 3-21, the effect of R_2 was found to be negligible. E_2 and f_2 had only slight effect, while N_2 produced a pronounced variation. From empirical data over the region examined, (CT) has the following functional relation with respect to the carrier circuit:

$$(CT) \rightarrow \frac{(E_2)^{1/5}}{(f_2)^{1/10} (N_2)^{1/2}} \quad (3-21)$$

These effects are difficult to explain because of the non-linear nature of the energy-storage elements, the saturable reactors. Since the analytic results, discussed in Chapter IV, do not confirm the experimental data for the variation

$$(7-18) \quad I_1(I_1) \approx \frac{K_1 K_2}{I_1}$$

In which K_1 is a constant of proportionality, and I_1 , because it is a function of I_1 , is identified by the additional subscript, (I_1) . The following relations can be

seen:

$$(7-19) \quad \left\{ \frac{K_2}{I_1} \right\} \frac{1}{I_1} \leftarrow \frac{K_1}{I_1} \leftarrow (GT)$$

or

$$(7-20) \quad \frac{I_1(I_1)}{I_1} \leftarrow (GT)$$

It is concluded, therefore, that the characteristic time is directly proportional to the square-root of the final value of the input impedance, and inversely proportional to the input resistance.

The effects of the carrier-circuit parameters,

R_2 , K_2 , I_2 , and I_3 , were next observed. As shown in Figure 7-21, the effect of R_2 was found to be negligible. I_2 and I_3 had only slight effect, while K_2 produced a pronounced variation. From empirical data over the region examined, (GT) has the following functional relation with

response to the carrier circuit:

$$(7-21) \quad \frac{I_2(I_2)}{I_2(I_2)} \leftarrow (GT)$$

These effects are difficult to explain because of the nonlinear nature of the energy-storage elements, the saturable reactor. Since the analytic results, discussed in Chapter IV, do not confirm the experimental data for the variation

$f_2 = 400 \text{ cps}$
 $E_2 = 71 \text{ VOLTS (rms)}$
 $R_2 = 500 \Omega$
 $R_1 = 10,000 \Omega$
 $N_1 = 3600 \text{ turns}$
 $N_2 = 1000 \text{ turns}$
 $I_1 = 2.2 \text{ ma}$

CT ↑

CHARACTERISTIC TIME IN MILLISECONDS

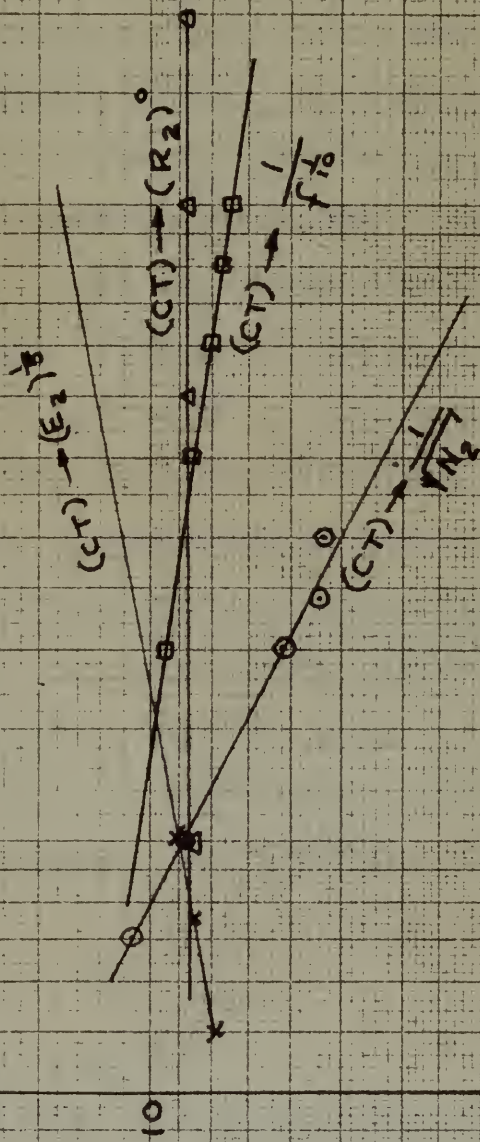


FIG. 3-21 EFFECT OF CARRIER-CIRCUIT PARAMETERS AND EXCITATION UPON THE CHARACTERISTIC TIME AS OBTAINED FROM EXPERIMENTAL TRANSIENT DATA.

of (CT) with the carrier-circuit parameters, some effect not taken into account in the formulation of the system equations for the analytic study must be responsible for the discrepancy between the two. This discrepancy is attributed to the fact that the functional dependence of core loss was neglected in establishing the analytic equations. The analytic solution assumed the eddy-current and copper losses to be lumped into the resistance R_2 , while hysteresis was neglected entirely by using the normal magnetization curve as the functional relation between flux and magnetizing force. Although these assumptions, as will be shown in Chapter IV, satisfy the steady-state solution and correctly describe the transient effects of the control circuit, they appear to misrepresent the transient effects which take place in the carrier circuit. The relation of the core loss to the carrier-circuit constants and excitation will be developed in order to point out the effects which were neglected. For symmetrical alternating-magnetization, eddy-current and hysteresis loss can be expressed by

$$P_e = k_1 f_2^2 \beta_{\max}^2 \quad (3-22)$$

$$P_h = k_2 f_2 \beta_{\max}^{\eta} \quad (3-23)$$

where β is the Steinmetz coefficient, and k_1 and k_2 constants of proportionality.

As discussed in Chapter II, these formulae do not necessarily hold for asymmetrical magnetization such

of (27) with the previously defined parameters, and also
 not taken into account in the formulation of the system
 conditions for the multiple input case be responsible for
 the discrepancy between the two. This discrepancy is
 attributed to the fact that the theoretical dependence of
 the loss was neglected in calculating the multiple
 equations. The multiple equations were solved by the
 method of least squares as is shown in the appendix 2.
 While the multiple equations were neglected, the normal
 regression curve as the theoretical relation between the
 and regression force. Although these assumptions, as will
 be shown in Chapter IV, satisfy the steady-state relation
 and correctly describe the transient effects of the control
 system, they do not in themselves the transient effects
 which take place in the control system. The relation of
 the loss to the steady-state conditions and transi-
 tion will be developed in order to help out the effects
 which were neglected. For simplicity, the following
 approximation, which neglects the transient loss can be
 expressed by

$$(27-2)$$

$$L = \frac{1}{2} \left(\frac{1}{\omega} \right)^2 \left(\frac{1}{\omega} \right)^2$$

$$(27-3)$$

$$L = \frac{1}{2} \left(\frac{1}{\omega} \right)^2 \left(\frac{1}{\omega} \right)^2$$

where L is the steady-state condition, and ω is the
 value of the frequency.
 As discussed in Chapter II, these losses do
 not necessarily hold for the approximation equation with

as occurs in magnetically-biased saturable reactors. In the absence of more accurate loss functions, these relations will be assumed to describe the total core loss which is the sum of its two components

$$P_T = P_e + P_h \quad (3-24)$$

$$P_T = k_1 f^2 \beta_{\max}^2 + k_2 f \beta_{\max}^\eta \quad (3-25)$$

From the induction law the following equation expresses the flux amplitude for peak sinusoidal induction voltage, \hat{E}

$$\beta_{\max} = \frac{\hat{E}}{2 f_2 N_2} \quad (3-26)$$

Eliminating the flux amplitude in Equation 3-25 by means of the Equation 3-26, the following expression for total core loss is obtained

$$P_T = k_3 \left(\frac{\hat{E}}{N_2} \right)^2 + k_4 \left(\frac{\hat{E}}{N_2} \right) \frac{1}{[f_2]^{\eta-1}} \quad (3-27)$$

where k_3 and k_4 are constants of proportionality. This relation clearly shows that the equivalent core-loss resistor is a function of the coil induction voltage, the carrier frequency, and the number of turns in the carrier windings. Although the core loss in the experimental reactors has been minimized by careful design, it is still appreciable and is believed to be intimately related to the effect of the carrier circuit upon the transient response, and hence should be accounted for in the differential equations of the system if the analytic solution is to reveal these carrier-circuit transient effects.

Before leaving this discussion of transient effects, the fact that (CT) measured by opening the switch

in the control circuit is somewhat less than measured when closing the switch should be mentioned. This phenomenon occurs because the response envelope is not a simple exponential, but builds up or decays at a slower rate for lower values of control current. It, therefore, takes a shorter time for the carrier envelope to fall through 63% of the total change than it does to rise through the same percentage. This would explain the differences in "time off" and "time on" noted by Fitzgerald.¹

Amplifier Dynamics Studied by Frequency Response

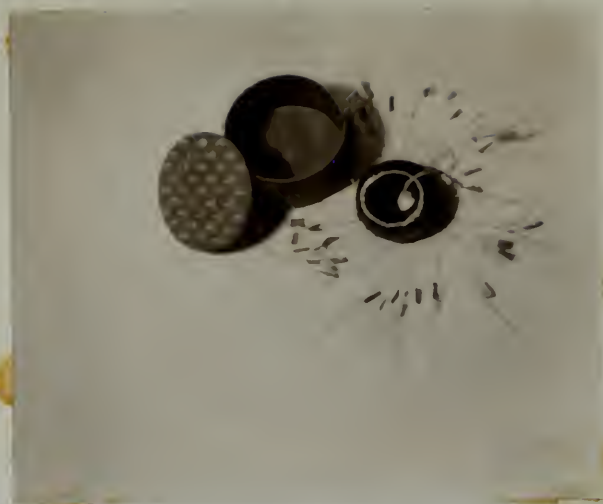
The practical value of the magnetic amplifier for many applications depends upon its ability to behave as a linear amplifier in spite of the inherent nonlinearity of the circuit. A study of the frequency response of a system to a sinusoidal driving function yields information both as to the static and dynamic behavior of the system. As mentioned earlier in the chapter, Therkelsen pointed out that the magnetic amplifier had a frequency response similar to that of a first order system. It will be the objective of this section to investigate in greater detail the nature of the frequency response as a function of the various amplifier parameters, and from the study correlate the observed frequency characteristics with observed transient behavior. The laboratory arrangement for these frequency studies was essentially the same as that used for the measurement of the static characteristics, with

1. Fitzgerald, A.B., "Magnetic Amplifier Characteristics-Neutral Type," J.F.I., 244, (1947), 415-439.

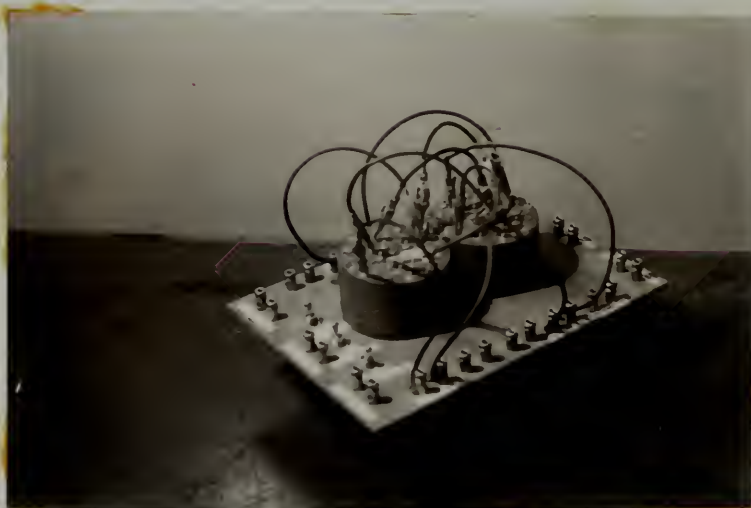
in the control circuit is somewhat less than measured when closing the switch should be mentioned. This phenomenon occurs because the response envelope is not a simple exponential, but rather as a damped sine wave. Lower values of external current, i.e., therefore, takes a shorter time for the carrier envelope to fall through 50% of the total change than it does to rise through the same percentage. This would explain the difference in "time off" and "time on" noted by Fitzgerald.

Amplifier Response Studied by Frequency Response

The practical value of the magnetic amplifier for many applications depends upon its ability to behave as a linear amplifier in spite of the inherent nonlinearity of the circuit. A study of the frequency response of a system to a sinusoidal driving function yields information both as to the static and dynamic behavior of the system. As mentioned earlier in the report, theoretical points and that the magnetic amplifier had a frequency response similar to that of a first order system. It will be the objective of this section to investigate in greater detail the nature of the frequency response as a function of the various amplifier parameters, and from the study correlate the observed frequency characteristics with observed transient behavior. The laboratory arrangement for these frequency studies was essentially the same as that used for the measurements of the static characteristics, with



(a) TOROIDAL CORE AND CONTAINER



(b) PAIR OF EXPERIMENTAL SATURABLE REACTORS

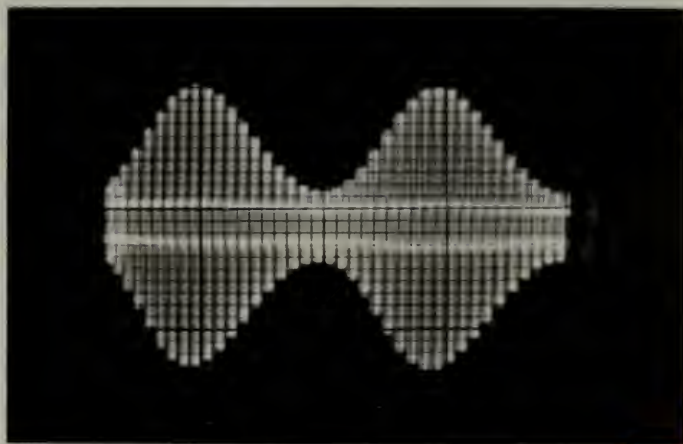
FIGURE 3-22



(14) VANDERBILT COLLEGE AND UNIVERSITY



(15) VANDERBILT COLLEGE AND UNIVERSITY



MODULATED CARRIER-CIRCUIT WAVEFORM
WITH SINUSOIDAL SIGNAL APPLIED TO INPUT.

FIGURE 3-23(A).



RECEIVED BY THE DIRECTOR OF THE
BUREAU OF THE ARMY AND NAVAL
COMMISSIONERS OF THE ARMY AND NAVAL
COMMISSIONERS OF THE ARMY AND NAVAL

FIGURE 1 (A)

the exception that a sinusoidal voltage is applied in series in the control circuit, and is thereby superimposed on a direct-current biasing level. This alternating-signal voltage was held constant and the amplitude of the response was observed on an oscilloscope. A typical modulation pattern obtained with a sinusoidal driving voltage is shown in Figure 3-23(A).

A few remarks will be made concerning the frequency response of first-order linear systems in order that a comparative study can be made with the frequency response of the magnetic amplifier. The sinusoidal response of a first-order linear system is characterized by the performance operator

$$[P] = \frac{1}{1 + j2\pi f(CT)} \quad (3-28)$$

where

(AR) = ratio of response amplitude
to input excitation amplitude,

f = input excitation frequency,

(CT) = time constant

ϕ = phase angle of the response

The relation in Equation 3-28 can further be broken down as

$$[P] = (AR) \angle \phi \quad (3-29)$$

where

$$(AR) = \frac{1}{\sqrt{1 + [2\pi f(CT)]^2}} \quad (3-30)$$

$$\text{and } \phi = \tan^{-1} [-2\pi f(CT)] \quad (3-31)$$

The exception that a sinusoidal voltage is applied in series in the control circuit, and an output proportional to a direct-current biasing level. This direct-current biasing level was held constant and the response of the response was observed on an oscilloscope. A typical modulation pattern obtained with a sinusoidal driving voltage is shown in

Figure 3-23(A).

A few remarks will be made concerning the frequency response of first-order linear systems in order that a comparative study can be made with the frequency response of the magnetic amplifier. The sinusoidal response of a first-order linear system is characterized by the performance

operator

$$[2] \quad \frac{1}{1 + j\omega\tau(C)} \quad (3-23)$$

where

$$(A) \quad \tau = \text{time constant of the system}$$

$$(B) \quad \omega = \text{input angular frequency}$$

$$(C) \quad \tau = \text{input resistance of the system}$$

$$(D) \quad \tau = \text{time constant}$$

$$(E) \quad \tau = \text{time constant of the response}$$

The relation in Equation 3-23 can therefore be broken down as

$$[3] \quad \frac{1}{1 + j\omega\tau(C)} \quad (3-24)$$

where

$$(A) \quad \tau = \frac{1}{\sqrt{1 + [\omega\tau(C)]^2}} \quad (3-25)$$

$$(B) \quad \phi = \tan^{-1} [\omega\tau(C)] \quad (3-26)$$

Figure 3-23 shows amplitude ratio and phase angle as a function of the normalized input-excitation frequency. The bandwidth of such a system is measured to the half-power point where the response is down 3db. The frequency at which this occurs is the critical frequency, f_c , and is related to the time constant by the relation

$$(CT) = 1/2 \pi f_c \quad (3-32)$$

The asymptote of the amplitude ratio at the high end of the frequency spectrum has a negative slope of 6 db/octave passing through the zero db line at the critical frequency when plotted on semi-logarithmic coordinates. The total associated change of phase is ninety degrees.

As seen from Figures 3-24 to 3-30, the magnetic amplifier has a frequency response which approximates a first-order linear system, as can be observed by the initial flat characteristic and the ultimate slope of negative 6 db/octave. The fact that the basic magnetic amplifier is a first-order system can be ascertained by inspection of the equations, or by noting that only one energy storage is involved. The important fact is that linear behavior is approximated. A plot of the transfer function of the magnetic amplifier on the complex plane is shown in Figure 3-31.

The effect of the various circuit parameters on bandwidth has been studied one at a time, and the observations plotted in Figures 3-24 to 3-30 respectively. From

Figures 3-23 show amplification factor and phase angle as a function of the normalized input frequency. The magnitude of such a system is measured in dB. The frequency power point where the response is down 3dB. The frequency at which this occurs is the critical frequency, f_c , and is related to the time constant by the relation

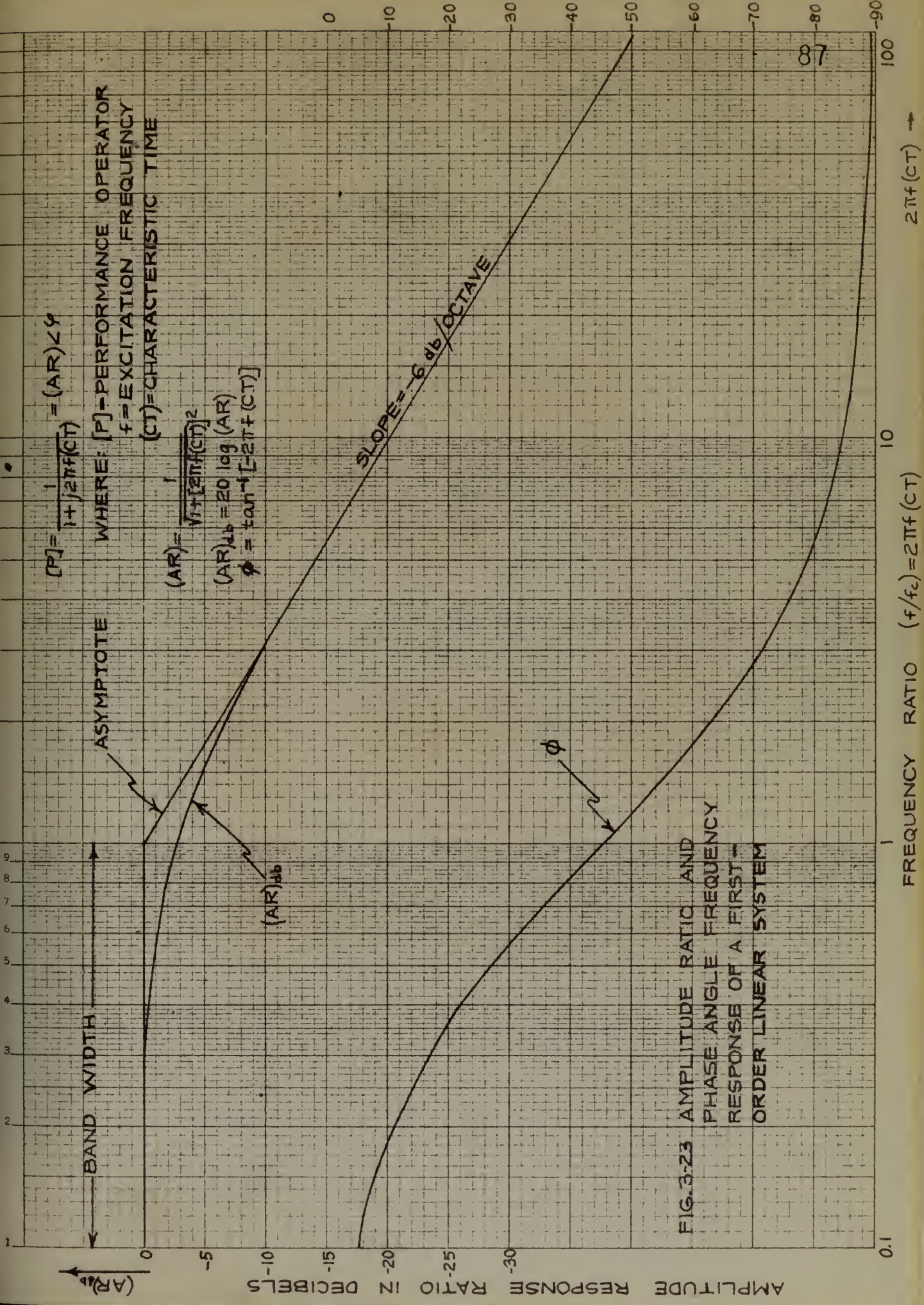
$$(3-24) \quad f_c = \frac{1}{2\pi\tau}$$

The response of the amplifier is of the form and the frequency response has a negative slope of 6 dB/octave. The gain at the time of the critical frequency is given by the semi-logarithmic plot. The total expected change of phase is nearly 90 degrees.

As seen from Figures 3-24 to 3-26, the amplifier has a frequency response with a magnitude a first-order linear system, as can be observed by the initial 6 dB/octave. The fact that the gain magnitude remains is a first-order system can be established by inspection of the equations, or by noting that only one energy storage is involved. The important part is that linear behavior is expected. A plot of the transfer function at the amplifier amplifier to the output signal is shown in Figure

3-27.

The effect of the transfer function between the bandwidth has been shown in Figure 3-28, and the phase-lead system in Figure 3-29 to 3-30 respectively. From



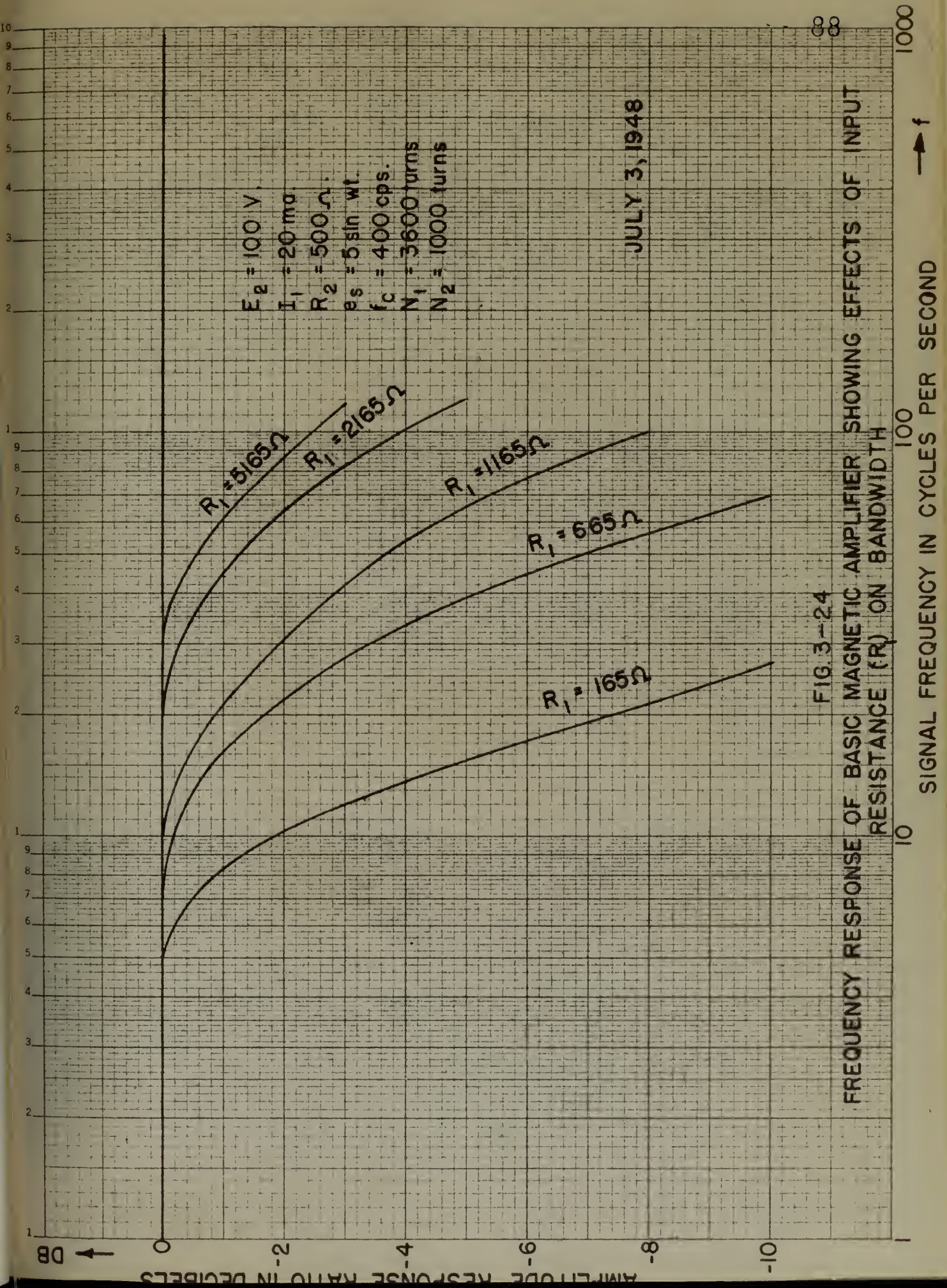
$$[P] = \frac{1}{1 + j2\pi f(CT)} = (AR) \angle \phi$$

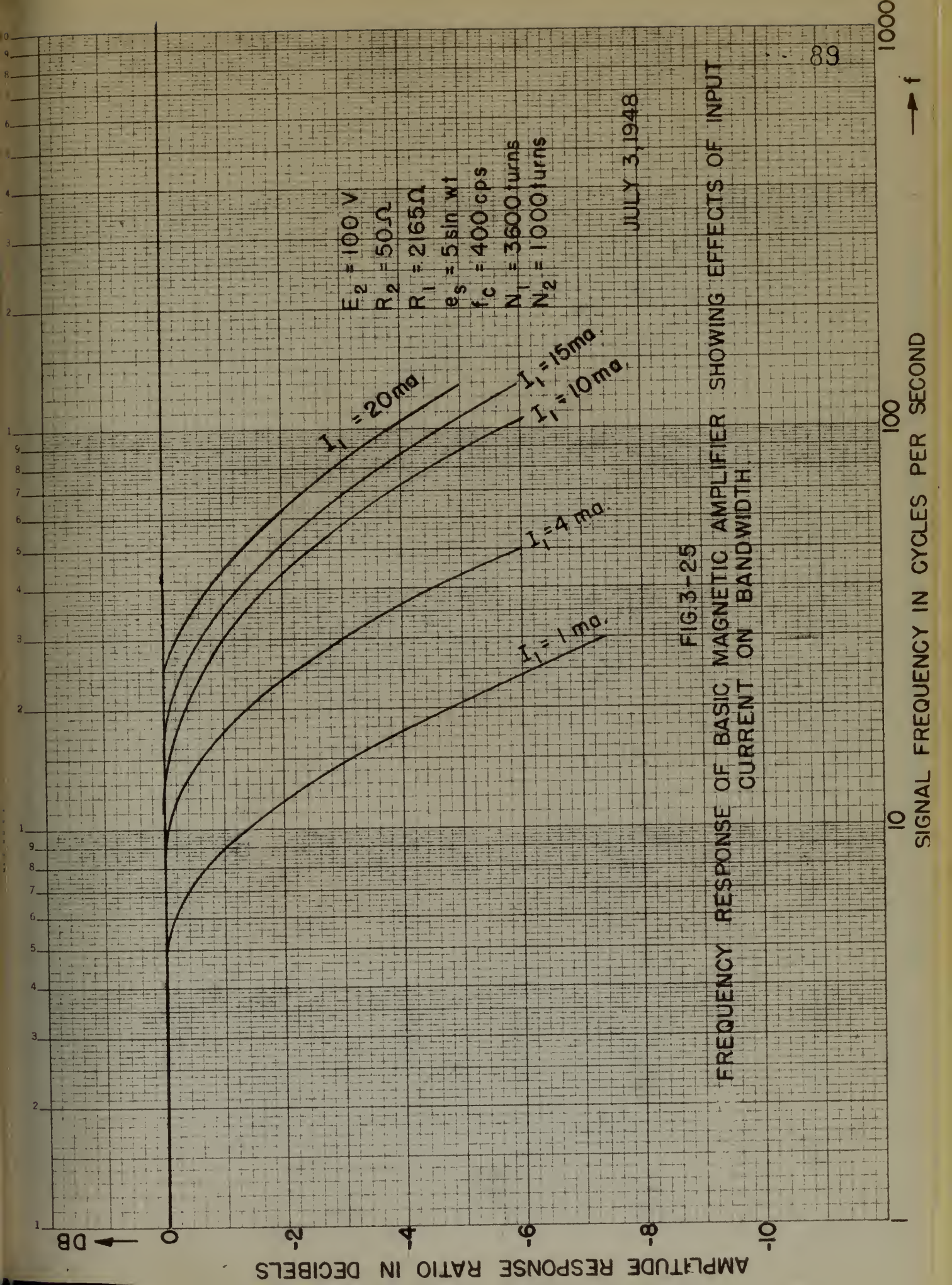
WHERE: $[P]$ - PERFORMANCE OPERATOR
 f - EXCITATION FREQUENCY
 (CT) - CHARACTERISTIC TIME

$$(AR) = \frac{1}{\sqrt{1 + [2\pi f(CT)]^2}}$$

$$(AR)_{dB} = 20 \log (AR)$$

$$\phi = \tan^{-1} [-2\pi f(CT)]$$





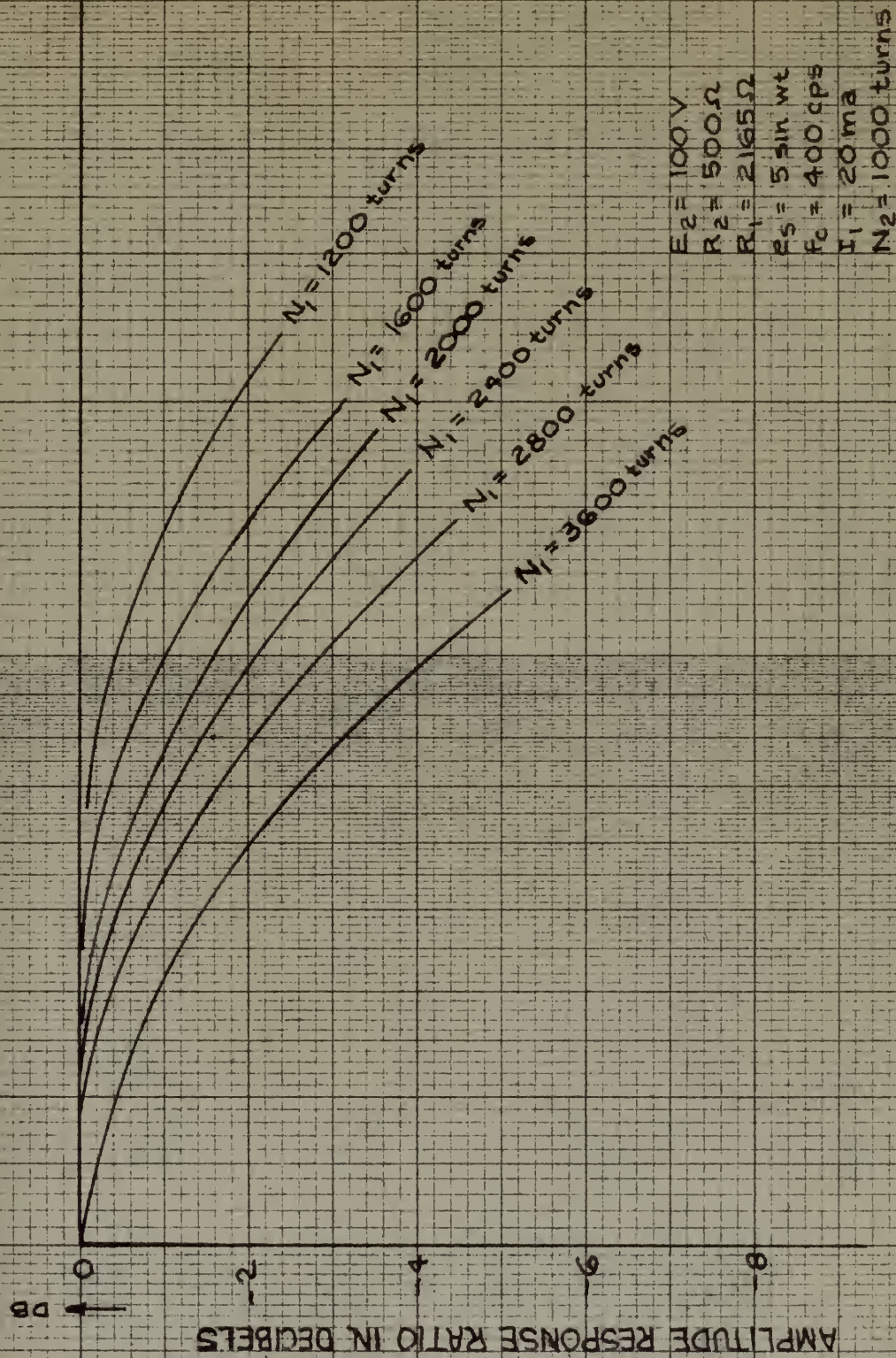


FIG. 3-26 FREQUENCY RESPONSE OF BASIC MAGNETIC AMPLIFIER SHOWING EFFECT OF INPUT TURNS ON BANDWIDTH

JULY 3, 1948

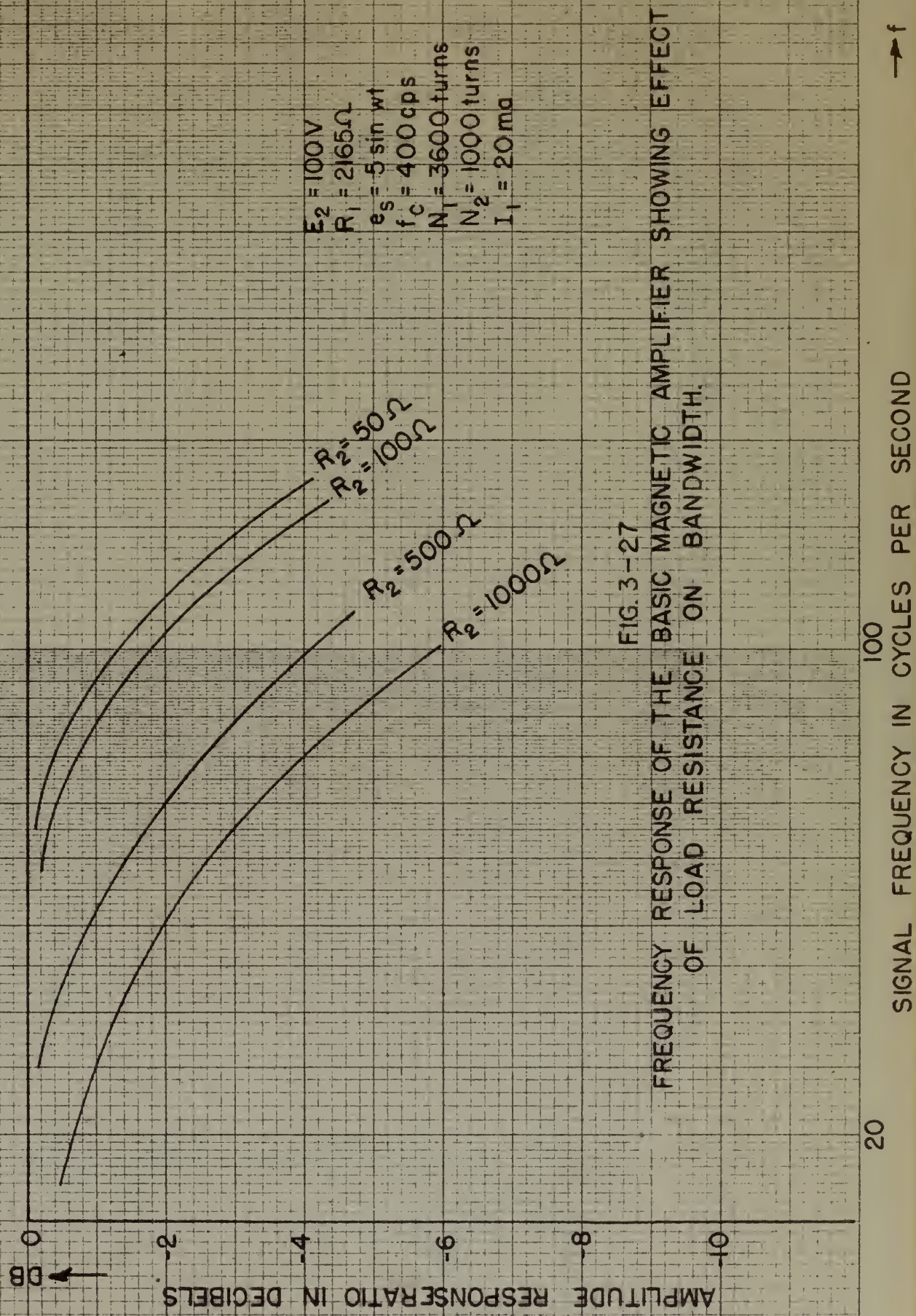


FIG. 3-27

FREQUENCY RESPONSE OF THE BASIC MAGNETIC AMPLIFIER SHOWING EFFECT OF LOAD RESISTANCE ON BANDWIDTH.

DB

AMPLITUDE RESPONSE RATIO IN DECIBELS

0 -2 -4 -6 -8 -10

2 3 4 5 6 7 8 9 10

1 2 3 4 5 6 7 8 9 10

10 9 8 7 6 5 4 3 2 1

$E_2 = 25V$
 $E_2 = 50V$
 $E_2 = 75V$
 $E_2 = 100V$

$R_2 = 500\Omega$
 $R_1 = 2165\Omega$
 $e_s = 5 \sin \omega t$
 $f_c = 400 \text{ cps}$
 $I_1 = 20 \text{ ma}$
 $N_1 = 3600 \text{ turns}$
 $N_2 = 2000 \text{ turns}$

FIG. 3-28_a

FREQUENCY RESPONSE OF THE BASIC MAGNETIC AMPLIFIER SHOWING EFFECT OF CARRIER POWER SUPPLY VOLTAGE (E_2) ON BANDWIDTH.

100

SIGNAL FREQUENCY IN CYCLES PER SECOND

1000

DB

AMPLITUDE RESPONSE RATIO IN DECIBELS

FIG. 3-29

FREQUENCY RESPONSE OF THE BASIC MAGNETIC AMPLIFIER SHOWING EFFECT OF OUTPUT TURNS ON BANDWIDTH.

$E_2 = 100V$
 $R_2 = 500\Omega$
 $R_1 = 2165\Omega$
 $e_s = 5 \sin wt$
 $f_c = 400 \text{ cps}$
 $I_1 = 20 \text{ ma}$
 $N_1 = 3600 \text{ turns}$

93
JULY 3, 1948

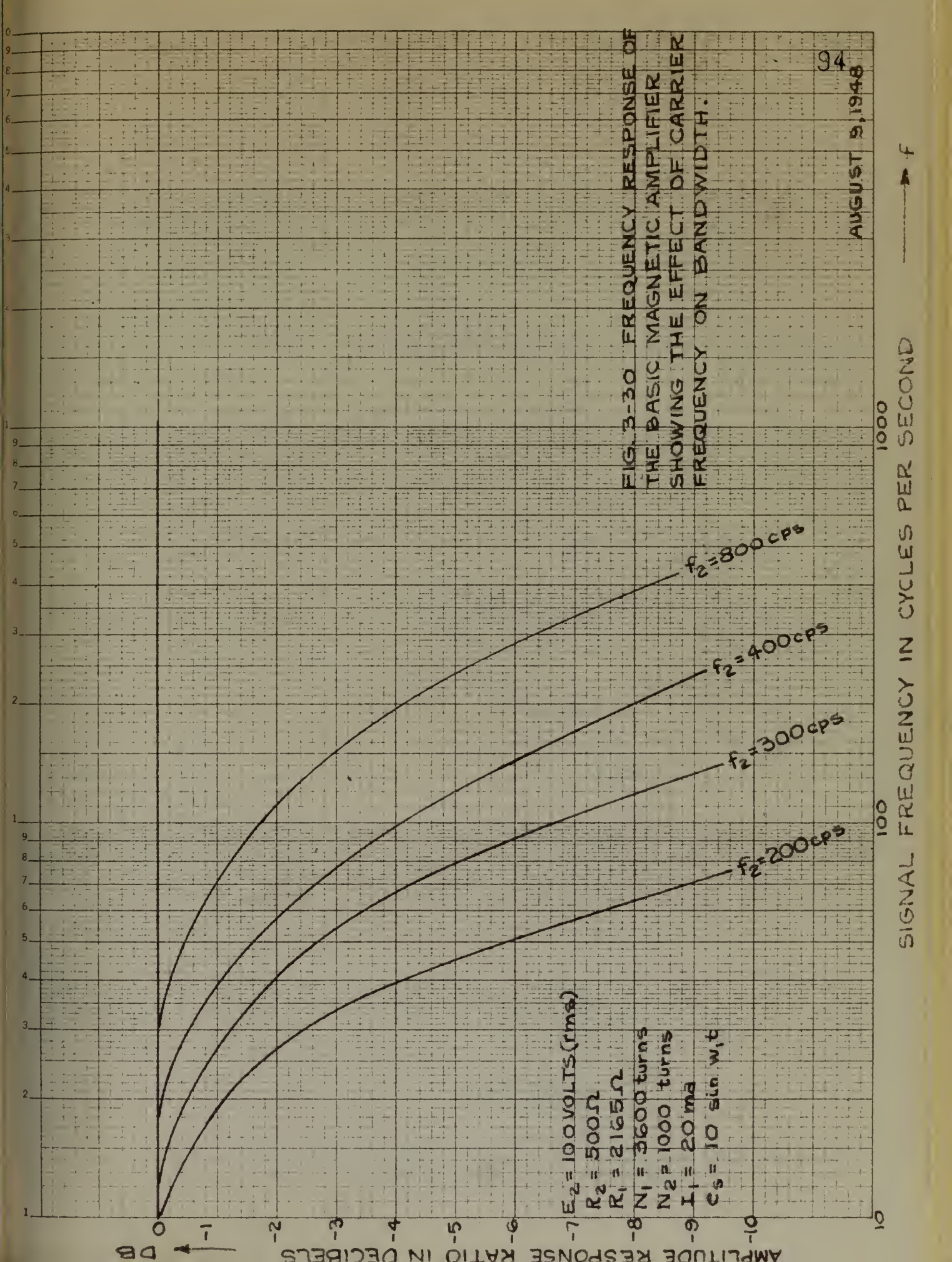
20

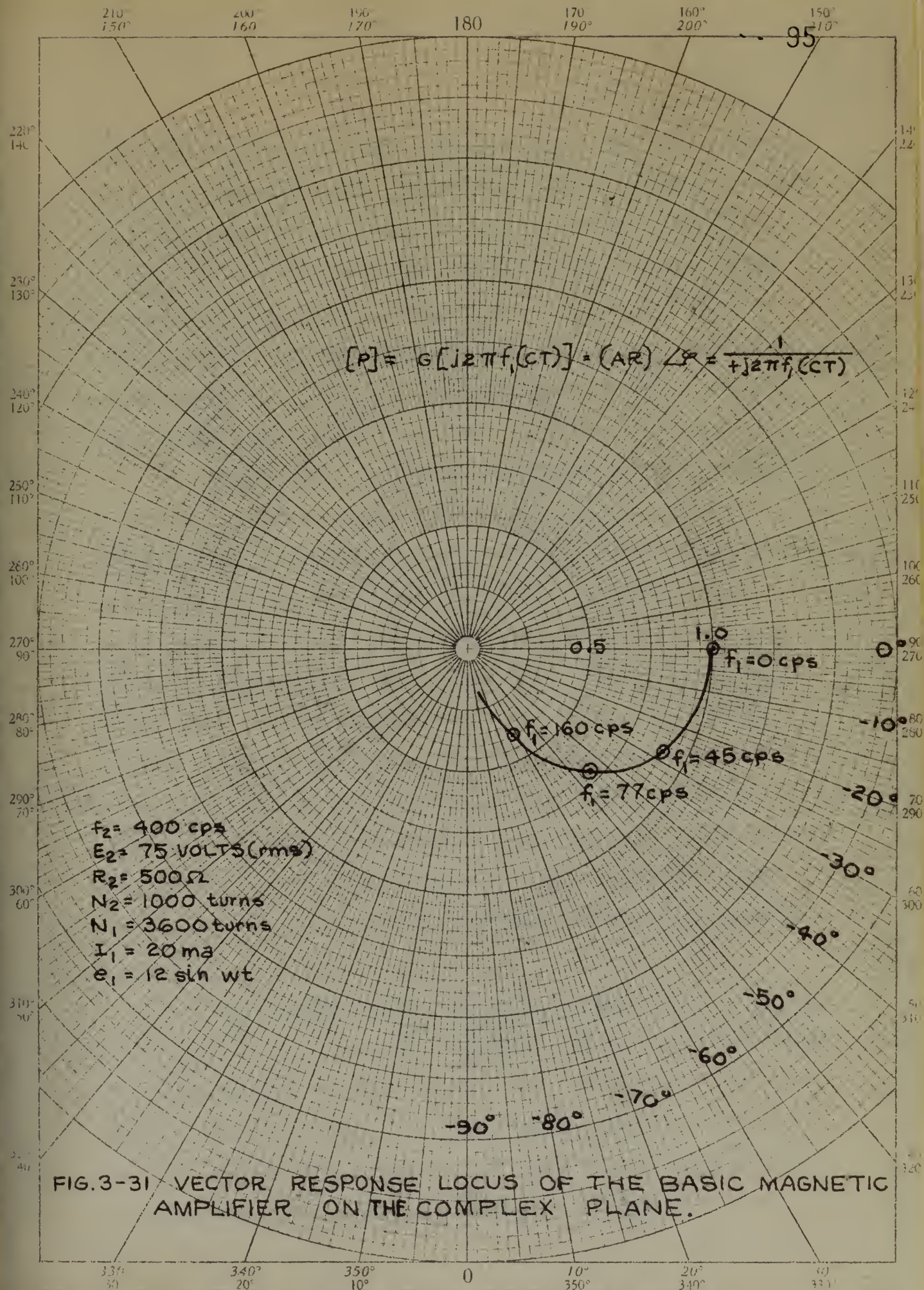
100

1000

SIGNAL FREQUENCY IN CYCLES PER SECOND

f





bandwidth measurements the characteristic time was computed using the Equation 3-32. Logarithmic plots of these results were then prepared for both control and carrier-circuit parameters, the former being shown in Figure 3-32 and the latter in Figure 3-33. As seen from the plots, (CT) was observed to be directly proportional to N_1 , and inversely proportional to R_1 and to the square-root of I_1 , thus confirming the results obtained from the transient studies.

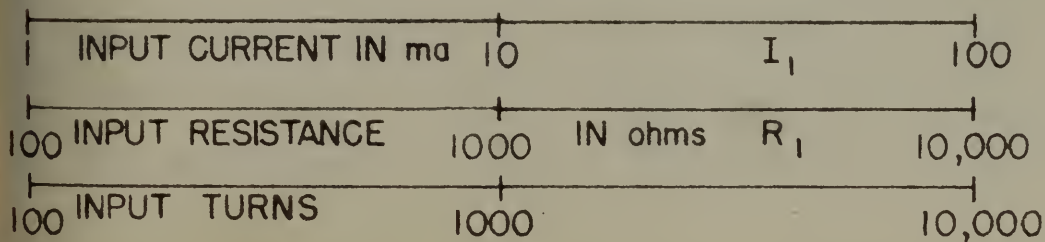
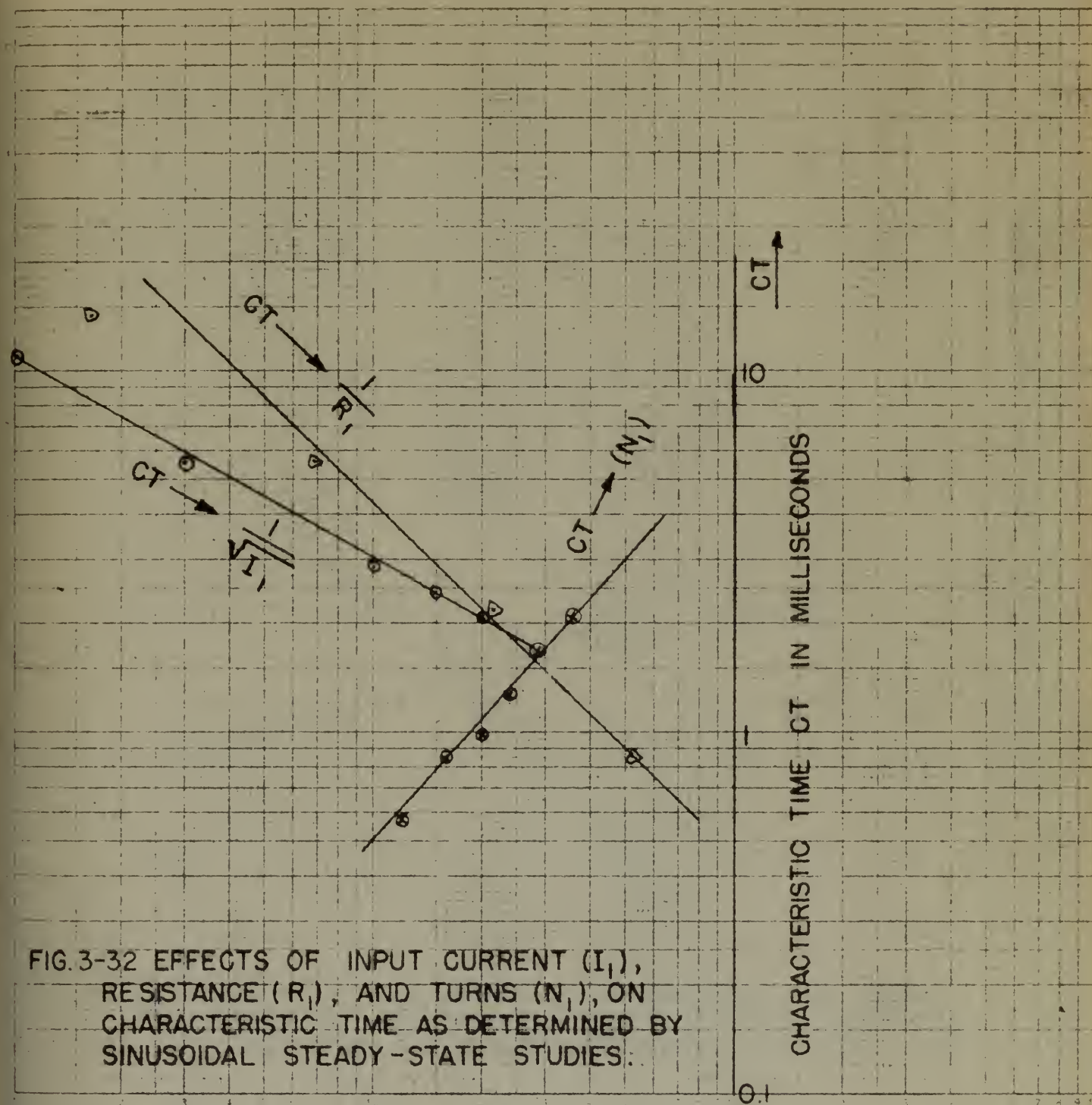
The effects caused by variations of the carrier-circuit parameters, as observed by frequency response methods, are in general agreement with those obtained from transient studies with some noticeable deviation. The variation of (CT) with E_2 and N_2 was identical. Whereas transient studies gave the result that (CT) depended very little upon f_2 , and almost not at all on R_2 , sinusoidal studies showed that (CT) varies directly with the one-third power of R_2 and inversely as f_2 . These differences are attributable to the fact that in the transient studies I_1 changes from zero to some discrete value, whereas in the sinusoidal studies I_1 varies periodically about a constant level.

The results of the dynamic studies, both transient and sinusoidal steady-state, indicate that in order to widen the bandwidth or shorten the characteristic time, it is desirable to increase R_1 , I_1 , f_2 , and N_2 , and to decrease N_1 and E_2 . In any case, f_2 would have to be sufficiently high to carry the intelligence as a modulated signal.

handicap between the two groups was not significant. Using the Bonferroni t -test, the difference between the two groups was not significant for each subject and within-subject parameter. The lowest value given is 0.05 (0.01 and 0.05) in Figure 3-11. As seen from the data, (0.01) was observed to be directly proportional to β_1 and inversely proportional to β_2 and to the square-root of β_3 . Thus one finding the results obtained from the constant method. The effects caused by variation in the subjects

clinical parameters, as observed by frequency response methods, are in general agreement with those obtained from frequency studies with more extensive techniques. The variation of (0.01) with β_1 and β_2 was identical. However, frequency studies gave the results that (0.01) increased very little upon β_1 , was almost constant with β_2 , and decreased studies about that (0.01) varied directly with the square-root of β_3 and inversely as β_4 . These differences are attributable to the fact that in the frequency studies β_1 appears from zero to some limited value, whereas in the clinical studies β_1 varies continuously about a constant level.

The results of the present study, with constant and variable step-size, indicate that the value of the handicap or step-size is not significant, it is variable to between 0.01, 0.05 and 0.10 and to between 0.01 and 0.10. In any case, β_1 would have to be sufficiently high to carry the information as a constant signal.



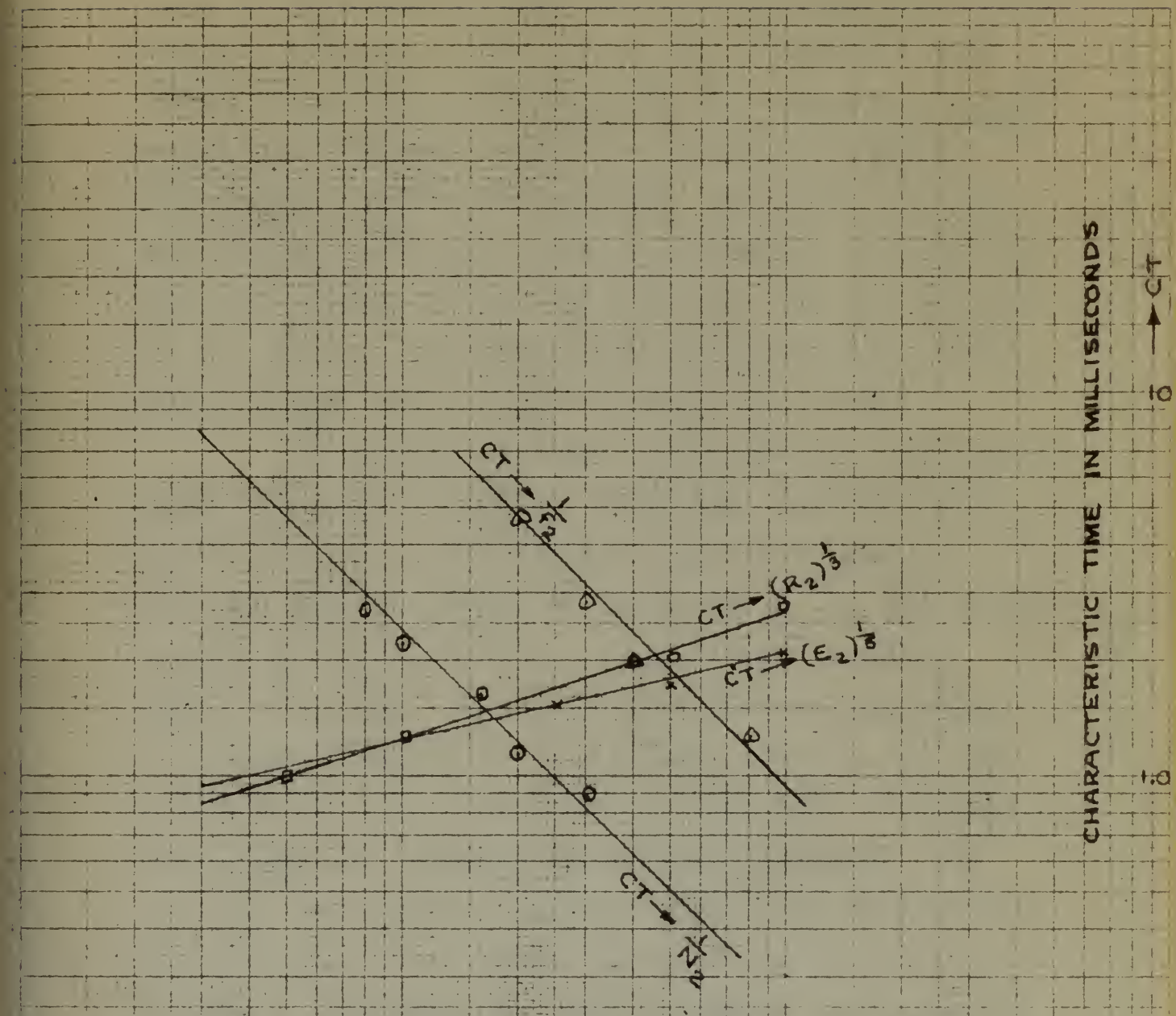


FIG. 3-33 EFFECT OF CARRIER-CIRCUIT PARAMETERS AND EXCITATION UPON CHARACTERISTIC TIME OBTAINED FROM EXPERIMENTAL SINUSOIDAL STEADY-STATE DATA.

10	CARRIER FREQUENCY	100	IN CYCLES/SECOND	1000 $\rightarrow f_2$
	RMS CARRIER VOLTAGE	10	IN VOLTS	$\rightarrow E_2$
100	OUTPUT WINDING	1000	IN TURNS	$\rightarrow N_2$
10	LOAD RESISTANCE	100	IN OHMS	$\rightarrow R_2$

Summary

The results of the experimental study of the basic magnetic-amplifier circuit reveal that a compromise must be made between gain and bandwidth. The adjustment of parameters in a direction to increase the gain is seen to simultaneously narrow the bandwidth. The design of a magnetic amplifier to meet a given specification is based first upon the selection of the core material. Once the material has been chosen, experimental data can be taken on a model, and the design scaled to meet specific requirements.

The carrier frequency is determined by the highest signal-frequency of interest. Amplifier bandwidth, sufficiently broad to pass the highest signal-frequency of interest, must be attained by increasing R_1 , I_1 , and by decreasing N_1 . The effects of E_2 and R_2 upon bandwidth appear to be small. To improve gain, however, exclusive of feedback techniques to be discussed later, R_1 , I_1 , and N_2 must be decreased, and N_1 and R_2 increased. A compromise between gain and bandwidth is obviously necessary. The fact that the magnetic amplifier, despite its nonlinearity, can approximate a first-order system, offers possibilities in certain applications in which electronic amplifiers are currently used.

The results of the experimental study of the basic negative-amplifier circuit reveal that a compensated amplifier must be made between gain and bandwidth. The adjustment of parameters in a direction to increase the gain is seen to simultaneously narrow the bandwidth. The design of a negative amplifier to meet a given specification is based first upon the selection of the core material. Once the material has been chosen, approximate data can be based on a model, and the design needed to meet specific requirements. The carrier frequency is determined by the desired signal-frequency of interest. Amplifier bandwidth, which is clearly based to pass the highest signal-frequency of interest, must be obtained by increasing R_1 , L_1 , and C_1 or decreasing R_2 . The effects of R_2 and C_2 upon bandwidth appear to be small. To improve gain, however, a negative of feedback technique to be discussed later, R_1 , L_1 , and C_1 must be decreased, and R_2 and C_2 increased. A comparison between gain and bandwidth is obviously necessary. The fact that the negative amplifier, despite its nonlinearity, can approximate a first-order system, offers possibilities in certain applications in which electronic amplifiers are currently used.

CHAPTER IV

THE MATHEMATICAL ANALYSIS OF THE MAGNETIC AMPLIFIER

Introduction to the Analytical Problem

The nonlinear character of the normal magnetizing curve of iron-cored saturable reactors has long placed a restraint on rigorous mathematical analysis of magnetic amplifiers. Since differential equations involving nonlinearities do not yield to ordinary methods of solution, a rigorous approach to this problem implies the use of machine methods of solution.

In the past, several approaches to the analysis and synthesis of the magnetic amplifier have been undertaken. Each method requires certain approximations. The two most important of these approaches are the linear-approximation technique, based on the division of the normal magnetization curve into linear regions,¹ and the reactor design technique developed at the Servomechanisms Laboratory at the Massachusetts Institute of Technology.²

Each of these techniques involves approximations which contribute to loss of rigor in the solution. In spite of these limitations, these approaches to the problem have been used with some success to predict and explain the steady-state performance of the magnetic amplifier. Unfortunately, neither technique is readily adaptable to the

-
1. Boyajian, A., "Mathematical Analysis of Nonlinear Circuits," G.E.Rev., 34, (1931), 531-539.
 2. Pease, W.M., "Design of a 400 Cycle Servomechanism," M.I.T. MS Thesis (1943).

prediction of the dynamic performance of the magnetic amplifier.

The use of the differential analyzer to solve the nonlinear differential equations of the magnetic amplifier circuit has offered an original method of attacking this important problem. Since there is no constraint on the nonlinearity of the character of the equations, the use of the analyzer has permitted a rigorous solution of the dynamic problem as well as the steady-state problem. The principal limitation imposed on the analytical solution is the necessity for neglecting hysteretic and eddy-current losses in the cores. If the cores used are of high quality, the neglect of hysteresis and eddy-current losses, as will be shown, is of no great consequence in the static or steady-state solution. The dynamic analytical solution will, however, suffer if losses are not considered. The physical effect of hysteretic loss in an iron-cored coil under excitation by fluxes of two or more different frequencies has not been fully explained, but in spite of this important fact, it was possible to make a semi-quantitative investigation of the effect of hysteresis in the magnetic-amplifier circuit. As has been described in Chapter III, and will be further considered later, hysteresis and eddy-current loss have a definite influence on the dynamic performance of the amplifier at different excitation-flux values, and consequently, the neglect of these phenomena

prediction of the dynamic performance of the machine in
 operation.

The use of the differential equation to solve
 the dynamic differential equation of the machine in
 operation has shown an original method of solving
 this important problem. Since there is no analytical
 the necessity of the solution of the equation, the use
 of the method has provided a rigorous solution of the
 dynamic problem as well as the steady-state problem. The
 principal limitation imposed on this analytical solution is
 the necessity for neglecting nonlinear and eddy-current
 losses in the system. In the case of low quality,
 the neglect of hysteresis and eddy-current losses, as will
 be shown, is not a great disadvantage in the study of
 steady-state behavior. The dynamic analysis solution
 will, however, require the use of the non-linear
 physical effect of hysteresis loss in an iron-core coil
 under excitation of fluxes of low or very different fre-
 quencies has not been fully explained, but in spite of this
 important fact, it was possible to make a satisfactory
 investigation of the effect of hysteresis in the magnetic
 circuit element. It has been suggested in Chapter III,
 and will be further considered later, hysteresis and eddy-
 current loss have a distinct influence on the dynamic
 performance of the machine at different excitation-time
 values, and consequently, the behavior of these phenomena

has somewhat hampered the mathematical investigation of the effects of certain parameters on the time-response of the amplifier. Variations in most of the circuit parameters have, however, been investigated satisfactorily by the analytical approach.

Formulation of the Equations

An investigation of the effect of fundamental parameters of the magnetic-amplifier circuit was established as the primary purpose of the analytical study. Accordingly, analytical investigations have been conducted, on the basic magnetic-amplifier circuit. The clarification of the fundamental behavior of the amplifier under the action of the various parameters which influence this behavior is intended to establish criteria which will then be applicable to the more complex magnetic-amplifier circuits involving feedback.

Experimental studies of the basic magnetic amplifier have indicated that the following circuit parameters influence the transient and steady-state performance of the amplifier: (1) Input-circuit resistance, R_1 , (2) Input-circuit coil turns, N_1 , (3) Input-circuit current, I_1 , (4) Output-circuit resistance, R_2 , (5) Output-circuit coil turns, N_2 , (6) Peak value of the output-circuit alternating voltage, E_2 , and (7) Frequency, ω , of the output-circuit alternating-voltage. These parameters are further identified in Figure 4-1. Analytical

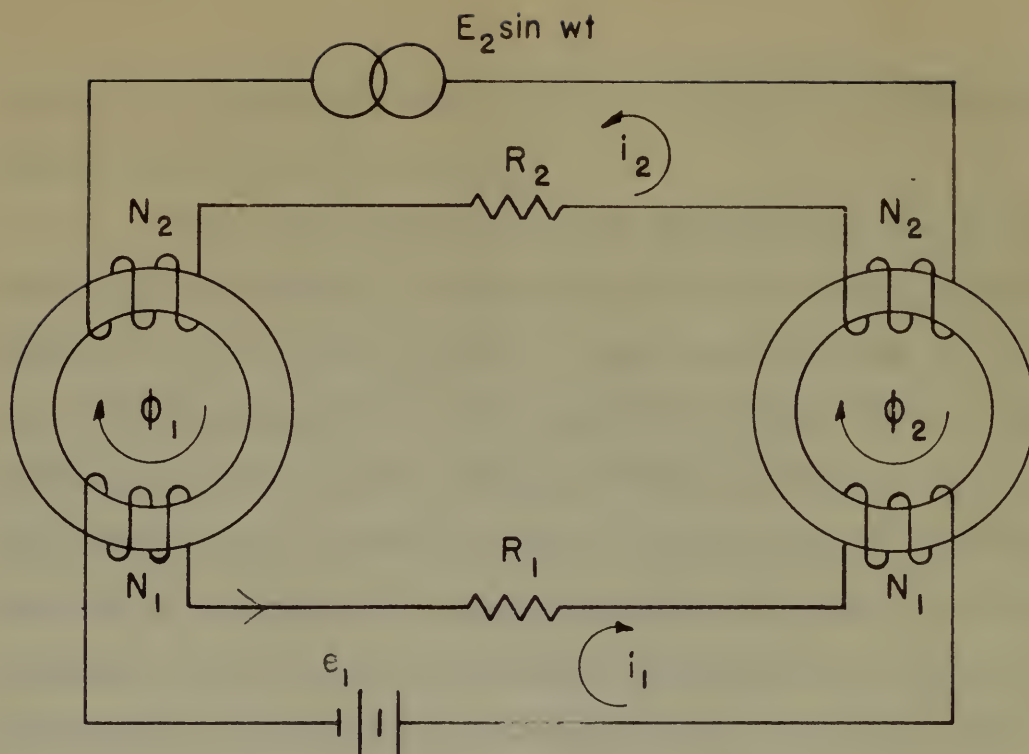


FIG. 4-1 BASIC MAGNETIC AMPLIFIER CIRCUIT

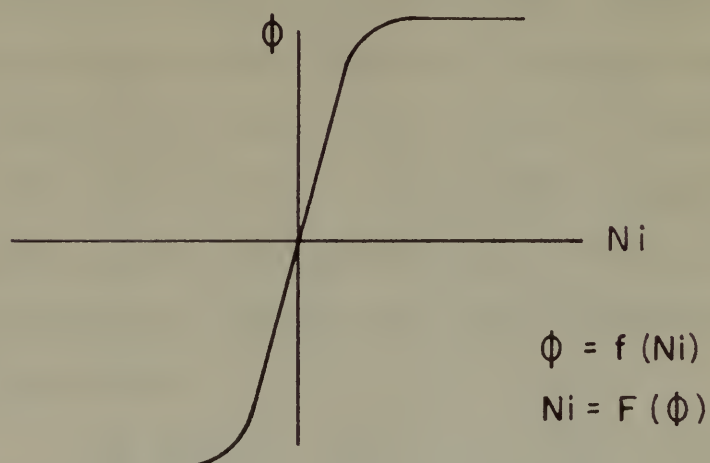


FIG. 4-2 NON-LINEAR RELATIONSHIP BETWEEN FLUX AND MAGNETIZING FORCE.

studies are conducted in a manner designed to indicate the effects of these parameters.

The analytical transient response of the magnetic amplifier is studied through the medium of a step function applied to the input circuit. This step function is applied as a voltage, e_1 , across the input terminals of the amplifier. The applied step voltage causes a current, i_1 , to flow in the input circuit, and a current, i_2 , to flow in the output circuit. In each case solved by the differential analyzer, the solution is carried through the transient period until steady-state conditions are reached. The even-harmonic currents, i_1 , which flow in the input circuit, and the odd-harmonic currents, i_2 , which flow in the output circuit, were recorded for each solution of the problem. The rate of buildup of current in the output circuit during the transient state establishes the characteristic time of the amplifier circuit for each condition observed. As was the case in the experimental studies described in Chapter III, the characteristic time of the amplifier is defined as the time required for the output current to reach 63% of its steady-state value after the application of the step function input.

In summary, then, the values of i_1 , i_2 and characteristic time, (CT), were observed for step function-input variations of e_1 for various conditions on the parameters R_1 , N_1 , R_2 , N_2 , E_2 , and ω . Minor deviations from this procedure will be discussed subsequently.

studies are contained in a separate volume in connection with the
 studies of the present volume.

The following studies are of the present volume.

Chapter I is devoted to the study of the present volume
 applied to the present volume. This study is applied
 as a whole, and the present volume of the present

time. The present volume is a whole, and the present

time in the present volume, and the present

The present volume is a whole, and the present

time, the present volume is a whole, and the present

period will be a whole, and the present

period will be a whole, and the present

and the present volume is a whole, and the present

period, and the present volume is a whole, and the present

The present volume is a whole, and the present

the present volume is a whole, and the present

The present volume is a whole, and the present

the present volume is a whole, and the present

the present volume is a whole, and the present

the present volume is a whole, and the present

the present volume is a whole, and the present

the present volume is a whole, and the present

In summary, the present volume is a whole, and the present

the present volume is a whole, and the present

the present volume is a whole, and the present

the present volume is a whole, and the present

the present volume is a whole, and the present

The equations used in the analytical solution are based upon the circuit of Figure 4-1, and the non-linear function of Figure 4-2. In Figure 4-1, the flux in Core 1 is defined as ϕ_1 while the flux in Core 2 is defined as ϕ_2 . The positive directions of these fluxes are shown by the arrows on the figure. Similarly, the positive directions of the currents i_1 and i_2 are indicated by arrows. The remaining parameters of this circuit have been identified. Figure 4-2 is a sketch of the normal magnetization curve of the core material used in the study. This figure is based on empirical data which was measured as described in Chapter II. In the figure, the flux in the cores, ϕ , in webers, is plotted against the magnetizing force, Ni , expressed in ampere-turns. The studies were conducted using the MKS system of units with all voltages expressed in volts, all currents expressed in amperes, resistances expressed in ohms, and time expressed in seconds.

From the circuit of Figure 4-1, it is possible to write the equilibrium equations of the system on the loop basis for the input and output circuits, respectively:

$$e_1 = R_1 i_1 + N_1 \frac{d\phi_1}{dt} - N_1 \frac{d\phi_2}{dt} \quad (4-1)$$

$$e_2 = R_2 i_2 + N_2 \frac{d\phi_1}{dt} + N_2 \frac{d\phi_2}{dt} \quad (4-2)$$

From Figures 4-1 and 4-2, the relationships between flux and magnetizing force are established:

The question arises in the analytical solution
 are based upon the theory of Figure 4-1, and the non-
 linear function of Figure 4-1. In Figure 4-1, the stress
 in case I is defined as σ_1 and the stress in case II as
 defined as σ_2 . The positive directions of these stresses
 are shown by the arrows in the figure. Similarly, the
 positive directions of the strains ϵ_1 and ϵ_2 are indi-
 cated by arrows. The resulting positions of this element
 have been indicated. Figure 4-2 is a sketch of the
 linear relationship curve at the core material used in
 the study. This figure is based on experimental data which
 has been used as described in Figure II. In the figure,
 the line in the center, σ , is shown, is plotted against
 the compressive force, σ , measured in pounds-per-inch. The
 strains were computed from the σ - ϵ curve of units with
 all stresses expressed in σ , all strains expressed in
 ϵ , and the relationship between σ and ϵ is shown
 in Figure 4-2.

From the sketch of Figure 4-1, it is possible
 to write the equilibrium equations of the stress of the
 two cases for the input and output elements, respectively:

$$\sigma_1 = \sigma_2 + \frac{\partial \sigma}{\partial x} \Delta x \quad (4-1)$$

$$\sigma_2 = \sigma_1 + \frac{\partial \sigma}{\partial x} \Delta x \quad (4-2)$$

From Figures 4-1 and 4-2, the relationship between
 the two resulting forces are established:

$$\phi = f(N_i) \quad (4-3)$$

$$N_i = f(\phi) \quad (4-4)$$

$$\phi_1 = f(N_2 i_2 + N_1 i_1) \quad (4-5)$$

$$\phi_2 = f(N_2 i_2 - N_1 i_1) \quad (4-6)$$

Equations 4-1 and 4-2 are next manipulated as shown in the following series of expressions:

$$e_1 - i_1 R_1 = N_1 \left(\frac{d\phi_1}{dt} - \frac{d\phi_2}{dt} \right) \quad (4-7)$$

$$e_2 - i_2 R_2 = N_2 \left(\frac{d\phi_1}{dt} + \frac{d\phi_2}{dt} \right) \quad (4-8)$$

If Equation 4-7 is divided by N_1 , and Equation 4-8 is divided by N_2 , the expressions may be added and subtracted to yield Equations 4-9 and 4-10 respectively:

$$\left(\frac{e_1 - i_1 R_1}{N_1} \right) + \left(\frac{e_2 - i_2 R_2}{N_2} \right) = 2 \frac{d\phi_1}{dt} \quad (4-9)$$

$$-\left(\frac{e_1 - i_1 R_1}{N_1} \right) + \left(\frac{e_2 - i_2 R_2}{N_2} \right) = 2 \frac{d\phi_2}{dt} \quad (4-10)$$

or

$$\frac{d\phi_1}{dt} = \frac{1}{2} \left[\left(\frac{e_2 - i_2 R_2}{N_2} \right) + \left(\frac{e_1 - i_1 R_1}{N_1} \right) \right] \quad (4-11)$$

$$\frac{d\phi_2}{dt} = \frac{1}{2} \left[\left(\frac{e_2 - i_2 R_2}{N_2} \right) - \left(\frac{e_1 - i_1 R_1}{N_1} \right) \right] \quad (4-12)$$

Integrating Equations 4-11 and 4-12 with respect to time, and combining these expressions with Equations 4-5 and 4-6, gives:

$$\begin{aligned} (11-1) \quad & \frac{\partial}{\partial x} \left(\frac{\partial \phi}{\partial x} + \frac{\partial \psi}{\partial y} \right) = 0 \\ (12-1) \quad & \frac{\partial}{\partial y} \left(\frac{\partial \phi}{\partial x} + \frac{\partial \psi}{\partial y} \right) = 0 \\ (13-1) \quad & \frac{\partial}{\partial x} \left(\frac{\partial \phi}{\partial y} - \frac{\partial \psi}{\partial x} \right) = 0 \\ (14-1) \quad & \frac{\partial}{\partial y} \left(\frac{\partial \phi}{\partial y} - \frac{\partial \psi}{\partial x} \right) = 0 \end{aligned}$$

Equations (11-1) and (12-1) are not independent as they are identical. Equations (13-1) and (14-1) are also identical.

$$\begin{aligned} (15-1) \quad & \frac{\partial}{\partial x} \left(\frac{\partial \phi}{\partial x} + \frac{\partial \psi}{\partial y} \right) = 0 \\ (16-1) \quad & \frac{\partial}{\partial y} \left(\frac{\partial \phi}{\partial x} + \frac{\partial \psi}{\partial y} \right) = 0 \end{aligned}$$

If Equation (15-1) is divided by $\frac{\partial \phi}{\partial x}$ and Equation (16-1) is divided by $\frac{\partial \psi}{\partial y}$, the expressions may be added and subtracted to yield Equations (17-1) and (18-1) respectively:

$$(17-1) \quad \frac{\partial}{\partial x} \left(\frac{\partial \phi}{\partial x} + \frac{\partial \psi}{\partial y} \right) = 0$$

$$(18-1) \quad \frac{\partial}{\partial y} \left(\frac{\partial \phi}{\partial x} + \frac{\partial \psi}{\partial y} \right) = 0$$

or

$$(19-1) \quad \left[\frac{\partial}{\partial x} \left(\frac{\partial \phi}{\partial x} + \frac{\partial \psi}{\partial y} \right) + \frac{\partial}{\partial y} \left(\frac{\partial \phi}{\partial x} + \frac{\partial \psi}{\partial y} \right) \right] = 0$$

$$(20-1) \quad \left[\frac{\partial}{\partial x} \left(\frac{\partial \phi}{\partial x} + \frac{\partial \psi}{\partial y} \right) - \frac{\partial}{\partial y} \left(\frac{\partial \phi}{\partial x} + \frac{\partial \psi}{\partial y} \right) \right] = 0$$

Integrating (19-1) and (20-1) with respect to x and y respectively, and combining these expressions with Equations (11-1) and (12-1) gives

$$\phi_1 = r (N_2 i_2 + N_1 i_1) = \frac{1}{2} \int_0^t \left[\frac{e_2 - i_2 R_2}{N_2} + \frac{e_1 - i_1 R_1}{N_1} \right] dt \quad (4-13)$$

$$\phi_2 = r (N_2 i_2 - N_1 i_1) = \frac{1}{2} \int_0^t \left[\frac{e_2 - i_2 R_2}{N_2} - \frac{e_1 - i_1 R_1}{N_1} \right] dt \quad (4-14)$$

By applying Equation 4-4 to Equations 4-13 and 4-14, the following expressions which define the behavior of the magnetic amplifier are obtained:

$$H_1 = N_2 i_2 + N_1 i_1 = F_1 \left\{ \frac{1}{2} \int_0^t \left[\frac{e_2 - i_2 R_2}{N_2} + \frac{e_1 - i_1 R_1}{N_1} \right] dt \right\} \quad (4-15)$$

$$H_2 = N_2 i_2 - N_1 i_1 = F_2 \left\{ \frac{1}{2} \int_0^t \left[\frac{e_2 - i_2 R_2}{N_2} - \frac{e_1 - i_1 R_1}{N_1} \right] dt \right\} \quad (4-16)$$

In Equations 4-15 and 4-16, the functions H_1 and H_2 are defined for convenience in the differential analyzer solution. From these expressions, it is now possible to define i_1 and i_2 in terms of H_1 and H_2 :

$$i_1 = \frac{H_1 - H_2}{2N_1} \quad (4-17)$$

$$i_2 = \frac{H_1 + H_2}{2N_2} \quad (4-18)$$

Recalling that the input voltage is applied as a step function, and that the output voltage is sinusoidal, the following equations are written:

$$e_1 = E_1 u(t) \quad (4-19)$$

$$e_2 = E_2 \sin \omega_2 t \quad (4-20)$$

The differential analyzer problem is formulated from Equations 4-15 through 4-20 inclusive.

$$H_1 = \frac{1}{2} \left(\frac{1}{2} + \frac{1}{2} \right) = \frac{1}{2} \quad (11-11)$$

$$H_2 = \frac{1}{2} \left(\frac{1}{2} + \frac{1}{2} \right) = \frac{1}{2} \quad (11-12)$$

By applying Equation 11-10 to Equations 11-11 and 11-12, the following expressions which define the behavior of the magnetic amplifier are obtained:

$$H_1 = \frac{1}{2} \left(\frac{1}{2} + \frac{1}{2} \right) = \frac{1}{2} \quad (11-13)$$

$$H_2 = \frac{1}{2} \left(\frac{1}{2} + \frac{1}{2} \right) = \frac{1}{2} \quad (11-14)$$

In Equations 11-13 and 11-14, the functions H_1 and H_2 are defined for convenience in the differential analysis. From these expressions, it is now possible to obtain i_1 and i_2 in terms of H_1 and H_2 :

$$i_1 = \frac{H_1}{2} \quad (11-15)$$

$$i_2 = \frac{H_2}{2} \quad (11-16)$$

Assuming that the input voltage is applied as a step function, and that the output voltage is measured, the following equations are obtained:

$$H_1 = \frac{1}{2} \quad (11-17)$$

$$H_2 = \frac{1}{2} \quad (11-18)$$

The differential analysis problem is formulated as follows: Equations 11-17 through 11-18 inclusive.

Preparation of the Differential Analyzer Problem

The M.I.T. Differential Analyzer No. 1 was employed for the solution of the equations of the magnetic amplifier. The operation of this machine is totally mechanical, in that all process of integration, addition and subtraction, multiplication, the generation and introduction of functions, and the recording of results, are accomplished by mechanical means. The machine has been described in detail in the literature^{1,2} and no further description will be attempted in this report. Similarly, the nature of the development of scale factors for use on this analyzer has been discussed in detail, and will not be dealt with further here. The reader is referred to the references given for further study of the analyzer and for further understanding of the method by which the scale factors were established for this problem.

After the equations of the problem have been formulated, limits over which the various parameters of the equations may be expected to vary are established. The knowledge of these limits permits the selection of scale factors which will allow the greatest flexibility of the parameters with minimum requisite changes in the layout of the machine. A schematic diagram of the analyzer layout is then constructed. Gear boxes, differ-

-
1. Bush, V., "The Differential Analyzer," J.F.I., 212, (1931), 447-448.
 2. Bush, V. and Caldwell, S.H., "A New Type Differential Analyzer," J.F.I., 240, (1945), 255-326.

PREPARATION OF THE HYDROLYZABLE ANALYTICAL SYSTEM

The M.I.T. Hydrolyzable Analytical System is a

designed for the solution of the equations of the hydrolyzable

analytical. The equations of the hydrolyzable are

mechanical, in that all phases of hydrolyzable, including

and hydrolyzable, including, the hydrolyzable and

hydrolyzable of hydrolyzable, and the hydrolyzable of hydrolyzable,

are described by mechanical means. The hydrolyzable and

has been described in detail in the literature^{1,2} and in the

first description will be attempted in this report.

Similarly, the nature of the development of hydrolyzable

for use in this system has been discussed in detail, and

will not be dealt with further here. The reader is re-

ferred to the references given for further study of the

analytical and for further understanding of the nature of

which the hydrolyzable was established for this system.

After the equations of the hydrolyzable have been

formulated, it is over which the various parameters of

the equations are to be varied so that the hydrolyzable

The knowledge of these hydrolyzable is the selected of

several factors which will allow the greatest flexibility

of the hydrolyzable with various mechanical changes in the

hydrolyzable of the hydrolyzable. A schematic diagram of the

hydrolyzable system is shown in Figure 1. The hydrolyzable, which

1. Hydrolyzable Analytical System, U.S. Pat. 2,711,111

2. Hydrolyzable Analytical System, U.S. Pat. 2,711,112

ential units and integrator units are provided to perform the necessary functions of the equations. Scale factors are then established to meet the conditions of the equations and these factors are fitted to a schematic diagram. The selection of scale factors is restricted somewhat by the actual gear-ratios available, but, in general, there is sufficient flexibility that scale factors may be chosen in a manner which very closely approximates any desired physical condition. Figure 4-3 shows the actual schematic diagram which was made for the initial problem applied to the machine in this study. In this figure, integrators are identified by number, differentials are identified by number, and gear boxes are identified by letters. In this problem, the sinusoidal voltage of the output circuit, E_2 , is generated by integrators No. 3 and 4. The fluxes in each core are integrated in accordance with equations (15) and (16) in integrator units No. 1 and 2. The nonlinear relationship between flux and magnetizing force is inserted by the manually-operated input tables No. 1 and 2, and the resultant currents, i_1 and i_2 , are plotted on the output table. The step voltage, e_1 , is applied to the lead screws of the integrators No. 1 and 2.

The problem shown in Figure 4-3 represents the conditions which obtained during Runs 1-13 inclusive of the analyzer study. The actual values of the parameters

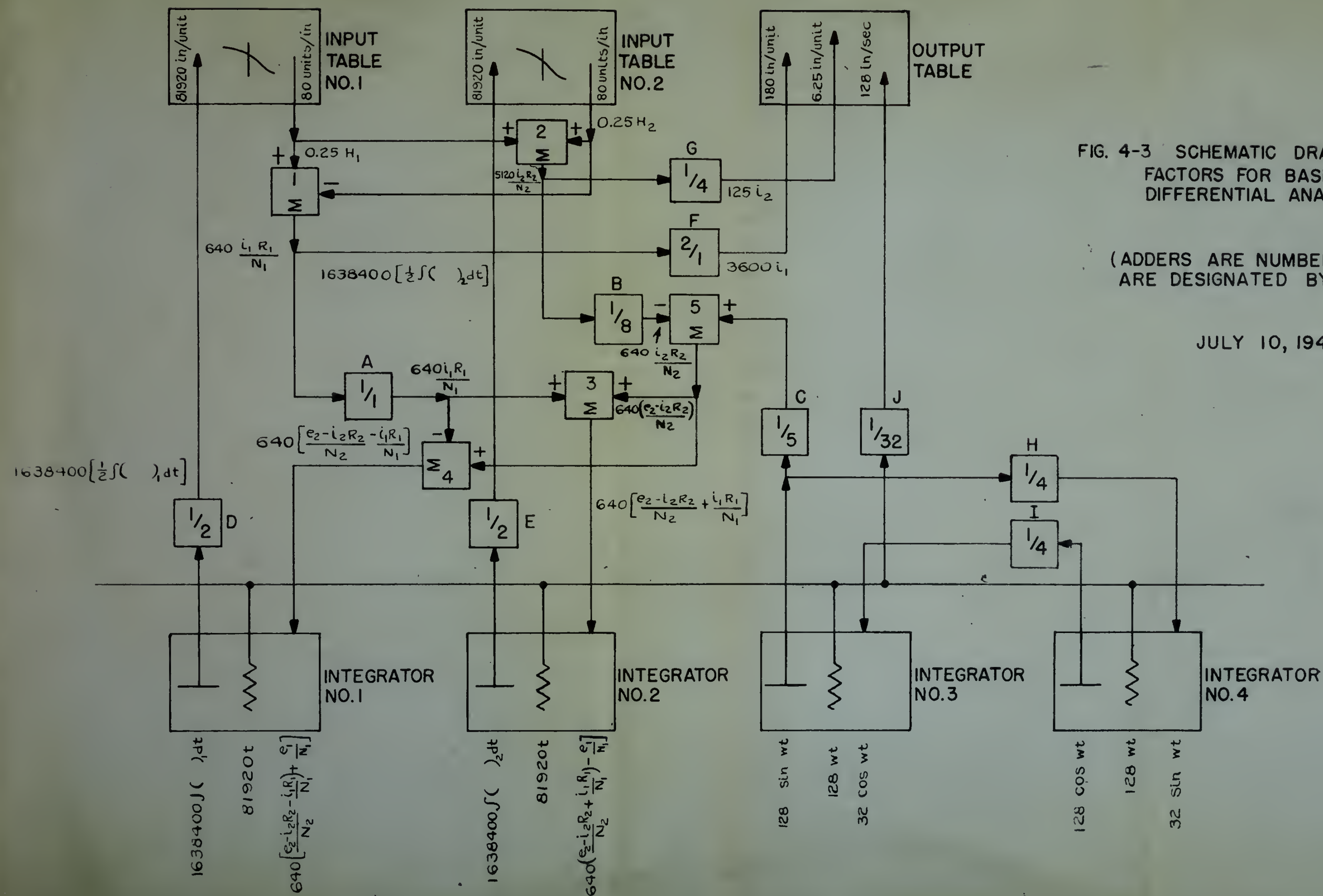


FIG. 4-3 SCHEMATIC DRAWING AND SCALE FACTORS FOR BASIC MECHANICAL DIFFERENTIAL ANALYZER PROBLEM.

(ADDERS ARE NUMBERED; GEAR BOXES ARE DESIGNATED BY LETTERS.)

JULY 10, 1948

$f_c = 102 \text{ c.p.s.}$
 $R_1 = 97.8 \text{ ohms}$
 $R_2 = 10125 \text{ ohms}$
 $E_2 = 40 \sin \omega t$
 $N_1 = 3600 \text{ T}$
 $N_2 = 1000 \text{ T}$

for these runs are tabulated on Chart 4-1. On this chart the parameters and the scale factors, as well as the gear ratios which provide the scale factors, are tabulated for each solution of the equations. The scale factors, and the means by which these were obtained, are shown on Figure 4-3, and may be correlated with the tabulated data of Chart 4-1.

After the schematic diagram and the scale factors have been determined, it is necessary to formulate the actual layout of the problem on the differential analyzer. This phase is subject to limitations on the physical positioning of the various problem components within the machine structure. In the layout used for this problem, a special effort was made to provide a maximum of flexibility to permit the variation of the several parameters with a minimum of required changes of the actual physical layout. With this objective in mind, an effort was made to anticipate the changes in scale factors occasioned by the parameter changes, and wherever possible, additional gear ratios were set up in the gear boxes, and these were left disconnected except when actually in use. Considerable saving in time is enabled by a procedure of this type. The physical layout of the differential analyzer for the problems shown in the schematic drawing of Figure 4-3, Runs 1-13, is shown in Figure 4-4. Changes in the layout for the remaining solutions are tabulated on Charts 4-1 and 4-2.

for these two are indicated on Chart 4-1. On this
chart the horizontal and the vertical factors, as well as
the gear ratios which provide the basic factors, are
indicated for each selected of the equations. The same
factors, and the same of which there were selected, are
shown on Figure 4-2, and may be correlated with the later
factors of Chart 4-1.

After the equations are given and the basic fac-
tors have been determined, it is necessary to formulate
the actual layout of the problem on the differential
analyzer. This phase is subject to limitations on the
physical positioning of the various problem components
within the machine structure. In the layout used for
this problem, a special effort was made to provide a maxi-
mum of flexibility to permit the variation of the various
parameters with a minimum of mechanical changes of the ma-
chine physical layout. This was achieved in such a way
effort was made to establish the changes in basic factors
indicated by the parameter changes, and wherever possible,
additional gear ratios were put up in the gear boxes, and
these were left disconnected except when actually in use.
Consequently moving in time is needed by a procedure of
this type. The physical layout of the differential
analyzer for the problem used in the mechanical drawing
of Figure 4-2, (see 4-3), is shown in Figure 4-4. Changes
in the layout for the various solutions are indicated on
Charts 4-1 and 4-2.

PETER
WERNER

July 1943

22.7

No 1

D.A 131

[illegible]

PETZER
WERNER
GROSSMAN

VULY 1948

MIT DIFFERENTIAL HYPER No. 1

DN 131

RW No	W	E ₂ VOLTS	R ₁ OHMS	R ₂ OHMS	N ₁ TURNS	N ₂ TURNS	GEAR BOX RATIOS												INPUT SPEED RPM'S (IN AMP)												STEP FORWARD TURNS	REMARKS																																																																																																																																																																																																																																																																																																																																																																																																																																																																																																																																																																																																																																																																																																																																																																																																																																																																																																																																																																																																																																																																																																																																																																																																																								
							A	B	C	D	E	F	G	H	I	J	K	L	M	N	O	P	Q	R	S	T	U	V	W	X			Y	Z																																																																																																																																																																																																																																																																																																																																																																																																																																																																																																																																																																																																																																																																																																																																																																																																																																																																																																																																																																																																																																																																																																																																																																																																																						
63	2560	100	10125	422.5	2543	1000	1	5	16	1	2	1	2	1	2	1	2	1	2	1	2	1	2	1	2	1	2	1	2	1	2	1	2	1	2	1	2	1	2	1	2	1	2	1	2	1	2	1	2	1	2	1	2	1	2	1	2	1	2	1	2	1	2	1	2	1	2	1	2	1	2	1	2	1	2	1	2	1	2	1	2	1	2	1	2	1	2	1	2	1	2	1	2	1	2	1	2	1	2	1	2	1	2	1	2	1	2	1	2	1	2	1	2	1	2	1	2	1	2	1	2	1	2	1	2	1	2	1	2	1	2	1	2	1	2	1	2	1	2	1	2	1	2	1	2	1	2	1	2	1	2	1	2	1	2	1	2	1	2	1	2	1	2	1	2	1	2	1	2	1	2	1	2	1	2	1	2	1	2	1	2	1	2	1	2	1	2	1	2	1	2	1	2	1	2	1	2	1	2	1	2	1	2	1	2	1	2	1	2	1	2	1	2	1	2	1	2	1	2	1	2	1	2	1	2	1	2	1	2	1	2	1	2	1	2	1	2	1	2	1	2	1	2	1	2	1	2	1	2	1	2	1	2	1	2	1	2	1	2	1	2	1	2	1	2	1	2	1	2	1	2	1	2	1	2	1	2	1	2	1	2	1	2	1	2	1	2	1	2	1	2	1	2	1	2	1	2	1	2	1	2	1	2	1	2	1	2	1	2	1	2	1	2	1	2	1	2	1	2	1	2	1	2	1	2	1	2	1	2	1	2	1	2	1	2	1	2	1	2	1	2	1	2	1	2	1	2	1	2	1	2	1	2	1	2	1	2	1	2	1	2	1	2	1	2	1	2	1	2	1	2	1	2	1	2	1	2	1	2	1	2	1	2	1	2	1	2	1	2	1	2	1	2	1	2	1	2	1	2	1	2	1	2	1	2	1	2	1	2	1	2	1	2	1	2	1	2	1	2	1	2	1	2	1	2	1	2	1	2	1	2	1	2	1	2	1	2	1	2	1	2	1	2	1	2	1	2	1	2	1	2	1	2	1	2	1	2	1	2	1	2	1	2	1	2	1	2	1	2	1	2	1	2	1	2	1	2	1	2	1	2	1	2	1	2	1	2	1	2	1	2	1	2	1	2	1	2	1	2	1	2	1	2	1	2	1	2	1	2	1	2	1	2	1	2	1	2	1	2	1	2	1	2	1	2	1	2	1	2	1	2	1	2	1	2	1	2	1	2	1	2	1	2	1	2	1	2	1	2	1	2	1	2	1	2	1	2	1	2	1	2	1	2	1	2	1	2	1	2	1	2	1	2	1	2	1	2	1	2	1	2	1	2	1	2	1	2	1	2	1	2	1	2	1	2	1	2	1	2	1	2	1	2	1	2	1	2	1	2	1	2	1	2	1	2	1	2	1	2	1	2	1	2	1	2	1	2	1	2	1	2	1	2	1	2	1	2	1	2	1	2	1	2	1	2	1	2	1	2	1	2	1	2	1	2	1	2	1	2	1	2	1	2	1	2	1	2	1	2	1	2	1	2	1	2	1	2	1	2	1	2	1	2	1	2	1	2	1	2	1	2	1	2	1	2	1	2	1	2	1	2	1	2	1	2	1	2	1	2	1	2	1	2	1	2	1	2	1	2	1	2	1	2	1	2	1	2	1	2	1	2	1	2	1	2	1	2	1	2	1	2	1	2	1	2	1	2	1	2	1	2	1	2	1	2	1	2	1	2	1	2	1	2	1	2	1	2	1	2	1	2	1	2	1	2	1	2	1	2	1	2	1	2	1	2	1	2	1	2	1	2	1	2	1	2	1	2	1	2	1	2	1	2	1	2	1	2	1	2	1	2	1	2	1	2	1	2	1	2	1	2	1	2	1	2	1	2	1	2	1	2	1	2	1	2	1	2	1	2	1	2	1	2	1	2	1	2	1	2	1	2	1	2	1	2	1	2	1	2	1	2	1	2	1	2	1	2	1	2	1	2	1	2	1	2	1	2	1	2	1	2	1	2	1	2	1	2	1	2	1	2	1	2	1	2	1	2	1	2	1	2	1	2	1	2	1	2	1	2	1	2	1	2	1	2	1	2	1	2	1	2	1	2	1	2	1	2	1	2	1	2	1	2	1	2	1	2	1	2	1	2	1	2	1	2	1	2	1	2	1	2	1	2	1	2	1	2	1	2	1	2	1	2	1	2	1	2	1	2	1	2	1	2	1	2	1	2	1	2	1	2	1	2	1	2	1	2	1	2	1	2	1	2	1	2	1	2	1	2	1	2	1	2	1	2	1	2	1	2	1	2	1	2	1	2	1	2	1	2	1	2	1	2	1	2	1	2	1	2	1	2	1	2	1	2	1	2	1	2	1	2	1	2	1	2	1	2	1	2	1	2	1	2	1	2	1	2	1	2	1	2	1	2	1	2	1	2	1	2	1	2	1	2	1	2	1	2	1	2	1	2	1	2	1	2	1	2	1	2	1	2	1	2	1	2	1	2	1	2	1	2	1	2	1	2	1	2	1	2	1	2	1	2	1	2	1	2	1	2	1	2	1	2	1	2	1	2	1	2	1	2	1	2	1	2	1	2	1	2	1	2	1	2	1	2	1	2	1	2	1	2	1	2	1	2	1	2	1	2	1	2	1	2	1	2	1	2	1	2	1	2	1	2	1	2	1	2	1	2	1	2	1	2	1	2	1	2	1	2	1	2	1	2	1	2	1	2	1	2	1	2	1	2	1	2	1	2	

Continued on
Page 114

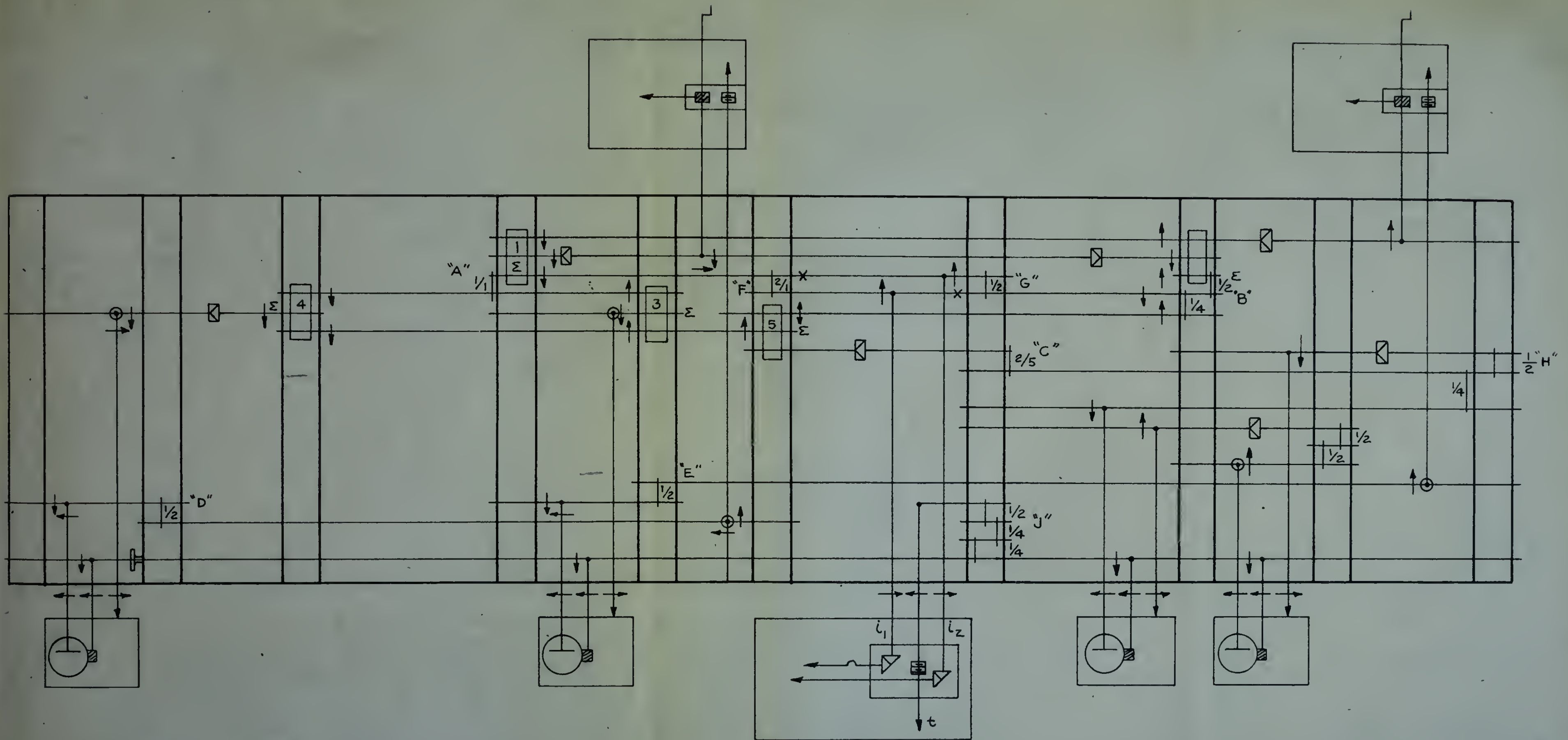


FIG. 4-4 DIFFERENTIAL ANALYZER LAYOUT FOR BASIC PROBLEM OF FIGURE 4-3.

JULY 11, 1948

Approximations, Limitations, and Difficulties

As has been stated, the effects of eddy-current and hysteresis losses have been neglected in this study. For all observations of parametric variations in the input circuit, the neglect of the losses in the core has imposed no serious limitation. The nature of the effect of eddy-current and hysteresis loss on the dynamic behavior of the amplifier when the output-circuit parameters are varied will be discussed.

The magnetic amplifier has an inherently long time-response. The nature of this long response requires that a large number of cycles of the fundamental applied voltage must occur before the final steady-state conditions are reached. When the differential analyzer is operated through a large number of cycles, the cumulative error resulting from the backlash in the many gears in the system can be of serious consequence, and may cause considerable error in the output of the machine. Furthermore, in the machine solution of the simultaneous equation-pair used in this problem, the cumulative error in the mechanical circuit which operates basically on one equation of the pair may be greatly in variance with the cumulative error which builds up in the circuit which operates primarily on the other equation. The accuracy of the solution will be seriously impaired when there is a definite unbalance in the mechanical error arising in different sections of the machine.

Nonlinear, Time-Varying, and Difficult

As was noted, the effects of non-linear and hysteretic losses have been neglected in this study. For all observations of hysteretic variation in the input circuit, the output of the device in the case has been an active limitation. The nature of the effect of non-linear and hysteretic loss on the dynamic behavior of the amplifier when the output-circuit parameters are varied will be discussed.

The magnetic amplifier has an inherently long time-constant. The nature of this long response requires that a large number of cycles of the input signal be applied before the output signal is established. When the differential amplifier is operated through a large number of cycles, the cumulative error resulting from the feedback in the next cycle in the system can be of various magnitudes, and may even occur. Although error in the output of the amplifier is small, in the present context of the analysis, the error is not negligible. The cumulative error in this problem, the cumulative error in the mechanical system which operates basically on one cycle of the input may be greatly in variance with the cumulative error which builds up in the circuit with operation primarily on the other variation. The nature of the solution will be seriously impaired when there is a definite variation in the mechanical error which is different sections of the machine.

The mechanical differential analyzer is provided with frontlash units which are inserted judiciously in the layout in a manner designed to compensate for the errors which result from backlash over a period of many cycles of operation. A total of seven frontlash units, as shown in Figure 4-4, were employed in this problem. The adjustment of these units to compensate for the backlash errors is accomplished mainly by trial-and-error, and requires a great deal of skill which, it seems, is acquired mainly by practice. The adjustment of error compensation was perhaps the largest single difficulty encountered by the authors in their work on the differential analyzer. The initial adjustment of the machine required a great deal of time and some rather substantial rearrangement of components to minimize backlash. Each time the circuit parameters were changed with resultant changes in the scale factors and, of course, in the gears and gear-ratios in the system, it was necessary to re-adjust the frontlash units. The time required to re-adjust the compensating units seems to be an inverse function of the experience of the operators. Actually, the later adjustments were made quite readily and with a minimum loss in time. In general, however, since the machine was required to operate through many cycles, the adjustment of frontlash units was found to be very critical and extremely important in obtaining accurate, precise solutions.

The mechanism of the machine is provided with facilities which are intended to facilitate in the layout in a manner designed to compensate for the errors which would result from wear over a period of many years of operation. A total of seven thousand miles as shown in Figure 4-1, was employed in this problem. The adjustment of these miles to compensate for the wear in the system is accomplished mainly by trial-and-error, and requires a great deal of skill which, in some, is required mainly by practice. The adjustment of every component in the system is perhaps the most delicate and important of the whole in that work on the other hand requires. The initial adjustment of the machine requires a great deal of time and also a great deal of experience of components in similar machines. Each time the circuit parameters were changed with resultant changes in the whole system and, of course, in the time and gear-ratios in the system, it was necessary to re-adjust the front-end meter. The time required to re-adjust the compensating units seems to be an inverse function of the experience of the operator. Usually, the later adjustments were made with speedily and with a minimum loss of time. In general, however, since the machine was required to operate through many cycles, the adjustment of front-end units was found to be very costly and extremely important in obtaining accurate, precise solutions.

Before the analytical problem was formulated, experimental work had shown that the characteristic time of the magnetic amplifier is an inverse function of the input-circuit resistance, R_1 . In order to keep the number of cycles through which the machine was required to operate at a minimum, most of the analytical observations were made with a large value of the input-circuit resistance. The exception to this condition was a set of observations which were made to determine the effect of R_1 on the dynamic and steady-state operation of the analyzer for smaller values of the input resistance. It has been pointed out in Chapter III that the gain of the amplifier is inversely proportional to the input-circuit resistance. Since the value of R_1 used in the analytical study was quite large, many of the observations made on the differential analyzer were made under conditions in which the power-gain of the amplifier was less than unity. Actually, this situation imposed no limitation whatever on the worth of the observations made, and mention of this condition is made here only to justify the choice of a large value of input resistance as imposed by mechanical considerations of the differential-analyzer performance.

The nonlinear relationship between the flux in the cores and the applied magnetizing force was inserted by two input tables. The input functions, drawn to scale, are shown in Figure 4-5. This curve, of course, represents the normal magnetization curve of the core material, and

Before the analytical method was developed, experimental work had shown that the characteristic curve of the magnetic amplifier is an inverse function of the input circuit resistance, R_i . In order to keep the number of cycles through which the magnetic core was required to operate at a minimum, most of the analytical observations were made with a large value of the input-circuit resistance. The assumption in this condition was a set of observations which were made to determine the effect of R_i on the dynamic and steady-state operation of the amplifier for smaller values of the input resistance. It has been pointed out in Chapter III that the gain of the amplifier is inversely proportional to the input-circuit resistance. Since the value of R_i used in the analytical study was quite large, many of the observations made in the laboratory were made under conditions in which the power-gain of the amplifier was less than unity. Actually, this observation imposed no limitation whatever on the study of the observation made, and mention of this condition is made here only to justify the choice of a large value of input resistance as imposed on mechanical measurements of the differential-amplifier performance.

The nonlinear relationship between the flux in the core and the applied magnetizing force was illustrated by two input values. The input resistance, shown in Figure 4-5, was chosen in Figure 4-5. This curve, of course, represents the overall magnetization curve of the core material, and

MAGNETIZING FORCE IN AMPERE-TURNS

400

320

240

160

80

-80

-160

-240

-320

-400

FLUX IN WEBERS $\times 10^5$

118

FIG. 4-5 PLOT OF THE NONLINEAR FUNCTION INPUT TO THE DIFFERENTIAL ANALYZER.

the unconventional coordinates of the plot were necessitated by the mechanical layout of the machine. Recalling that the coordinates are rotated 90° , reference to Figure 4-5 will show that the initial slope, i.e., the ratio of flux to ampere-turns, is very great. Mechanically, the abscissas of this function were inserted by the analyzer, while the ordinates were inserted manually by the operators. In practice, it was found that the errors introduced by backlash in the gears when the ordinates were manually introduced were greater than the changes in magnetizing force introduced by following the curve, and it was therefore necessary to assume an infinite initial slope of the magnetization curve in order to avoid the effect of backlash when small input magnetizing forces were applied. Consequently, the initial slope of the curve was assumed infinite (actually zero, as viewed on Figure 4-5); the initial permeability and inductance were then infinite. The slope was assumed infinite until the flux reached a value of 4×10^{-5} webers, after which the empirical curve of the normal magnetization of the core material was followed. This approximation actually imposes no great limitation on the solutions observed. It is clear from Figure 4-5 that the changes in magnetizing force are very minute over the range from the origin to the value of flux mentioned.

It has been shown in the discussions of empirical results in Chapter III that the output ampere-turns over

It has been noted in the literature that the
of this material.

very minute over the range from the origin to the value
of the figure 5-5 that the change in magnetizing force
no great limitation on the magnetic moment. It is
material was followed. This approximation actually improves
divided curve of the normal magnetization at the same
reached a value of 4×10^{-5} gauss, after which the re-
initial. The slope was deemed constant until the limit
5-5; the initial permeability was determined with the
was assumed infinite (initially zero), as shown in figure
were applied. Consequently, the initial slope of the curve
effect of permeability when small magnetizing forces
slope of the magnetization curve in order to avoid the
it was therefore necessary to assume an infinite initial
magnetizing force introduced by following the curve, and
manually introduced were greater than the change in
found by looking in the figure when the ordinate was
zero. In practice, it was found that the order intro-
while the ordinates were plotted manually by the ap-
ordinates of this function were affected by the material,
time to compare-figures, is very great. Consequently, the
5-5 will show that the initial slope, i.e., the value of
that the coordinate was plotted 50, referred to figure
noted by the mathematical layout of the material. Recalling
the experimental conditions of the plot were normal.

the normal range of the amplifier or modulation characteristic are very nearly equal to the input ampere-turns. Reference to Equation 4-16 will then indicate another rather serious limitation for the mechanical solution, namely, the measurement of the small difference:

$$N_1 i_1 - N_2 i_2$$

between two relatively large quantities. Again, the necessity for careful error compensation is implied by the nature of the equations to be solved.

It has been the purpose of this section of the report to emphasize the nature of the difficulties anticipated and encountered in solution of the analytical equations of the differential analyzer, and to describe the methods used to minimize these difficulties.

Nature of the Analytical Solutions

Conditions for the various analytical problems were formulated to closely simulate conditions existent during experimental observations. In the case of transient analytical observations, actual oscilloseopic photographs of equivalent experimental situations were made. Throughout the study, all analytical solutions were matched by a series of experimental observations in which circuit conditions were made as nearly identical as possible. The results of all analytical observations are tabulated in Charts 4-3 and 4-4.

As has been stated, the currents i_1 and i_2 which

the normal range of the analysis of metabolism studies. The results are very similar to the data reported in the literature. It is well known that the results of the analysis of the metabolism of the various amino acids for the metabolic studies, namely, the measurement of the small differences

Fig. 1 - 1953

between the various large quantities. Again, the results for the analysis of the metabolism of the various amino acids are similar to the data reported in the literature.

It has been the purpose of this section of the report to emphasize the nature of the analytical results obtained and summarized in relation to the analysis of the metabolism of the various amino acids, and to describe the methods used to minimize these differences.

Nature of the Analytical Results

Conditions for the various analytical procedures were formulated to closely simulate conditions existing during experimental observations. In the case of the various analytical observations, actual conditions were simulated by the use of experimental conditions. The results of the analysis of the various amino acids were similar to the data reported in the literature. It is well known that the results of the analysis of the metabolism of the various amino acids for the metabolic studies, namely, the measurement of the small differences

As has been stated, the results of the analysis of the metabolism of the various amino acids are similar to the data reported in the literature.

CHART 4-3

RESULTS OF ANALYTICAL STUDIES

RUN NO.	W RAPEL	E ₂ VOLTS	R ₁ OHMS	R ₂ OHMS	N ₁ TURNS	N ₂ TURNS	SCALE IN/AMP	I ₁		I ₂		SCALE IN/SEC	(ST)					
								MEAS IN ²	AVER INPUT MA	MEAS IN ²	AVER OUTPUT MA		MEAS IN ²	IN M-EC				
1	640	40	10125	977	3600	1000	180	0.17	1.47	1.11	4	6.25	0.004	1.09	1.09	128	2.58	20.1
2	↑	↑	↑	↑	↑	↑	↑	0.21	1.82	1.66	6	25	0.10	6.25	6.25	↑	1.25	3.77
3	↑	↑	↑	↑	↑	↑	↑	0.24	2.08	1.95	7	↑	0.13	8.12	8.12	↑	1.20	3.37
4	↑	↑	↑	↑	↑	↑	↑	0.26	2.26	2.20	8	↑	0.15	4.37	4.37	↑	1.12	2.75
5	↑	↑	↑	↑	↑	↑	↑	0.29	2.51	2.50	9	↓	0.15	4.37	4.37	↑	1.00	2.81
6	↑	↑	↑	↑	↑	↑	↑	0.35	3.04	3.05	11	25	0.18	11.25	11.25	↑	2.82	6.4
7	↑	↑	↑	↑	↑	↑	↑	0.15	1.30	1.11	4	50	0.16	5.63	5.63	↑	1.90	14.9
8	↑	↑	↑	↑	↑	↑	↑	0.42	3.64	3.61	13	↑	0.46	14.4	14.4	↑	0.75	5.85
9	↑	↑	↑	↑	↑	↑	↑	0.49	4.25	4.16	15	↑	0.51	15.4	15.9	↑	0.70	5.47
10	↑	↑	↑	↑	↑	↑	↑	0.58	5.02	4.72	17	↑	0.56	18.1	18.1	↑	0.60	4.6
11	↑	↑	↑	↑	↑	↑	↑	0.60	5.20	5.27	13	↑	0.66	13.4	13.4	↑	0.68	5.31
12	↑	↑	↑	↑	↑	↑	↑	0.69	5.98	5.83	21	↑	0.65	20.3	20.3	↑	0.52	4.36
13	640	40	↑	↑	↑	↑	↑	0.77	6.67	6.37	23	↑	0.73	24.7	24.7	↑	0.48	3.75
14	2560	50	↑	↑	↑	↑	↑	—	—	1.11	4	↑	—	—	—	128	3.40	25.8
15	↑	↑	↑	↑	↑	↑	↑	0.10	1.15	2.22	8	↑	2.18	11.25	1.25	250	3.33	12
16	↑	↑	↑	↑	↑	↑	↑	0.19	3.30	3.33	12	↑	2.21	13.1	13.1	↑	2.35	3.18
17	↑	↑	↑	↑	↑	↑	↑	—	—	4.44	16	↑	—	—	—	↑	1.10	7.53
18	↑	↑	↑	↑	↑	↑	↑	0.32	5.55	5.55	20	↑	0.31	13.4	13.4	↑	1.42	5.50
19	↑	↑	↑	↑	↑	↑	↑	0.39	6.78	6.66	24	↑	0.40	25.0	25.0	↑	1.25	4.88
20	↑	↑	↑	↑	↑	↑	↑	—	—	3.33	12	↑	—	—	—	↑	—	—
21	↑	50	↑	↑	↑	↑	↑	—	—	1.11	4	↑	—	—	—	↑	—	—
22	↑	100	↑	↑	↑	↑	↑	0.06	1.04	1.11	4	↑	0.07	3.13	3.13	↑	4.25	12.2
23	↑	↑	↑	↑	↑	↑	↑	0.15	2.60	2.22	8	↑	0.15	7.5	7.5	↑	2.15	11.1
24	↑	↑	↑	↑	↑	↑	↑	0.17	2.35	3.33	12	↑	0.13	11.88	11.88	↑	2.10	8.20
25	↑	↑	↑	↑	↑	↑	↑	0.24	4.17	4.44	16	↑	0.24	15.0	15.0	↑	1.60	6.25
26	↑	↑	↑	↑	↑	↑	↑	0.31	5.39	5.55	20	↑	0.32	20.0	20.0	↑	1.40	5.47
27	↑	↑	↑	↑	↑	↑	↑	0.34	5.40	6.39	23	↑	0.35	21.9	21.9	↑	1.25	4.78
28	↑	↑	↑	↑	↑	↑	↑	0.05	0.57	1.11	4	↑	0.05	3.13	3.13	↑	4.25	12.2
29	↑	↑	↑	↑	↑	↑	↑	0.13	2.25	2.22	8	↑	0.14	5.20	5.20	↑	2.55	12.00
30	↑	↑	↑	↑	↑	↑	↑	0.19	3.30	3.33	12	↑	0.13	11.3	11.3	↑	2.03	8.16
31	↑	↑	↑	↑	↑	↑	↑	0.24	4.18	4.44	16	↑	0.25	15.0	15.0	↑	1.55	6.25
32	↑	↑	↑	↑	↑	↑	↑	0.24	5.03	5.55	20	↑	0.35	14.8	14.8	↑	1.40	5.47
33	↑	↑	↑	↑	↑	↑	↑	0.37	6.43	6.39	23	↑	0.35	24.2	24.2	↑	1.28	5.00
34	↑	↑	↑	↑	↑	↑	↑	0.05	0.87	1.11	4	↑	0.06	3.75	3.75	↑	4.25	12.2
35	↑	↑	↑	↑	↑	↑	↑	0.12	2.08	2.22	8	↑	0.14	8.20	8.20	↑	3.50	11.1
36	↑	↑	↑	↑	↑	↑	↑	0.19	3.30	3.33	12	↑	0.17	12.50	12.50	↑	2.55	2.00
37	↑	↑	↑	↑	↑	↑	↑	0.25	4.34	4.44	16	↑	0.26	16.25	16.25	↑	1.60	6.25
38	↑	↑	↑	↑	↑	↑	↑	0.32	5.40	5.55	20	↑	0.35	1.00	1.00	↑	1.40	5.47
39	↑	↑	↑	↑	↑	↑	↑	0.24	5.40	6.39	23	↑	0.35	21.9	21.9	↑	1.25	4.78
40	↑	↑	↑	↑	↑	↑	↑	0.05	0.87	1.11	4	↑	0.05	3.13	3.13	↑	4.25	12.2
41	↑	↑	↑	↑	↑	↑	↑	0.13	2.25	2.22	8	↑	0.11	6.87	6.87	↑	2.40	4.4
42	↑	↑	↑	↑	↑	↑	↑	0.18	3.13	3.33	12	↑	0.18	11.20	11.20	↑	2.10	8.20
43	↑	↑	↑	↑	↑	↑	↑	0.24	4.16	4.44	16	↑	0.26	16.5	16.5	↑	1.60	6.25
44	↑	↑	↑	↑	↑	↑	↑	0.32	5.53	5.55	20	↑	0.31	19.4	19.4	↑	1.48	5.75
45	↑	↑	↑	↑	↑	↑	↑	0.35	6.03	6.39	23	↑	0.37	23.50	23.50	↑	1.34	7.20
46	↑	↑	↑	↑	↑	↑	↑	0.04	0.63	0.55	2	↑	0.05	0.24	0.24	↑	10.4	40.6
47	↑	↑	↑	↑	↑	↑	↑	0.07	1.22	1.11	4	↑	0.03	1.88	1.88	↑	6.4	25.0
48	↑	↑	↑	↑	↑	↑	↑	0.11	1.91	1.66	6	↑	0.05	3.13	3.13	↑	4.2	16.4
49	↑	↑	↑	↑	↑	↑	↑	0.15	2.60	2.22	8	↑	0.07	4.87	4.87	↑	3.7	14.5
50	↑	↑	↑	↑	↑	↑	↑	0.18	3.13	2.78	10	↑	0.08	5.00	5.00	↑	2.7	10.6
51	↑	↑	↑	↑	↑	↑	↑	0.21	3.65	3.19	11.5	↑	0.08	5.00	5.00	↑	2.55	10.0
52	↑	↑	↑	↑	↑	↑	↑	0.15	2.60	2.22	8	↑	0.27	16.9	16.9	↑	1.20	5.08
53	↑	↑	↑	↑	↑	↑	↑	0.26	4.51	4.44	16	↑	0.47	23.4	23.4	↑	1.00	3.91
54	↑	↑	↑	↑	↑	↑	↑	0.105	1.80	1.11	4	↑	0.145	20.6	20.6	↑	1.30	7.43
55	↑	↑	↑	↑	↑	↑	↑	0.185	3.21	3.33	12	↑	0.20	24.4	24.4	↑	1.15	4.49
56	↑	↑	↑	↑	↑	↑	↑	0.308	5.30	5.55	20	↑	0.53	36.8	36.8	↑	0.85	3.32
57	↑	↑	↑	↑	↑	↑	↑	0.02	0.35	0.56	1	↑	0.015	0.94	0.94	↑	4.60	18.0
58	↑	↑	↑	↑	↑	↑	↑	0.05	0.87	1.11	2	↑	0.045	2.81	2.81	↑	2.30	7.00
59	↑	↑	↑	↑	↑	↑	↑	0.10	1.73	1.66	3	↑	0.055	3.44	3.44	↑	1.55	6.05
60	2560	100	10125	489	1800	1000	180	0.15	2.60	2.22	4	50	0.065	4.1	4.1	256	1.25	4.88

CHART 4-4

RESULTS OF ANALYTICAL STUDIES

RUN NO.	f ₁										f ₂									
	W RAD/SEC	E ₂ VOLTS	R ₁ OHMS	R ₂ OHMS	N ₁ TURNS	N ₂ TURNS	SCALE IN/AMP	MEAS IN ²	AVER IN/MA	INPUT MA	N ₁ I ₁	SCALE IN/AMP	MEAS IN ²	AVER OUTPUT MA	N ₂ I ₂	SCALE IN/AMP	MEAS IN ²	AVER IN/MA	(CT) M/SEC	
61	2560	100	10125	489	1800	1000	180	0.13	3.13	2.77	5	50	0.03	5.65	5.05	250	1.05	4.1		
62	↑	↑	↑	↑	1800	↑	180	0.20	3.47	3.19	5.75	↑	0.2	7.50	7.50	↑	0.30	3.51		
63					2543		159	0.04	0.79	0.79	2		0.33	1.88	1.88		4.8	13.8		
64								0.17	1.95	1.57	4		0.55	3.44	3.44		2.5	3.76		
65								0.125	2.46	2.36	6		0.075	5.20	5.20		1.8	7.03		
66								0.16	3.15	3.12	5		0.13	5.2	5.2		1.4	5.47		
67			10125		2543		159	0.105	4.03	2.32	10		0.17	12.6	10.6		1.15	4.49		
68			5063		3600		150	0.105	1.52	2.22	5		0.12	7.50	7.50		5.25	20.5		
69								0.125	4.34	4.44	10		0.26	16.3	16.3		5.2	12.5		
70								0.33	6.59	6.66	24		0.38	23.8	23.8		2.3	4.98		
71								0.25	5.76	5.88	32		0.25	32.8	32.8		1.9	7.43		
72								0.31	5.58	5.55	20		0.325	20.2	20.2		2.7	10.6		
73			5063					0.55	2.69	3.33	12		0.12	11.5	11.5		1.38	15.39		
74			2531					0.25	3.83	4.44	16		0.255	14.6	14.0		5.8	24.3		
75								0.375	6.50	6.66	24		0.330	24.3	24.3		4.5	17.0		
76								0.505	5.16	5.88	32		0.53	33.1	33.1		3.85	15.1		
77			2531					0.03	1.53	2.22	8		0.12	7.50	1.50		10.0	10.0		
78			1265					0.175	5.25	5.88	32		0.44	27.5	27.5		3.07	14.32		
79								0.315	5.50	6.66	24		0.35	22.2	22.2		5.9	34.7		
80								0.23	4.00	4.44	16		0.240	15.0	15.0		12.75	12.0		
81			1265					0.08	1.53	2.22	8		0.1	6.70	6.70		13.10	74.60		
82			10125					—	—	—	—		—	—	—		1.35	5.26		
83								—	—	—	—		—	—	—		—	—		
84			100					0.12	2.88	1.66	2		0.25	2.75	3.75		2.55	16.0		
85			150					0.225	5.50	5.00	18		0.30	20.8	20.8		1.65	6.45		
86								0.465	7.90	6.66	24		0.42	26.2	26.2		0.84	3.28		
87			150					0	0	0	0		0.065	16.25	16.25		—	—		
88			300					0.05	0.87	0.53	3		0.07	17.5	17.5		3.24	0.337		
89								0.11	1.91	1.60	6		0.105	25.2	25.2		0.20	2.78		
90								0.18	3.22	3.32	12		0.13	32.5	32.5		0.20	2.75		
91	2560	300						0.255	4.42	4.44	16		0.26	16.2	16.2		3.15	6.05		
92	5120	200						0.355	6.69	6.66	24		0.38	23.8	23.8		2.38	4.65		
93								0.125	2.17	2.22	8		0.12	7.5	7.5		5.02	3.80		
94								—	—	—	—		—	—	—		—	—		
95	5120	200	10125	489	3600	1000	180	—	—	3.88	16	50	—	—	—	512	1.80	3.51		

flow in the input and output circuits of the amplifier respectively, were plotted as outputs of the differential analyzer. The magnitudes of these currents were obtained by integrating the area under the curves by use of a planimeter, and then computing the values of the currents by application of the proper scale factors. Actually, the average value of the second-harmonic alternating current in the input circuit, i_1 , is equal to the value of current applied to the circuit when the step voltage is connected to the input-circuit terminals. Stated in a different manner: the average value of i_1 is equal to I_1 , which is equal to the magnitude of the step voltage divided by the total input-circuit resistance. The comparison of values obtained by planimetric integration and values obtained by division are shown in Charts 4-3 and 4-4. As will be noticed, agreement is quite good.

Figure 4-6 is a tracing of an actual solution plotted by the differential analyzer after steady-state conditions were reached. The nature of the odd-harmonic composition of the output-circuit current, i_2 , is apparent in this figure. Similarly, the even-harmonic composition of the input-circuit current, i_1 , is shown by the nature of the tracing. For comparison with the curves of Figure 4-6, actual photographs of the face of a cathode-ray oscillograph are shown in Figures 4-7 and 4-8. It should be emphasized that the photographs of Figure 4-7 are not shown to scale.

flow in the input and output elements of the amplifier respectively, were plotted as functions of the differential amplifier. The magnitudes of these currents were obtained

by integrating the wave across the source by use of a planimeter, and then computing the values of the currents by application of the power factor. Actually, the average value of the second-harmonic alternating current in

the input circuit, i_1 , is equal to the value of current applied to the circuit when the step voltage is connected

to the input-circuit terminals. Hence in a different manner: the average value of i_1 is equal to i_1 , which is equal to the magnitude of the step voltage divided by the total input-circuit resistance. The percentage of voltage obtained by planimetric integration and values obtained by

division are shown in Curves 4-7 and 4-8. As will be noted, agreement is quite good.

Figure 4-6 is a tracing of an actual solution plotted by the differential analyzer after steady-state conditions were reached. The nature of the non-harmonic composition of the output-circuit current, i_2 , is apparent in this figure. Similarly, the even-harmonic composition of the input-circuit current, i_1 , is shown by the nature of the tracing. For comparison with the waves of Figure 4-6, actual photographs of the trace of a cathode-ray oscilloscope are shown in Figures 4-7 and 4-8. It should be emphasized that the photographs of Figure 4-7 are not shown to scale.

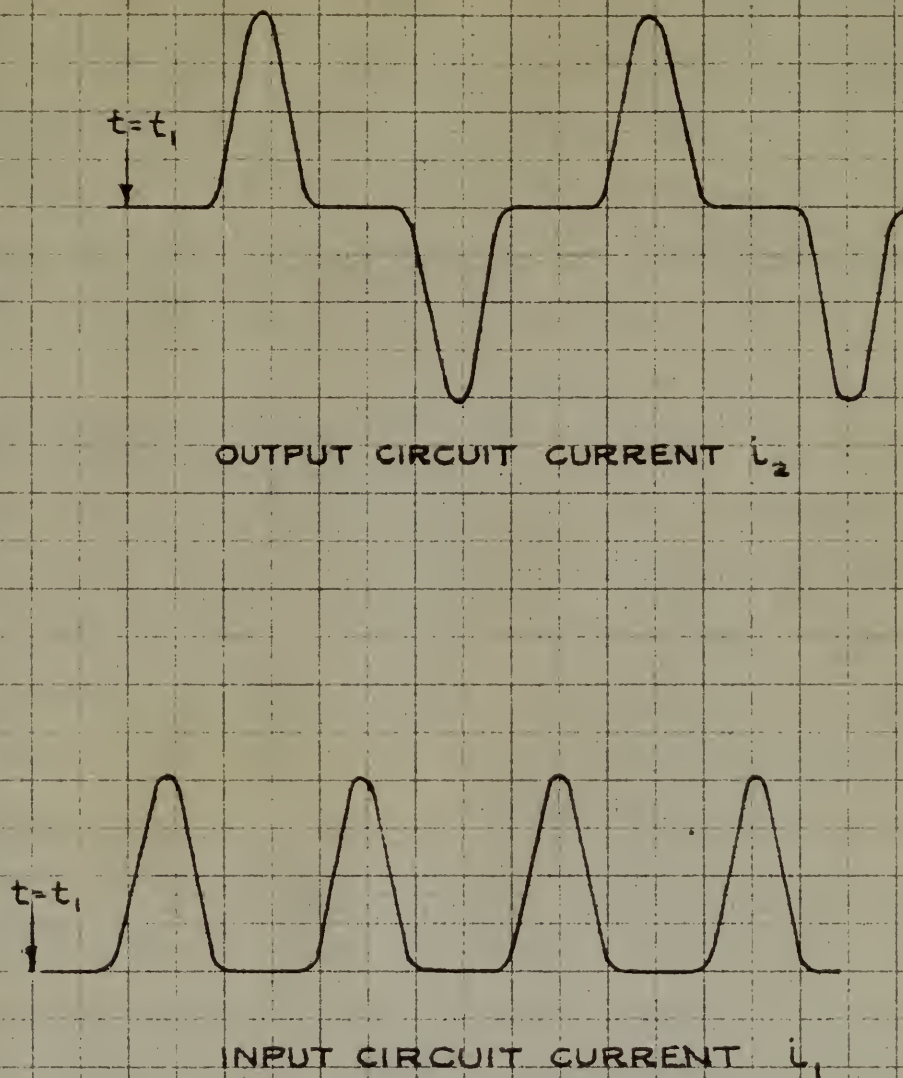
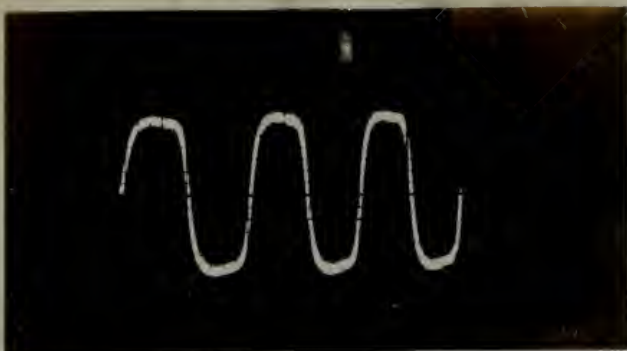


FIG. 4-6 FORM OF THE PLOTTED SOLUTIONS OF THE DIFFERENTIAL ANALYZER PROBLEM. (NOTICE THAT THE DISSYMMETRY OF THE EXPERIMENTAL CURRENTS IS ABSENT BECAUSE LOSSES ARE NEGLECTED IN THE ANALYTICAL SOLUTION.)

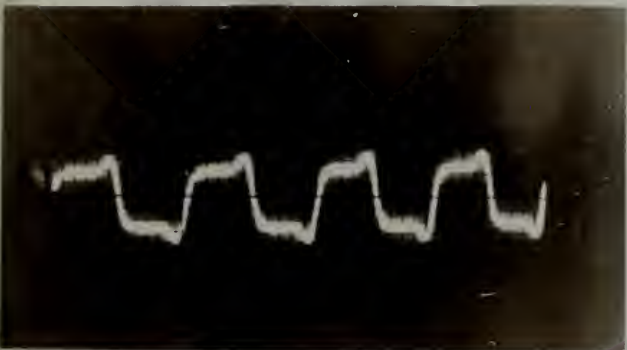
Figure 4-7(a) shows the flow of current in the output circuit when the input current is zero. The square wave obtained is due almost wholly to the effects of hysteresis which have been neglected in the analyzer solution. The frequency of the square wave is that of the applied alternating flux. As the input current increases to a small value, small peaks appear on the output-current waveform when the flux excursions begin to extend into the knee of the magnetization curve. This effect is shown on Figure 4-7(b). A further slight increase in input current yields the waveform of Figure 4-7(c). When the input current is increased to a larger value and flux excursions extend well into the knee, as shown in Figure 4-7(d), the hysteresis current becomes a relatively small portion of the total waveform, and the overall effect is merely to cause a slight difference in the levels of the shoulders of the output waveform. Figure 4-7(d) is analogous to the differential analyzer output-wave shown in Figure 4-6. The dissymmetry of the levels of the shoulders does not, of course, appear in the analytical solution because hysteresis was neglected. If the input current is made sufficiently great, the flux excursion in one core of the amplifier may extend above the knee of the magnetization curve at the same time the flux excursion in the other core is also on the knee. Under these conditions, the output waveform is

Figure 6-7(a) shows the flow of current in the output circuit when the input current is zero. The square wave obtained in this circuit is due to the effects of hysteresis which have been neglected in the analysis. The frequency of the square wave is that of the applied sinusoidal flux. As the input current increases to a small value, small peaks appear on the output-current waveform when the flux excursions begin to extend into the base of the magnetization curve. This effect is shown in Figure 6-7(b). A further slight increase in input current yields the waveform of Figure 6-7(c). When the input current is increased to a larger value and the excursions extend well into the knee, as shown in Figure 6-7(d), the hysteresis current becomes a relatively small portion of the total waveform, and the overall effect is merely to cause a slight difference in the levels of the shoulders of the output waveform. Figure 6-7(e) is analogous to the differential analysis output-wave shown in Figure 6-6. The dissymmetry of the levels of the shoulders does not, of course, appear in the simplified relation because hysteresis was neglected. If the input current is made sufficiently great, the flux excursion in one cycle of the amplifier may extend above the knee of the magnetization curve to the point where the flux excursion in the other cycle is also in the knee. Under these conditions, the output waveform is

(a)



(b)



(c)



(d)



(e)



FIGURE 4-7

OSCILLOSCOPIC PHOTOGRAPHS
WHICH SHOW THE INCREASE IN
THE STEADY-STATE VALUE OF
THE OUTPUT CURRENT, i_2 ,
FOR INCREASING VALUES OF
THE INPUT CURRENT, i_1 .

f = 100 cps.
 N_1 = 3600 T.
 N_2 = 1000 T.
 R_1 = 10125 ohms.
 R_2 = 100 ohms.
 ϕ_2 = 40 sin wt.

KEY TO FIGURES

(a) i_1 = 0.
 i_2 = 1.8 ma.
(Hysteresis only)

(b) i_1 = 0.1 ma.
 i_2 = 1.85 ma.

(c) i_1 = 0.3 ma.
 i_2 = 1.90 ma.

(d) i_1 = 2.5 ma.
 i_2 = 5.4 ma.

(e) i_1 = 10.0 ma.
 i_2 = 12.5 ma.

The Photographs are not
Shown to Scale

FIGURE 4-7

OSILLIGOSCOPTIC PHOTOGRAPHY
WHICH SHOW THE INCREASE IN
THE STRENGTH OF THE
THE OUTPUT CURRENT, IS
FOR INCREASING VALUES OF
THE INPUT CURRENT, IS.

100 sec.	1
5000 ft.	2
1000 ft.	3
10000 ft.	4
100000 ft.	5
1000000 ft.	6
40 min wt.	7

KEY TO FIGURES

10.0 sec.	1	(a)
1.0 sec.	2	(b)
0.1 sec.	3	(c)
0.01 sec.	4	(d)
0.001 sec.	5	(e)
0.0001 sec.	6	(f)
0.00001 sec.	7	(g)

The Photographs are not
shown to scale

(a)



(b)



(c)

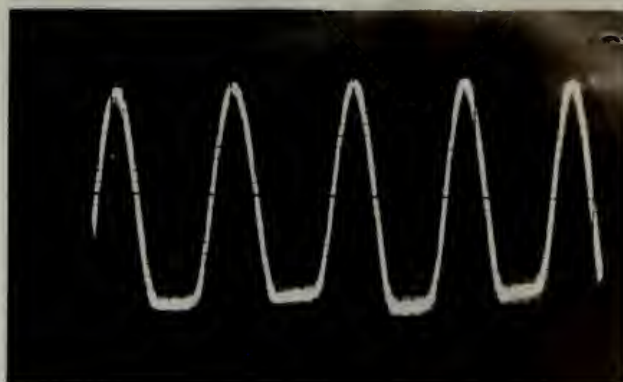


(d)



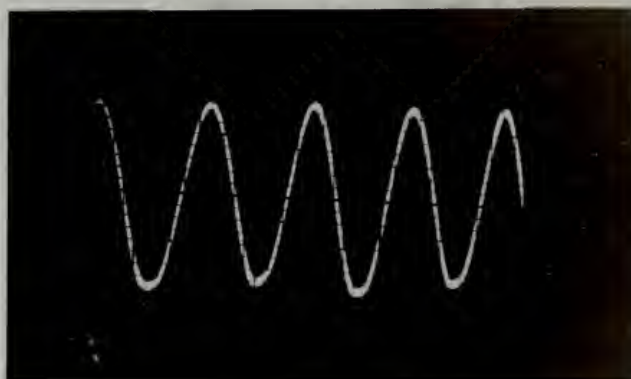
(e)





(a)

INPUT CURRENT, $i_1 = 5.0$ ma.



(b)

INPUT CURRENT, $i_1 = 10.0$ ma.

FIGURE 4-8

OSCILLOSCOPIC PHOTOGRAPHS SHOWING THE INPUT-CIRCUIT CURRENT, i_1 , AT THE SECOND-HARMONIC FREQUENCY OF THE APPLIED ALTERNATING VOLTAGE.



(a)

10.0 in. x 1.0 in. (10.0 in. x 1.0 in.)



(b)

10.0 in. x 1.0 in. (10.0 in. x 1.0 in.)

10.0 in. x 1.0 in.

COPIES OF THIS REPORT ARE AVAILABLE TO THE PUBLIC AT THE NATIONAL ARCHIVES, COLLEGE PARK, MARYLAND, 20740-6001. FOR MORE INFORMATION, CONTACT THE NATIONAL ARCHIVES AT (301) 837-1122.

shaped as shown in Figure 4-7(e). The shoulder has virtually disappeared, because there is no period in the cycle when current ceases to flow because the fluxes in each core are simultaneously passing over the knee of the magnetization curve.

The path of the flux and magnetizing force in an iron core is, of course, affected by the presence of the hysteresis loop. Since the number of loops formed by hysteresis is infinite, it is difficult to determine the proper value of the loop path to follow when the value of the flux versus magnetizing-force function is applied manually as an input to the differential analyzer. It was considered, however, very important to observe, if possible, the effects of hysteresis on the analytical waveform, and consequently, the particular member of the hysteresis loop family shown for 4750 Alloy in Figure 2-7 was utilized as an input to the differential analyzer for several solutions. The observed effect was, of course, qualitative, since it has been pointed out that an infinite number of loops will actually exist, but it is extremely significant to note that output-current curves exactly similar to the experimental waveforms of Figure 4-7 were obtained through the simulated hysteresis method. It may then be stated that much of the current which flows in the output circuit when the input-circuit current is zero is due to hysteresis. Furthermore, the difference in levels of the shoulders of

placed as shown in Figure 4-7(c). The electrode has been
 usually disconnected, because there is no action in the
 circle when current ceases at this moment. The change in
 each case are simultaneously passing over the line in the
 organization curve.

The path of the line and resulting force in the
 line were in of course, situated in the presence of the
 hysteretic loop. Since the nature of this force is
 hysteretic in nature, it is difficult to determine the
 proper value of the loop path to follow when the value of
 the flux varies accordingly. Therefore it is required
 manually as an input to the differential analyzer. It was
 considered, however, very important to observe, if possible,
 the effects of hysteresis on the resulting system, and
 consequently, the particular nature of the hysteretic loop
 really shows the type of input in Figure 4-7 was utilized as
 an input to the differential analyzer for several minutes.
 The observed effect was, of course, qualitative, since it
 has been pointed out that we have no means of force with
 actually exist, but it is extremely significant to note
 that output-current curves exactly similar to the input-
 current curves of Figure 4-7 were obtained through the
 simulated hysteretic system. It was then in Figure 4-7
 none of the current which flows in the output circuit when
 the input-current current is zero in the hysteretic
 Furthermore, the difference in levels of the hysteresis

of the output waveforms is definitely attributable to hysteresis effect, and not to unbalance in the cores, as was previously thought. It is questionable whether these statements could have been made without the aid of the differential analyzer observations.

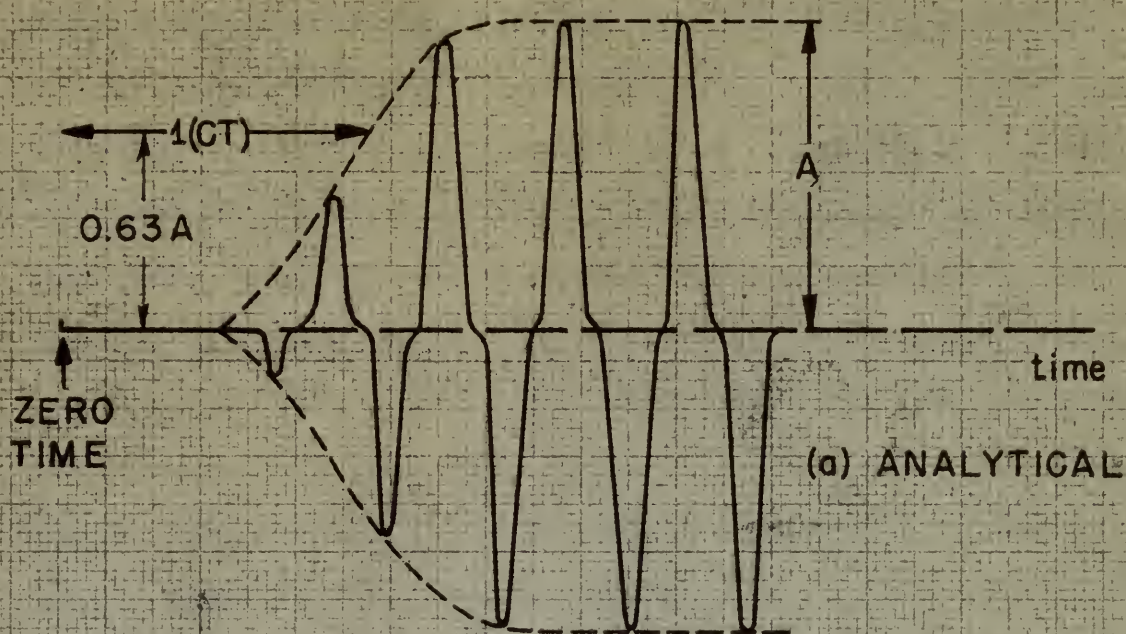
Figure 4-6(b) shows a tracing of an analytical solution of the second-harmonic input-circuit current, i_1 . Similar oscilloscope photographs are shown in Figure 4-8. It is worth noticing that just as the shoulders disappear from the output current waveform when the input current becomes large, so do the flat portions disappear from the lower portions of the input-circuit current waveform when the input circuit current becomes greater. This effect may be seen by comparing Figure 4-8(a), which was made for the conditions which prevailed for the analytical solution shown in Figure 4-6(b), with the waveform of Figure 4-8(b), which was made for a somewhat larger input current. The disappearance of these flat portions is attributed to the same reason given for disappearance of the shoulders of the output-circuit waveform, namely: there is no time in the cycle during which the flux excursions in the two cores are simultaneously on the linear portion of the magnetization curve.

A tracing of the buildup of output-circuit current, i_2 , as produced by a solution of the differential analyzer, is shown in Figure 4-9(a). The nature of the

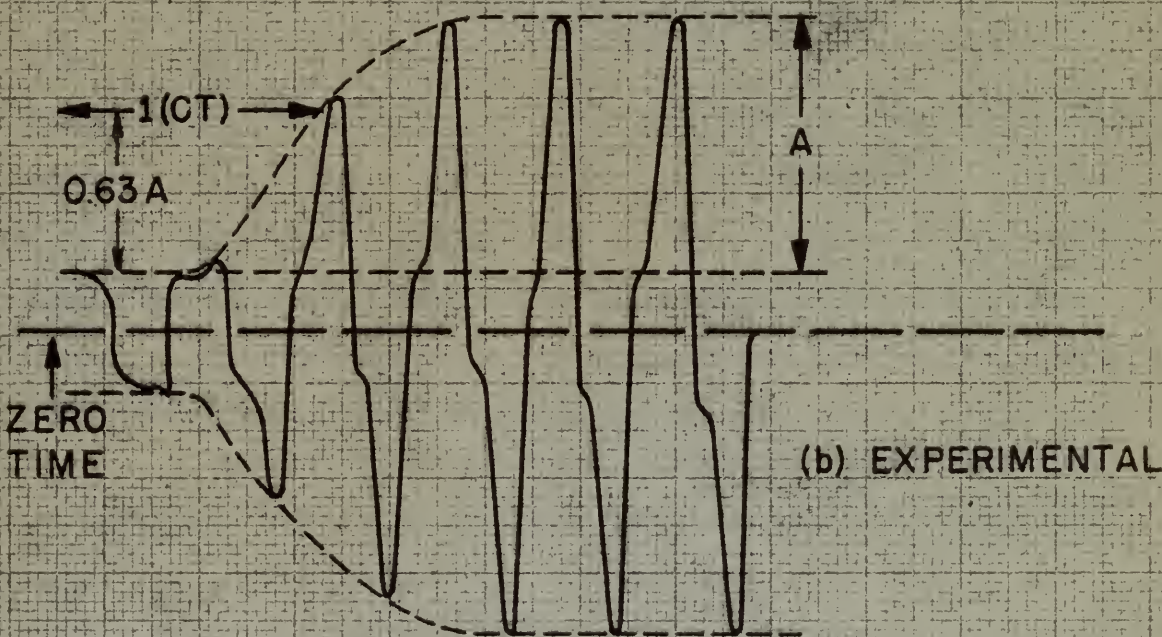
of the output waveform is definitely sinusoidal in
character, and not as undulating in the wave, as
was previously thought. It is questionable whether these
oscillations could have been made without the aid of the
differential amplifier circuit.

Figure 2-6(a) shows a tracing of an analytical
solution of the second-order linear differential equation, $y'' + 2y' + 2y = 0$.
Similar oscillatory behavior is shown in Figure 2-6(b).
It is worth noting that just as the amplitude decreases
from the output current waveform when the input current
becomes larger, so in the first position diagram, from the
lower portion of the input current waveform, the
The input current is greater than the output. This is the way
be seen by comparing Figure 2-6(a) with the output for the
conditions which prevail for the analytical solution
shown in Figure 2-6(b), with the waveform of Figure 2-6(c),
which was made for a constant input current. The
disappearance of the first portion is attributed to the
some reason given for disappearance of the amplitude of
the output current waveform, namely, there is no limit in
the rate at which the first portion is in the first
two simultaneously in the input portion of the waveform
from curve.

A tracing of the output of the input current is
given in Figure 2-6(d) as a comparison of the analytical
solution, as shown in Figure 2-6(a). The output of the



(a) ANALYTICAL



(b) EXPERIMENTAL

FIG. 4-9

COMPARISON OF THE BUILDUP OF OUTPUT CIRCUIT CURRENT, I , FOR ANALYTICAL AND EXPERIMENTAL OBSERVATIONS.

defined characteristic time has been discussed previously, and is shown pictorially on this figure. Figure 4-9(b) is a drawing made from an oscilloscopic photograph of the output current of the amplifier when the conditions of operation were identical to those shown on the analytical solution. The effect of hysteresis is apparent in the practical case, and the definition of characteristic time for the practical case is apparent from the drawing. It is clear from Figure 4-9(a) that initially, since infinite permeability was assumed, and since hysteresis was neglected, there is no flow of current. A waveform identical to the analytical waveform of Figure 4-9(a) can be simulated experimentally if the input current is made very large; this results in such a large output current that the hysteresis current is negligible by comparison, and the flat line shown initially in Figure 4-9(a) for an analytical solution can be very neatly shown on the oscilloscope for an experimental situation.

The Concept of Buildup of Flux Bias.

There is a certain intangible benefit that may be obtained from working with the mechanical differential analyzer that is difficult to describe. The effect is related somewhat to an intuitive feeling that is acquired while actually observing mechanical parts operate on the differential equations, and this intuitive feeling is of value in understanding the actual behavior of the physical circuit which is represented by the motion of mechanical

parts. This "intangible" benefit, so-called, does not appear in the tabulated solutions of the analyzer problem, and seems to depend principally on actually observing the behavior of the various integrators, differentials, gears, and input tables, as the problem is carried through. It was this type of observation which led to an appreciation of the theoretical behavior of the magnetic amplifier under transient conditions.

Since initial permeability was assumed to be infinite and hysteresis was neglected, no current flows in the input circuit immediately after the application of the step voltage to the input terminals, unless the initial flux applied to the cores is sufficiently great to cause excursions above the break of the knee of the magnetization curve. Under these conditions of zero initial current flow in the input circuit, there is, of course, no current flow in the output circuit. When the step voltage is applied, the flux in each core begins to be biased outward toward the region of the knee. Once the flux excursion extends into the knee, current begins to flow in both the input and output circuits; these currents contribute nonlinearly to the further buildup of flux, in accordance with Equations 4-15 and 4-16, and it becomes difficult to reason the behavior from physical concepts after current flow starts, because of the nonlinear nature of the equations. During the interval of time, however, before the flux excursions extend

part. This "induced" current, however, does not
 appear in the calculated magnetic field of the primary circuit,
 and hence no induced potential is induced in the
 secondary of the various instruments. Furthermore, the
 induced current, as the current is induced through it
 and this type of observation which has been a reproduction
 of the theoretical behavior of the magnetic field in
 the transient conditions.

Along with permeability was assumed to be
 infinite and constant, and neglected, in current flow
 in the primary circuit, the induced current in
 the secondary is the induced current, which the induced
 flux applied to the core is not induced, but to which
 examples show the work of the core of the magnetization
 curve. When these conditions are taken into account
 the induced current, there is, of course, no induced
 flux in the core circuit. When the induced flux is ap-
 plied, the flux in each wire begins to be induced between
 toward the center of the core. Once the flux is induced
 extends into the core, current begins to flow in both the
 inner and outer circuit, then current continues to
 increase as the induced flux is induced with
 question 4-11 and 12, and it becomes difficult to answer
 the behavior of the induced magnetic field in the core,
 because of the nonlinear nature of the magnetic field
 interval of time, however, before the flux commences to

into the knee, the theoretical system, since infinite initial permeability was assumed, behaves as a linear system and linear concepts are applicable. This fact was first recognized while actually observing the behavior of the differential analyzer, and probably would not have been recognized from experimental observations alone. In many cases of magnetic-amplifier operation, the original buildup of flux consumes a large portion of the total characteristic time, and, therefore, is of importance when considerations of the transient behavior of the theoretical amplifier are made. The time of flux-bias buildup, t , is defined as the time after the application of the voltage step-function to the input terminals until current begins to flow in the output and input circuits.

The development of the equation which defines flux buildup in the theoretical case follows. It is first necessary to define certain quantities, and in each case the defined quantities refer to only a single core of the magnetic amplifier core-pair. It is possible to deal with a single core because the rise in d-c flux is identical in each core of an amplifier, although the directions of rise are opposite in phase. Let

ϕ_{dc} = applied direct flux as supplied by the input circuit.

ϕ_s = the value of flux at which permeability becomes finite, i.e., the value of flux required to cause flow of currents. Designated as saturation flux.

into the form, the theoretical system, since initial
 initial pattern-unity was assumed. However as a linear
 system and linear concepts are applicable. This leads to
 first approximation while actually observing the behavior of
 the differential system, and possibly would not have
 been recognized from experimental observations alone. In
 many cases of experimentally observed, the solution
 pattern of the system is a linear pattern of the total
 characteristic time, and, therefore, is of importance when
 consideration of the structure behavior of the theoretical
 system is made. The time of first-line behavior, T_1 , is
 defined as the time after the application of the voltage
 step-function to the input terminals until current begins
 to flow in the circuit and is denoted by T_1 .

The development of the equation which defines
 this behavior in the theoretical case follows. It is first
 necessary to define certain quantities, and in each case
 the defined quantity refers to only a single case of the
 specific behavior characteristic. It is defined as time with
 a single case because the time in each case is identical
 in each case of an equation, although the discussion of
 this case appears in general. Let

$$R = \text{resistance of the circuit in ohms} \\
L = \text{inductance of the circuit in henries} \\
C = \text{capacitance of the circuit in farads} \\
V = \text{voltage of the source in volts} \\
I = \text{current in the circuit in amperes} \\
t = \text{time in seconds}$$

ϕ_p = the peak value of the applied alternating flux as supplied by the output circuit.

N_1, E_1, N_2, \hat{E}_2 - Defined as previously.

Since permeability was initially assumed to be infinite in the theoretical case, there is, as has been pointed out, no initial flow of current in the output circuit. Consequently, the total alternating voltage applied to the output circuit appears across the reactor system, and half of this voltage appears across a single reactor. Similarly, no current flows initially in the input circuit, and half of the total applied stop voltage appears across the control coils of a single reactor. In order to establish the time of bias building, the applied flux, ϕ_{dc} , must equal the difference between the value of flux required for flow of current and the peak magnitude of the applied alternating flux. This is the flux required to bias the alternating flux to a position sufficiently high that peak excursions extend into the nonlinear region of the magnetization curve during some portion of the cycle. Therefore

$$\phi_{dc} = \phi_s - \phi_p \quad (4-21)$$

By the law of induction

$$\phi = -\frac{1}{N} \int e \, dt \quad (4-22)$$

Thus, from Equations 4-19 and 4-22

$$\phi_{dc} = \frac{E_1}{2N_1} t \quad (4-23)$$

and similarly, from Equations 4-22 and 4-20 (which assume a sinusoidal flux in the output circuit):

(The rest of the page is illegible)

...and the ...

These responsibilities are usually assumed to be within the
the editorial team, hence it has been assigned out,
we intend to provide in the next issue.

on output there liability in the input circuit, and will
of this voltage appears across a simple resistor. Similarly,
output circuit appears across the resistor network, and half
eventually, the level of receiving voltage applied to the

of the total applied and volume against the position
coils of a single resistor. In order to determine the size

of time building the positive time, but must equal the difference between the value of time required for the of various and the same negative of the applied alternating flux. This is the time required to drive the alternating flux to a position sufficiently high that the alternating current into the coil is zero. The negative current wave extends into the coil and region of the magnetization wave during some portion of the cycle. Therefore

1234-1

$$a^2 - b^2 = (a+b)(a-b)$$

65-211

22 12-1-00

CONFIDENTIAL

4. 1993

11/1/76

$$\phi_p = \frac{\hat{E}_2}{2\omega N_2} \quad (4-24)$$

In each case the factor of 2 appearing in the denominator is made necessary because only one coil of the pair is under consideration. By combining Equations 4-21, 4-23 and 4-24, the following expression is written:

$$\phi_{dc} = \phi_s - \phi_p = \frac{E_1}{2N_1} t = \phi_s - \frac{\hat{E}_2}{2\omega N_2} \quad (4-25)$$

or

$$t = \frac{N_1}{2E_1} \left[\phi_s - \frac{\hat{E}_2}{2\omega N_2} \right] \quad (4-26)$$

Equation 4-26 has been checked analytically for all of the differential analyzer solutions and agreement has been found to be excellent. ϕ_s is found empirically from the measured magnetization curve, and in this problem, in accordance with Figure 4-5, ϕ_s was found to equal 4×10^{-5} webers. The value of Equation 4-26 will become more apparent later in this chapter.

The Analytical Steady-State Behavior of the Magnetic Amplifier

The experimental behavior of the magnetic amplifier has been examined quite thoroughly in Chapter III. The remainder of Chapter IV will be devoted to (1) presentation of analytical results, and (2) correlation of the experimental results with the analytical results which were obtained through use of the differential analyzer.

Throughout this report, all considerations of the steady-state characteristics of the magnetic amplifier

$$\hat{A}_0 = \frac{1}{\omega_0} \frac{d}{dt} \hat{A}_0$$

In each case the factor of 2 appearing in the denominator is made necessary because only one half of the field is under consideration. By combining equations (4-21) and (4-22) the following expression is obtained:

$$(4-23) \quad \hat{A}_0 = \frac{1}{\omega_0} \frac{d}{dt} \hat{A}_0 = \frac{1}{\omega_0} \frac{d}{dt} \left(\frac{1}{\omega_0} \frac{d}{dt} \hat{A}_0 \right)$$

$$(4-24) \quad \left[\frac{1}{\omega_0} \frac{d}{dt} \hat{A}_0 \right] \frac{1}{\omega_0} = \frac{1}{\omega_0} \frac{d}{dt} \left(\frac{1}{\omega_0} \frac{d}{dt} \hat{A}_0 \right)$$

Equation (4-24) has been derived and is valid for all of the differential amplifier solutions and represents the same result as the previous. \hat{A}_0 is found experimentally from the measured excitation wave, and in this problem, is assumed with value $\hat{A}_0 = 1$ was found to equal 1×10^{-2} volt. The value of Equation (4-24) will be used here as a first order in this chapter.

The Analytical Steady-State Behavior of the Amplifier

The experimental behavior of the magnetic amplifier has been examined with knowledge in Chapter III. The remainder of Chapter IV will be devoted to (1) derivation of analytical results, and (2) comparison of the experimental results with the analytical results. The results of the analytical analysis were obtained through use of the differential amplifier. Throughout this report, all derivations of the steady-state characteristics of the magnetic amplifier

have been based upon consideration of the modulation characteristic of the magnetic amplifier. This approach has been continued in the analytical studies.

In Figure 4-10, modulation characteristics for experimental and analytical observations are plotted. The circuit parameters for these observations were identical for each case. It will be noticed from Figure 4-10 that the modulation characteristic observed experimentally lies above the analytical characteristic by a constant value of approximately 2 ampere-turns. The fact that the average value of the output ampere-turns is larger by a constant factor in the experimental case is directly attributed to two factors: (1) the fact that infinite initial-permeability was assumed in the theoretical case while in the practical case the initial permeability is not infinite and some current will surely flow in the output circuit, and (2) the more important fact that hysteresis and eddy-current losses were neglected in the theoretical case while in the practical case it has been pointed out that the initial hysteresis current is of a definitely measurable magnitude. Since measured magnetization characteristics for the cores employed have indicated that the initial permeability, while certainly not approaching infinity, is very great, the assumption of infinite initial permeability in the analytical case is construed to be of less importance than the neglect of hysteresis in the analyzer problem, and, therefore, the major part of

have been based upon consideration of the modulation characteristics of the negative amplifier. This assumption has been confirmed by the analytical studies.

In Figure 4-10, modulation characteristics for experimental and analytical observations are plotted.

The circuit parameters for these observations were identical for each case. It will be noticed from Figure

4-10 that the modulation characteristics observed experimentally are in good agreement with the analytical characteristics of a

constant value of approximately 1.25. The fact that the average value of the output signal is

larger by a constant factor in the experimental case is directly attributed to the fact that the

initial value of the output signal is not zero in the experimental case while in the analytical case the initial value is

zero. It is not infinite and some constant will result from the output signal, and (2) the fact that the

output signal is not zero in the experimental case is due to the fact that the initial value of the output signal is not zero

in the analytical case. The fact that the initial value of the output signal is not zero in the experimental case is due to the fact that the

initial value of the output signal is not zero in the analytical case. The fact that the initial value of the output signal is not zero in the experimental case is due to the fact that the

initial value of the output signal is not zero in the analytical case. The fact that the initial value of the output signal is not zero in the experimental case is due to the fact that the

initial value of the output signal is not zero in the analytical case. The fact that the initial value of the output signal is not zero in the experimental case is due to the fact that the

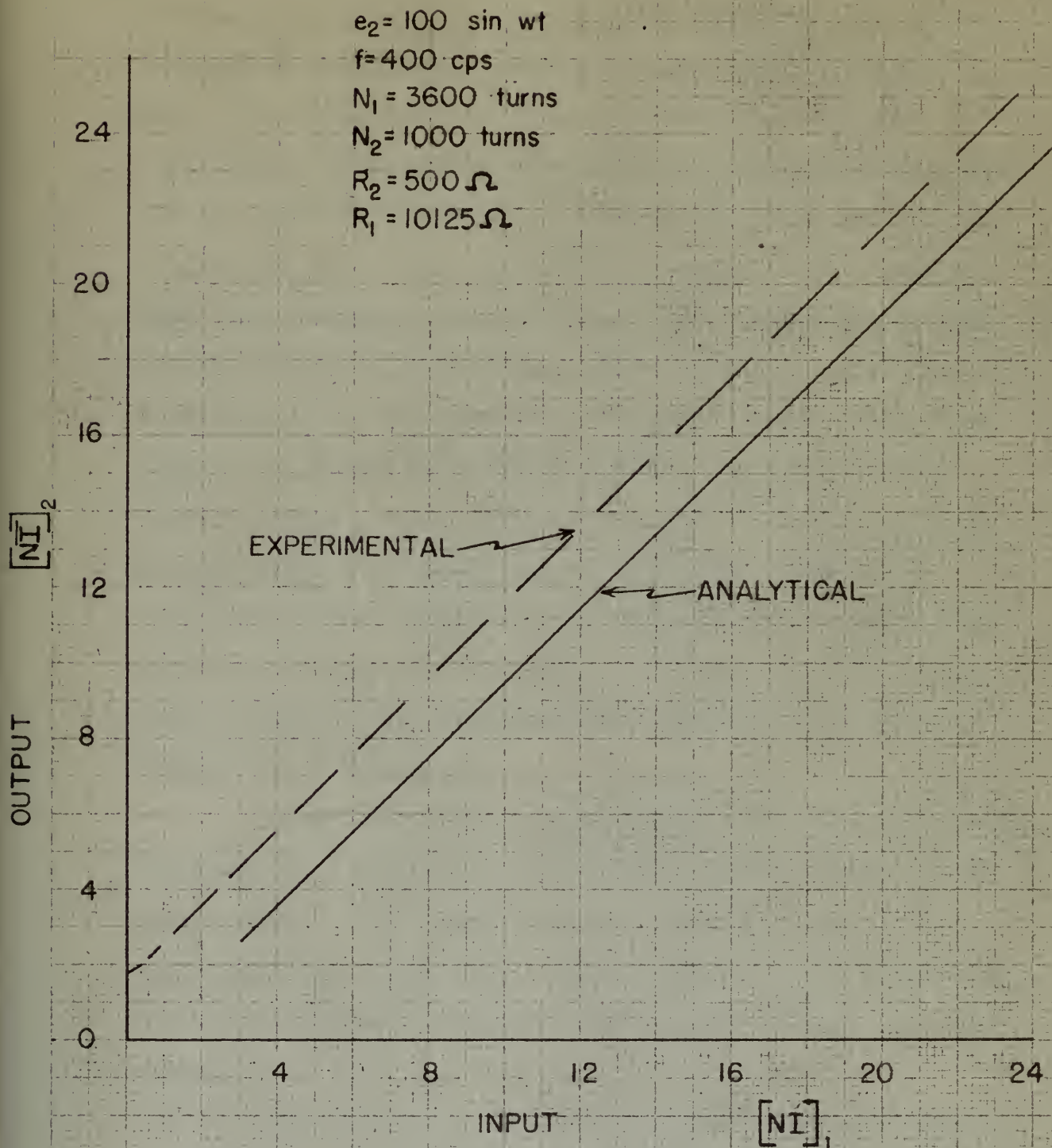


FIG. 4-10 COMPARISON OF ANALYTICAL AND EXPERIMENTAL MODULATION CHARACTERISTICS AT 400 CPS

the variation between observed and analytical cases is assigned to hysteresis effects. As is shown in Figure 4-10, the neglect of hysteresis has not had a marked derogatory effect on the analytical steady-state solution and the error introduced is constant and does not affect the usefulness of the theoretical observations. In further discussions of the effects of the various parameters on the analytical modulation characteristics, the observed variations from experimental conditions which result from neglect of losses are exactly similar to the variation shown in Figure 4-10. It may be stated that the neglect of losses and the assumption of infinite initial permeability in the analytical solutions have not materially affected the value of the data obtained from these solutions, insofar as the steady-state modulation characteristics are concerned.

The discussion of the steady-state and transient response of the analytical amplifier is best divided into discussions of the input-circuit parameters and of the output-circuit parameters. The modulation characteristics obtained analytically will be discussed in these two categories.

(a) The Effects of Input Circuit Parameters on the Modulation Characteristic ---

The reader will recall that all output currents were measured with a planimeter and thence calculated by the application of scale factors. Since the planimeter is not a precise instrument, it is conceivable

The variation between observed and analytical curves is assigned to systematic errors. As is shown in Figure 4-10, the analysis of hydrocarbons has not a simple derivative effect on the analytical steady-state solution and the error introduced is constant and does not affect the usefulness of the theoretical observations. In the first discussion of the effects of the various parameters on the analytical solution characteristics, the observed variations from experimental conditions which result from neglect of losses are exactly similar to the variation shown in Figure 4-10. It may be noted that the neglect of losses and the assumption of infinite initial concentration in the analytical solution have not materially affected the value of the data obtained from these experiments, insofar as the steady-state analytical characteristics are concerned.

The discussion of the steady-state and transient response of the analytical solution is now divided into discussions of the input-output parameters and of the output-analytical parameters. The modification characteristics obtained analytically will be discussed in these two chapters.

(a) The Effects of Input Output Parameters on the Analytical Characteristics --- The reader will recall that all output curves were measured with a galvanometer and known calculated by the application of a sine wave. Since the galvanometer is not a perfect instrument, it is necessary

that errors may be present in some measurements which may cause inconsistencies in the results. In general, these inconsistencies have been relatively unimportant.

The measured analytical modulation-characteristic showing the effect of the input-circuit resistance, R_1 , is shown on Figure 4-11. It will be noticed on this figure that the effect of R_1 on the analytical modulation characteristic is virtually negligible, as would be expected from the form of the equations, because it is the input-circuit current, which determines the magnitude of the current flowing in the output circuit. In the analytical studies, the magnitude of the input step-voltage was adjusted as R_1 was varied, such that the input current was maintained at an equivalent level for the various observations of the effects of different values of R_1 . It may be concluded, therefore, that in accordance with both analytical and experimental observations, the input circuit resistance does not materially affect the shape of the modulation characteristic as long as the input current is maintained unaffected by changes in this resistance. If the input current is to be unaffected by changes in R_1 , changes in the magnitude of the input step-voltage are implied.

The effect of the number of turns on the input coils of the amplifier is shown by the modulation characteristics of Figure 4-12. The bending and cross-over of the characteristic at 1000 turns is attributed to inaccuracy of

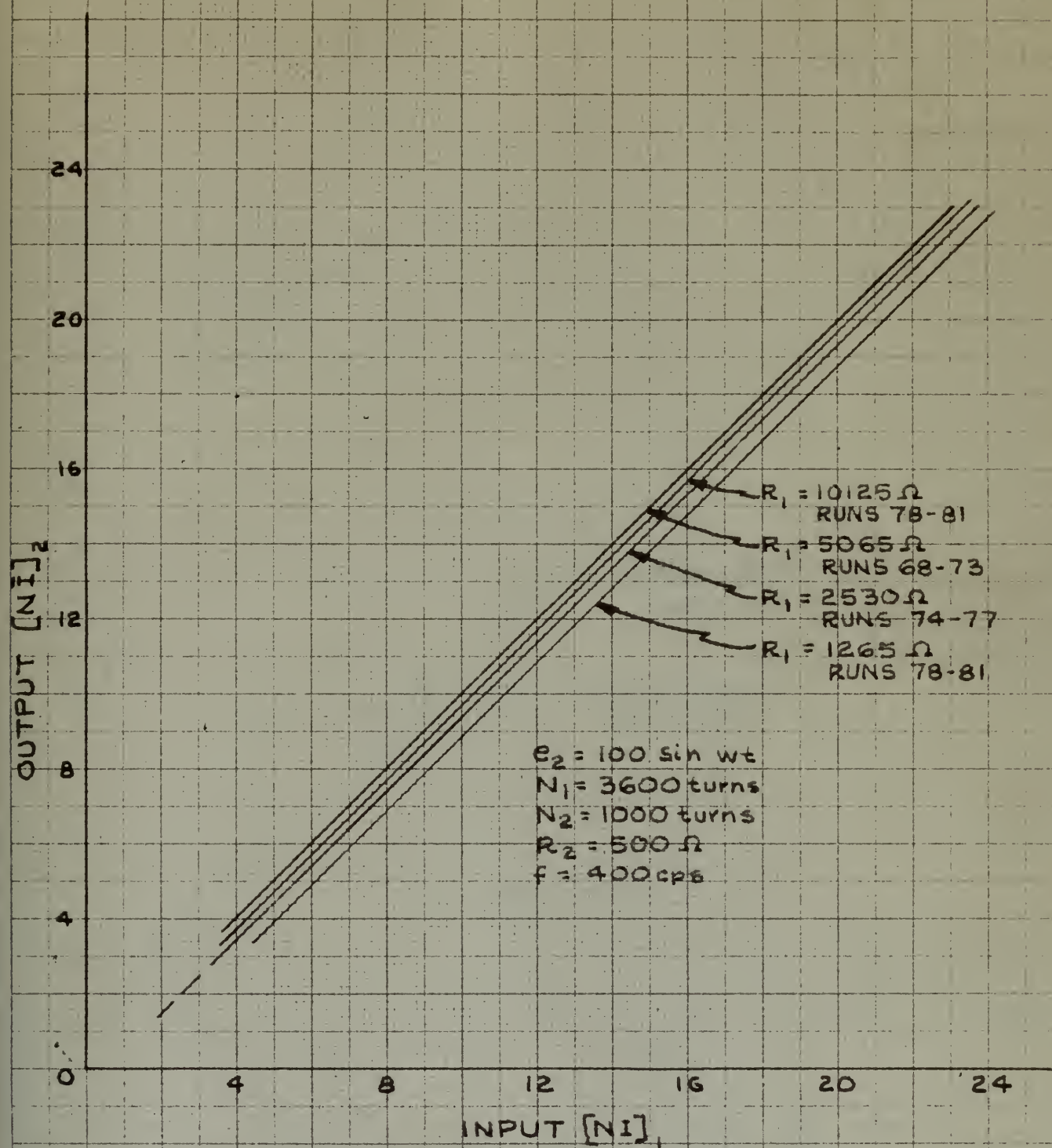


FIG. 4-11 ANALYTICAL OBSERVED EFFECT OF INPUT RESISTANCE, R_1 , ON STEADY-STATE OPERATION.

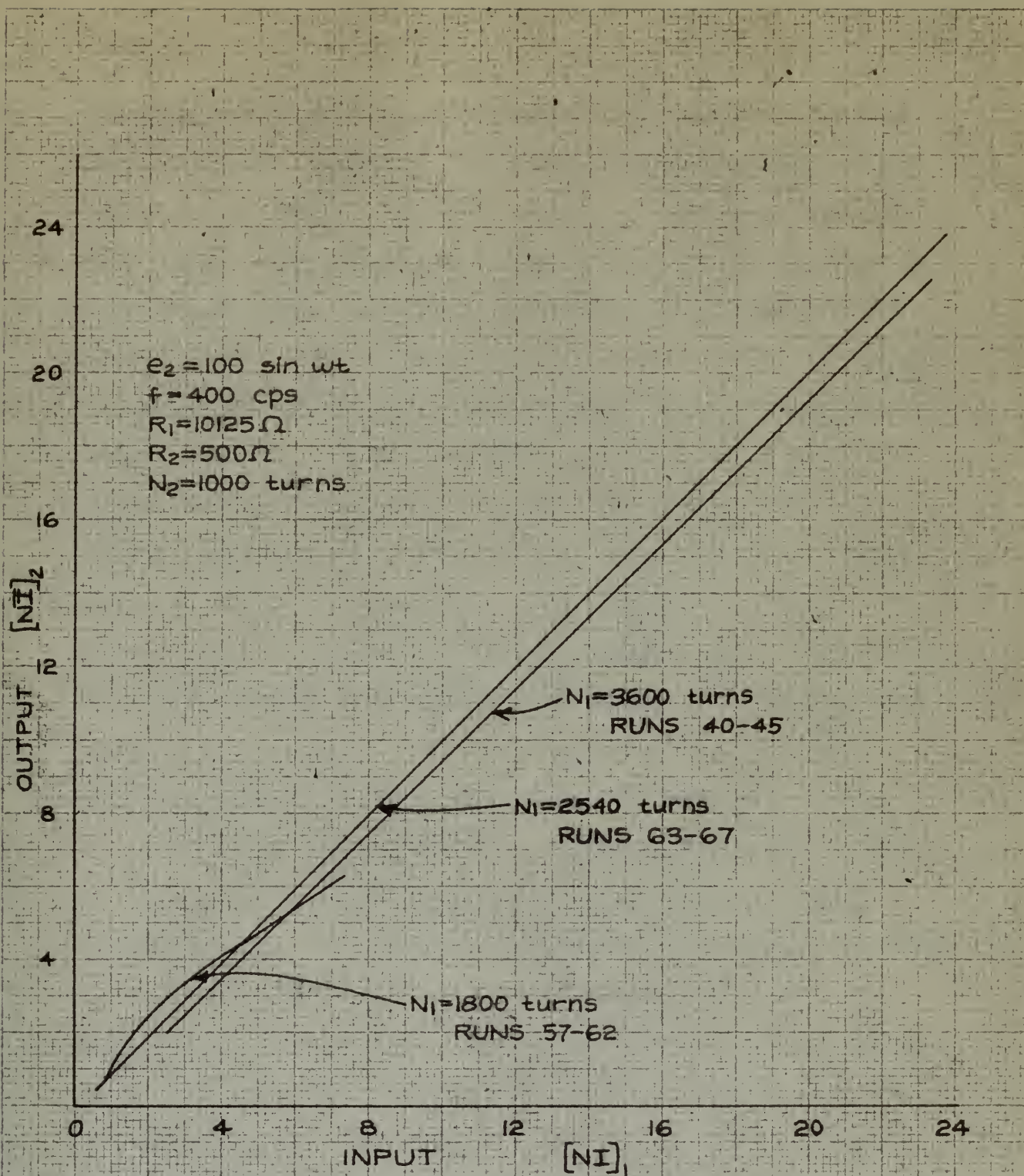
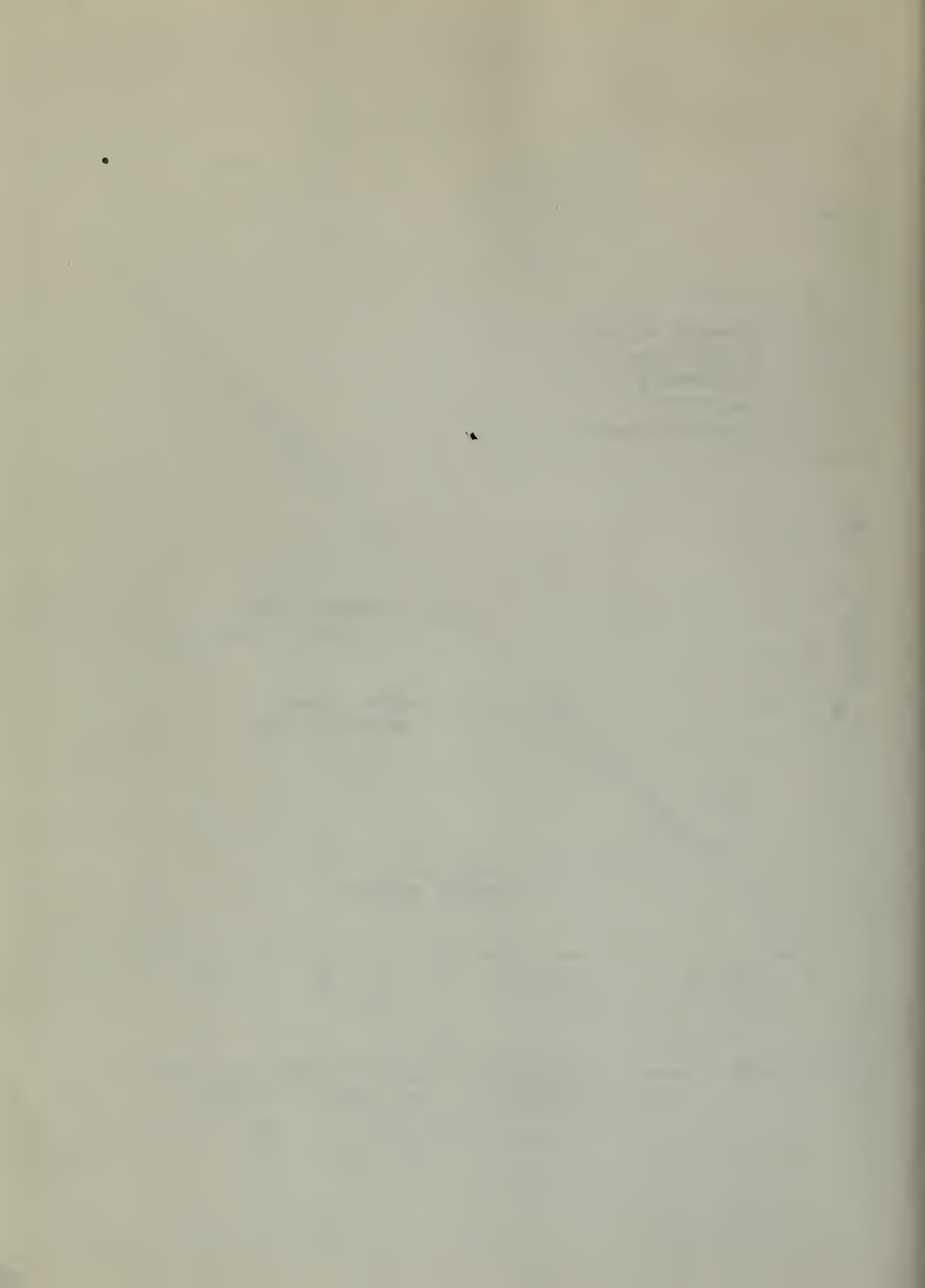


FIG. 4-12 ANALYTICAL OBSERVED EFFECT OF INPUT CIRCUIT TURNS, N_1 , ON STEADY STATE OPERATION



of measurement with the planimeter at the lower values of input current. Actually, this characteristic would be expected to be similar to those shown at 2540 turns and at 3600 turns. The modulation characteristics are plotted in ampere-turns and, therefore, the characteristics for the lower values of N_1 actually require larger values of input currents to produce the same amount of ampere-turns in the output circuit. It is therefore apparent that the input power required to produce a given ampere-turn output is greater when the input turns are decreased because larger input-currents are required. The analytical effect of the input turns on the modulation characteristic, as expressed in ampere-turns, is virtually negligible, and this observation is in agreement with experimental investigations.

(b) The Effects of the Output Circuit Parameters on the

Modulation Characteristic --- The experimental effect of the output-circuit resistance, R_2 , which is largely composed of the system-load resistance, has been considered in detail in Chapter III. As explained previously, the manner in which the load resistance affects static behavior is contingent upon simultaneous magnetic effects and electrical effects in the output circuit. The flattening of the modulation characteristic in the higher ranges of input ampere-turns for large values of R_2 has been explained on the basis of the voltage distribution in the carrier circuit and will not be considered further at this time. Figure 4-13

of measurement with the amplifier at the lower values of input current. Actually, this characteristic would be expected to be similar to those shown at 5000 cycles and at 5000 cycles. The modulation characteristics are limited in range-factors and, therefore, the characteristics for the lower values of ω actually require higher values of input current to produce the same amount of range-factors in the output circuit. It is therefore apparent that the input power required to produce a given range-factor output is greater when the input tones are decreased because higher input-currents are required. The analytical effect of the input tones on the modulation characteristics, as represented in range-factors, is virtually negligible, and this observation is in agreement with experimental measurements.

(d) The effect of the input current on the modulation characteristics — The experimental effect of the output-current magnitude, ω , which is largely composed of the system-level resistance, has been indicated in detail in Chapter III. As explained previously, the amount is which the load resistance affects the behavior is confined upon similar manner regarding effects and also typical effects in the output circuit. The frequency of the modulation characteristics in the higher ranges of input range-factors for large values of ω has been explained on the basis of the voltage distribution in the output circuit and will not be considered further at this time. (Figure 4-1)

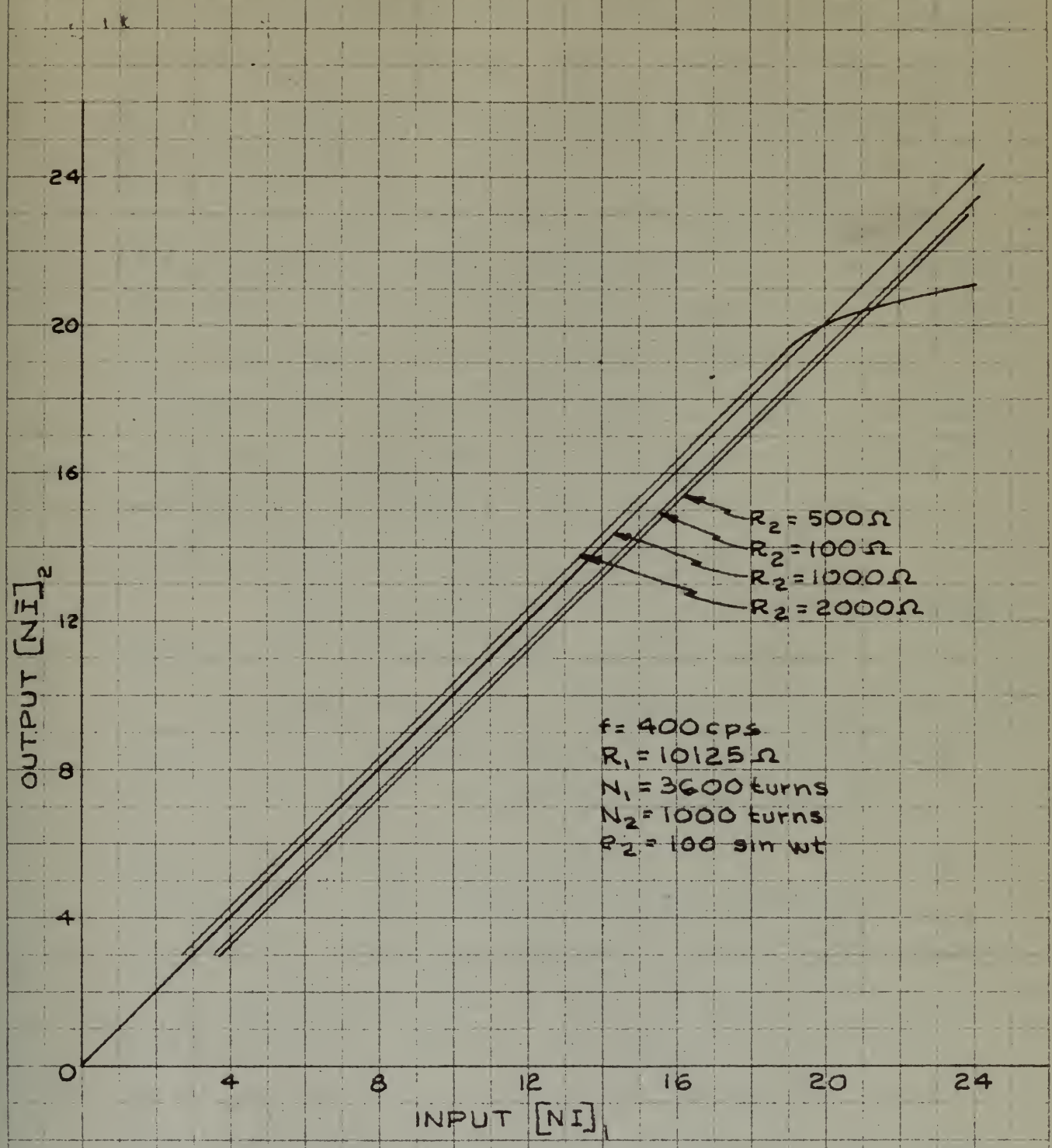


FIG. 4-13 ANALYTICAL OBSERVED EFFECT OF OUTPUT CIRCUIT RESISTANCE, R_2 , ON STEADY-STATE OPERATION.

shows the analytically observed effect of the output-circuit resistance on the modulation characteristic. Notice that at the value of $R_2 = 2000$ ohms the modulation characteristic has commenced to fall off and the effect of saturation of the modulation characteristic is becoming apparent. The other values of R_2 , being of lower magnitude, do not exhibit this effect within the range of the observations which were made. The behavior of the analytical circuit is again analogous to the experimentally-observed behavior and tends to confirm the conclusions made previously with regard to the nature of the effect of increasing values of load resistance on the static behavior of the amplifier.

Similarly, the nature of the analytically-observed effects of the variation of the output-circuit turns confirms the observations and conclusions drawn from experimental evidence in the previous chapter. The analytical results for turns variations in the output circuit are shown in Figure 4-14. As was the case experimentally, there is no definite trend of the effect. A definite flattening of the modulation characteristic occurs when the N_2 is reduced to the value of 500 turns per coil, and comparison of this result with Figure 3-10, in which similar characteristics are plotted for similar parameters, will show the marked similarity between analytical and experimental observations. As was the case empirically, so does the analytical solution indicate an optimum value of N_2 for maximum ampere-

shows the analytically observed effect of the output-voltage regulation on the modulation characteristics. It is seen that at the value of $V_g = 2000$ volts the modulation characteristics has decreased by half and the effect of modulation on the modulation characteristics is reduced. The other values of V_g , being of lower magnitude, do not exhibit this effect within the range of the modulation voltage used. The behavior of the analytical results is again compared to the experimentally-observed behavior and found to confirm the conclusions made, especially with regard to the effect of the effect of increasing value of V_g on the behavior of the output behavior of the amplifier.

Similarly, the effect of the analytically-observed

effect of the variation of the output-voltage regulation on the modulation and modulation characteristics (see experimental evidence in the previous chapter). The analytical results for some variations in the output voltage are shown in Figure 4-10. As was the case experimentally, there is no definite trend of the effect. A definite increasing of the modulation characteristics occurs when the V_g is reduced to the value of 2000 volts per volt, and decreases of the results with Figure 4-10. In other words, the modulation characteristics are plotted for higher modulation, with the same modulation characteristics between analytical and experimental characteristics. As was the case experimentally, so was the analytical results also indicate an increase in the modulation characteristics.

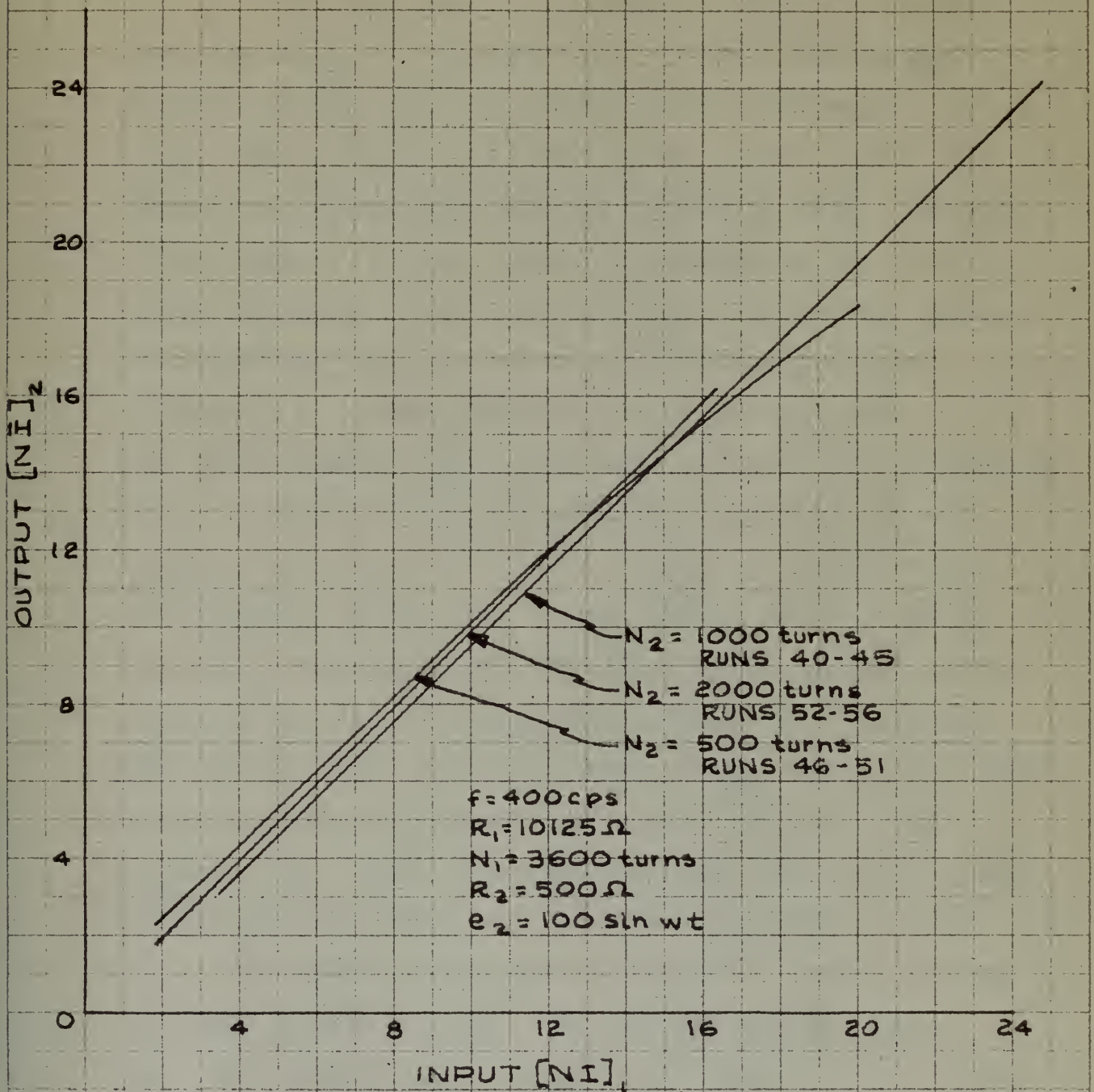


FIG. 4-14. ANALYTICAL OBSERVED EFFECT OF OUTPUT CIRCUIT TURNS, N_2 , ON STEADY-STATE PERFORMANCE.

turn sensitivity of the amplifier. The semi-quantitative procedure for optimizing N_2 was discussed in Chapter III.

The peak value of alternating flux in a single core was defined by Equation 4-24. It has been pointed out that if the peak value of this flux exceeds the saturation flux, a current will flow in the output circuit although the applied input circuit current is zero. Analytically, because of scale factor limitations on the differential analyzer, it was not practicable to decrease either the secondary turns, N_2 , or the alternating frequency, f , sufficiently to obtain fluxes of adequate magnitude to exceed the saturation flux at the peak value of the alternating flux. A simple computation made from Equation 4-24 will indicate that if ϕ_s is 4×10^{-5} webers, N_2 is 1000 turns and frequency is 400 cps., a peak voltage of 102.4 volts per coil, or approximately 205 volts total supplied to the secondary circuit, is required to produce an alternating flux sufficient to exceed the value of ϕ_s . The differential analyzer was readily adapted to produce an alternating voltage of 300 volts peak amplitude, and the results of the observations made with this voltage are plotted on Figure 4-15. The output ampere-turns are noted to exceed 16 when the input current is zero. For various reasons, which have been discussed previously in this report and in detail in the literature,¹ the presence of a large initial output current is highly undesirable, and it is, therefore, essen-

1. Fitzgerald, A.S., "Magnetic Amplifier Circuits," J.F.I., 244, (1947), 249-263.

turn sensitivity of the amplifier. The non-linearities
 procedure for obtaining H_2 was discussed in Chapter III.
 The peak value of alternating flux is a single

core was defined by Equation 4-14. It has been pointed
 out that if the peak value of this flux exceeds the sat-
 uration flux, a current will flow in the output circuit al-
 though the applied input signal current is zero. Analyti-
 cally, because of finite vector limitations on the differ-
 ential amplifier, it was not possible to determine either
 the secondary current, I_2 , or the alternating flux density, B_2 ,
 sufficiently to obtain values of maximum signals to ex-
 ceed the saturation flux at the peak value of the alternating

flux. A single computation was from Equation 4-14 will
 indicate that if B_2 is 2×10^5 gauss, H_2 is 1000 gauss
 and frequency is 500 cps., a peak voltage of 100.4 volts
 per cell, or approximately 200 volts total applied to the
 secondary circuit, is required to produce an alternating
 flux sufficient to exceed the value of B_2 . The differential

amplifier was readily capable of producing an alternating
 voltage of 500 volts peak amplitude, and the results of the
 observations with this voltage are shown in Figure
 4-15. The output wave-forms are noted in Figure 4-15 when

the input current is zero. The various waveforms, which
 have been discussed previously in this report and in detail
 in the literature,¹ are produced at a large initial output
 current is highly undistorted, and as I_2 , increases, wave-
 1. Richardson, A. G., "Magnetic Amplifier Circuit," *IEEE*,
 Vol. 11, No. 1, 1964.

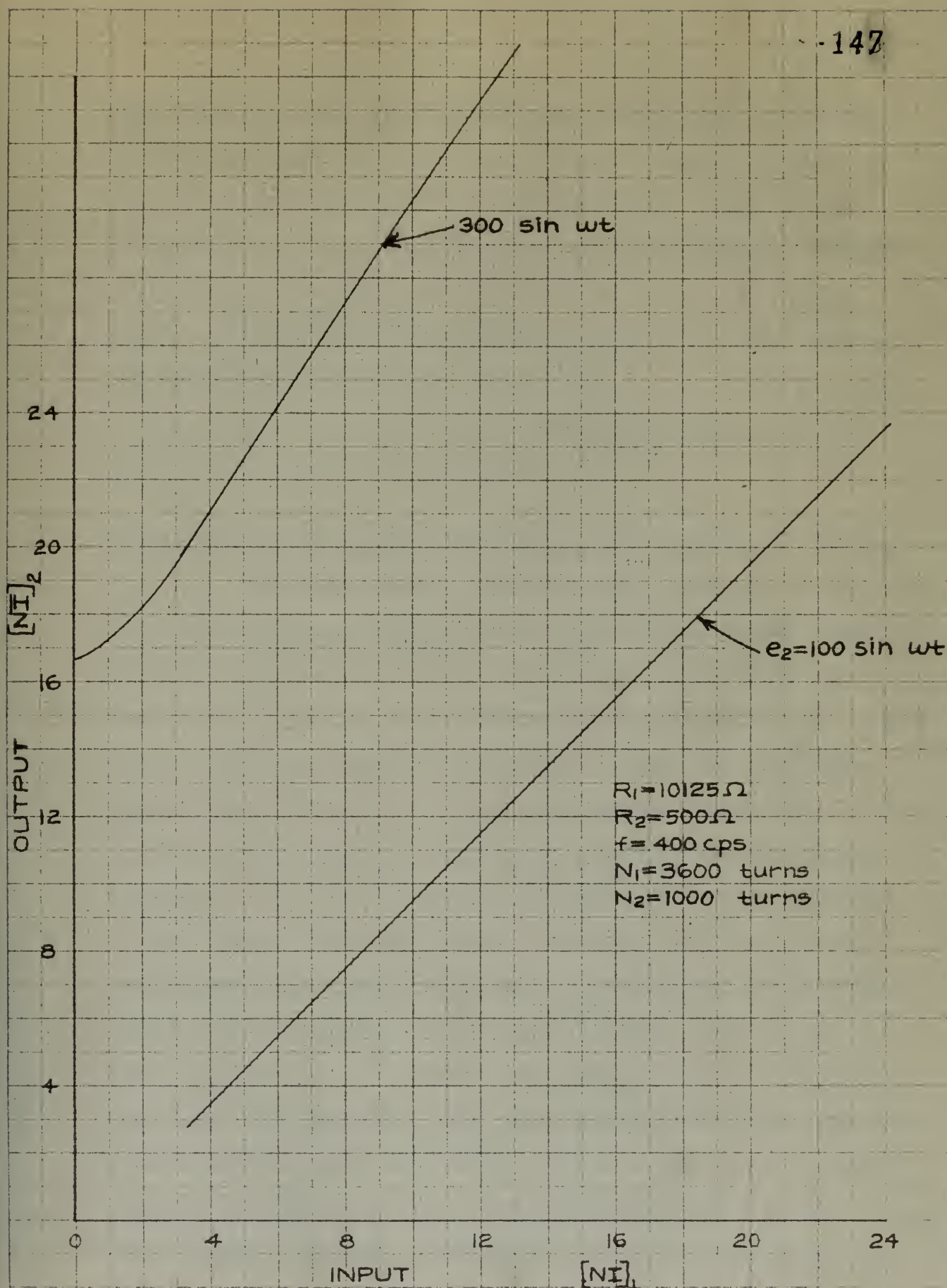


FIG. 4-15 ANALYTICAL OBSERVED EFFECT OF ALTERNATING VOLTAGE, e_2 , ON STEADY-STATE OPERATION

tial that the flux excursions of the output circuit be restricted to less than ϕ_g if the effect of large initial output-circuit currents is to be minimized. Limitations of the voltage-generating and amplifying equipment available in the laboratory made it difficult to create an experimental situation having the same circuit parameters used in the analytical observation at 300 volts, and again, the value of the machine solution in observing the fundamental behavior of the circuit is apparent.

The Analytical Transient Behavior of the Magnetic Amplifier

The Elmen theory regarding the nature of hysteresis loss in iron-cored reactors under excitation at more than one frequency has been discussed previously. The theory has been further confirmed by analytical studies of the transient behavior of the magnetic amplifier. In review, the Elmen theory states that if a core is excited at separate circuits in which the frequencies of the alternating parameters are different, the major portion of hysteresis loss is supplied by the higher frequency source. In accordance with this hypothesis, the effect of hysteresis loss would be expected to be more pronounced in the output circuit than in the input circuit of the magnetic amplifier. Such is, indeed, the case. Analytically, the effects of variations in the input-circuit parameters on the transient response of the magnetic amplifier are very nearly exactly equal to the corresponding effects of variations of these parameters as

that the flux component of the output circuit is not
 expected to have any effect on the output of the
 output-circuit amplifier is to be minimal. The
 of the output-circuit and amplifying elements available
 in the laboratory made it difficult to obtain an output
 normal amplifier having the same circuit parameters used in
 the analytical treatment as 100 volts, and equal the value
 of the machine output in operating the fundamental be-
 havior of the circuit is expected.

The Analytical Treatment of the Output Amplifier

The linear theory regarding the nature of the output
 loss in iron-core transformers under excitation at more than one
 frequency has been discussed previously. The theory has
 been further confirmed by analytical studies of the behavior
 of the magnetic amplifier. In view of the linear
 theory stated that it is not to be expected at higher frequencies
 in which the frequency of the alternating component may
 differ, the major portion of the output loss is expected
 of the higher frequency losses. In accordance with this
 hypothesis, the effect of transformer loss would be expected
 to be more pronounced in the output circuit than in the
 input circuit of the magnetic amplifier. Such is, indeed,
 the case. Analytically, the effect of transformer loss in the
 input-circuit parameters on the transient response of the
 magnetic amplifier are very nearly equally small to the
 corresponding effects of variations of these parameters on

observed experimentally. Quite on the contrary, the effects of analytical variations of the output-circuit parameters on the transient response of the amplifier are very different from the effects observed experimentally. The difference, as was pointed out in Chapter III, is almost totally due to loss effects which are very pronounced in the output circuit.

As was done in the preceding section, the output and input circuits will be dealt with separately in discussions of the analytical transient behavior of the magnetic amplifier.

(a) The Effects of the Input-Circuit Parameters on the

Transient Behavior of the Magnetic Amplifier -- The characteristic time of the response of the magnetic amplifier to an applied step voltage for variations in the input-circuit current, i_1 , was shown experimentally to be inversely proportional to the square-root of the input current. The nature of this variation has been discussed in Chapter III. The effect of i_1 upon the transient-time of the amplifier was confirmed by the analytical equations, and the inverse square-root function was shown to hold in the theoretical case. In Figure 4-16 the variation of characteristic time with increasing values of input circuit current is plotted from observed analytical data as obtained from the analyzer solutions for a particular set of circuit parameters, as indicated on the figure. The curve of Figure 4-16 is replotted on log-log coordinates in Figure

observed experimentally. Quite on the contrary, the effect of analytical variations of the output-circuit parameters on the transient response of the amplifier are very different from the effects observed experimentally. The difference, as was pointed out in Chapter III, is almost totally due to loss effects which are very pronounced in the output circuit.

As was done in the preceding section, the output and input circuits will be dealt with separately in the questions of the analytical transient behavior of the magnetic amplifier.

(a) The effects of the input-circuit parameters on the transient behavior of the magnetic amplifier -- The characteristic time of the response of the magnetic amplifier to an applied step voltage for variations in the input-circuit current, i_1 , was shown experimentally to be inversely proportional to the square-root of the input current. The nature of this variation has been discussed in Chapter III. The effect of i_1 upon the transient-time of the amplifier was confirmed by the analytical treatment, and the inverse square-root function was shown to hold in the theoretical case. In Figure 4-15 the variation of characteristic time with increasing value of input circuit current is plotted from observed analytical data as obtained from the analytical solution for a particular set of circuit parameters, as indicated on the figure. The curve of Figure 4-15 is replotted on log-log coordinates in Figure

$e_2 = 100 \sin \omega t$
 $N_1 = 3600$ turns
 $N_2 = 1000$ turns
 $R_1 = 10125 \Omega$
 $R_2 = 500 \Omega$
 $f = 400$ cps

(CT) IN $\text{sec} \times 10^5$

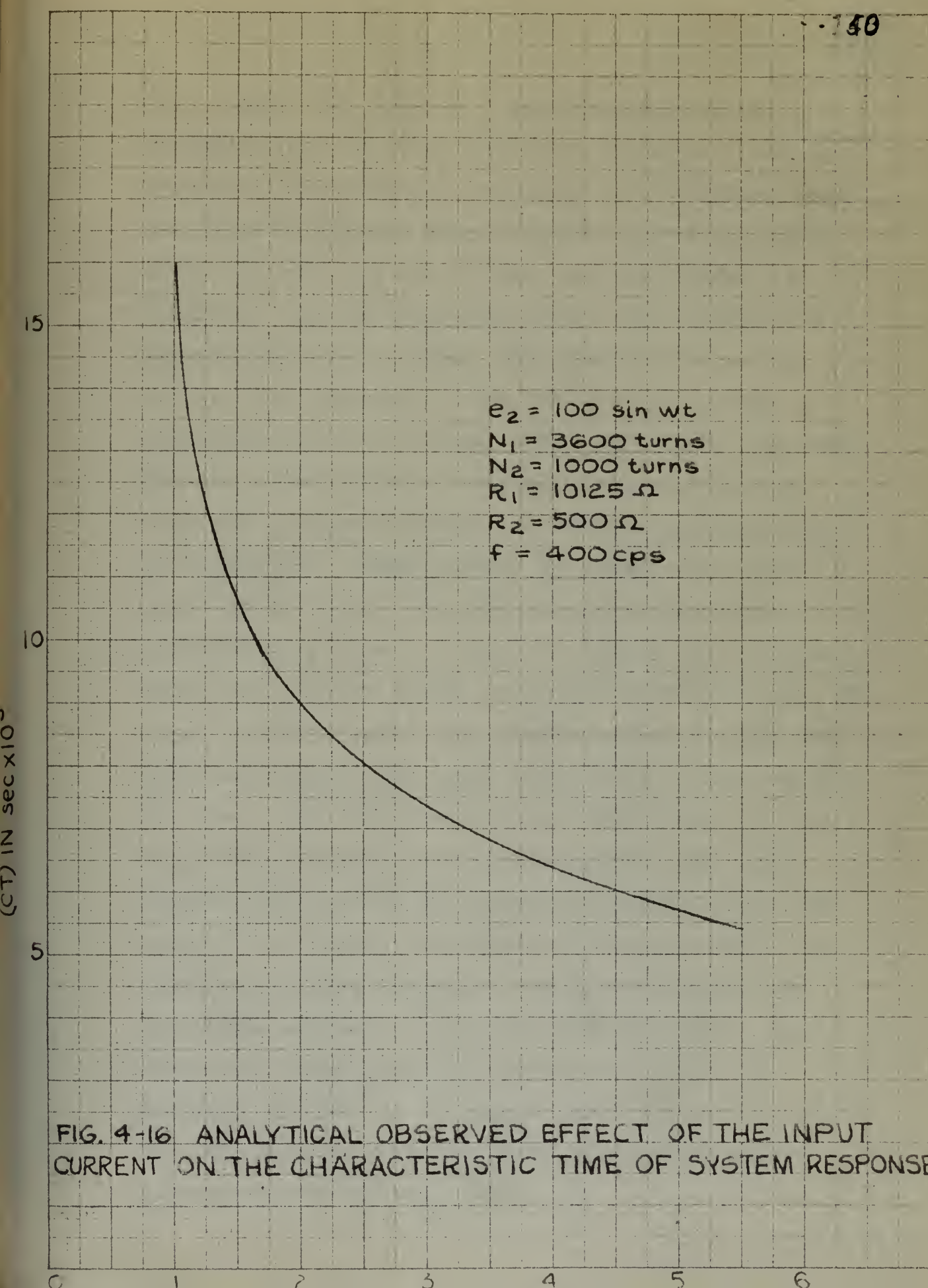


FIG. 4-16 ANALYTICAL OBSERVED EFFECT OF THE INPUT CURRENT ON THE CHARACTERISTIC TIME OF SYSTEM RESPONSE.

4-17, which also shows the experimentally observed variation for equivalent parametric conditions. The experimental data used for comparison with analytical data was taken by photographing a single sweep of an oscilloscope when the transient in the amplifier circuit was in progress. This technique has proved very valuable for observations of this type. The effects of increasing values of i_1 are shown by the series of photographs of transient behavior in Figure 4-18. It will be noted that the characteristic-time variation plots as a straight line with a slope of minus $\frac{1}{2}$ on the log-log coordinates of Figure 4-17, which confirms the inverse square-root variation due to i_1 . It will also be noticed that the experimentally observed curve lies beneath the analytical curve, or, in other words, the experimental variations indicate somewhat lesser magnitudes of characteristic time than were observed for equal values of i_1 in the analytical case. This phenomena is attributed to the presence of a small additional variable resistor in the input circuit which appears as a result of the hysteresis and eddy-current losses. The magnitude of this resistor is dependent on the magnitude of the i_1 and changes with increasing currents in a manner which maintains a constant difference between the curves of Figure 4-17. Actually, as shown by the figure, the difference is small over the observed range and might be caused by normal fluctuations of the data.

4-17, which also shows the experimentally observed variation for equivalent permeability conditions. The experimental data used for comparison with analytical data was taken by photographing a single sweep of an oscilloscope when the transient in the amplifier circuit was in progress. This technique has proved very valuable for observations of this type. The effects of increasing values of i_1 are shown by the series of photographs of transient behavior in Figures 4-18. It will be noted that the characteristic-time variation plots as a straight line with a slope of minus $\frac{1}{2}$ on the log-log coordinates of Figure 4-17, which confirms the inverse square-root variation due to i_1 . It will also be noticed that the experimentally observed curve lies beneath the analytical curve, or, in other words, the experimental variations in these somewhat lesser magnitudes of characteristic time than were observed for equal values of i_1 in the analytical case. This phenomenon is attributed to the presence of a small additional variable resistor in the input circuit which appears as a result of the inductance and eddy-current losses. The magnitude of this resistor is dependent on the magnitude of the i_1 and changes with increasing currents in a manner which maintains a constant difference between the curves of Figure 4-17. Actually, as shown by the figure, the difference is small over the observed range and might be caused by normal fluctuations of the data.

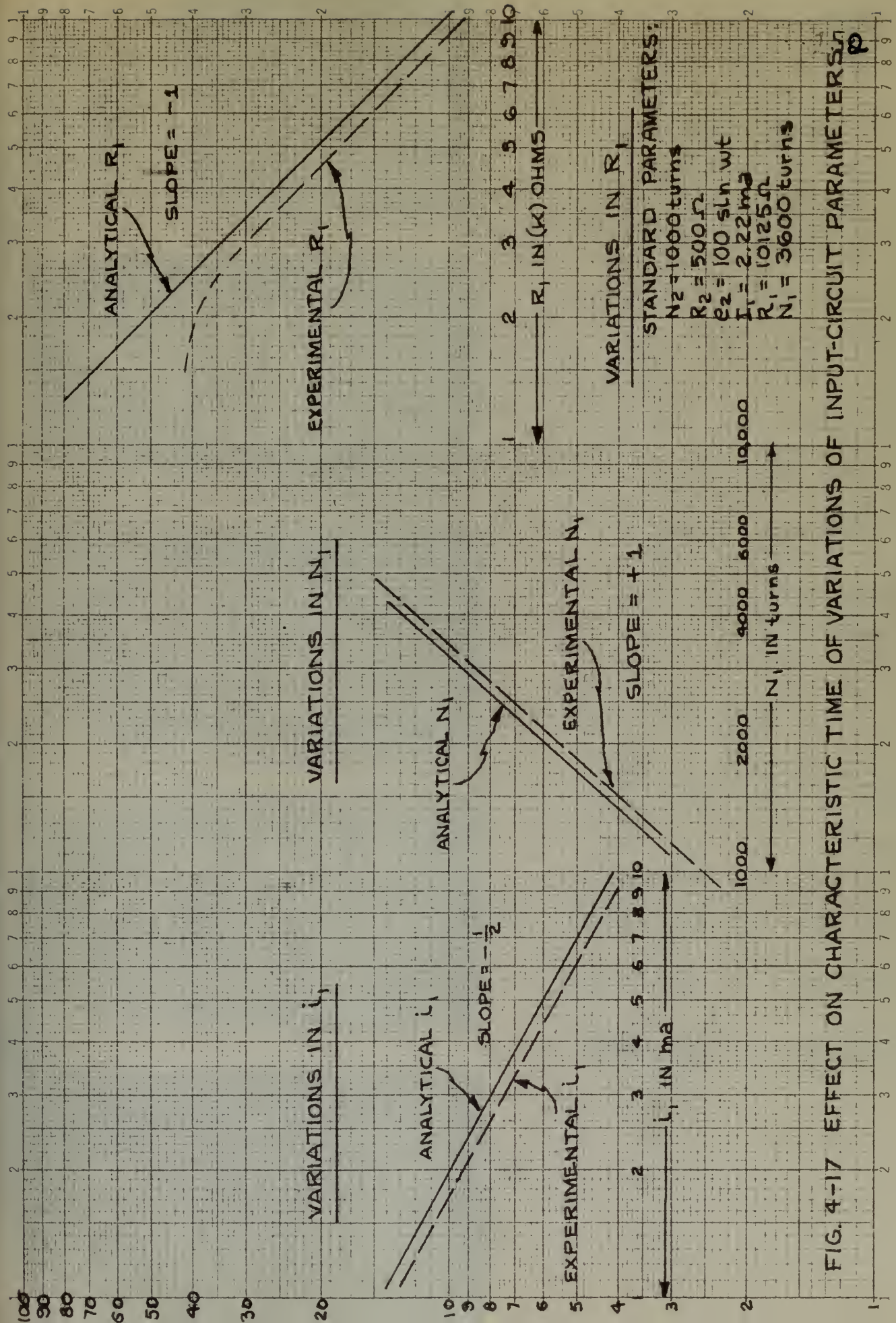
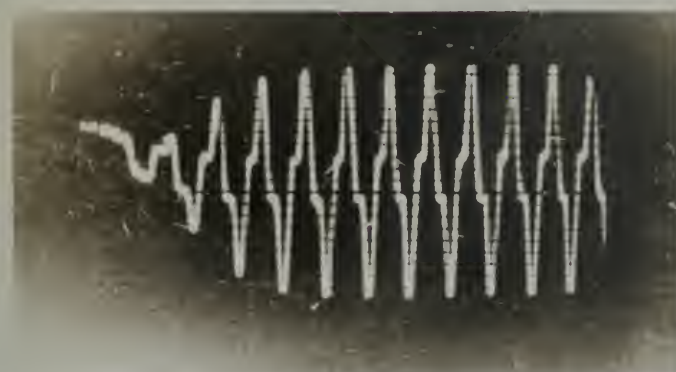


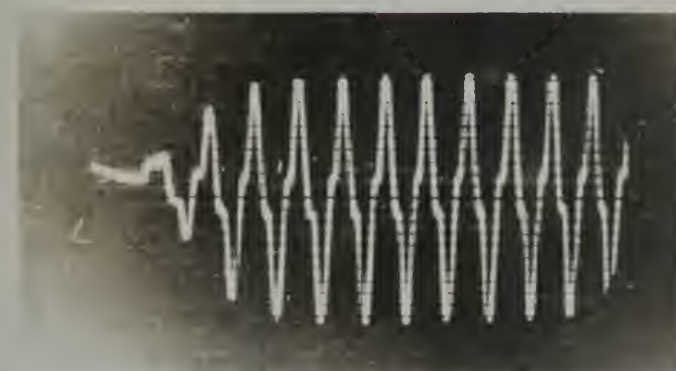
FIG. 4-17 EFFECT ON CHARACTERISTIC TIME OF VARIATIONS OF INPUT-CIRCUIT PARAMETERS p



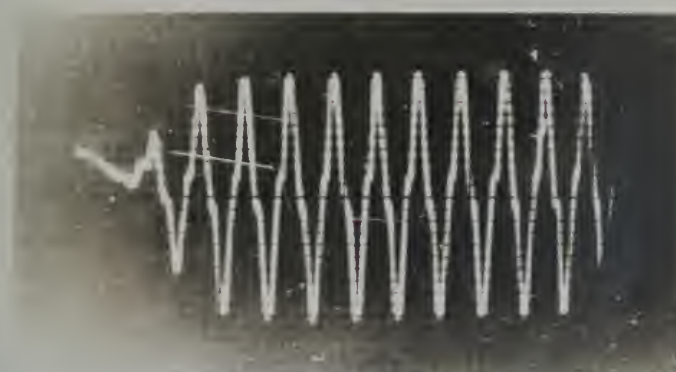
(a)



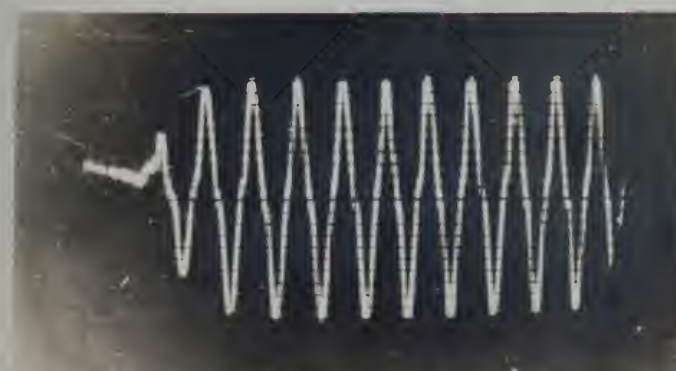
(b)



(c)



(d)



(e)

FIGURE 4-18

OSCILLOSCOPIC PHOTOGRAPHS
SHOWING THE BUILDUP OF THE
OUTPUT-CIRCUIT CURRENT, i_2 ,
FOR INCREASING VALUES OF THE
INPUT CURRENT, i_1 , WHEN A
STEP-FUNCTION OF VOLTAGE IS
APPLIED TO THE INPUT-CIRCUIT
TERMINALS

f = 400 cps.
 N_1 = 3600 T
 N_2 = 1000 T
 R_1 = 10125 ohms
 R_2 = 500 ohms
 e_2 = 100 sin ωt volt

KEY

(a) i_1 = 1.11 ma.
(C_T) = 12.5 msec.
(b) i_1 = 2.22 ma.
(C_T) = 8.6 msec.
(c) i_1 = 3.33 ma.
(C_T) = 7.2 msec.
(d) i_1 = 4.44 ma.
(C_T) = 6.0 msec.
(e) i_1 = 5.55 ma.
(C_T) = 5.25 msec.

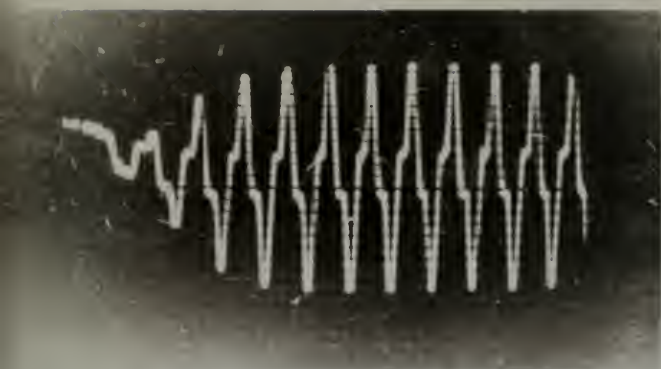
Observations made analytically have permitted the plotting of families of curves similar to those in Figure 4-16 with the various parameters of the circuit represented by different curves of the family. The data from which each of these analytical curves was plotted are tabulated in Charts 4-3 and 4-4. The families of curves show the variation of characteristic time with I_1 for different values of each parameter. It is then possible to select a constant value of the input-circuit current and to determine the variation of characteristic time as any individual parameter is varied. In these studies the value of I_1 of 2.22 milliamperes has been selected as a standard for observation of parametric effects.

The variation of the characteristic time of amplifier-response with changes in the input-circuit resistance when the other parameters are held constant is shown plotted on log-log coordinates in Figure 4-17. Also plotted on this figure is the experimentally observed variation in characteristic time for the same circuit conditions as were existent in the analytical case. The experimental characteristic times were obtained from the series of oscilloscopic photographs shown in Figure 4-19. As was the case with the analytical and experimental variations of I_1 , the comparison of analytical and experimental variations of R_1 also indicates the presence of a small additional variable resistance in the input

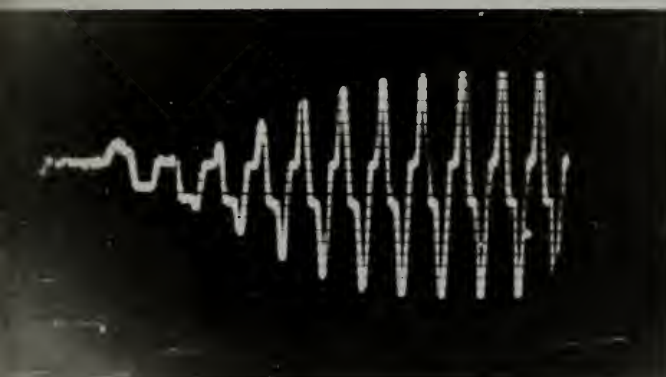
Observations made analytically have permitted the plotting of families of curves similar to those in Figure 4-16 with the various parameters of the circuit represented by different curves of the family. The data from which each of these analytical curves was plotted are tabulated in Charts 4-3 and 4-4. The families of curves show the variation of characteristic time with I_1 for different values of each parameter. It is then possible to select a constant value of the input-circuit current and to determine the variation of characteristic time as any individual parameter is varied. In these studies the value of I_1 at 5.25 milliamperes has been selected as a standard for observation of parametric effects.

Tests.

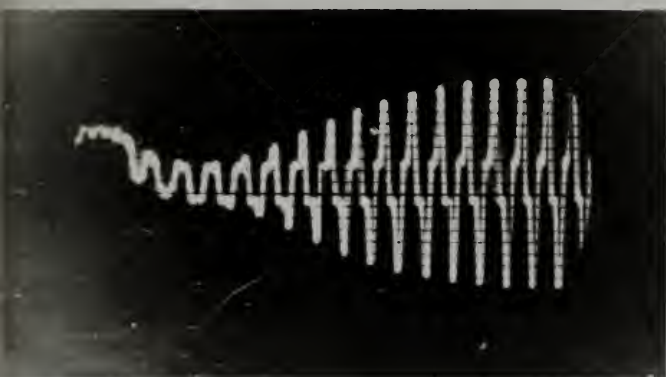
The variation of the characteristic time of amplifier-response with changes in the input-circuit resistance when the other parameters are held constant is shown plotted on log-log coordinates in Figure 4-17. Also plotted on this figure is the experimentally observed variation in characteristic time for the same circuit conditions as were existent in the analytical case. The experimental characteristic times were obtained from the series of oscilloscopic photographs shown in Figure 4-18. As was the case with the analytical and experimental variations of I_1 , the comparison of the present and experimental variations of t_c also indicates the presence of a small additional variable resistance in the input



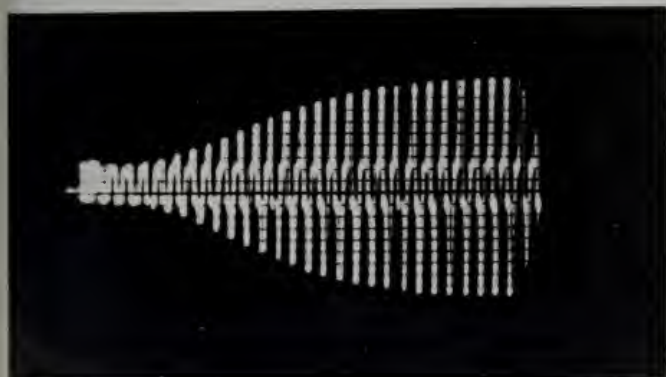
(a)



(b)



(c)



(d)

FIGURE 4- 19

OSCILLOSCOPIC PHOTOGRAPHS
SHOWING THE BUILDUP OF THE
OUTPUT-CIRCUIT CURRENT, i_2 ,
FOR INCREASING VALUES OF THE
INPUT-CIRCUIT RESISTANCE, R_1 ,
WHEN A STEP-FUNCTION OF VOLTAGE
IS APPLIED TO THE INPUT-
CIRCUIT TERMINALS.

f	=	400 cps.
N_1	=	3600 T
N_2	=	1000 T
R_2	=	500 ohms
i_1	=	2.22 ma.
e_2	=	100 $\sin \omega t$ volts

KEY

(a)	R_1	=	10125 ohms
	(C_T)	=	8.6 msec.
(b)	R_1	=	5065 ohms
	(C_T)	=	15.0 msec.
(c)	R_1	=	2530 ohms
	(C_T)	=	33.0 msec.
(d)	R_1	=	1265 ohms
	(C_T)	=	40.0 msec.

circuit as caused by hysteresis and eddy-current effects. In general, however, the agreement between experimental and analytical data is excellent. The variation of characteristic time, (CT), with R_1 plots as a straight line with a slope of negative one on log-log coordinates, confirming the fact that the response time of the amplifier is an inverse function of the total input-resistance of the magnetic-amplifier circuit.

The effects of variations of the input-circuit turns were observed in a similar manner. The points plotted in log-log coordinates in Figures 4-17 were selected from the N_1 family of curves for variations of characteristic time with input-circuit current. The experimental points, also plotted on this figure, were derived from the oscilloscope photographs shown in Figure 4-20. Again agreement between experimental and analytical observations is good, with the expected effect of hysteresis apparent for experimental cases. The slope of the straight line variation of characteristic time with input turns is observed to be equal to positive unity. The nature of this variation has been discussed in Chapter III and the analytical observations confirm the experimentally observed trend.

The effects of input-circuit parameter variations on the characteristic time of the magnetic amplifier have been shown analytically to agree very closely with experimental data. The neglect of losses has imposed no serious limitation to the analytically rigorous approach to the

circuit as caused by hysteretic and eddy-current effects. In general, however, the agreement between experimental and analytical data is excellent. The variation of characteristic time, (τ) , with R_1 plots as a straight line with a slope of negative one on log-log coordinates, confirming the fact that the response time of the amplifier is an inverse function of the total input-resistance of the magnetic-amplifier circuit.

The effects of variations of the input-current turns were observed in a similar manner. The points plotted in log-log coordinates in Figure 4-17 were selected from the R_1 family of curves for variations of characteristic time with input-current. The experimental points, also plotted on this figure, were derived from the oscilloscope photographs shown in Figure 4-20. Again agreement between experimental and analytical observations is good, with the expected effect of hysteretic agreement for experimental cases. The slope of the straight line variation of characteristic time with input turns is observed to be equal to positive unity. The nature of this variation has been discussed in Chapter III and the analytical observations confirm the experimentally observed trend.

The effects of input-current's parameter variations on the characteristic time of the magnetic amplifier have been shown analytically to agree very closely with experimental data. The neglect of losses has imposed no serious limitation on the analytical response approach to the

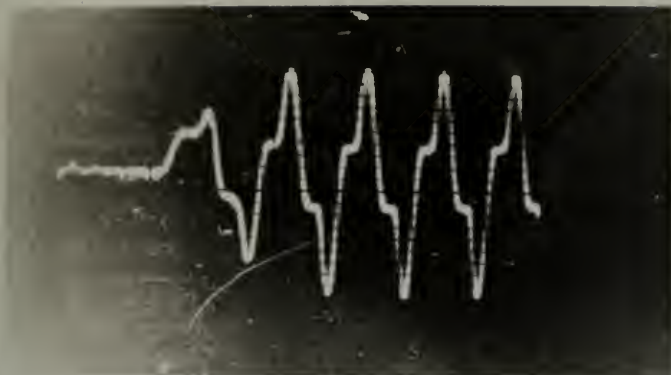
FIGURE 4-20

OSCILLOSCOPIC PHOTOGRAPHS
SHOWING THE BUILDUP OF THE
OUTPUT-CIRCUIT CURRENT, i_2 ,
FOR INCREASING VALUES OF THE
INPUT-CIRCUIT TURNS, N_1 ,
WHEN A STEP-FUNCTION OF VOLTAGE
IS APPLIED TO THE INPUT-
CIRCUIT TERMINALS.

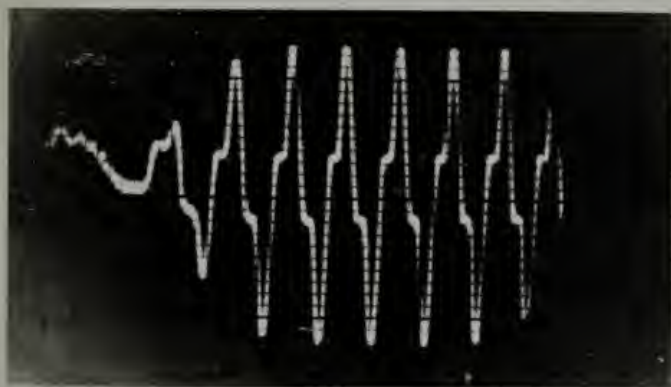
$$\begin{aligned}
 f &= 400 \text{ cps.} \\
 N_2 &= 1000 \text{ T} \\
 R_1 &= 10125 \text{ ohms} \\
 R_2 &= 500 \text{ ohms} \\
 i_1 &= 2.22 \text{ ma.} \\
 e_2 &= 100 \sin \omega t \text{ volts}
 \end{aligned}$$

KEY

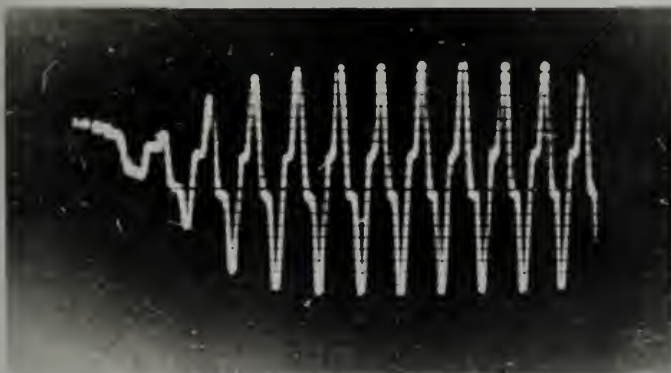
$$\begin{aligned}
 \text{(a)} \quad N_1 &= 1800 \text{ T} \\
 (CT) &= 4.7 \text{ msec.} \\
 \text{(b)} \quad N_1 &= 2600 \text{ T} \\
 (CT) &= 6.6 \text{ msec.} \\
 \text{(c)} \quad N_1 &= 3600 \text{ T} \\
 (CT) &= 8.6 \text{ msec.}
 \end{aligned}$$



(a)



(b)



(c)

solution of the equations of the magnetic amplifier insofar as variations in the input-circuit parameters are concerned.

(b) The Effects of the Output-Circuit Parameters on the Transient Behavior of the Magnetic Amplifier. -- The concept of the buildup of biasing flux has been introduced previously. Since the buildup of flux bias consumes an appreciable portion of the total characteristic time of the amplifier, the amplitude of the flux in the coils of the output circuit is of great importance in the transient behavior of the magnetic amplifier. Ideally, the alternating flux-amplitude should be initially equal to the saturation flux. It is necessary that the flux amplitude not exceed this value because, as has been pointed out in the discussion of the static effects of flux, large initial currents will flow if the initial flux extends into the nonlinear region of the curve. It is, however, desirable that currents begin to flow as soon as possible after the application of the step function to the input terminals, and in order to accomplish this end, the excursions of the alternating flux should be as great as possible initially without exceeding the break value. Since the flux amplitude plays an important part in the transient behavior of the amplifier, it is convenient to discuss the effects of output-circuit parameters through the medium of the effect of these parameters on the alternating flux.

The effects of losses in the output circuit are pronounced in the practical case, and in general, the agreement between analytical and experimental variations

isolation of the equations of the magnetic amplifier in the form of variations in the input-circuit parameters are unnecessary. (b) The Effects of the Output-Circuit Parameters on the Transient Behavior of the Magnetic Amplifier. — The concept of the behavior of the amplifier has been introduced previously. Since the behavior of the amplifier is an appreciable portion of the total characteristic time of the amplifier, the amplification of the flux in the coils of the output circuit is of great importance in the transient behavior of the magnetic amplifier. Ideally, the amplifier flux-amplitude should be initially equal to the saturation flux. It is necessary that the flux amplitude not exceed this value because, as has been pointed out in the discussion of the static effects of flux, large initial currents will flow if the initial flux exceeds into the nonlinear region of the curve. It is, however, desirable that currents begin to flow as soon as possible after the application of the step function to the input terminals, and in order to accomplish this end, the excitation of the saturating flux should be as great as possible initially without exceeding the peak value. Since the flux amplitude plays an important part in the transient behavior of the amplifier, it is convenient to discuss the effects of output-circuit parameters through the medium of the effect of these parameters on the saturating flux.

The effects of losses in the output circuit are pronounced in the practical case, and in general, the agreement between analytical and experimental variations

of the output-circuit parameters has been poor. The nature of the effects of losses on the magnetic-electric circuit has been considered in detail in the chapter devoted to discussion of experimental results.

As shown by Equation 4-24, the flux in the output circuit is directly proportional to E_2 , and inversely proportional to frequency and to N_2 . Since large initial flux-excursions lead to small values of characteristic time, it would seem apparent that an increase in E_2 would, in the analytical case, lead to reduction of the characteristic time. As shown on the plot of characteristic time versus E_2 on log-log coordinates of Figure 4-22, the expected decrease of characteristic time with increases in E_2 does not occur. As is consistent with the linear-circuit theory defined by Equation 4-26, the initial drop in characteristic time with E_2 is an inverse function of this parameter. After the value of E_2 becomes sufficiently great to produce fluxes of amplitude in excess of ϕ_s , nonlinear effects of the circuit take place, the buildup of flux is aided by the flow of currents, and the drop in characteristic time becomes much more rapid. The variation ceases to follow linear theory. The value of voltage required to produce ϕ_s was shown to be approximately 205 volts peak, or 145.5 volts rms, for the standard-parameter conditions, and therefore, above this flux value the nonlinear characteristics become apparent. Because of the losses in the out-

of the output-current parameter has been poor. The nature of the effect of losses on the magnetic-field circuit has been considered in detail in the chapter devoted to discussion of experimental results.

As shown by equation 8-24, the flux in the

output circuit is directly proportional to E_2 , and in-

versely proportional to impedance and to N_2 . Since

large initial flux-captations lead to small values of

characteristic time, it would seem apparent that an in-

crease in N_2 would, in the practical case, lead to re-

duction of the characteristic time. As shown on the

plot of characteristic time versus N_2 on log-log co-

ordinates of Figure 8-2, the expected behavior of

characteristic time with increasing N_2 does not occur.

As is consistent with the linear-current theory defined

by equation 8-25, the initial drop in characteristic

time with N_2 is an inverse function of E_2 in power.

After the value of E_2 becomes sufficiently great to pro-

duce fluxes of magnitude in excess of H_2 , nonlinear effects

of the circuit take place, the buildup of time is aided by

the rise of impedance, and the drop in characteristic time

becomes more rapid. The variation ceases to follow

linear theory. The value of voltage required to produce

H_2 was shown to be approximately 600 volts peak, or 140.5

volts rms, for the aluminum-permeability conditions, and

therefore, above this time value the nonlinear character-

istics become apparent. Because of the losses in the out-

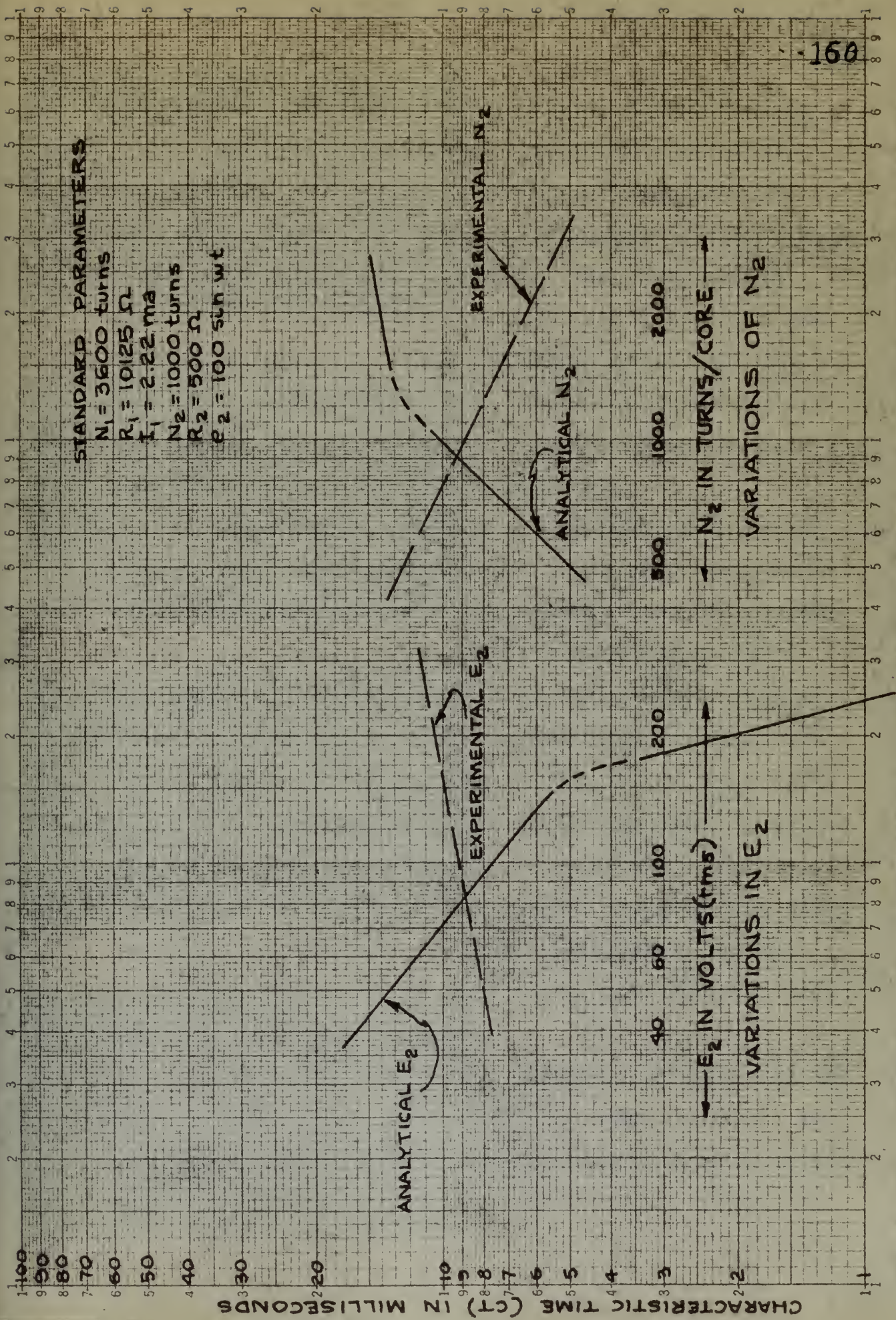


FIG. 4-22 EFFECT ON CHARACTERISTIC TIME OF VARIATIONS OF OUTPUT-CIRCUIT PARAMETERS.

put circuit, the effect of experimental variation of E_2 is radically different, having a positive slope of approximately $1/5$, as plotted on Figure 4-22, from the data represented by the photo-oscillographs of Figure 4-21. Since the reasons for this behavior were discussed in Chapter III, it is only necessary to state here that the analytical approach, because of core losses, does not adequately indicate the nature of the effects of variations in E_2 upon the transient characteristics of the magnetic amplifier in the practical case.

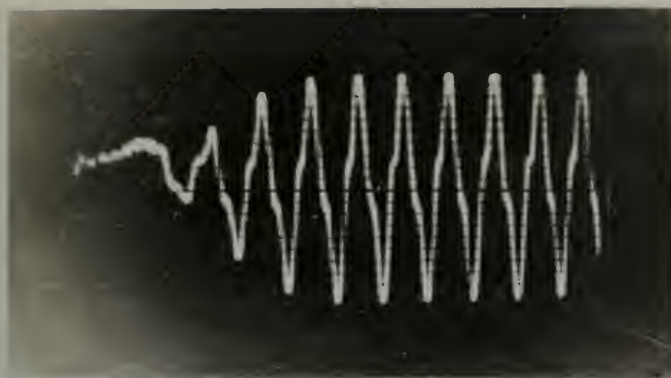
The effect of the output-circuit resistance on characteristic time was observed analytically and experimentally to be negligible. This result is to be expected because the effect of the output-circuit resistance on the amount of voltage available to the reactors is constant and independent of the output-circuit losses. Examination of the photographs of Figure 4-23 shows quite clearly that the transient time of the amplifier is practically constant regardless of the magnitude of the load resistor. The results of differential analyzer Runs 27-45 inclusive, as tabulated on Charts 4-3 and 4-4, confirm analytically the lack of effect of R_2 upon transient behavior in the region observed.

The flux-bias buildup concept, Equation 4-26 and Equation 4-24, would indicate that an increase in the output-circuit turns would result in an increase in characteristic time. This expected trend was found to be true in

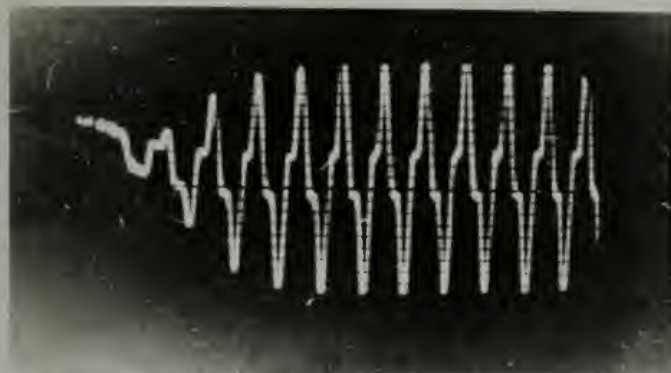
but almost, the effect of experimental variation of ϵ_2 is radically different, having a positive slope of approximately $1/2$, as plotted on Figure 4-12, from the data represented by the photo-conductivity of Figure 4-11. Since the reasons for this behavior were discussed in Chapter III, it is only necessary to state here that the analytical approach, because of our losses, does not adequately indicate the nature of the effects of variations in ϵ_2 upon the transient characteristics of the negative amplifier in the present case.

The effect of the output-circuit resistance on characteristic time was observed analytically and experimentally to be negligible. This result is to be expected because the effect of the output-circuit resistance on the amount of voltage available to the reactor is constant and independent of the output-circuit losses. Examination of the photograph of Figure 4-13 shows quite clearly that the transient time of the amplifier is practically constant regardless of the magnitude of the load resistor. The results of differential analysis from 4-12 inclusive, as tabulated on Charts 4-3 and 4-4, indicate analytically the lack of effect of ϵ_2 upon transient behavior in the region covered.

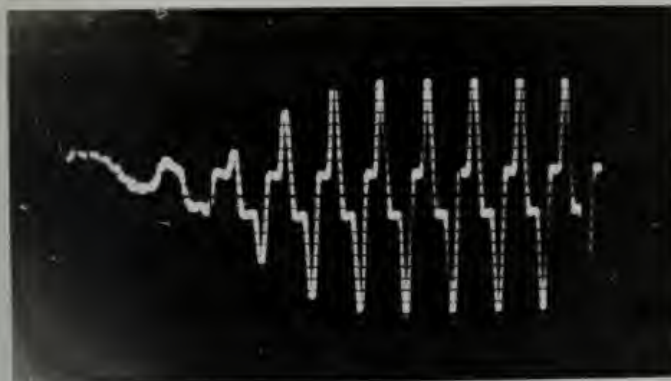
The time-lag during recovery, sections 4-14 and Equation 4-15, would indicate that an increase in the output-circuit time would result in an increase in characteristic time. This expected trend was found to be true in



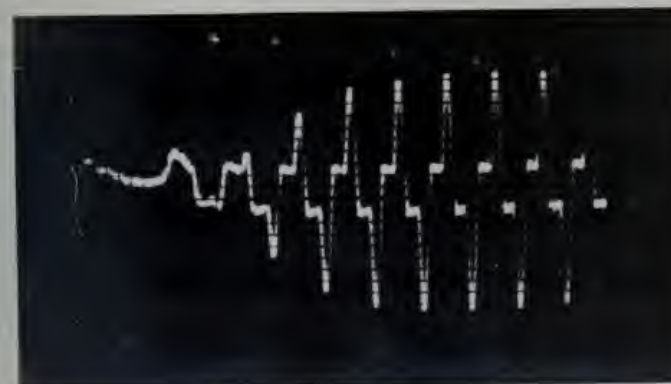
(a)



(b)



(c)



(d)

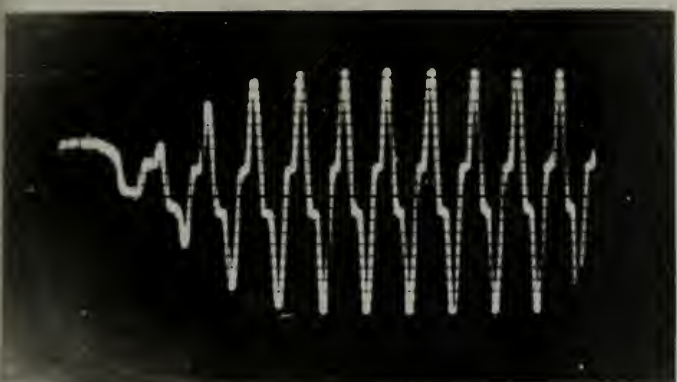
FIGURE 4-21

OSCILLOSCOPIC PHOTOGRAPHS
SHOWING THE BUILDUP OF THE
OUTPUT-CIRCUIT CURRENT, i_2 ,
FOR INCREASING VALUES OF THE
PEAK VALUE OF THE APPLIED
ALTERNATING VOLTAGE, E_2 ,
WHEN A STEP-FUNCTION VOLTAGE
IS APPLIED TO THE INPUT-
CIRCUIT TERMINALS.

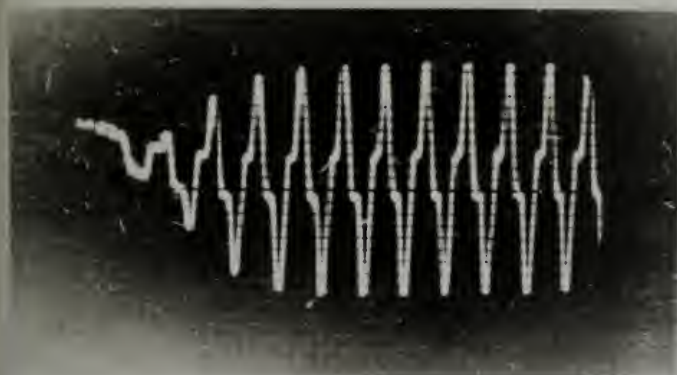
$f = 400$ cps.
 $N_1 = 3600$ T
 $N_2 = 1000$ T
 $R_1 = 10125$ ohms
 $R_2 = 500$ ohms
 $i_1 = 2.22$ ma.

KEY

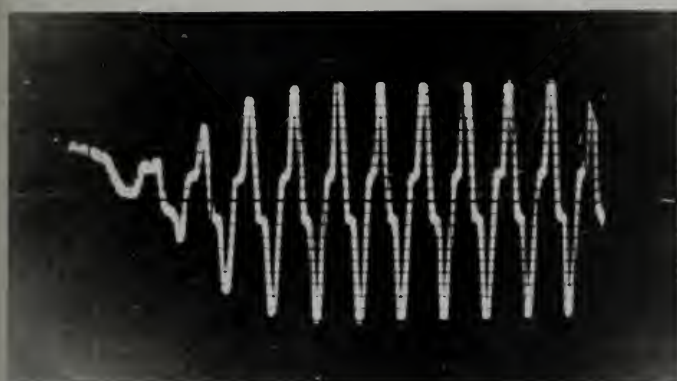
(a) $E_2 = 80$ volts
(CT) = 8.0 msec.
(b) $E_2 = 100$ volts
(CT) = 8.6 msec.
(c) $E_2 = 150$ volts
(CT) = 9.2 msec.
(d) $E_2 = 185$ volts
(CT) = 11.9 msec.



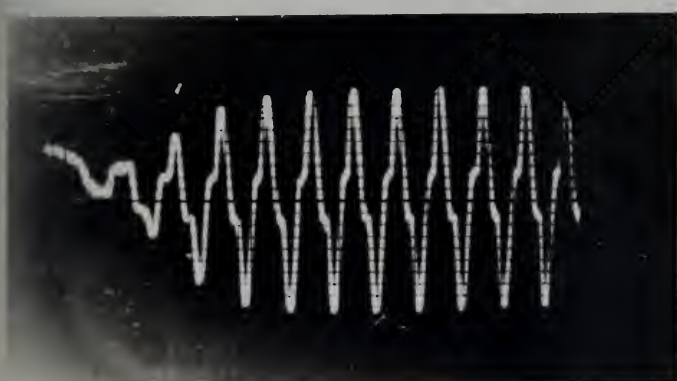
(a)



(b)



(c)



(d)

FIGURE 4-23

OSCILLOSCOPIC PHOTOGRAPHS
SHOWING THE BUILDUP OF THE
OUTPUT-CIRCUIT CURRENT, i_2 ,
FOR INCREASING VALUES OF THE
OUTPUT-CIRCUIT RESISTANCE
 R_2 , WHEN A STEP-FUNCTION OF
VOLTAGE IS APPLIED TO THE
INPUT-CIRCUIT TERMINALS.
(NOTICE THAT THE EFFECT OF VARIA-
TIONS IN R_2 IS VERY SMALL.)

f = 400 cps.
 N_1 = 3600 T
 N_2 = 1000 T
 R_1 = 10125 ohms
 i_1 = 2.22 ma.
 e_2 = 100 $\sin \omega t$ volts

KEY

(a) R_2 = 100 ohms
(CT) = 8.65 msec.
(b) R_2 = 500 ohms
(CT) = 8.60 msec.
(c) R_2 = 1000 ohms
(CT) = 8.70 msec.
(d) R_2 = 2000 ohms
(CT) = 8.73 msec.

the analytical case, and in accordance with Equation 4-26, the time response increases, analytically, approximately with the number of turns in the output circuit windings. The observed analytical effect, as well as the experimental effect, are shown plotted on log-log coordinates in Figure 4-22. The experimental effect of increasing N_2 , as obtained from the photographs of Figure 4-24, shows that the characteristic time is an inverse function of the square-root of N_2 . The wide deviation between experimental and analytical results must again be attributed to output-circuit losses, and it is necessary to conclude that the analytical approach, because of these losses, does not present a true picture of the actual transient behavior of a practical magnetic-amplifier circuit.

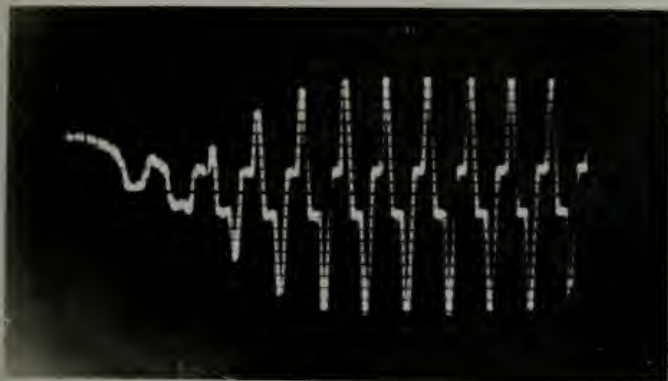
Time limitations did not permit investigation of the effect of the output-circuit alternating-frequency on the transient behavior of the amplifier, but since the frequency, in accordance with Equation 4-24, affects the flux amplitude in the same manner as the output turns, N_2 , it is anticipated that frequency effects observed analytically would be similar to the observed analytical effects of N_2 . Since the analytical effects of N_2 are not confirmable experimentally, it is presumed that the analyzer would not show correct frequency effects, again as a result of the circuit losses of hysteresis and eddy-currents.

the analytical case, and in accordance with Equation 4-36, the time response increases, analytically, approximately with the number of turns in the output circuit windings. The observed analytical effect, as well as the experimental effect, are shown plotted on log-log coordinates in Figure 4-32. The experimental effect of increasing N , as obtained from the photographs of Figure 4-32, shows that the characteristic time is an inverse function of the square-root of N . The wide deviation between experimental and analytical results must again be attributed to output circuit losses, and it is necessary to recognize that the analytical approach, because of these losses, does not present a true picture of the actual transient behavior of a practical magnetic-amplifier circuit.

Time limitations did not permit investigation of the effect of the output-circuit inductance-frequency on the transient behavior of the amplifier, but since the frequency, in accordance with Equation 4-36, affects the flux magnitude in the same manner as the output turns, N , it is anticipated that frequency effects observed analytically would be similar to the observed analytical effects of N . Since the analytical effects of N are not non-linear experimentally, it is presumed that the amplifier would not show output frequency effects, again as a result of the circuit losses of resistance and eddy-currents.

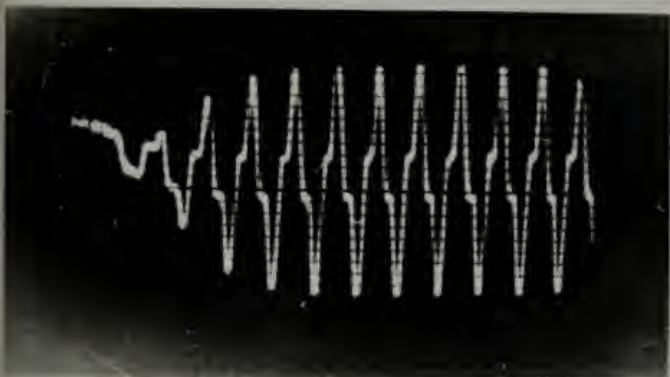
FIGURE 4-24

(a)



OSCILLOSCOPIC PHOTOGRAPHS
SHOWING THE BUILDUP OF OUTPUT-
CIRCUIT CURRENT, i_2 , FOR
INCREASING VALUES OF THE
OUTPUT-CIRCUIT TURNS, N_2 ,
WHEN A STEP-FUNCTION OF VOLTAGE
IS APPLIED TO THE INPUT-CIRCUIT
TERMINALS.

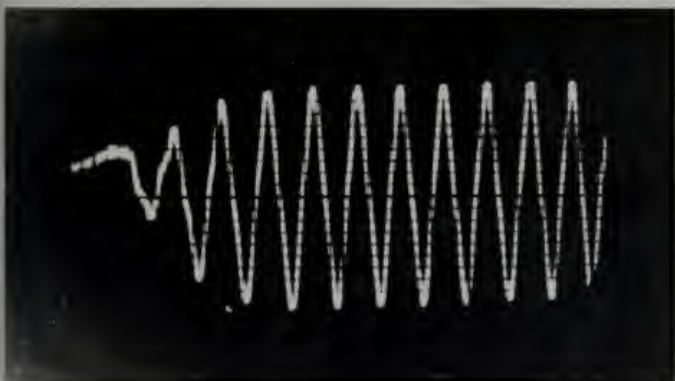
(b)



$f = 400$ cps.
 $N_1 = 3600$ T
 $R_1 = 10125$ ohms
 $R_2 = 500$ ohms
 $i_1 = 2.22$ ma.
 $e_2 = 100 \sin \omega t$ volts

KEY

(a) $N_2 = 600$ T
(CT) = 11.6 msec.
(b) $N_2 = 1000$ T
(CT) = 8.6 msec.
(c) $N_2 = 2000$ T
(CT) = 6.1 msec.



Conclusions Regarding the Analytical Studies

The analytical approach to the magnetic amplifier problem has given excellent indications of the steady-state performance which might be expected from a given magnetic-amplifier design. It has further indicated the nature of choice of parameters which might be selected to permit optimum operation in the steady-state to meet the requirements of a particular situation. The analytical approach has also indicated the nature of the effects of the input-circuit parameters upon the transient performance of the magnetic amplifier. Unfortunately, the analytical solution fails to give true indications of the effects of the output-circuit parameters which affect the magnitude of the alternating flux in affecting the transient performance of the device.

It should be remembered that the analytical studies were made using the most simple magnetic-amplifier circuit. In general, usable magnetic-amplifier circuits are further complicated by feedback windings and by rectifier-demodulator units which will contribute decidedly toward complicating the equations of amplifier performance, and would seem to make the analytical approach extremely difficult.

This particular investigation was, however, devoted to examination of the fundamentals which affect magnetic-amplifier performance, and as such, the use of

Conclusions Regarding the Analytical Studies

The analytical approach to the magnetic amplifier problem has given excellent indications of the steady-state performance which might be expected from a given magnetic amplifier design. It has further indicated the nature of choices of parameters which might be selected to obtain optimum operation in the steady-state to meet the requirements of a particular situation. The analytical approach has also indicated the nature of the effects of the input-circuit parameters upon the transient performance of the magnetic amplifier. Unfortunately, the analytical solution fails to give true indications of the effects of the output-circuit parameters which affect the magnitude of the saturating time in affecting the transient performance of the device.

It should be remembered that the analytical studies were made using the most simple magnetic-amplifier circuit. In general, simple magnetic-amplifier circuits are further complicated by feedback windings and by regenerative characteristics which will contribute decidedly toward complicating the questions of amplifier performance, and would need to make the analytical approach extremely difficult.

This particular investigation was, however, devoted to examination of the fundamentals which affect magnetic-amplifier performance, and as such, the use of

the mechanical differential analyzer has been very valuable, both in indicating the precise nature of the amplifier performance, and in crystallizing concepts which affect magnetic-amplifier performance.

the mechanical differential analyzer has been very valuable, both in indicating the precise nature of the amplifier performance, and in explaining concepts which affect numerical-amplifier performance.

CHAPTER V

REGENERATIVE FEEDBACK IN MAGNETIC AMPLIFIERS

The Use of Regenerative Feedback in Magnetic Amplifiers

As a means of improving the gain of the magnetic amplifier, the use of regenerative feedback has proved valuable. Since the magnetic amplifier is limited in time-response to relatively low values, conceivably part of the additional gain obtainable by feedback circuitry might well be sacrificed in an effort directed toward reduction of characteristic time, with a resultant over-all improvement in the performance of the feedback circuit as contrasted with the performance of the basic circuit.

The first noted use of regenerative-feedback techniques was that of P. H. Dowling of the Union Switch and Signal Company, who patented a positive-feedback amplifier in 1929. The techniques used by Dowling were greatly extended by two German engineers, Theodor Buchhold and Wilhelm Geyger, during and in the few years preceding World War II. Recently, under the auspices of the Navy Department, Bureau of Ordnance, experimental investigations of positive feedback techniques have been continued in detail at the Naval Ordnance Laboratory, White Oak, Maryland.

In view of the interest being currently shown in the use of regenerative feedback, it was deemed advisable to examine briefly the use of positive feedback in magnetic amplifiers as an extension of the basic studies which were defined as the primary objective of this research.

REGENERATIVE FEEDBACK IN MAGNETIC AMPLIFIERS

The Use of Regenerative Feedback in Magnetic Amplifiers

As a means of increasing the gain of the magnetic

amplifier, the use of regenerative feedback has proved valuable. Since the magnetic amplifier is limited in its response to relatively low values, considerably more of the additional gain obtainable by feedback circuitry might well be sacrificed in an effort directed toward reduction of characteristic time, with a resultant over-all improvement in the performance of the feedback circuit as contrasted with the performance of the basic circuit.

The first noted use of regenerative-feedback

techniques was that of P. H. Dowling of the Union Electric and Signal Company, who patented a positive-feedback amplifier in 1929. The techniques used by Dowling were greatly extended by two German engineers, Theodor Reichold and Wilhelm Geiger, during and in the few years preceding World War II. Recently, under the auspices of the Navy Department, Bureau of Ordnance, experimental investigations of positive feedback techniques have been conducted in detail at the Naval Ordnance Laboratory, White Oak, Maryland.

In view of the interest being currently shown in the use of regenerative feedback, it was deemed advisable to examine briefly the use of positive feedback in magnetic amplifiers as an extension of the basic studies which were defined as the primary objective of this research.

Theory of Regenerative Feedback in Magnetic Amplifiers*

Let us consider for a moment a basic magnetic amplifier in which an additional set of windings have been applied to each core. The additional set of windings is to be wound with exactly the same number of turns as employed on the output circuit of the basic amplifier; that is

$$N_2 = N_3, \quad (5-1)$$

where N_3 is the number of turns per core of the additional winding. The tertiary windings are connected in a manner which will cause the fluxes produced by currents in these windings to be additive to the fluxes produced by currents in the input-circuit coils. The current flowing in the output circuit of the amplifier is rectified in an ordinary full-wave-rectifier bridge, and the rectified current is applied to the tertiary or feedback windings. The nature of the connections required is shown in Figure 3-1.

It has been pointed out previously that the average value of the output ampere-turns of the basic amplifier is approximately equal to the average value of the input ampere-turns over the region of normal amplification. When the output current is rectified and applied to the feedback windings, which, we recall, have the same turns as the output circuit, it is clear that the ampere-turns of magnetizing force in the feedback circuit are approximately equal to the ampere-turns of the input circuit.

*The basic theory in the next 2½ pages is adapted from Buchhold, T., "Über Gleichstromvormagnetisierte Wechselstromdrosselspulen und der Rückkopplung," A.f.E., 36, (1942), p. 514-534.

Theory of Regenerative Feedback in Magnetic Amplifiers

Let us consider for a moment a basic magnetic

amplifier in which an additional set of windings have been applied to each core. The additional set of windings is to be wound with exactly the same number of turns as employed on the output circuit of the basic amplifier;

that is

$$N_2 = N_1 \quad (2-1)$$

where N_2 is the number of turns per core of the additional winding. The tertiary windings are connected in a manner which will cause the fluxes produced by currents in these windings to be additive to the fluxes produced by currents in the input-output coils. The current flowing in the

output circuit of the amplifier is restricted in an ordinary full-wave-rectifier bridge, and the restricted current is applied to the tertiary or feedback windings. The nature of the connections required is shown in Figure 2-1.

It has been pointed out previously that the

average value of the output average-value of the basic amplifier is approximately equal to the average value of the input average-value over the region of normal amplification. When the output current is restricted and applied to the feedback windings, which, we recall, have the same turns as the output circuit, it is clear that the average-value of magnetizing force in the feedback circuit and approximately equal to the average-value of the input circuit.

"The Basic Theory in the next 24 pages is adapted from
Buckley, J., "The Regenerative Feedback Amplifier," A.I.E.E. 56
(1937), p. 31-32."

Since the fluxes produced by the magnetizing force in the feedback circuit are additive to those produced by the input-circuit magnetizing force, it is possible to state that the feedback magnetizing force may be represented by the distance $(NI)_3$ on the modulation characteristic of Figure 5-1. It will be noted that $(NI)_3$ is of sufficient magnitude to provide the magnetizing force necessary to extend just to the 45° slope line, which represents the ideal case. If the amplifier is to be operated at the point "P", it is then necessary that the input circuit provide only the magnetizing force represented by the distance $(NI)_1'$. The magnitude of $(NI)_1'$ depends upon the permeability of the core material, and can be made very small if the permeability is great. Since $(NI)_1'$ is of much lesser magnitude than $(NI)_1$, the power gain of the amplifier operating at point "P" is much improved by the addition of the feedback windings. The new condition in the amplifier input circuit may be expressed

$$(NI)_1 = (NI)_3 + (NI)_1' . \quad (5-2)$$

The average value of the output ampere-turns remains unchanged although the required input ampere-turns have been reduced. It may be seen in the exaggerated drawing of Figure 5-1 that below the point "A", the value of $(NI)_1'$ required to operate along the modulation characteristic is measured in the negative direction. At point "A", $(NI)_1'$ becomes zero and above this point the feedback input-magnetizing-force, $(NI)_1'$, becomes positive, eventually

Since the linear process by the magnifying force in the feedback circuit are similar to those produced by the input circuit magnifying force, it is possible to state that the feedback magnifying force may be represented by the distance $(NI)_2$ on the modulation characteristic of Figure 2-1. It will be noted that $(NI)_2$ is of sufficient magnitude to provide the magnifying force necessary to extend just to the 45° slope line, which represents the ideal case. If the amplifier is to be operated at the point 45° , it is then necessary that the input circuit provide only the magnifying force represented by the distance $(NI)_1$. The magnitude of $(NI)_1$ depends upon the permeability of the core material, and can be made very small if the permeability is great. Since $(NI)_1$ is of small least magnitude even $(NI)_1$, the power gain of the amplifier operating at point 45° is much increased by the action of the feedback winding. The net condition is the amplifier input circuit may be expressed

$$(NI)_1 = (NI)_2 + (NI)_1 \quad (2-2)$$

The average value of the output square-wave remains unchanged although the average input square-wave has been reduced. It may be seen in the exaggerated drawing of Figure 2-1 that below the point 45° , the value of $(NI)_1$ required to operate along the modulation characteristic is less than the negative direction. At point 45° , $(NI)_1$ becomes zero and above this point the feedback input magnifying-force, $(NI)_1$, becomes positive, eventually

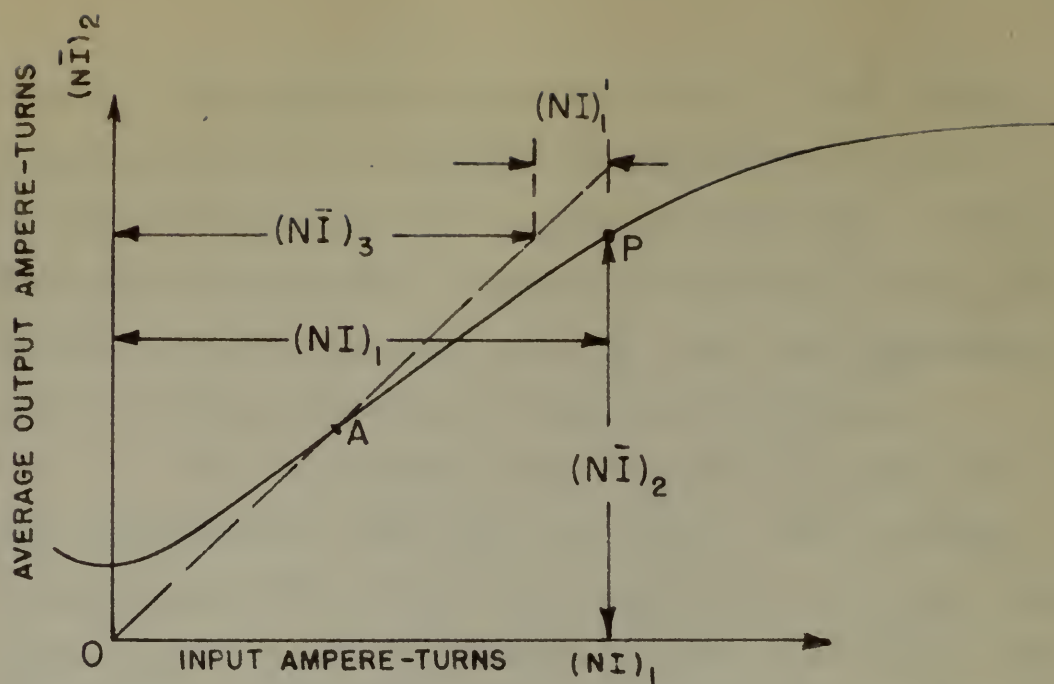


FIG. 5-1 (a) FULLY-COMPENSATED FEEDBACK.

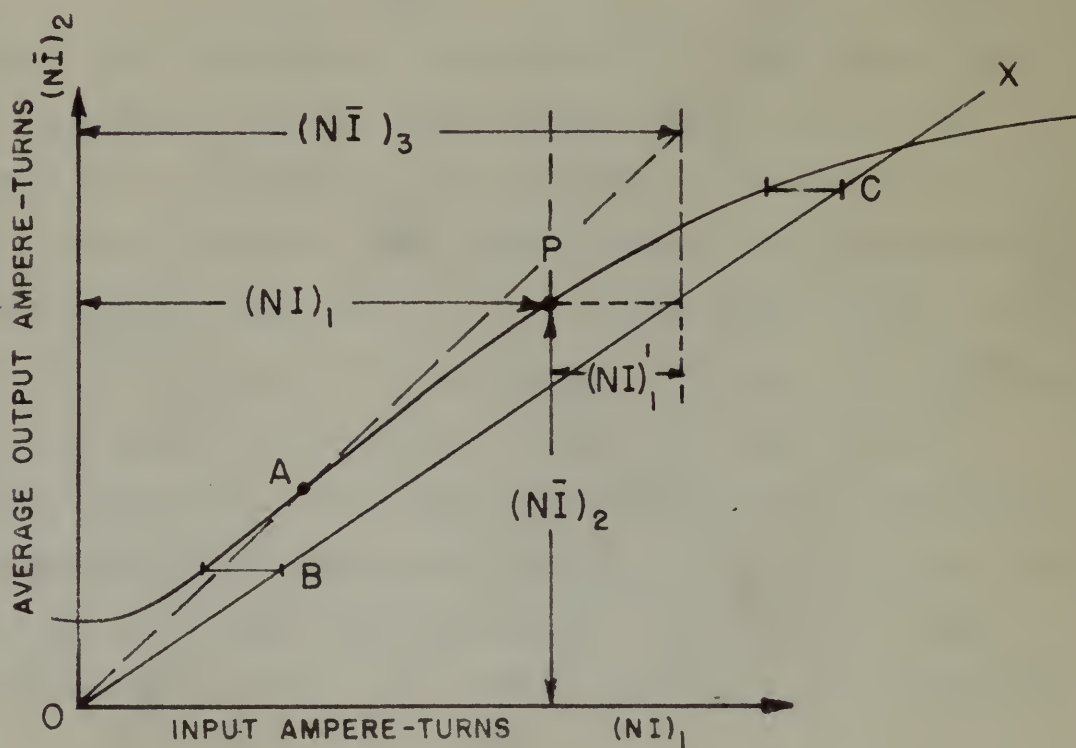


FIG. 5-1 (b) OVER-COMPENSATED FEEDBACK.

becoming very great as saturation occurs. From these considerations it is possible to construct a revised modulation characteristic for the feedback case. Such a revised characteristic is shown in Figure 5-7. The case which has been discussed, i.e., $N_2 = N_3$, has been designated as fully-compensated regenerative-feedback.

If the feedback turns, N_3 , are increased to some value greater than N_2 , the value of $(NI)_3$ becomes greater than $(NI)_2$, since the currents are the same. Consequently, $(NI)_3$ is of greater magnitude than $(NI)_1$. On a modulation characteristic, as shown in Figure 5-1(b), it is seen that $(NI)_3$ is measured to the line O-X which has a slope of less than 45° , the actual value of this slope being dependent on the ratio of N_3 to N_2 and defined by

$$\tan \theta = \frac{N_2}{N_3} \quad (5-3)$$

Under these conditions the point "A" is seen to occur at an increased value of output ampere-turns. Above the point "A", saturation occurs rapidly, and consequently, the usable portion of the characteristic is represented by that portion lying below "A". In this region $(NI)_1^i$ is at all times measured in the negative direction. It will be noticed that at two points, "B" and "C", the values of $(NI)_1^i$ are equal. This equality results in an instability in the amplifier performance and in a discontinuity in the revised modulation characteristic. The nature of this singularity is shown more clearly in Figure 5-7, where it

becoming very great as saturation occurs. From these considerations it is possible to construct a revised modulation characteristic for the feedback case. Such a revised characteristic is shown in Figure 2-7. The case which has been discussed, i.e., $\mu_2 = 1$, has been designated as fully-compensated negative-feedback.

If the feedback factor, μ_2 , are increased to some value greater than μ_2 , the value of $(M)_2$ becomes greater than $(M)_2$, since the outputs are the same. Consequently, $(M)_2$ is of greater magnitude than $(M)_1$. On a modulation characteristic, as shown in Figure 2-1(b), it is seen that $(M)_2$ is measured to the line O-K which has a slope of less than μ_2 . The actual value of this slope being dependent on the value of μ_2 to μ_2 and defined by

$$\tan \theta = \frac{\mu_2}{\mu_2} \quad (2-7)$$

Under these conditions the point "A" is seen to occur at an increased value of output negative-feedback. Above the point "A", saturation occurs rapidly, and consequently the middle portion of the characteristic is represented by that portion lying below "A". In this region $(M)_1$ is at all times measured in the negative direction. It will be noticed that at two points, "B" and "C", the values of $(M)_1$ are equal. This equality results in an instability in the amplifier performance and is a discontinuity in the revised modulation characteristic. The nature of this discontinuity is shown more clearly in Figure 2-7, where it

$f_2 = 400 \text{ cps}$
 $N_1 = N_2 = 2000 \text{ turns}$
 $E_2 = 100 \text{ V}$
 $R_2 = 1000 \Omega$

I_1

I_2

AVERAGE CARRIER CURRENT (I_2) IN MILLIAMPERES

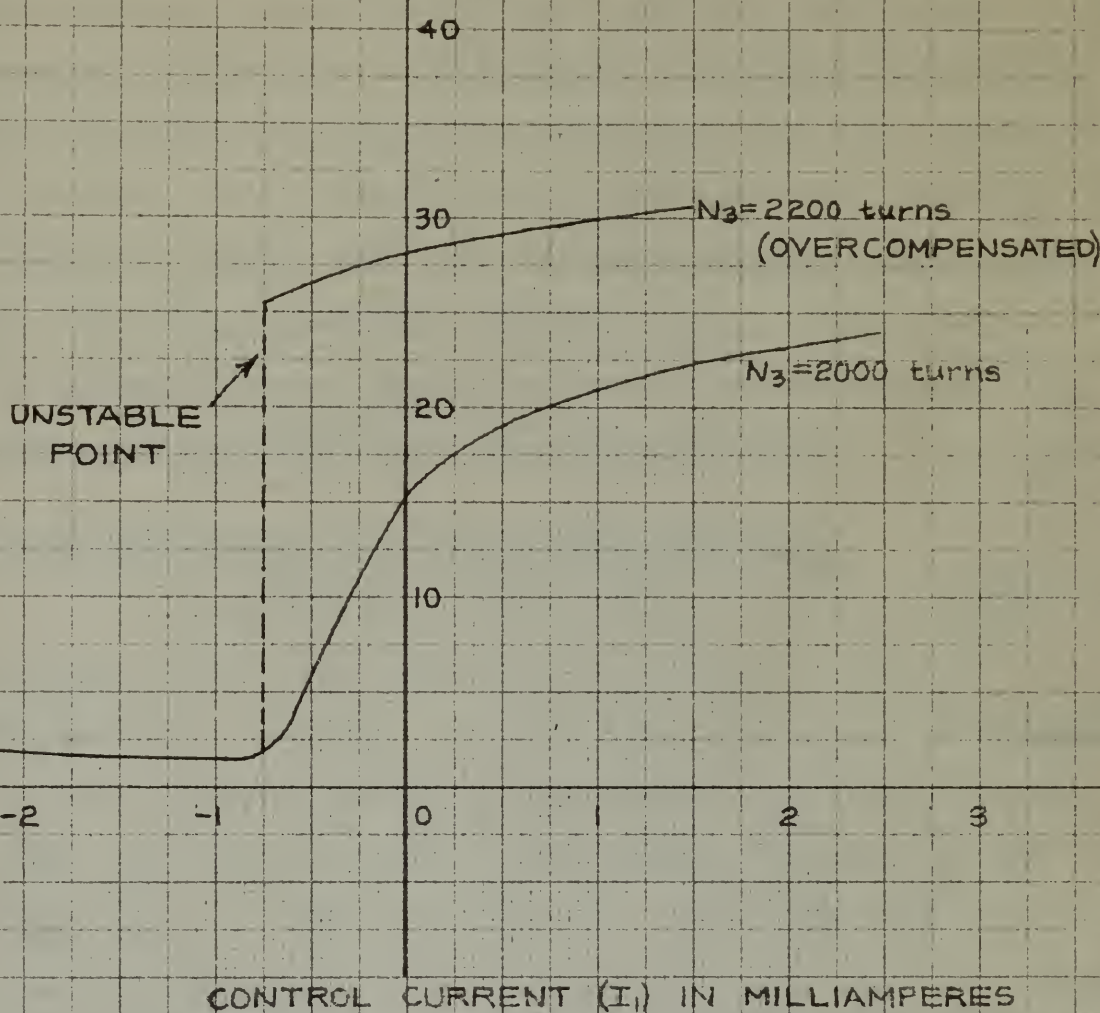


FIG. 5-7. MODULATION CHARACTERISTIC FOR MAGNETIC AMPLIFIER WITH POSITIVE FEEDBACK SHOWING EFFECT OF OVERCOMPENSATION

may be seen that, because of the discontinuity, there is a very rapid rise in $(NI)_2$ for a minute change in the input magnetizing force, corresponding to the double-valued function of $(NI)_2$ at the value of $(NI)_1$ represented by "B" and "C" of Figure 5-1(a). The value of overcompensated feedback, as this situation is designated, for on-off control, is obvious. Large output currents are controlled by extremely small changes in the input current. It is possible to add a fourth set of windings to the magnetic amplifier, which, when fed with an additional supply, will bias the overcompensated characteristic of Figure 5-7 toward the right in Figure 5-7 in a manner which will cause the singularity to occur at the origin.

Static Characteristics of Feedback Operation

A comparison between practical cases of fully-compensated and overcompensated feedback is shown on Figure 5-7. Actually, there is some question as to whether the case represented by the modulation characteristic for fully compensated feedback does indeed represent the optimum value of 100% compensation. The reader will recall that the windings of the cores used for the study were tapped every 200 turns, and under these conditions, it is thus theoretically possible to make $(NI)_2$ equal to $(NI)_3$. In the practical situation, however, although N_2 is equal to N_3 , it is likely that I_3 is slightly less than I_2 because some losses and distortion are inevitable in the rectifier

may be seen from the behavior of the characteristic, there is a very rapid rise in $(W)_2$ for a minute change in the input magnetizing force, corresponding to the small change in the value of $(W)_2$ at the value of $(W)_1$ represented by "B" and "C" of Figure 5-1(a). The value of overcompensated feedback, as this situation is designated, for on-off control, is obvious. Large output changes are controlled by extremely small changes in the input current. It is possible to add a fourth set of windings to the magnetic amplifier, which, when fed with an additional supply, will bias the overcompensated characteristics of Figure 5-1 toward the right in Figure 5-1 in a manner which will cause the amplifier to operate at the origin.

Stable Characterization of Feedback Operation

A comparison between practical cases of fully-compensated and overcompensated feedback is shown on Figure 5-7. Actually, there is some question as to whether the cases represented by the non-linear characteristic for fully compensated feedback have indeed represented the optimum value of 100% compensation. The reader will recall that the windings of the cores used for the study were tapped every 200 turns, and under these conditions, it is thus theoretically possible to make $(W)_2$ equal to $(W)_1$. In the practical situation, however, although it is equal to $(W)_1$, it is likely that it is slightly less than $(W)_1$ because some losses and distortion are inevitable in the reactor

units. It would, therefore, have been desirable to have provided a means of increasing the turns in the feedback winding by some small amount in order to maintain $(NI)_3$ equal to $(NI)_2$ by compensation for the rectifier distortion and losses. Unfortunately, such a procedure was precluded in this brief study because the toroids were potted in Ceresin Wax in order to increase the breakdown-voltage between windings during studies made of the basic circuit. In general, it is recommended that means be provided in the breadboard circuit to make smaller adjustments of the number of turns in the feedback windings. Perhaps under these conditions, a steeper curve than that shown for fully compensated feedback in Figure 5-7 would then be attainable.

It is essential, whenever regenerative feedback is employed, that the rectifier bridge be perfectly symmetrical. If such symmetry does not exist, an unbalanced waveform will be observed in the current in the feedback windings, which results in an unbalance in the output current waveform. Four Benwood-Linze Type 32681 selenium rectifier units were available for this study. Dissimilarity between these units made it undesirable to use the dry-disc rectifier bridge, however, because of the unbalanced waveforms produced. Consequently, a rectifier bridge composed of two 6H6 double diodes was constructed. Approximately ten of these tubes were tested before a sufficiently matched pair was found to eliminate asymmetry

It is well known that the human ear is not a simple receiver of sound waves, but a complex organ capable of discriminating between different frequencies and intensities of sound. The ear is also capable of localizing sound sources in space. This is achieved by the brain interpreting the time and intensity differences between the sounds reaching the two ears. The ear is also capable of detecting the direction of movement of sound sources. This is achieved by the brain interpreting the changes in the time and intensity differences between the sounds reaching the two ears. The ear is also capable of detecting the pitch of sound. This is achieved by the brain interpreting the frequency of the sound waves. The ear is also capable of detecting the timbre of sound. This is achieved by the brain interpreting the complex pattern of frequencies that make up a sound. The ear is also capable of detecting the loudness of sound. This is achieved by the brain interpreting the intensity of the sound waves. The ear is also capable of detecting the quality of sound. This is achieved by the brain interpreting the complex pattern of frequencies that make up a sound. The ear is also capable of detecting the duration of sound. This is achieved by the brain interpreting the time interval between the onset and offset of a sound. The ear is also capable of detecting the location of sound. This is achieved by the brain interpreting the time and intensity differences between the sounds reaching the two ears. The ear is also capable of detecting the direction of movement of sound. This is achieved by the brain interpreting the changes in the time and intensity differences between the sounds reaching the two ears. The ear is also capable of detecting the pitch of sound. This is achieved by the brain interpreting the frequency of the sound waves. The ear is also capable of detecting the timbre of sound. This is achieved by the brain interpreting the complex pattern of frequencies that make up a sound. The ear is also capable of detecting the loudness of sound. This is achieved by the brain interpreting the intensity of the sound waves. The ear is also capable of detecting the quality of sound. This is achieved by the brain interpreting the complex pattern of frequencies that make up a sound. The ear is also capable of detecting the duration of sound. This is achieved by the brain interpreting the time interval between the onset and offset of a sound. The ear is also capable of detecting the location of sound. This is achieved by the brain interpreting the time and intensity differences between the sounds reaching the two ears.

in the output waveform of the amplifier. In the practical magnetic amplifier, the use of dry-disc type rectifiers is highly desirable, because the filament-supply problem is eliminated. In the laboratory tests, convenience indicated the use of the diode bridge. A comparison of the modulation characteristics produced by the bridge composed of type 326S1 selenium rectifiers and the 6H6 diode bridge is shown in Figure 5-2. The steeper slope associated with the dry-disc rectifier bridge justifies the use of these units when matched pairs are selected. In general, the use of dry-disc rectifiers is desirable because the amplifier circuit is then wholly without tubes.

The subject of the choice of rectifier units for the feedback magnetic-amplifier requires further study.

The shape of the modulation characteristics for magnetic amplifiers utilizing fully-compensated feedback depends on the factors which influence the shape of the modulation characteristics for the basic circuit. This statement is borne out by the measured feedback modulation-characteristics of Figures 5-3, 5-5 and 5-6, which show the effects of R_2 , E_2 and N_2 respectively.

The modulation characteristics of Figure 5-3 are quite similar to those of the basic circuit in which a variation in the load resistance R_2 is made. The falling off of the characteristic for large load resistances is again apparent. The nature of this flattening has been discussed in connection with investigations of the basic

in the output waveform of the amplifier. In the presence of magnetic coupling, the use of thy-ristor type rectifier is highly desirable, because the thy-ristor-type rectifier is eliminated. In the laboratory tests, convenience indicated the use of the above bridge. A comparison of the modulation characteristics provided by the bridge composed of type 250A selenium rectifiers and the QM class bridge is shown in Figure 3-5. The output also measured with the thy-ristor rectifier bridge justifies the use of QM class when modulation pairs are required. In general, the use of thy-ristor rectifier is desirable because the amplifier circuit is then wholly without tubes.

The subject of the choice of rectifier class for the feedback magnetic-coupling amplifier circuit is the subject of the modulation characteristics for magnetic amplifiers utilizing fully-saturated feedback signals on the output which influence the shape of the modulation characteristics for the basic circuit. This statement is borne out by the measured feedback modulation characteristics of Figures 3-5, 3-6 and 3-7, which show the effects of R_L and R_F respectively.

The modulation characteristics of Figure 3-5 are quite similar to those of the basic circuit in which variation in the load resistance R_L is made. The variation of the characteristic for large load resistance is again apparent. The nature of this fluctuation has been discussed in connection with investigations of the basic

$$f_2 = 400 \text{ cps}$$

$$E_2 = 100 \text{ V}$$

$$R_2 = 50 \Omega$$

$$N_1 = N_2 = N_3 = 2000 \text{ turns}$$

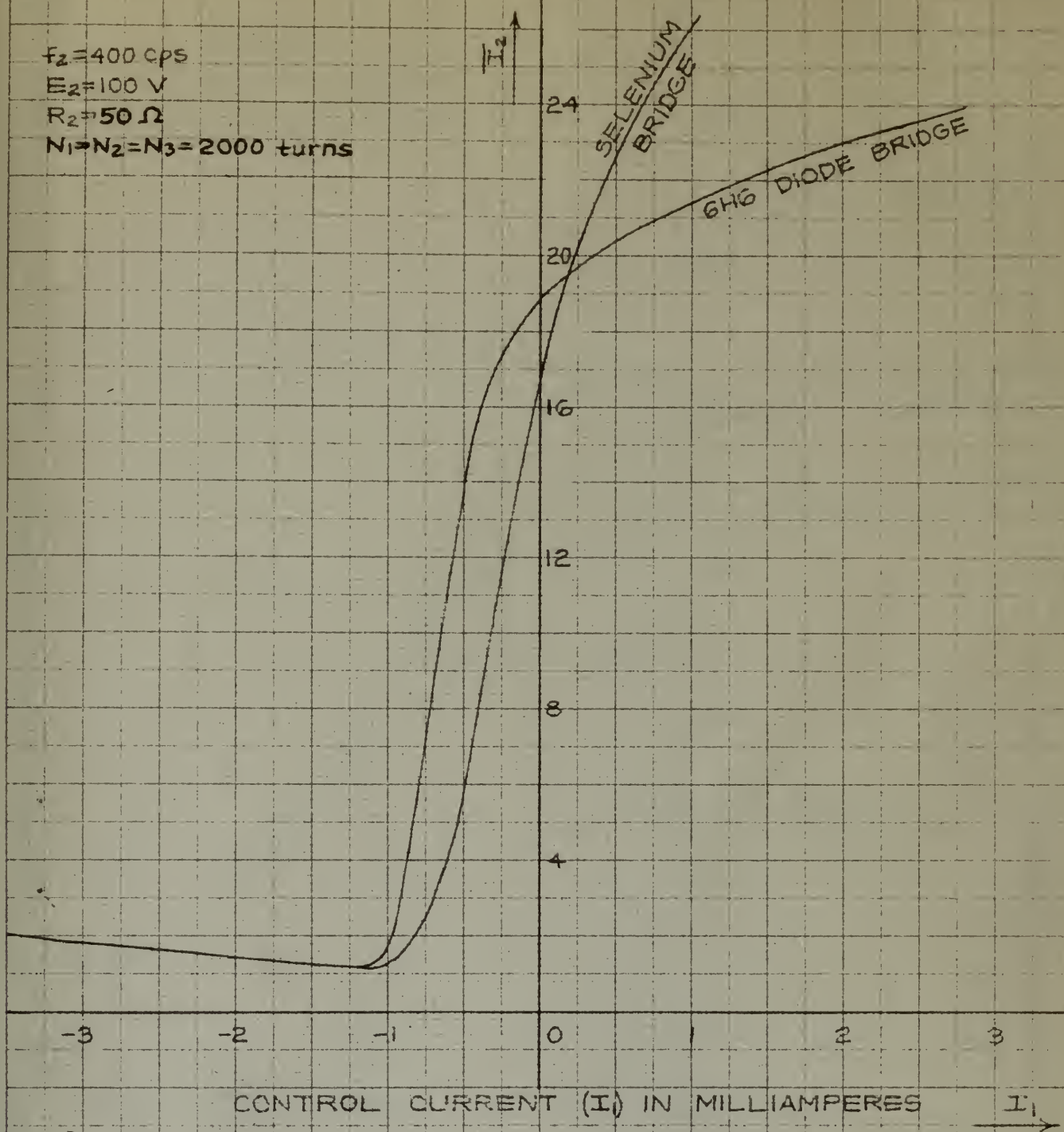


FIG. 5-2 MODULATION CHARACTERISTIC OF MAGNETIC AMPLIFIER WITH POSITIVE FEEDBACK SHOWING COMPARISON OF PERFORMANCE OF A SELENIUM AND A DIODE RECTIFIER BRIDGE.

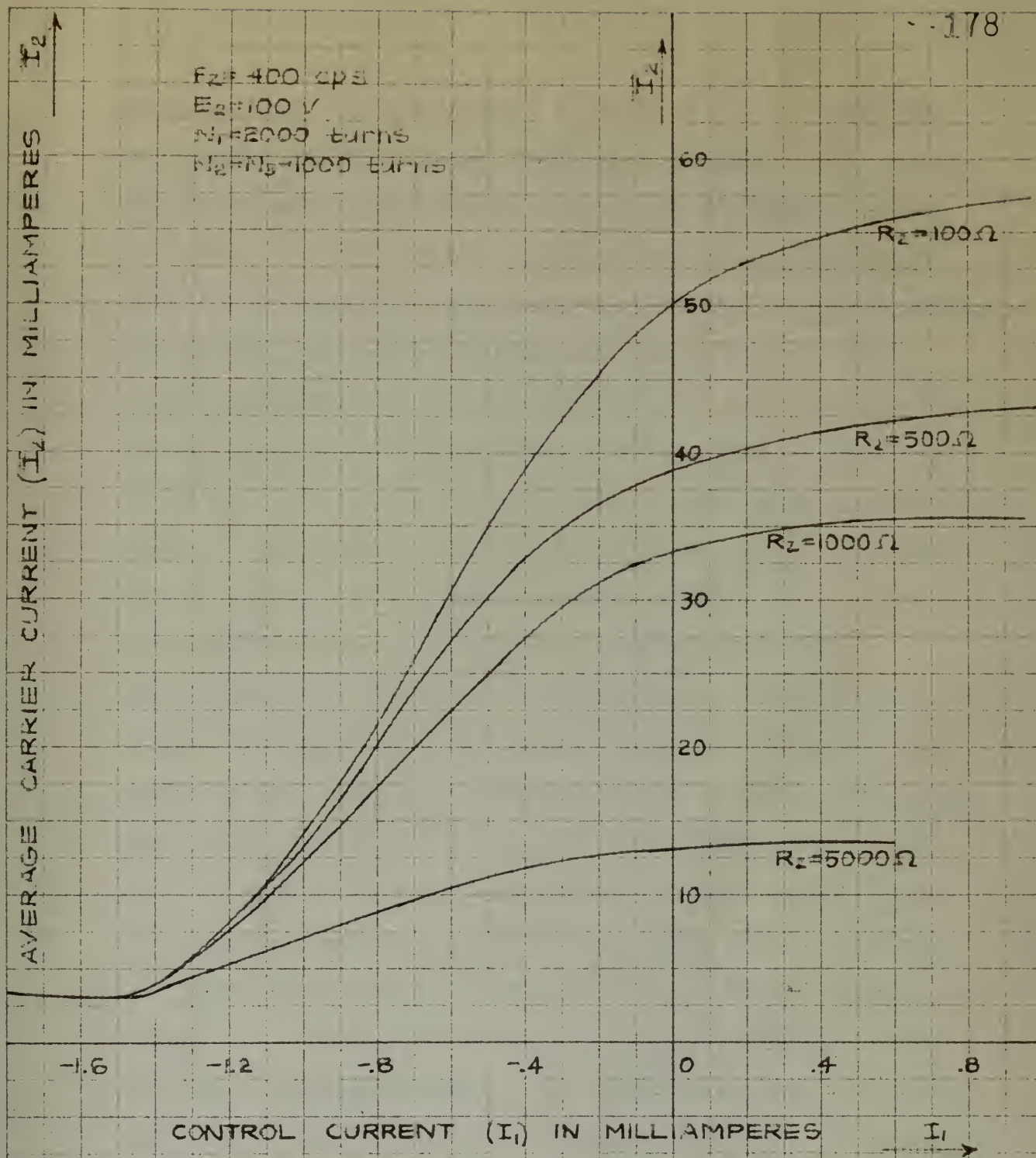


FIG. 5-3 MODULATION CHARACTERISTIC OF MAGNETIC
 AMPLIFIER WITH POSITIVE FEEDBACK
 SHOWING EFFECTS OF CHANGING THE LOAD
 RESISTANCE (R_L).

circuit, and the discussions in Chapter III are directly extendable to the present feedback situation. The curves of Figure 5-3 attain further practical significance when converted to curves which indicate the power output and gain of the magnetic amplifier at given input power levels. Invariably, when the feedback connection is used in a single amplifier, the additional set of windings, called either biasing or compensation windings, and designed to shift the modulation characteristic to the right, are employed. The shift is made such that the dip of the modulation characteristic occurs at the origin, i.e., for zero input current. In the power-output and gain characteristics shown, it is assumed that such an additional winding has been employed to shift the characteristic to the right by 1.5 milliamperes on the input scale. The power necessary to supply the additional windings is readily available from the a-c power supply after a portion of the supply current is rectified. This conversion has been carried out and the results are shown plotted in Figure 5-4. The power output in watts is plotted versus the input current squared. The input resistance is again omitted, as was the case with similar curves for the basic circuit, in order to allow flexibility in the selection of this parameter, because of the important effect of R_1 in determining the characteristic time of the dynamic performance of the amplifier. On the same figure, the gain of the amplifier times the input circuit resistance is plotted

circuits, and the discussion in Chapter III are directly extendable to the present feedback situation. The curves of Figure 5-3 attain further practical significance when converted to curves which indicate the power output and gain of the negative amplifier at given input power levels. Inversely, when the feedback connection is used in a single amplifier, the additional set of windings, called either biasing or compensation windings, and designed to shift the modulation characteristic to the right, are employed. The shift is such that the tip of the modulation characteristic occurs at the origin, i.e., for zero input current. In the power-output and gain characteristics shown, it is assumed that such an additional winding has been employed to shift the characteristic to the right by 1.5 milliamperes on the input scale. The power necessary to supply the additional windings is readily available from the a-c power supply after a portion of the supply current is rectified. This conversion has been carried out and the results are shown plotted in Figure 5-4. The power output in watts is plotted versus the input current in amperes. The input resistance is again omitted, as we have seen with similar curves for the basic circuit, in order to allow flexibility in the selection of this parameter, because of the important effect of R_i in determining the characteristic line of the dynamic performance of the amplifier. On the same figure, the gain of the amplifier times the input circuit resistance is plotted

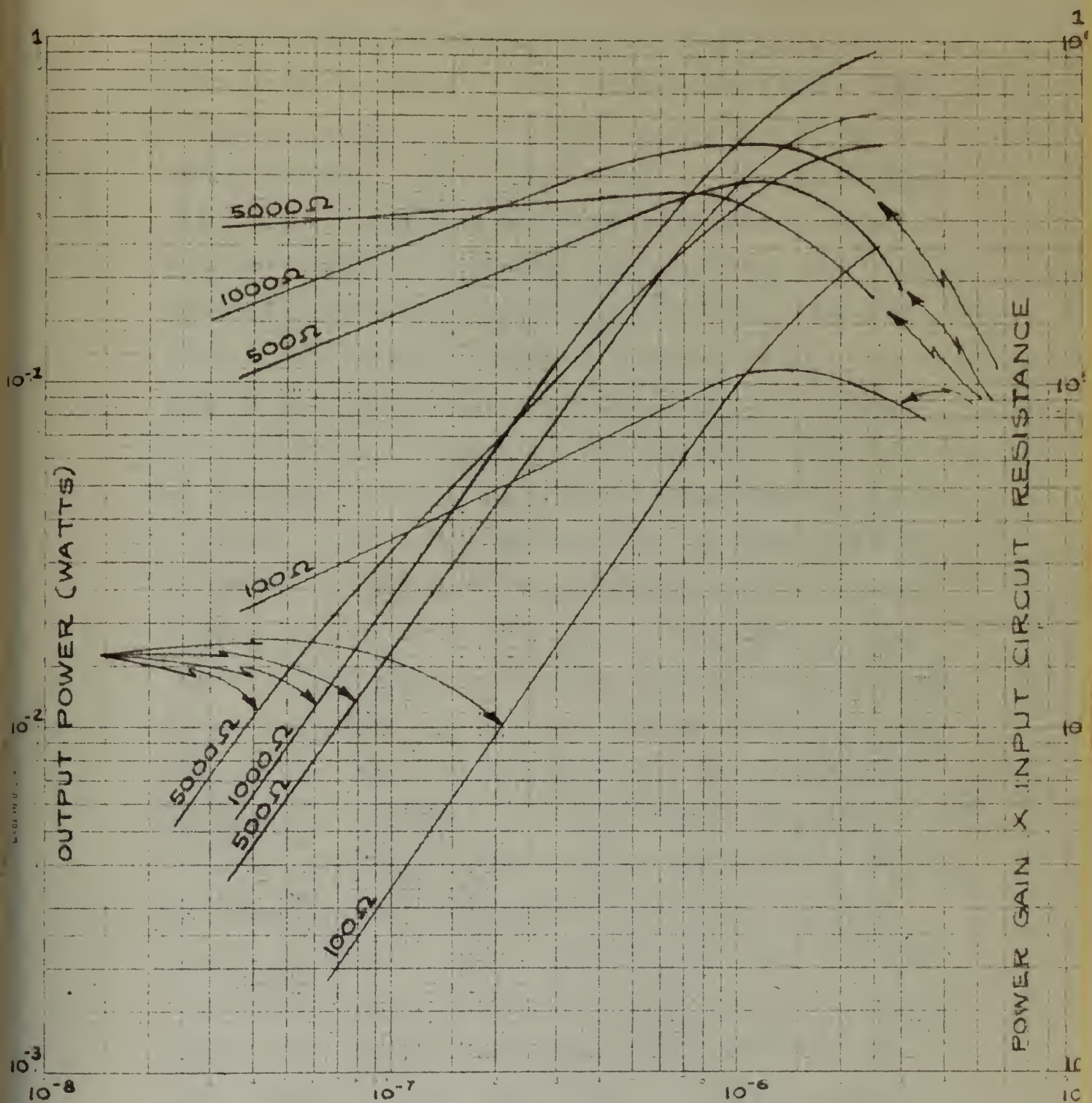


FIG.5-4 POWER OUTPUT AND GAIN FOR THE FULLY-COMPENSATED FEEDBACK CONNECTION PLOTTED VERSUS $(\text{INPUT CURRENT})^2$.

versus $(I_1)^2$. It is apparent, from these curves, that there is a definite optimum value of R_2 at which the gain reaches a maximum. This peaking occurs for a value of R_2 of approximately 1000 ohms, and at a value of $(\text{input current})^2$ equal to 10^{-6} amps.². The curves indicate that the choice of load resistance must be based upon the level of input power (represented by $(I_1)^2$) and then selected from the optimum gain conditions at this level. In some cases it may be necessary to sacrifice gain in order to obtain larger values of output power. The gain curves of Figure 5-4 were made with 2000 turns on the input windings, while gain curves shown in Figure 3-19 were observed for 3600 turns on the input windings. If the curves of Figure 5-4 are corrected by the squared turns ratio criterion established by Equation 3-17, it may be seen by comparing Figures 3-19 and 5-4 that a gain improvement, depending on the magnitude of the input resistance, of the order of 100 to 150, is possible with regenerative feedback in the region where the squared value of the input current is approximately 10^{-6} . This is the value of $(I_1)^2$ at which the gain of the feedback circuit reaches a maximum, and also is a value at which the basic-circuit gain-characteristic is at its maximum point. For identical conditions, the improvement in power output is of the same order as the improvement in gain with positive feedback. A careful adjustment of the feedback turns as described to obtain perfect 100% feed-

versus $(I_1)^2$. It is apparent, from these curves, that there is a definite optimum value of I_1 at which the gain reaches a maximum. This peak occurs for a value of I_1 of approximately 1000 gauss, and at a value of (input current) I_1 equal to 10^{-4} amp. The curves indicate that the choice of load resistance must be based upon the level of input power (represented by $(I_1)^2$) and then selected from the optimum gain conditions at this level. In some cases it may be necessary to sacrifice gain in order to obtain larger values of output power. The gain curves of figure 2-4 were made with 5000 turns on the input winding, while gain curves shown in figures 2-19 were observed for 3000 turns on the input winding. If the curves of figure 2-4 are corrected by the indicated turns ratio criterion established by equation 2-17, it may be seen by comparing figures 2-19 and 2-4 that a gain improvement, depending on the magnitude of the input resistance, of the order of 100 to 150, is possible with regenerative feedback in the region where the observed value of the input current is approximately 10^{-4} . This is the value of $(I_1)^2$ at which the gain of the feedback circuit reaches a maximum, and also is a value at which the basic circuit gain characteristic is at its maximum point. For identical conditions, the improvement in power output is of the same order as the improvement in gain with positive feedback. A careful adjustment of the feedback turns as described to obtain perfect 100% feed-

back might permit a better gain improvement than that shown in these limited observations. Both Figure 3-19 and Figure 5-4 emphasize the important and somewhat unfortunate part played by the input resistance in determining the gain available from a given magnetic amplifier. Again, these figures emphasize the significant fact that excellent gains are obtainable with a magnetic amplifier if dynamic response is of sufficiently small importance to permit the use of a minimum input resistance.

The effect of the magnitude of the peak alternating voltage, E_2 , in the feedback case is also analogous to this effect in the basic amplifier. The value selected should, for optimum operation, be sufficient to produce a flux with peak amplitude equal to ϕ_s . Values of applied voltage of lesser magnitude result in premature flattening of the modulation characteristic, as shown in Figure 5-5. If E_2 is sufficiently great to produce alternating fluxes of magnitudes greater than ϕ_s , the minimum or dip point of the feedback modulation characteristic will be increased, and the excitation current flowing in the output windings for zero input-current is increased to an undesirable figure. The discussion here implies that the modulation characteristic has been shifted to the right by an additional set of coils so that the minimum of the characteristic occurs at zero input current.

The effects of N_2 , which must equal N_3 theoretically, are also similar in the feedback case to those

been slighter than that shown in these limited observations. Both figures 5-12 and figure 5-13 emphasize the important and somewhat unfortunate fact played by the input resistance in determining the gain available from a given magnetic amplifier. Again, these figures emphasize the significant fact that excellent gains are obtainable with a magnetic amplifier if dynamic response is of sufficiently small importance. To permit the use of a minimum input resistance.

The effect of the magnitude of the gain is determined by the value of R_2 in the feedback circuit. The value selected for this effect in the basic amplifier. The value selected should, for optimum operation, be sufficient to produce a gain with load resistance equal to R_2 . Values of applied voltage of input resistance result in a constant relationship by the modulation characteristics, as shown in figure 5-5. It is sufficiently great to produce a constant value of gain of magnitude greater than R_2 , the minimum at the point of the feedback modulation characteristics will be determined and the resulting current flowing in the output winding for zero input-current is determined to an undesirable figure. The characteristic were taken that the modulation characteristics have been shifted to the right by an additional set of coils so that the minimum of the characteristic occurs at zero input current.

The effect of R_2 , which must equal R_1 for zero input-current, are also similar in the feedback case to those

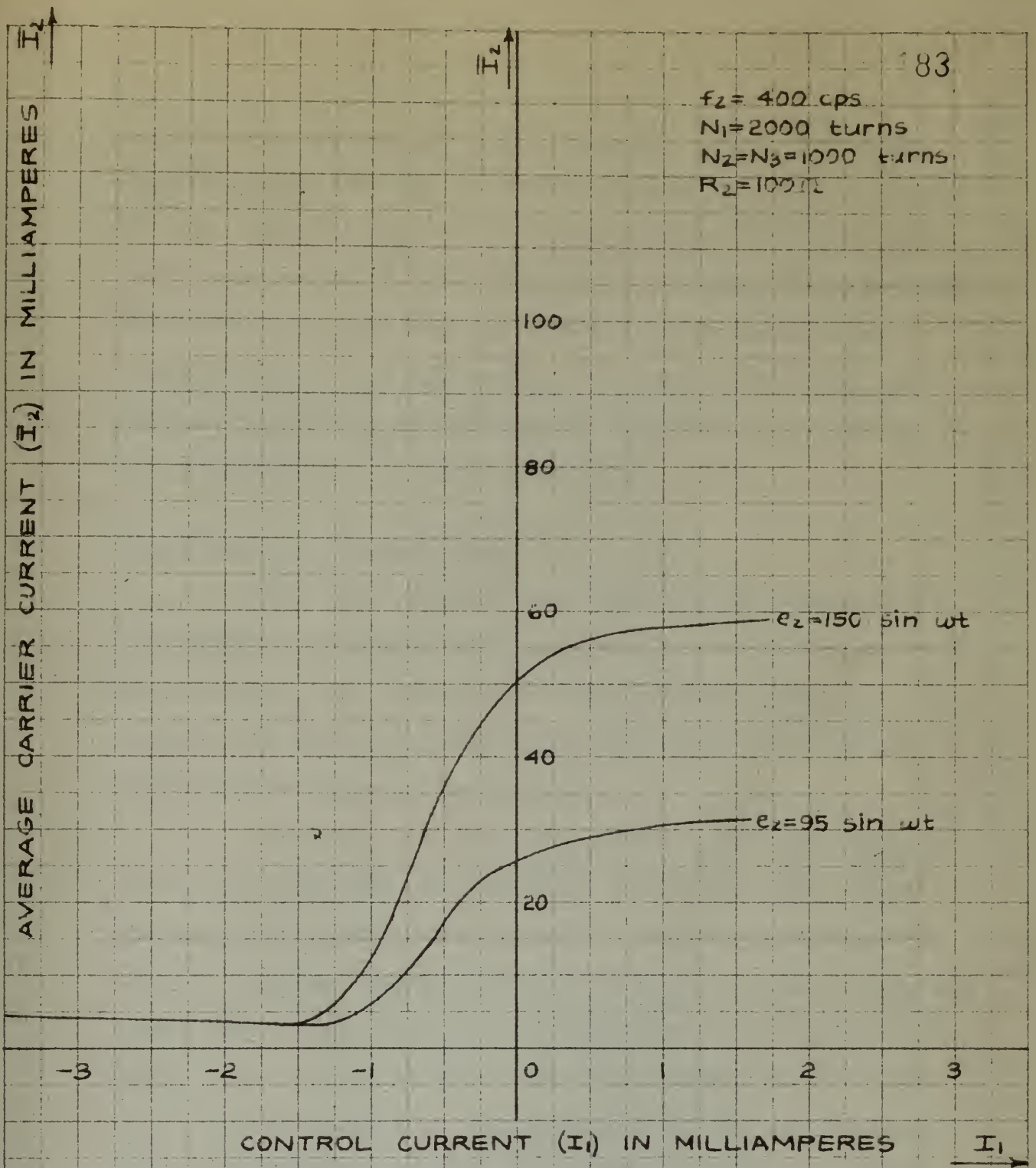


FIG. 5-5 MODULATION CHARACTERISTIC OF MAGNETIC AMPLIFIER WITH POSITIVE FEEDBACK SHOWING EFFECTS OF CHANGING THE APPLIED ALTERNATING VOLTAGE.

effects observed in the basic circuit. N_2 must also be adjusted such that the peak excursion of the alternating flux is equal to ϕ_g , or the minimum points of the modulation characteristic will be raised, as shown in Figure 5-6. This effect is particularly evident in the modulation curve for $N_2 = N_3 = 600$ turns. The selection of N_2 , as well as that of E_2 and frequency, is governed by the optimum magnitude of alternating flux.

The Theory of Feedback Gain

The basic concepts of regenerative-feedback, as introduced by Buchhold and discussed in the early pages of this chapter, are extended in the following paragraphs to explain the gain characteristics obtainable with fully-compensated regenerative-feedback.

Formulas for the power gain of the basic amplifier were developed and presented in Chapter III. When dealing with magnetic amplifiers it is also convenient to consider either ampere-turn gain or current gain, since the power gain of the amplifier depends upon the currents in the input and output circuits. The developments of this section will be devoted to consideration of the ampere-turn gain of the basic magnetic amplifier and of the magnetic amplifier with regenerative feedback.

In the idealized magnetic amplifier, as discussed in Chapter III, it has been shown that

effects observed in the basic circuit. H_2 must also be adjusted such that the peak excitation of the alternating flux is equal to H_2 , or the minimum points of the modulation characteristic will be raised, as shown in Figure 5-6. This effect is particularly evident in the modulation curve for $H_2 = H_2 \approx 500$ gauss. The reduction of H_2 , as well as that of H_1 and frequency, is governed by the same magnitudes of alternating flux.

The Theory of Feedback Gain

The basic concepts of regenerative-feedback, as introduced by Arnold and discussed in the early pages of this chapter, are extended in the following paragraphs to explain the gain characteristics obtainable with self-compensated regenerative-feedback.

Formulas for the power gain of the basic amplifier were developed and presented in Chapter III. When dealing with magnetic amplifiers it is also convenient to consider either power-current gain or current gain, since the power gain of the amplifier depends upon the currents in the input and output circuits. The development of this section will be devoted to consideration of the power-current gain of the basic magnetic amplifier and of the magnetic amplifier with regenerative feedback.

In the idealized magnetic amplifier, as discussed in Chapter III, it has been shown that

$$f_2 = 400 \text{ cps}$$

$$E_2 = 100 \text{ V}$$

$$N_1 = 2000 \text{ turns}$$

$$R_2 = 100 \Omega$$

[NOTE: 6H6 DIODE BRIDGE
RECTIFIER USED IN
FEEDBACK CIRCUIT]

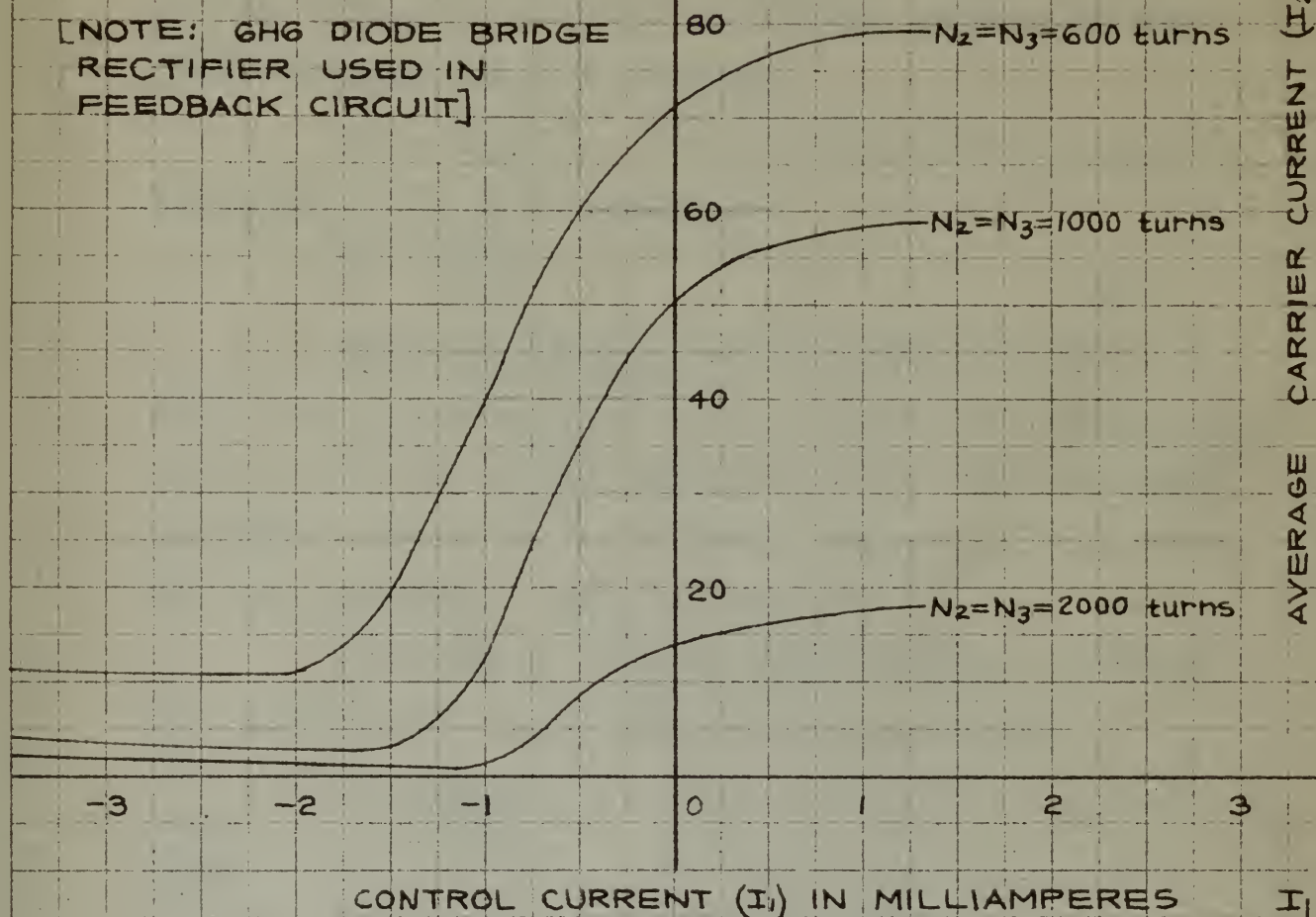


FIG. 5-6 MODULATION CHARACTERISTIC OF MAGNETIC AMPLIFIER WITH POSITIVE FEEDBACK SHOWING EFFECT OF CHANGING THE NUMBER OF TURNS IN OUTPUT (N_2) AND FEEDBACK (N_3) WINDINGS.

$$(NI)_1 = (N\bar{I})_2 \quad (5-4)$$

In the practical basic-amplifier, the equivalent concept, because permeability is not infinite, is

$$(NI)_1 \approx (N\bar{I})_2 \quad (5-5)$$

Actually $(NI)_1$ is slightly greater than $(N\bar{I})_2$, the amount greater being, as was shown, an inverse function of the permeability of the core material.

It is possible, then, to define the ampere-turn gain, K_I , of the basic amplifier:

$$K_I = \frac{(N\bar{I})_2}{(NI)_1} \quad (5-6)$$

The value of K_I is ideally unity; in the practical case K_I is less than unity. Although the ampere-turn gain is equal to or less than unity, it is still possible to obtain power gains in the basic circuit and the method has been developed. (See Equation 3-17.)

According to accepted feedback-theory, the gain of a system with regenerative feedback is defined

$$K' = \frac{K}{1 - \beta K} \quad (5-7)$$

where

K' = gain of the feedback system,

K = gain of the system without feedback,

β = feedback ratio.

By reference to Figure 5-1(a) and Equation 5-2, the following relationships for the feedback system are established:

(4-4)

$$(M)_1 = (M)_2$$

In the immediate feedback, the equivalent

concept, because permeability is not infinite, is

(4-5)

$$(M)_1 \approx (M)_2$$

Actually $(M)_1$ is slightly greater than $(M)_2$, the amount

greater being, as was shown, an inverse function of the

permeability of the area material.

It is possible, then, to define the negative-gain

gain, K_1 , of the basic amplifier

(4-6)

$$K_1 = \frac{(M)_2}{(M)_1}$$

The value of K_1 is unity only; in the zero-

gain case K_1 is less than unity. Although the negative-gain

gain is equal to or less than unity, it is still possible

to obtain power gain in the basic circuit and the method

has been developed. (See Equation 3-17.)

According to accepted feedback-theory, the gain

of a system with regenerative feedback is defined

(4-7)

$$K' = \frac{K}{1 - \beta K}$$

where

K' = gain of the feedback system,

K = gain of the system without feedback,

β = feedback ratio.

By reference to Figure 2-1(a) and Equation 2-2,

the following relationships for the feedback system are

established:

$$K = \frac{(\bar{N}I)_2}{(\bar{N}I)_1} = \frac{(\bar{N}I)_2}{(\bar{N}I)_1' + (\bar{N}I)_3} \quad (5-8)$$

Ideally for full compensation

$$(\bar{N}I)_2 = (\bar{N}I)_3, \quad (5-9)$$

but in the practical case $(\bar{N}I)_2$ is slightly greater than $(\bar{N}I)_3$ because of loss in the rectifier system. The feedback ratio is defined

$$\beta = + \frac{(\bar{N}I)_3}{(\bar{N}I)_2} \quad (5-10)$$

From Equations 5-7, 5-8 and 5-10

$$K' = \frac{\frac{(\bar{N}I)_2}{(\bar{N}I)_1' + (\bar{N}I)_3}}{1 - \frac{(\bar{N}I)_2}{(\bar{N}I)_1' + (\bar{N}I)_3}} \quad (5-11)$$

or

$$K' = \frac{(\bar{N}I)_2}{(\bar{N}I)_1' + (\bar{N}I)_3 - (\bar{N}I)_2} \quad (5-12)$$

Let us consider Equation 5-12 in the light of the idealized situation of infinite permeability. Under these conditions $(\bar{N}I)_1'$ is identically zero, $(\bar{N}I)_2$ and $(\bar{N}I)_3$ are equal, the denominator is zero and K' becomes infinite. We see that the ampere-turn gain has been increased in the ideal case from unity for the basic circuit to infinity for the case of fully-compensated feedback.

In the practical case, of course, $(\bar{N}I)_1'$ is a finite value and an inverse function of permeability, while the difference between $(\bar{N}I)_2$ and $(\bar{N}I)_3$ is small and a direct function of the rectifier losses and distor-

$$(2-8) \quad \bar{X}_2 = \frac{\bar{X}_1}{1 + \frac{\bar{X}_1}{\bar{X}_2}} = \frac{\bar{X}_1}{1 + \frac{\bar{X}_1}{\bar{X}_2}}$$

ideally for full compensation

$$(2-9) \quad \bar{X}_2 = \bar{X}_1$$

but in the practical case, \bar{X}_2 is slightly greater than \bar{X}_1 because of loss in the feedback system. The loss has been taken as defined

$$(2-10) \quad \bar{X}_2 = \bar{X}_1 + \frac{\bar{X}_1}{\bar{X}_2}$$

From equations 2-7, 2-8 and 2-10

$$(2-11) \quad \bar{X}_2 = \frac{\bar{X}_1}{1 + \frac{\bar{X}_1}{\bar{X}_2}} = \frac{\bar{X}_1}{1 + \frac{\bar{X}_1}{\bar{X}_2}}$$

$$(2-12) \quad \bar{X}_2 = \frac{\bar{X}_1}{1 + \frac{\bar{X}_1}{\bar{X}_2}} = \frac{\bar{X}_1}{1 + \frac{\bar{X}_1}{\bar{X}_2}}$$

Let us consider equation 2-12 in the limit as the idealized relation of infinite permeability. When there is no loss, \bar{X}_2 is a constant, and \bar{X}_1 and \bar{X}_2 are equal. The permeability is zero and \bar{X}_1 becomes infinite. We see that the negative feedback has been introduced in the ideal case from which the basic circuit is infinity for the case of fully-compensated feedback. In the practical case, of course, \bar{X}_1 is a finite value and an inverse relation of permeability, while the difference between \bar{X}_1 and \bar{X}_2 is small and a direct function of the feedback losses and delay.

tion. The value of K' is still very large. Equation 5-12 indicates that high-permeability core-materials and low-loss rectifiers are essential for feedback magnetic-amplifier designs.

Dynamic Performance with Regenerative Feedback

The time available for dynamic feedback studies was very limited, and did not permit a thorough investigation of this subject. A few remarks relative to the effect of regenerative feedback on the dynamic performance of the amplifier are, however, presented here.

It would be desirable to be able to predict the dynamic performance of the feedback amplifier from the dynamic performance of the basic circuit, since it is possible, within reasonable limits, to anticipate the dynamic behavior of the basic circuit by methods which have already been described in the earlier chapters. A means for such a prediction is not, however, apparent to the authors at the present time. The additional feedback windings, and the buildup in current in these windings, involve factors which greatly complicate the dynamic behavior. The effect of input-circuit current on dynamic performance is also complicated by the addition of feedback windings. In the basic circuit, the biasing input-current for an alternating signal may be selected anywhere in a wide range of linear ampere-turn sensitivity. Reference to any of the feedback modulation characteristics in this chapter will show that, in the feedback case, the

tion. The value of β is still very large. Consider
5-12 consider the high-frequency characteristics and
low-frequency characteristics are essential for feedback systems
amplifier designs.

Dynamic Performance with Regenerative Feedback

The time available for dynamic feedback analysis
was very limited, and did not permit a thorough investiga-
tion of this subject. A few remarks relative to the
effect of regenerative feedback on the dynamic performance
of the amplifier are, however, presented here.
It would be desirable to be able to predict the

dynamic performance of the feedback amplifier from the
dynamic performance of the basic circuit, since it is
possible, within reasonable limits, to anticipate the
dynamic behavior of any basic circuit by methods which
have already been described in the earlier chapters. A
means for such a prediction is not, however, apparent in
the analysis of the present case. The additional feedback
windings, and the shifting in current in these windings,
involve factors which greatly complicate the dynamic be-
havior. The effect of input-output current on dynamic
performance is also complicated by the addition of feed-
back winding. In the basic circuit, the blocking input-
current for an alternating signal may be calculated anywhere
in a wide range of linear system analysis. But
even so any of the feedback modulation characteristics in
this chapter will show that in the feedback case, the

range of selection is greatly narrowed, and is, in general, limited to somewhere in the range from 0.3 to 1.3 milliamperes. The limitation is a result of the fact that much of the effective "input" magnetizing force is, in effect, supplied by the feedback windings, since these windings are connected in a manner additive to the input circuit windings.

A single sinusoidal band-pass characteristic for a feedback amplifier is shown in Figure 5-8. The input resistance is approximately 7000 ohms plus the resistance of the windings. The biasing current is 0.7 ma., which insures operation over the most linear portion of the feedback modulation-characteristic. The observed bandwidth is seen to be of the order of 12 cycles per second, which is rather low for many applications, and certainly lower than what might be expected from the basic circuit with a 7K input resistance and a moderately large biasing current. The fact that the biasing current may be lower in the feedback case is no specific advantage, since this current can be readily supplied by rectifying a portion of the main supply voltage; the power consumed is thence independent of the signal source. At any rate, a substantial reduction in bandpass is apparent for the feedback circuit as compared with the basic circuit under similar conditions. Of course, the gain has been improved by the use of regenerative feedback.

range of selection is greatly increased, and in the
control, limited to somewhere in the range from 0.5 to
1.5 milliamperes. The limitation is a result of the
fact that most of the effective "input" representing force
is, in effect, supplied by the feedback winding, since
these windings are connected in a manner similar to
the input circuit windings.

A single sinusoidal band-pass characteristic
for a feedback amplifier is shown in Figure 3-3. The
input resistance is approximately 7000 ohms plus the re-
sistance of the winding. The damping constant is 0.7 sec.,
which insures operation over the most linear portion of
the feedback characteristic. The feedback
characteristic is seen to be of the order of 10 cycles per
second, which is rather low for many applications, and
certainly lower than what might be expected from the basic
circuit with a 75 input resistance and a moderately large
damping constant. The fact that the damping constant may
be lower in the feedback case is an obvious advantage,
since this system can be readily supplied by controlling
a portion of the main supply voltage; the power consumed
is hence independent of the signal source. At any rate,
a substantial reduction in feedback is required for the
feedback circuit as compared with the basic circuit under
similar conditions. Of course, this gain has been improved
by the use of regenerative feedback.

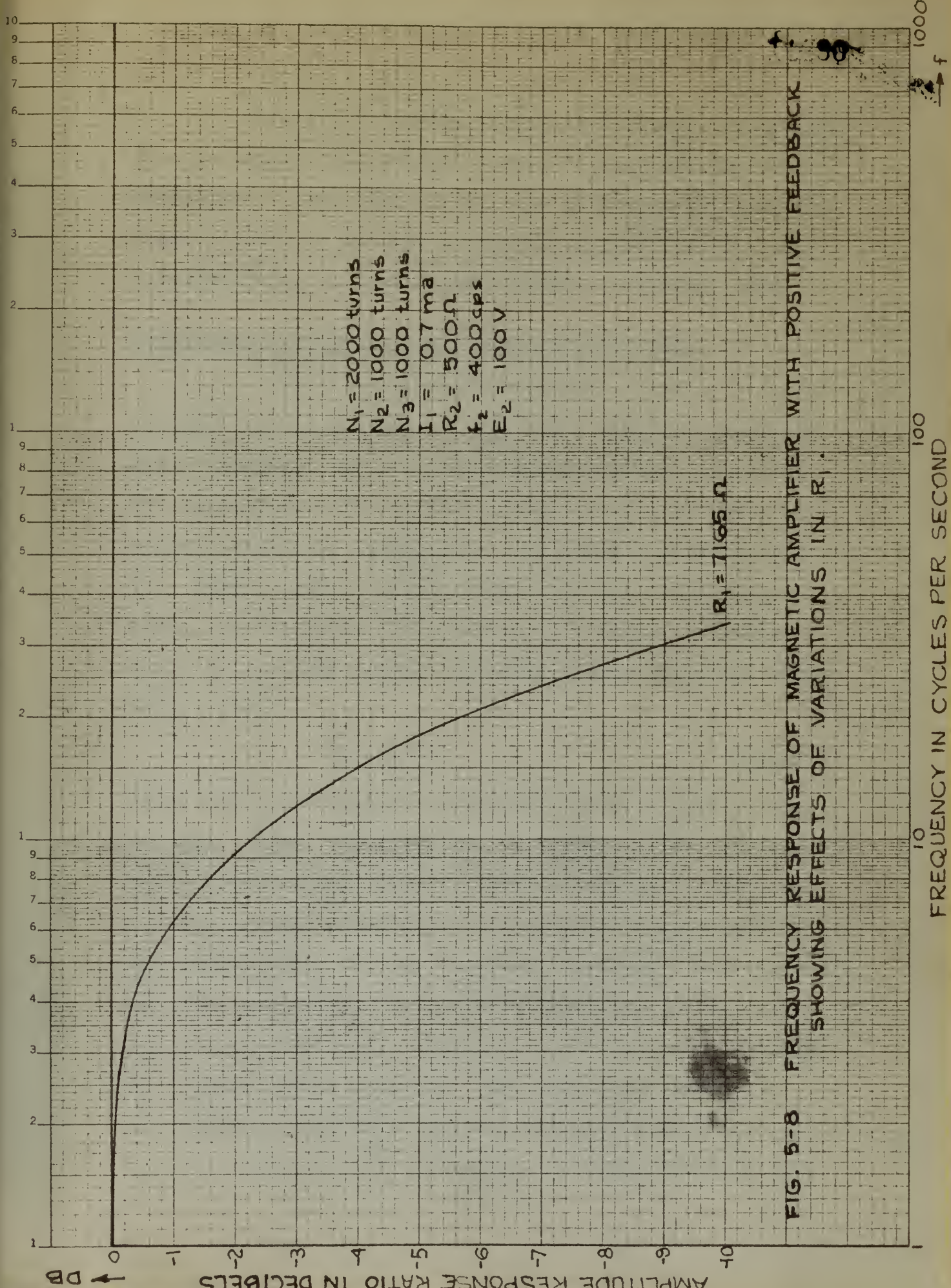


FIG. 5-8 FREQUENCY RESPONSE OF MAGNETIC AMPLIFIER WITH POSITIVE FEEDBACK SHOWING EFFECTS OF VARIATIONS IN R_1 .



The proportionate improvement in gain and reduction in dynamic performance should be investigated more thoroughly. The effect of the use of regenerative-ampere-turn feedback on the gain-bandwidth product, rather than on gain alone, is particularly worthy of further study.

Analytical Equations of the Feedback Amplifier

A set of analytical equations, similar to those employed in the solution of the basic magnetic amplifier, may be prepared for the regenerative-feedback amplifier. The regenerative-feedback amplifier-circuit is shown in schematic form in Figure 5-9. New parameters defined by this figure include the resistance of the feedback windings, R_3 , the forward resistance of a single rectifier unit, R_f , and the current i_3 which is the rectified value of i_2 . Thus

$$i_3 = \pm i_2 \quad (5-13)$$

where the signs alternate each half-cycle of the carrier voltage. Ideal rectification is assumed in the rectifier units to the extent that the back resistance is infinite and the forward resistance is a constant independent of the value of i_2 . In the practical rectifier, both forward and back resistance are nonlinear functions of the exciting current, and such a function could be readily handled by a differential analyzer. The equivalent circuit of the idealized rectifier and the feedback circuit as seen by i_2 is shown for one half-cycle in Figure 5-10(a), and

The proposed improvements in gain and regulation in dynamic performance should be investigated more thoroughly. The effect of the use of regenerative-negative feedback on the gain-bandwidth product, rather than on gain alone, is particularly worthy of further study.

Analytical Solution of the Feedback Amplifier

A set of analytical equations, similar to those employed in the solution of the basic magnetic amplifier, may be prepared for the regenerative-feedback amplifier. The regenerative-feedback amplifier circuit is shown in schematic form in Figure 5-9. Two parameters defined by this figure include the resistance of the feedback winding, R_f , the forward resistance of a single rectifier unit, r_f , and the current i_f which is the rectified value of i_g . Thus

$$i_f = \frac{1}{2} i_g \quad (5-13)$$

where the signs alternate each half-cycle of the carrier voltage. Ideal rectification is assumed in the rectifier units to the extent that the back resistance is negligible and the forward resistance is a constant independent of the value of i_g . In the practical rectifier, both forward and back resistance are nonlinear functions of the exciting current, and such a function could be readily handled by a differential analyzer. The equivalent circuit of the idealized rectifier and the feedback circuit as seen by i_g is shown for one half-cycle in Figure 5-10(a), and

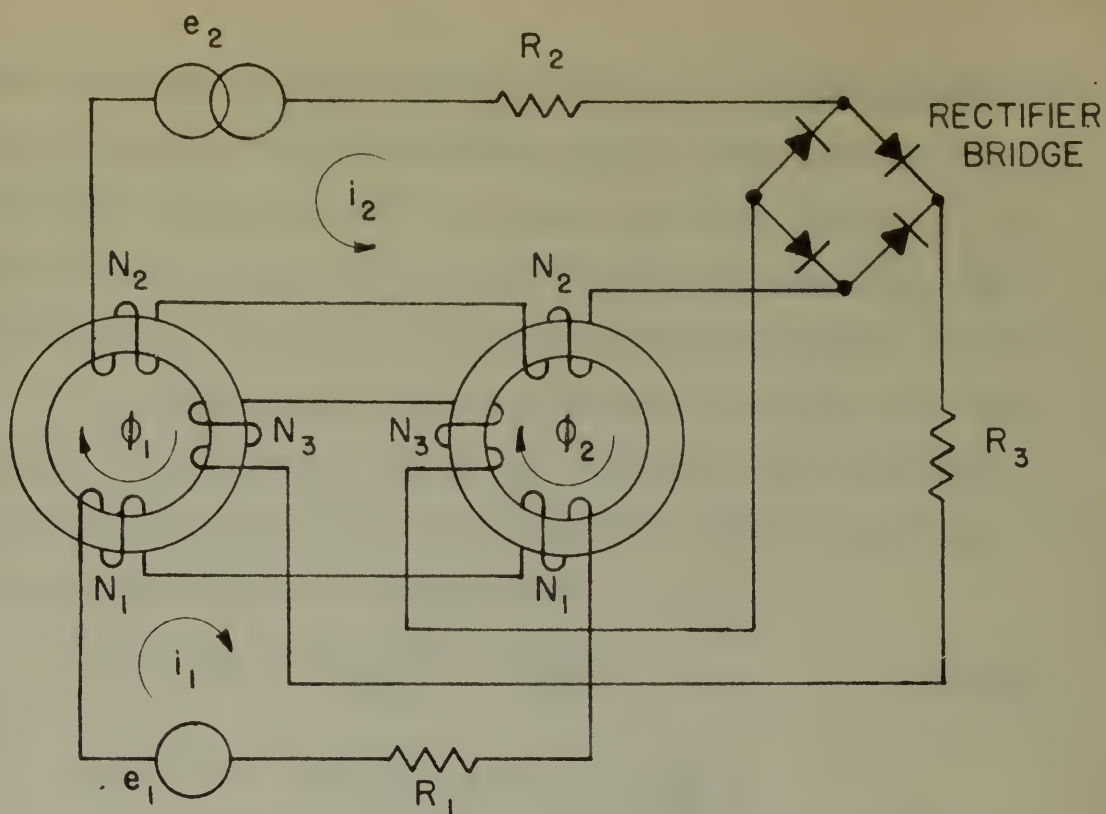
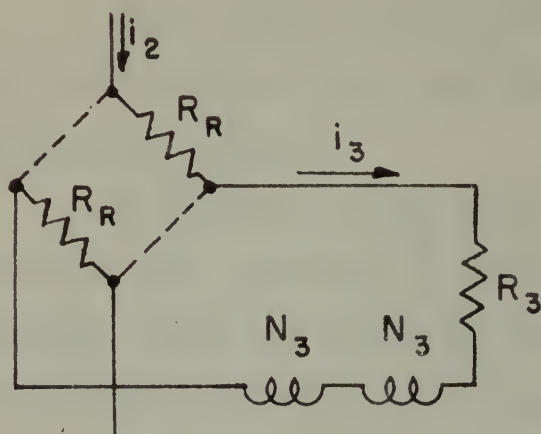
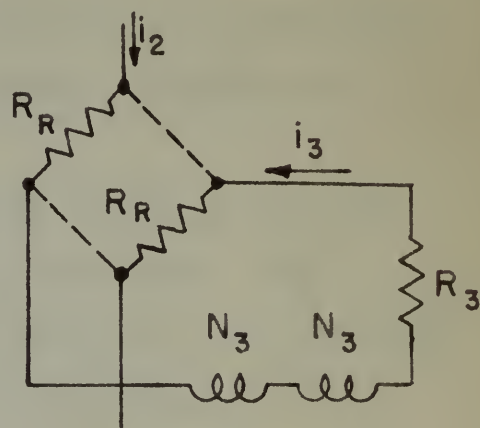


FIG. 5-9 REGENERATIVE FEEDBACK CIRCUIT.



(a) EQUIVALENT RECTIFIER CIRCUIT FOR 1ST HALF CYCLE.



(b) EQUIVALENT RECTIFIER CIRCUIT FOR 2ND HALF CYCLE.

FIG. 5-10 RECTIFIER CIRCUITS.

... and the ...
 ... the ...
 ... the ...
 ... the ...

... the ...
 ... the ...
 ... the ...
 ... the ...

... the ...
 ... the ...
 ... the ...
 ... the ...

... the ...
 ... the ...
 ... the ...
 ... the ...

... the ...
 ... the ...
 ... the ...
 ... the ...

for the next alternating half-cycle in Figure 5-10(b). The reversal of i_2 each half-cycle as this current flows in the feedback circuit is shown in these figures. It is also apparent that an additional resistance, $2R_r$, is included in the path of i_2 through the feedback circuit.

The system loop-equilibrium equations for the loops defined by i_1 and by i_2 (including the feedback loop and recalling Equation 5-13) are formulated from Figure 5-9 and from Figure 4-2:

$$e_1 = R_1 i_1 + N_1 \frac{d\phi_1}{dt} - N_1 \frac{d\phi_2}{dt} \quad (5-14)$$

$$e_2 = (R_2 + 2 R_r + R_3) i_2 + N_2 \frac{d\phi_1}{dt} + N_2 \frac{d\phi_2}{dt} + N_3 \frac{d\phi_1}{dt} + N_3 \frac{d\phi_2}{dt} \quad (5-15)$$

$$\phi_1 = f (N_2 i_2 + N_1 i_1 + N_3 i_3) \quad (5-16)$$

$$\phi_2 = f (N_2 i_2 - N_1 i_1 + N_3 i_3) \quad (5-17)$$

The \pm signs in the above equations are associated with rectification of i_2 when this current is applied to the feedback circuit.

A problem for the differential analyzer could be formulated from Equations 5-14 to 5-17 inclusive. The mechanical layout of the differential analyzer would require provision for reversing the signs each half-cycle, as indicated in the equations. The reversal might be accomplished by including a set of idler gears in each appropriate gear

For the next alternating half-cycle in Figure 5-10(b). The reversal of i_2 each half-cycle as this current flows in the feedback circuit is shown in these figures. It is also apparent that an additional resistance, R_2 , is included in the path of i_2 through the feedback circuit. The system loop-differential equations for the

loops defined by i_1 and by i_2 (including the feedback loop and feedback equation 5-13) are formulated from Figure 5-9 and from Figure 5-11:

$$e_1 = R_1 i_1 + L_1 \frac{di_1}{dt} - R_1 \frac{di_2}{dt} \quad (5-14)$$

$$e_2 = (R_2 + R_3 + R_4) i_2 + L_2 \frac{di_2}{dt} + R_2 \frac{di_1}{dt}$$

$$R_2 \frac{di_2}{dt} = R_3 \frac{di_1}{dt} + R_4 \frac{di_2}{dt} \quad (5-15)$$

$$e_1 = r (R_2 i_2 + R_1 i_1 + R_3 i_2) \quad (5-16)$$

$$e_2 = r (R_2 i_2 - R_1 i_1 + R_3 i_2) \quad (5-17)$$

The + signs in the above equations are associated with restriction of i_2 when this current is applied to the feedback circuit.

A problem for the differential analyzer could be formulated from Equations 5-14 to 5-17 inclusive. The mechanical layout of the differential analyzer would require provision for reversing the signs each half-cycle, as indicated in the equations. The reversal might be accomplished by including a set of index gears in each appropriate gear

box. As i_2 passes through zero in the solution, it would then be necessary to stop the machine and reverse the necessary shafts through use of the idlers. The value of an analytical study based upon these equations would be weighed, as was the investigation of the basic circuit of this thesis, against the importance of the losses in the carrier circuit, but would undoubtedly be of significant value in elucidating many of the features of regenerative-feedback magnetic-amplifier performance.

Now, as it passes through zero in the solution, it would then be necessary to stop the machine and reverse the necessary shafts through use of the latter. The value of an analytical study based upon these conditions would be weighed, as was the investigation of the basic circuit of this theory, against the importance of the losses in the system circuit, but would undoubtedly be of significant value in elucidating many of the features of regenerative-feedback magnetic-amplifier performance.

(1-10)

$$V = I \cdot R + L \frac{dI}{dt}$$

(1-11)

$$\frac{dV}{dt} = R \frac{dI}{dt} + L \frac{d^2I}{dt^2}$$

(1-12)

$$V = I \cdot R + L \frac{dI}{dt}$$

(1-13)

$$V = I \cdot R + L \frac{dI}{dt}$$

The above is the basic equation for the regenerative-feedback magnetic-amplifier circuit. It is a second-order differential equation, and its solution is given by the following expression:

The solution of the above equation is given by the following expression:

$$I = I_0 e^{-\alpha t} \cos(\omega_d t + \phi)$$

where I_0 is the initial current, α is the damping coefficient, ω_d is the damped natural frequency, and ϕ is the phase angle. The values of α and ω_d are given by the following expressions:

$$\alpha = \frac{R}{2L}$$

$$\omega_d = \sqrt{\frac{1}{LC} - \left(\frac{R}{2L}\right)^2}$$

The phase angle ϕ is given by the following expression:

$$\phi = \tan^{-1} \frac{\omega_d L}{R}$$

The above expressions are valid for the case where the circuit is underdamped, i.e., where $\alpha < \omega_d$. If the circuit is overdamped, i.e., where $\alpha > \omega_d$, the solution is given by a different expression.

CHAPTER VI

SUMMARY AND CONCLUSIONS

Summary of the Research

This thesis has attempted to investigate the fundamental behavior of the magnetic amplifier both from experimental and analytic studies. Although various articles have appeared in the literature pertaining to the static performance of the amplifier, relatively little has been published concerning circuit dynamics. Both static and dynamic aspects have been explored in this research, with particular emphasis on dynamic studies based upon both transient and frequency-response data. The mathematical analysis of the circuit is complicated by the nonlinear nature of the differential equations which characterize the system. The solution of these equations by means of the differential analyzer is believed to be an original effort. In order to arrive at circuit fundamentals, the simplest case of interest was chosen as the starting point of the investigation. This circuit is the basic magnetic amplifier which involves no feedback techniques. A thorough study was made of the basic circuit correlating experimental and analytical data wherever possible. A rather large amount of experimental characteristics have been included in the thesis because of the paucity of concrete design data in the literature. It is hoped that the inclusion of this data may be of some value to future investigators. After studies of the basic circuit

CHAPTER VI

NONLINEAR AND CHAOTIC BEHAVIOR

Summary of the Chapter

This chapter has attempted to investigate the fundamental behavior of the magnetic amplifier both from experimental and analytical studies. Although various articles have appeared in the literature pertaining to the static performance of the amplifier, relatively little has been published concerning circuit dynamics. Both static and dynamic aspects have been explored in this review, with particular emphasis on dynamic studies based upon both transient and frequency-response data. The mathematical analysis of the circuit is conducted by the nonlinear nature of the differential equations which characterize the system. The solution of these equations by means of the differential analyzer is believed to be an original effort. In order to arrive at circuit transfer functions, the algebraic laws of circuit analysis are used. The starting point of the investigation. This circuit is the basic magnetic amplifier which involves no feedback mechanism. A thorough study was made of the basic circuit containing experimental and analytical data wherever possible. A rather large amount of experimental data has been included in the thesis because of the paucity of accurate design data in the literature. It is hoped that the inclusion of this data may be of some value to future investigators. After analysis of the basic circuit

were completed, the remaining available time was devoted to experimental investigations of regenerative ampere-turn feedback.

Results of the Research

A thorough study was made of the basic magnetic amplifier and quantitative design criteria were obtained. The effects of all circuit parameters were studied, a family of curves being plotted for each parametric variation. These curves, as determined experimentally, are reproduced in Chapter III. An analytic formulation of the basic-circuit problem in terms of the differential loop-equilibrium equations was made, neglecting hysteresis and eddy-current losses, and the machine solutions were compared with experimentally determined steady-state and transient response. The results of this study, which are tabulated in Figure 6-1, indicate satisfactory agreement between experimental and theoretical steady-state performance. Important differences were obtained, however, between experimental and theoretical dynamic behavior. Although the effect of the control-circuit parameters upon the effective characteristic time agreed in both cases, the dependence of characteristic time upon carrier-circuit conditions revealed major discrepancies. These inconsistencies are attributable to the functional relation of the core losses upon the carrier-circuit conditions, as expressed by Equation 3-27, and which was neglected in the analytic solutions.

very complete, the remaining available time was devoted to experimental investigation of regenerative capacity.

Downloaded At: 11:53 11 September 2009

A thorough study was made of the head weights, heights and accelerative design criteria were obtained. The effects of all dynamic parameters were studied, a series of curves being plotted for each parameter variation. These curves, as determined experimentally, are reproduced in Chapter III. An analytical formulation of the basic-dynamic problem in terms of the differential equations of motion was made, neglecting rotational and body-control forces, and the solution relations were compared with experimentally-determined steady-state and transient responses. The results of this study, which are tabulated in Figure 3-1, indicate satisfactory agreement between experimental and theoretical steady-state performance. In contrast, differences were observed, however, between experimental and theoretical dynamic behavior. Although the effect of the control-system parameters upon the effective characteristic time agreed in both cases, the dependence of characteristics time upon system-steady conditions required major discrepancies. These discrepancies are attributable to the mechanical relation of the two masses upon the carrier-theoretical conditions, as explained by Figures 3-2, 3-3, and which are indicated in the weight reduction.

TABULATION OF RESULTS

1-197

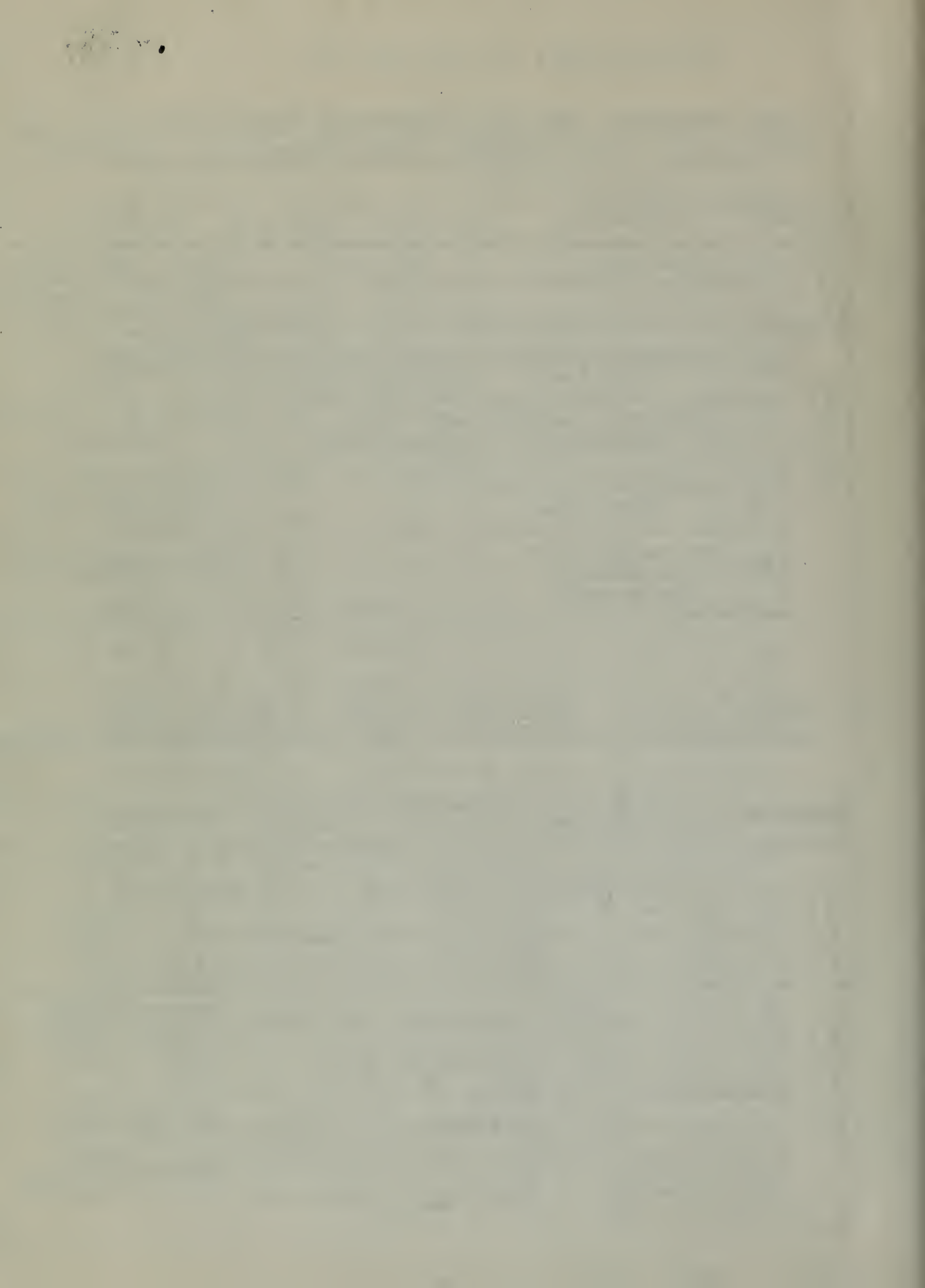
I STATIC TRENDS - THE EFFECT OF ONE PARAMETER UPON THE MODULATION CHARACTERISTIC, OTHER PARAMETERS CONSTANT.

PARAMETER		EXPERIMENTAL	ANALYTICAL	REMARKS
CONTROL CIRCUIT	R_1	NEGLIGIBLE	NEGLIGIBLE	NATURAL MAGNETIZATION- LOW CONTROL CIRCUIT IMPEDANCE TO CARRIER EVEN HARMONICS
	N_1	NEGLIGIBLE	NEGLIGIBLE	
CARRIER CIRCUIT	R_2	INCREASING R_2 INCREASES LINEAR RANGE	ANALYTIC RESULTS CHECK EXPERIMENTAL TRENDS OVER THE LOWER INPUT RANGE; NOT EXAMINED OVER HIGHER INPUT RANGE.	AFFECTS ONLY E_L/E_2 CHARACTERISTIC (FIG. 3-5)
	E_2	INCREASING E_2 INCREASES LINEAR RANGE		AFFECTS ONLY A.C. FLUX AMPLITUDE
	f_2	INCREASING f_2 DECREASES LINEAR RANGE		AFFECTS BOTH E_L/E_2 AND FLUX AMPLITUDE
	N_2	OPTIMUM N_2 EXISTS FOR MINIMUM LINEAR RANGE		AFFECTS BOTH E_L/E_2 AND FLUX AMPLITUDE

II DYNAMIC TRENDS - THE EFFECT OF ONE PARAMETER UPON THE EFFECTIVE CHARACTERISTIC TIME, OTHER PARAMETERS CONSTANT.

PARAMETER		EXPERIMENTAL FREQUENCY-RESPONSE	EXPERIMENTAL TRANSIENT	ANALYTICAL TRANSIENT	REMARKS
CONTROL CIRCUIT	I_1	$(CT) \rightarrow \frac{1}{\sqrt{I_1}}$	$(CT) \rightarrow \frac{1}{\sqrt{I_1}}$	$(CT) \rightarrow \frac{1}{\sqrt{I_1}}$	ALL CHECK
	R_1	$(CT) \rightarrow \frac{1}{R_1}$	$(CT) \rightarrow \frac{1}{R_1}$	$(CT) \rightarrow \frac{1}{R_1}$	ALL CHECK
	N_1	$(CT) \rightarrow N_1$	$(CT) \rightarrow N_1$	$(CT) \rightarrow N_1$	ALL CHECK
CARRIER CIRCUIT	R_2	$(CT) \rightarrow (R_2)^{1/3}$	NEGLIGIBLE	NEGLIGIBLE	ANALYSIS NEGLECTED CORE-LOSS FUNCTION THEREFORE DIFFERENT FROM EXPERIMENTAL DATA.
	E_2	$(CT) \rightarrow (E_2)^{1/5}$	$(CT) \rightarrow (E_2)^{1/5}$	$(CT) \rightarrow \frac{1}{E_2}$	
	f_2	$(CT) \rightarrow \frac{1}{f_2}$	$(CT) \rightarrow \frac{1}{(f_2)^{1/10}}$	NOT EXAMINED	FREQUENCY-RESPONSE DATA INVOLVES CONSTANT I_1 BIAS; WHILE I_1 TRANSIENT BUILDS UP FROM ZERO; HENCE THE DIFFERENCE.
	N_2	$(CT) \rightarrow \frac{1}{N_2}$	$(CT) \rightarrow \frac{1}{\sqrt{N_2}}$	$(CT) \rightarrow N_2$	

FIG. 6-1 BASIC CIRCUIT STUDIES.



The differential analyzer was directly responsible for disclosing two effects which otherwise might have escaped observation. These were, first, the concept of flux-bias buildup, and secondly, the relation of hysteresis to the carrier-current waveform. Finally, an approximate expression for power gain, Equation 3-17, was developed. By comparing this relation with the effects of circuit parameters upon characteristic time, tabulated in Figure 6-1, it is evident that a compromise between gain and bandwidth must be accepted.

Results from the studies of the regenerative ampere-turn feedback connection are more of a qualitative nature than quantitative. Lack of time curtailed a more thorough investigation of this circuit. As would be expected from a consideration of feedback-amplifier theory, the sensitivity of this circuit is much greater than that of the equivalent basic circuit, but the bandwidth is much less. Further study should indicate whether or not an overall improvement of the gain-bandwidth product can be obtained with the feedback connection. Experimentation with this circuit revealed that the rectifier bridge must be carefully balanced if a symmetrical carrier-current waveform is to be obtained.

Conclusions

The results indicate that certain design criteria have been obtained which will permit a prediction of both power-gain and amplifier-bandwidth. It has been shown that

The differential analysis was directly comparable for all the cases. The effects which otherwise might have been observed. These were, first, the change of the gain, delay, and secondly, the relation of the delay to the carrier-current wave. Finally, an approximate expression for power gain, Equation 3-17, was developed. By comparing this relation with the effects of circuit parameters upon characteristic time, tabulated in Figure 2-1, it is evident that a comparison between gain and bandwidth must be made.

Results from the analysis of the representative input-output feedback connection are more of a qualitative nature than quantitative. Lack of time prevented a more thorough investigation of this circuit. It would be expected from a consideration of feedback-amplifier theory, the sensitivity of this circuit is much greater than that of the equivalent basic circuit, but the bandwidth is much less. Further study should indicate whether or not an overall improvement of the gain-bandwidth product can be obtained with the feedback connection. Experimentation with this circuit revealed that the results of the analysis were essentially correct in a qualitative manner.

Conclusions

The results indicate that certain design criteria have been obtained which will permit a prediction of both power-gain and amplifier-bandwidth. It has been shown that

a compromise between the two, consistent with the requirements of the particular application, must be sought. In order to crystallize these concepts, a sample design to meet fixed specifications is outlined in the Appendix. Model theory could then be applied to miniaturize this design, a consideration of importance where space and weight must be minimized.

The value of the analytic approach cannot be overestimated. It has been valuable in disclosing the importance of hysteresis and eddy-current loss in the cores. It has been of assistance in establishing the transient behavior of flux bias. But perhaps the most beneficial result obtained from the solution of the problem on the differential analyzer was the appreciation of the physical significance of the differential equations acquired by watching the relative motion of the shafts which represented the system variables. This intuitive feeling for the fundamentals of the circuit would be most difficult, if not impossible, to acquire from experimental observations alone. Any variable of interest can readily be plotted by the analyzer as a function of time, and both the transient and steady-state behavior simultaneously determined.

A study of the frequency-response characteristics has disclosed that the magnetic amplifier can be characterized by a first-order time constant when an incremental signal is superimposed upon a direct-current

A comparison between the two, consistent with the results of the statistical analysis, may be made. In order to crystallize these concepts, a simple device is used. This device is outlined in the Appendix. These results should then be applied to maintain this design, a consideration of importance where space and weight must be obtained.

The value of the amplification system cannot be overestimated. It has been valuable in developing the importance of feedback and step-control loss in the cover. It has been of assistance in establishing the transient behavior of the line. At present the only practical result obtained from the solution of the problem is on the differential equation and the derivation of the physical significance of the differential equation. It is noted by using the relative motion of the electric which represented the system variables. This intuitive feeling for the importance of the electric field is not difficult, if not impossible, to acquire from experimental observation alone. Any variable of interest can readily be plotted by the analysis as a function of time, and both the transient and steady-state behavior simultaneously obtained.

A study of the frequency-response characteristics has disclosed that the magnetic amplifier can be characterized by a first-order time constant when an incremental signal is superimposed upon a direct-current

bias. Although the first-order concept is not original with this thesis, it does not appear that the above information has yet been used to clarify certain criteria that Alexanderson established in 1916 for the gain of the magnetic amplifier.¹ According to Alexanderson, the ratio of amplification is roughly proportional to the ratio of the carrier frequency to the signal frequency. The frequency response of the magnetic amplifier has been shown to be flat in the low-frequency range, and subsequently to fall off at 6 db/octave in the higher ranges. The critical frequency of the amplifier is inherently low, as can be observed from the frequency-response characteristics of Chapter III. The reason Alexanderson observed the gain to be inversely proportional to the audio frequency can be attributed to the fact that the bandwidth of his amplifier was very low and that he was actually operating in the cutoff region of the amplitude response where the slope is, indeed, inversely proportional to the frequency - in other words, in the region where the response falls off at 6 db/octave.

The magnetic amplifier has been used for a number of years in automatic-control,² measuring,³ and audio systems.¹ The principal limitation of this highly inductive

-
1. Alexanderson, E.F.W. and S.P. Nixdorf, "A Magnetic Amplifier for Radio Telephony," I.R.E. Proc., 4, (1916), 101-129.
 2. Giroz, H.E., "Application of Magnetic Amplifiers to the Control and Automatic Regulation of Furnace Temperatures," Bull. Soc. Franc. Elec., 1, (1941), 459-497.
 3. Geyger, W., "Magnetische Verstärker für die Mess und Regeltechnik," E.T.Z., 62, (1941), 849-853, 891-898.

Although the first-order concept is not original with this thesis, it does not appear that the above information has yet been used to clarify certain criteria that Alexander established in 1916 for the gain of the magnetic amplifier.¹ According to Alexander, the ratio of amplification is roughly proportional to the ratio of the center frequency to the signal frequency. The frequency response of the magnetic amplifier has been shown to be flat in the low-frequency region, and independently to fall off at a dy/dx rate in the higher region. The critical frequency of the amplifier is inherently low, as can be observed from the frequency-response characteristics of Chapter III. The reason Alexander observed the gain to be inversely proportional to the audio frequency can be attributed to the fact that the condition of the amplifier was very low and that he was actually operating in the cutoff region of the amplifier response where the gain is, indeed, inversely proportional to the frequency. In other words, in the region where the response falls off at a dy/dx rate.

The magnetic amplifier has been used for a number of years in automatic-control,² measuring,³ and radio systems.⁴ The principal limitation of this highly inductive

1. Alexander, S. F., and G. E. Alexander, "A magnetic amplifier for radio frequency," I.R.E. Trans., 3, (1916), 101-129.
2. Ulmer, H. E., "Application of magnetic amplifiers to the control and automatic regulation of machine systems," Gen. Elec. Engr. Bull., 1, (1911), 45-52.
3. Geyer, R., "Magnetic amplifier for the measurement of resistance," I.R.E. Trans., 3, (1916), 101-129.

device is its inherently narrow bandwidth. The future value of the amplifier in applications other than direct-current instruments lies in the success with which bandwidth can be increased while still maintaining reasonable gain. The use of the magnetic amplifier in automatic control has thus far been limited to medium and low-speed servomechanisms having bandwidths in the order of 1 cycle per second.¹ Within the last few months a recent development has occurred which indicates that higher bandwidths combined with reasonable gain can be obtained. This event was the announcement of a two-stage magnetic audio-amplifier having a 3ke. bandwidth, a power gain of about 10 per stage, and a 10.8 ke. power supply.² The saturable-reactor cores used in the design were made of improved magnetic material.

The attractive feature of long life under adverse operating conditions enjoyed by the magnetic amplifier has been the motivating force behind recent magnetic amplifier development, and results of this thesis indicate that some improvement of bandwidth while retaining reasonable gain is possible. Where high gain is desired and bandwidth is of little consequence, the magnetic amplifier has already proved its value.

Suggestions for Further Work

This thesis has investigated only the fundamentals of magnetic-amplifier performance, and a great

1. Rodemann, W.B., "A Study of the Magnetic Amplifier as a Servo Controller," E.E. Thesis, (M.I.T., 1947).
2. Logan, F.W., "Saturable Reactor and Magnetic Amplifier Circuits," N.O.R.L. 1091, Naval Ordnance Laboratory, White Oak, Md. (1945), 7-20.

device is an inherently narrow bandwidth. The future
 value of the amplifier in applications other than direct-
 current instruments lies in the success with which band-
 width can be increased while still maintaining reasonable
 gain. The use of the magnetic amplifier in automatic
 control has thus far been limited to medium and low-speed
 servomechanisms having bandwidths in the order of 1 cycle
 per second. Within the last few months a recent develop-
 ment has occurred which indicates that higher bandwidths
 associated with magnetic gain can be obtained. This event
 was the announcement of a two-stage magnetic audio-amplifier
 having a flat bandwidth, a power gain of about 10 per stage,
 and a 10.8 Mc. power supply.² The experimental results
 used in the design were made of improved magnetic material.
 The attractive feature of long life under adverse
 operating conditions enjoyed by the magnetic amplifier has
 been the activating factor toward recent magnetic amplifier
 development, and results of this work indicate that some
 improvement of bandwidth while retaining reasonable gain
 is possible. Where high gain is desired and bandwidth is
 of little consequence, the magnetic amplifier has already
 proved its value.

References for Further Work

1. "Magnetic Amplifier," J. E. Smith, *Electrical Engineering*, Vol. 68, No. 1, p. 1, 1949.
2. "Magnetic Amplifier," J. E. Smith, *Electrical Engineering*, Vol. 68, No. 1, p. 1, 1949.
3. "Magnetic Amplifier," J. E. Smith, *Electrical Engineering*, Vol. 68, No. 1, p. 1, 1949.

deal of work yet remains to be done before the potentialities are fully exploited and the limitations fully understood. A thorough investigation of regenerative ampere-turn feedback is essential to the development of high-gain amplifiers. Bandwidth and stability considerations of such a circuit should be put on a quantitative basis. The performance of the feedback varistor-bridge has, in the past, been a source of trouble since the varistors are affected by changes of voltage, frequency, and particularly of temperature. Such fluctuation results in considerable variation of amplifier sensitivity.¹ The solution of this problem would increase the accuracy of magnetic-amplifier instruments. Shock and fatigue studies should be conducted to give specific data on the ability of the magnetic amplifier to maintain uniform performance over long uninterrupted periods under adverse operating conditions. The problem of noise appears completely untouched, and information as to its importance should prove valuable in establishing performance limitations. The Barkhausen effect, or discrete reversals of electron spins, is somewhat analogous to the shot effect in electronic amplifiers. This and other sources of noise should be investigated. Rigorous theoretical studies could profitably be made taking into account core loss. These studies could be extended to the feedback case. The mathematics involved in rigorous analyses is, in general, too involved for practical design engineering, and

1. Geyger, W., "Magnetisch Verstärker für die Mess und Regeltechnik," E.F.Z., 62, (1941), 849-853.

deal of work yet remains to be done before the possibilities
are fully exploited and the limitations fully under-
stood. A thorough investigation of representative empha-
sized feedback is essential to the development of high-gain
amplifiers. Bandwidth and stability considerations of such
a circuit should be put on a quantitative basis. The per-
formance of the feedback amplifier-oscillator has, in the past,
been a source of trouble since the variables are affected
by changes of voltage, frequency, and particularly of tem-
perature. Such fluctuations result in considerable varia-
tion of amplifier sensitivity. The rejection of noise

problems would interest the student of magnetic amplifier
circuits. Open and closed circuit studies should be conducted
to give specific data on the ability of the magnetic ampli-
fier to maintain uniform performance over long uninter-
rupted periods under adverse operating conditions. The problem of
noise requires carefully understood, and information as to
its importance should prove valuable in establishing per-
formance limitations. The feedback effect, or decrease
in output of a system when it is connected to the
input, is a factor in amplifier design. This and other

sources of noise should be investigated. A more detailed
and studies could profitably be made taking into account
noise level. These studies could be extended to the feedback
case. The techniques involved in rigorous analysis is, in
general, not involved in practical design engineering, and

I. Gustaf, W. Gustafson, and J. Gustafson for his help and
technical assistance. (1941), 194-195.

hence, performance criteria should be reduced wherever possible to permit linear-system approximations. Further extension of familiar amplifier configurations, such as the cascaded circuit, balanced circuit, and push-pull circuit, will undoubtedly yield other useful designs.

hence, performance criteria should be reduced wherever possible to permit linear-space representations. Further extension of familiar amplifier configurations, such as the cascaded circuit, balanced circuit, and push-pull circuit, will undoubtedly yield other useful designs.

APPENDIX
SAMPLE DESIGN PROCEDURE

Specifications

Let us assume that the following specifications for a magnetic amplifier are given:

$$f = 400 \text{ cps.}$$

$$BW = 40 \text{ cps.}$$

Core type - Allegheny #4750 alloy
of dimensions shown in
Figure 2-4.

The amplifier is to employ the basic circuit, and is to be designed to produce maximum gain. The design will be based on empirical data, developed equations and the information of Figure 6-1.

Flux-Adjustment for Static Linear Operation

The applied alternating voltage is selected as 75 volts, rms, and the load resistance is chosen as 500 ohms from Figure 3-8. The optimum empirical value of N_2 is selected from Figure 3-10 as 1200 turns per core. The turns are to be made of No. 30 Formvar wire which has an approximate average resistance of 0.025 ohms per turn on the chosen cores.

It is desirable to use a large number of input turns in order to increase the gain, since the gain increases with the square of N_1 in accordance with Equation 3-17, whereas the bandwidth decreases directly with N_1 . The principal limitation on the maximum value of N_1 is the

APPENDIX

SAMPLE DESIGN PROCEDURE

Specifications

Let us assume that the following specifications

for a magnetic amplifier are given:

$$I = 400 \text{ amp.}$$

$$W = 50 \text{ amp.}$$

Core type - Alloyed 4-75 alloy
of dimensions shown in
Figure 2-1.

The amplifier is to employ the basic circuit, and is to be designed to produce maximum gain. The design will be based on empirical data, developed equations and the information of Figure 2-1.

First Adjustment for Basic Linear Operation

The applied alternating voltage is selected as 15 volts, rms, and the load resistance is chosen as 500 ohms. From Figure 3-8, the optimum saturation value of I_0 is selected from Figure 3-10 as 1500 turns per core. The turns are to be made of No. 30 wire with which has an approximate average resistance of 0.005 ohms per turn on the chosen core.

It is desirable to use a large number of input turns in order to increase the gain, since the gain increases with the square of I_0 in accordance with Equation 3-17, where the constant decreases directly with I_0 . The principal limitation on the maximum value of I_0 is the

available core window-space. For purposes of this design, there is ample window space for 8000 turns per core for the input windings. The windings are again made of No. 30 Formvar and the total winding resistance is therefore approximately 400 ohms.

From Equation 3-17

$$K_p R_1 = \left(\frac{8000}{1200}\right)^2 \times 500 = 22.25 \times 10^3.$$

Design for Dynamic Operation

The choice of R_1 for use in the gain equation must be based on the desired bandwidth. From Figure 3-28, the following conditions are established for a particular observation:

$$\begin{aligned} R_1 &= 2165 \text{ ohms} \\ BW &= 77 \text{ cps.} \\ f &= 400 \text{ cps.} \\ E_2 &= 75 \text{ volts rms.} \\ R_2 &= 500 \text{ ohms} \\ N_1 &= 3600 \text{ T.} \\ N_2 &= 1000 \text{ T.} \\ I_1 &= 20 \text{ ma.} \end{aligned}$$

The values of R_2 and E_2 for this design are identical to the above, and hence, need no further consideration. The variation of bandwidth with the effective parameters, R_1 , N_1 , N_2 , and I_1 , can be selected from Figure 6-1, recalling that bandwidth is the inverse of the defined characteristic time. The following equation may then be written:

available core window-space. For purposes of this design, there is ample window space for 8000 turns per core for the layout winding. The windings are again made of No. 30 copper and the total winding resistance is therefore approximately 400 ohms.

From Equation 3-17

$$R_p A^2 = \left(\frac{8000}{1200} \right)^2 \times 500 = 22.25 \times 10^3$$

Design for Dynamic Operation

The choice of A^2 for use in the gain equation must be based on the desired bandwidth. From Figure 3-25, the following conditions are established for a particular observation:

A^2	=	210 ohms
R_p	=	75 ohms
L	=	400 ohms
R_s	=	75 volts rms
R_L	=	500 ohms
M_A	=	3600 T.
R_g	=	1000 T.
I_1	=	20 ma.

The values of R_p and L for this design are identical to the above, and hence, need no further consideration. The variation of bandwidth with the effective parameters, A^2 , L , R_p , and I_1 , can be selected from Figure 3-1, resulting that bandwidth in the inverse of the defined characteristic time. The following equation may then be written:

$$BW = \frac{C_1 R_1 N_2 I_1^{\frac{1}{2}}}{N_1}$$

where C_1 is a constant. Substitution of the listed values in the above equation permits solution for C_1 :

$$C_1 = \frac{N_1 BW}{R_1 N_2 I_1^{\frac{1}{2}}} = \frac{3600 \times 77}{2165 \times 1000 \times 20^{\frac{1}{2}}} = 28.65 \times 10^{-3}$$

The value of the biasing current, I_1 , is chosen to insure operation in the linear range. A satisfactory value is 10.0 milliamperes. The biasing current may be applied in series with the control circuit.

It is now possible to solve for R_1 from the selected parameters

$$N_1 = 8000 \text{ turns}$$

$$N_2 = 1200 \text{ turns}$$

$$I_1 = 10.0 \text{ ma.}$$

$$BW = 40 \text{ cps.}$$

$$C_1 = 28.65 \times 10^{-3}$$

The expression for R_1 becomes:

$$\begin{aligned} R_1 &= \frac{N_1 \times BW}{C_1 N_2 I_1^{\frac{1}{2}}} = \frac{8000 \times 40}{28.65 \times 10^{-3} \times 1200 \times 10^{\frac{1}{2}}} \\ &= \underline{2950 \text{ ohms.}} \end{aligned}$$

The gain equation is now solvable:

$$K_p = \frac{22.25 \times 10^3}{R_1} = \frac{22.25 \times 10^3}{2950} = \underline{7.55}$$

The gain is relatively low, but the bandwidth of 40 cps. is excellent for this type amplifier.

If bandwidth considerations would permit the use of a minimum input resistance, that is, the resistance of

$$G_1 = \frac{G_2 R_2}{R_1 + R_2} = \frac{1000 \times 10^3}{10^3 + 10^3} = 500$$

where G_1 is a constant. Substitution of the listed values in the above equation permits solution for G_1 .

$$G_1 = \frac{R_2}{R_1 + R_2} \times 10^3 = \frac{1000}{10^3 + 10^3} \times 10^3 = 500$$

The value of the damping constant, ζ , is chosen so linear operation in the linear range. A satisfactory value is 10.0 milliseconds. The damping constant may be applied in series with the control circuit.

It is not possible to solve for ζ from the recorded parameters

$$R_1 = 800 \text{ ohms}$$

$$R_2 = 1000 \text{ ohms}$$

$$\zeta = 10.0 \text{ ms}$$

$$W = 60 \text{ cps}$$

$$G_1 = 500 \times 10^3$$

The expression for ζ becomes:

$$\zeta = \frac{R_2}{R_1 + R_2} \times 10^3 = \frac{1000}{10^3 + 10^3} \times 10^3 = 500$$

$$= 1000 \text{ ohms}$$

The gain equation is now solved:

$$K_p = \frac{G_1}{R_1} = \frac{500 \times 10^3}{10^3} = 500$$

The gain is relatively low, but the bandwidth of 60 cps is excellent for this type amplifier.

If feedback considerations would permit the use of a minimum input resistance, that is, the resistance of

the windings of the input circuit, which we recall is $2 \times 8000 \times 0.025$, or 400 ohms, the gain becomes

$$K_p = \frac{22.25 \times 10^3}{400} = 55.5 .$$

Under these conditions, the bandwidth is reduced to

$$BW = \frac{40 \times 400}{2950} = 5.43 \text{ cps.}$$

Obviously, further increases in the input turns to entirely fill the window space will result in further increases in the gain-bandwidth product. In this particular design, however, provision is made for the addition of feedback windings.

The Addition of Feedback Windings

Sufficient window space remains to add regenerative-feedback windings to equal the windings of the output circuit for fully-compensated feedback. The improvement in gain with the feedback connection will be of the order of at least 100, and if compensation is accurately made, may be well in excess of this value. A reduction in bandwidth will undoubtedly occur. The extent of this thesis investigation does not permit a prediction to be made as to the extent of this reduction.

The findings of the input circuit, which we recall is
 $2 \times 8000 \times 0.025$, or 400 ohms, the gain becomes

$$K_p = \frac{25,000 \pm 10^3}{400} = 62.5$$

Under these conditions, the bandwidth is reduced to

$$BW = \frac{10 \times 800}{2500} = 3.2 \text{ cps.}$$

Obviously, further increases in the input leads to only
 till the window space will result in further increases in
 the gain-bandwidth product. In this particular design,
 however, provision is made for the addition of feedback
 signals.

The Addition of Feedback Signals

Sufficient window space remains to add negative-
 feedback signals to equal the findings of the output
 circuit for fully-compensated feedback. The improvement
 in gain with the feedback compensation will be of the order
 of at least 100, and if compensation is accurately made,
 may be well in excess of this value. A reduction in band-
 width will undoubtedly occur. The extent of this decrease
 investigation does not permit a prediction to be made as to
 the extent of this reduction.

BIBLIOGRAPHY

1. Alexanderson, E.F.W., and Nixdorff, S.P., "A Magnetic Amplifier for Radio Telephony," I.R.E. Proc., 4, (1916), 101-129.
2. Boyajian, A., "Mathematical Analysis of Nonlinear Circuits," G.E. Rev., 34, (1931), 531-745.
3. Buchhold, T., "Für Theorie des Magnetischen Verstärken (On the Theory of the Magnetic Amplifier)," A.f.E., 37, (1943), 197-211.
4. Buchhold, T., "Über Gleichstromvormagnetisierte Wechselstromdrosselspuln und deren Rückkopplung (On D-C Premagnetized A-C Choke Coils and Their Feedback)," A.f.E., 36, (1942), 221-239, 514.
5. Burton, E.T., "Transformer," U. S. Patent #1,880,412, (1930).
6. Bush, V., "The Differential Analyzer," J.F.I., 212, (1931), 447-448.
7. Bush, V., and Caldwell, S.H., "A New Type Differential Analyzer," J.F.I., 240, (1945), 255-326.
8. Draper, C.S. and McKay, W., "Instrument Analysis," M.I.T. Notes, (1946).
9. Elmen, O.W., "High-Frequency Detector," U. S. Patent, #1,289,418, (1918).
10. Fitzgerald, A.S., "Magnetic Amplifier Characteristics, Neutral Type," J.F.I., 244, (1947), 415-439.
11. Fitzgerald, A.S., "Some Notes on the Design of Magnetic Amplifiers," J.F.I., 244, (1947), 323-362.
12. Fitzgerald, A.S., "Magnetic Amplifier Circuits, Neutral Type," J.F.I., 244, (1947), 249-265.
13. Geyger, W., "Magnetische Verstärken für die Mess und Regeltechnik (Magnetic Amplifiers for Measurement and Control)," E.T.Z., 62, (1941), 849-853, 891-898.
14. Giroz, H.E., "Application of Magnetic Amplifiers to the Control and Automatic Regulation of Furnace Temperatures," Bul. Soc. Franc. Elect., 1, (1941), 459-479.
15. Grafinger, L.N., "A Study of Magnetic Amplifiers for Servomechanisms," E.E. Thesis, (M.I.T., 1946).

BIBLIOGRAPHY

1. Alexander, E.H.W., and Alexander, E.H.W., "A Magnetic Amplifier for Radio Frequency," I.R.E. Trans., A, (1946), 101-102.
2. Bogdan, A., "Mathematical Analysis of Nonlinear Systems," I.R.E. Trans., A, (1947), 371-372.
3. Bruckner, T., "The Theory of the Magnetic Amplifier," A.I.E.E. Trans., (1947), 197-211.
4. Bruckner, T., "Some Characteristics of the Magnetic Amplifier," Proc. I.R.E., (1947), 351-352.
5. Burton, E.L., "Fundamentals," U. S. Patent 2,400,712, (1949).
6. Bush, V., "The Differential Analyzer," I.R.E. Trans., (1947), 107-108.
7. Bush, V., and others, "The New Type Differential Analyzer," I.R.E. Trans., (1947), 353-354.
8. Burton, E.L., and others, "The Magnetic Amplifier," I.R.E. Trans., (1947), 355-356.
9. Burton, E.L., "The Magnetic Amplifier," U. S. Patent 2,400,712, (1949).
10. Burton, E.L., "The Magnetic Amplifier," I.R.E. Trans., (1947), 357-358.
11. Burton, E.L., "The Magnetic Amplifier," I.R.E. Trans., (1947), 359-360.
12. Burton, E.L., "The Magnetic Amplifier," I.R.E. Trans., (1947), 361-362.
13. Burton, E.L., "The Magnetic Amplifier," I.R.E. Trans., (1947), 363-364.
14. Burton, E.L., "The Magnetic Amplifier," I.R.E. Trans., (1947), 365-366.
15. Burton, E.L., "The Magnetic Amplifier," I.R.E. Trans., (1947), 367-368.

16. Lamm, U., "The Transductor, D.C. Pre-Saturated Reactor," (Stockholm, Esselte Aktiebolag, 1943).
17. Lamson, H.W., "Alternating-Current Measurements of Magnetic Properties," I.R.E. Proc., 36, (1947), 266-277.
18. M.I.T. E.E. Staff, "Magnetic Circuits and Transformers," (New York, John Wiley and Sons, 1943), 198.
19. Naval Ordnance Laboratory Report, "Papers Presented at the Naval Ordnance Laboratory Magnetic Materials Symposium," N.O.L.R. #1091, (1948).
20. Pease, W.M., "Design of a 400 Cycle Servomechanism," E.E. Thesis, (M.I.T., 1943).
21. Rex, H.B., "The Transductor," Instruments, 20, (1947), 1102-1109.
22. Ricker and Tucker, "Electrical Engineering Laboratory Experiments," (New York, McGraw-Hill, 1940), 91-100.
23. Rockett, F., "Improved Material for Magnetic Amplifiers," Electronics, (August, 1948), 128-130.
24. Rodemann, W.B., "A Study of the Magnetic Amplifier as a Servo-Controller," E.E. Thesis, (M.I.T.), (1947).
25. Therkelsen, E.B., "A Low-Power Magnetic Amplifier for Servomechanisms," E.E. Thesis, (M.I.T.), (1946).
26. U. S. Naval Mission to Japan, "Magnetic Development in Japan during World War II," Target Report X-34N, (1946).

16. Lamm, U., "The Transformer, U.C. Pre-Saturated Reactor," (Stockholm, Kassel, Stockholm, 1943).
17. Lamm, U., "Electrical-Current Measurement of Magnetic Properties," I.E.E. Proc., 36, (1947), 265-277.
18. M.I.T. Staff, "Magnetic Circuits and Transformers," (New York, John Wiley and Sons, 1943), 158.
19. Naval Ordnance Laboratory report, "Paper Presented at the Naval Ordnance Laboratory Magnetic Materials Symposium," N.O.L.A. 41091, (1948).
20. Pappas, W.L., "Design of a 400 Cycle Transformer," A.S. Thesis, (M.I.T., 1943).
21. Ray, H.B., "The Transformer," Instrument, 20, (1947), 1102-1109.
22. Risher and Tucker, "Electrical Engineering Laboratory Experiments," (New York, McGraw-Hill, 1940), 21-100.
23. Roberts, F., "Improved Material for Magnetic Amplifiers," Electronics, (August, 1948), 123-130.
24. Robinson, W.B., "A Study of the Magnetic Amplifier as a Servo-Controller," A.S. Thesis, (M.I.T., 1947).
25. Therkelsen, E.M., "A Low-Power Magnetic Amplifier for Servomechanisms," A.S. Thesis, (M.I.T., 1946).
26. U.S. Navy, "Report on Japan, Magnetic Developments in Japan during World War II," Report X-344, (1946).



APR 30
AUG 31

244
BINDERY

SEP 30
12 SEP 67

171
509
15731

Thesis
B48

Betzer

Study of the magnetic
amplifier.

11256

12 SEP 67

15731

Thesis

11256

B48

Betzer

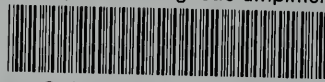
Study of the magnetic ampli-
fier.

Library
U. S. Naval Postgraduate School
Monterey, California



thesB48

A study of the magnetic amplifier /



3 2768 002 13794 5

DUDLEY KNOX LIBRARY